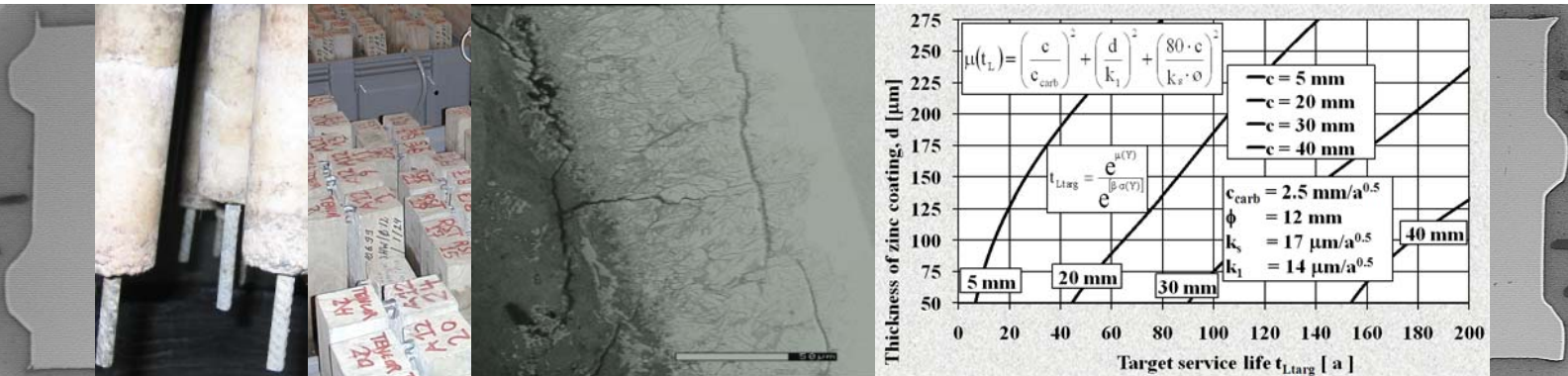# SERVICE LIFE OF HOT-DIP GALVANISED REINFORCEMENT BARS IN CARBONATED AND CHLORIDE-CONTAMINATED CONCRETE

Esko Sistonen

TEKNILLINEN KORKEAKOULU
TEKNISKA HÖGSKOLAN
HELSINKI UNIVERSITY OF TECHNOLOGY
TECHNISCHE UNIVERSITÄT HELSINKI
UNIVERSITE DE TECHNOLOGIE D'HELSINKI

SERVICE LIFE OF HOT-DIP GALVANISED REINFORCEMENT BARS IN CARBONATED AND CHLORIDE-CONTAMINATED CONCRETE

Esko Sistonen

Dissertation for the degree of Doctor of Science in Technology to be presented with due permission of the Faculty of Engineering and Architecture, Helsinki University of Technology for public examination and debate in Auditorium R1 (Rakentajanaukio 4A) at Helsinki University of Technology (Espoo, Finland) on the 4th of December, 2009, at 12 noon.

Helsinki University of Technology
Faculty of Engineering and Architecture
Department of Structural Engineering and Building Technology

Author's address:

Helsinki University of Technology
Department of Structural Engineering and Building Technology
P. O. Box 2100
FI-02015 TKK
FINLAND
esko.sistonen@tkk.fi

Author   Esko Sistonen

Name of the dissertation

Service Life of Hot-dip Galvanised Reinforcement Bars in Carbonated and Chloride-Contaminated Concrete

Faculty   Faculty of Engineering and Architecture

Department   Department of Structural Engineering and Building Technology

Field of research   Structural Engineering and Building Physics

Opponent(s)   Research Professor Carmen Andrade, Research Professor (Emeritus) Asko Sarja

Supervisor   Professor Jari Puttonen, Helsinki University of Technology, TKK

Instructor   Professor Jari Puttonen, Helsinki University of Technology, TKK

Abstract

The dissertation presents the work studying the factors influencing on the service life of hot-dip galvanised reinforcement bars. The experimental part of the study consisted of accelerated corrosion tests among others. The comparison of the measured crack width of concrete with the rate of corrosion values, and also with other measured values such as the corrosion potential, the resistivity of concrete, and the mechanical properties of the steel indicated no correlation irrespective of the duration of the exposure or type of aggressive liquid. The rate of corrosion decreased as a function of exposure time. This was not dependent on the water-to-cement ratio of concrete.

Three probable corrosion mechanisms are determined for hot-dip galvanised reinforcement bars in cracked concrete, based on long-term durability tests and other studies. The first mechanism consists of a local dissolution of the eta (η) and zeta (ζ) phases of the zinc layer. In the second mechanism, as a result of the non-uniformity of the zinc coating, local dissolution of the eta (η) and zeta (ζ) phases, together with longitudinal and perpendicular cracking in the zinc layer, may lead to the local separation of the zinc layer. In the third mechanism, as a result of the non-uniformity of the zinc coating, full dissolution of the eta (η) phase and partial dissolution of the zeta (ζ) phase, together with longitudinal and perpendicular cracking in the ferrite, may lead to the local separation of the zinc layer and the ferrite.

The effects of different reinforcing steels on the service life of outdoor concrete structures were estimated through calculations. A stochastic method based on the probability of damage, Monte Carlo simulation, and reliability and sensitivity analyses were also used. In carbonated intact and cracked concrete the use of hot-dip galvanised reinforcement bars could double the service life compared with the use of ordinary steel reinforcement bars. In chloride-contaminated intact concrete the service life as a result of using hot-dip galvanised reinforcement bars is 3-5 times longer compared with ordinary steel reinforcement bars. The conclusion is based on the results received with the critical water-soluble chloride content, 1.0-1.5 wt%$_{CEM}$, which is substantially higher than the critical water-soluble chloride content, 0.3-0.4 wt%$_{CEM}$, for ordinary steel reinforcement bars.

Keywords: hot-dip galvanised concrete reinforcement, crack width, corrosion mechanisms, service life

VÄITÖSKIRJAN TIIVISTELMÄ	TEKNILLINEN KORKEAKOULU PL 1000, 02015 TKK http://www.tkk.fi

Tekijä Esko Sistonen

Väitöskirjan nimi
Kuumasinkittyjen betoniraudoitetankojen käyttöikä karbonatisoituneessa ja kloridipitoisessa betonissa

Käsikirjoituksen päivämäärä 25.05.2009	Korjatun käsikirjoituksen päivämäärä 15.10.2009

Väitöstilaisuuden ajankohta   04.12.2009

☒ Monografia   ☐ Yhdistelmäväitöskirja (yhteenveto + erillisartikkelit)

Tiedekunta   Insinööritieteiden ja arkkitehtuurin tiedekunta
Laitos   Rakenne- ja rakennustuotantotekniikan laitos
Tutkimusala   Talonrakennustekniikka
Vastaväittäjä(t)   Tutkimusprofessori Carmen Andrade, Tutkimusprofessori (Emeritus) Asko Sarja
Työn valvoja   Professori Jari Puttonen, Teknillinen korkeakoulu, TKK
Työn ohjaaja   Professori Jari Puttonen, Teknillinen korkeakoulu, TKK

Tiivistelmä

Väitöskirjassa tutkittiin osatekijöitä, jotka vaikuttavat kuumasinkityn betoniterästangon käyttöikään. Työn kokeellinen osuus koostui muun muassa kiihdytetyistä korroosiokokeista. Mitattujen betonin halkeaman leveyden ja korroosionopeuden tai muiden mitattujen arvojen kuten korroosiopotentiaalin, betonin ominaisvastuksen ja teräksen mekaanisten ominaisuuksien välillä ei havaittu yhteyttä säilyvyyskokeen pituudesta tai rasitusolosuhteista riippumatta. Korroosionopeus oli hidastuvaa rasitusajan funktiona. Tämä ei riippunut betonin vesisementtisuhteesta.

Säilyvyyskokeisiin ja muihin tutkimuksiin perustuen kolme todennäköistä kuumasinkityn betoniterästangon korroosiomekanismia halkeilleessa betonissa määritettiin. Ensimmäinen mekanismi käsittää sinkkikerroksen eta (η) ja zeta (ζ) faasin paikallisen liukenemisen. Toisessa mekanismissa sinkkipinnoitteen epäyhtenäisyydestä johtuen eta (η) ja zeta (ζ) faasin liukeneminen yhdessä sinkkikerroksen pitkittäis- ja paksuussuuntaisen halkeilun kanssa saattaa aiheuttaa sinkkikerroksen paikallista irtoamista. Kolmannessa mekanismissa sinkkipinnoitteen epäyhtenäisyydestä johtuen täydellinen eta (η) ja osittainen zeta (ζ) faasin liukeneminen yhdessä raudassa tapahtuvan pitkittäis- ja paksuussuuntaisen halkeilun kanssa saattaa johtaa sinkkikerroksen ja raudan paikalliseen irtoamiseen.

Erityyppisten betoniraudoitteiden vaikutuksia ulkoteräsbetonirakenteen käyttöikään arvioitiin laskelmin. Stokastista vauriotodennäköisyyteen ja Monte Carlo–simulointiin perustuvaa menetelmää, sekä myös luotettavuus- ja herkkyystarkasteluja käytettiin laskelmissa. Kuumasinkityn betoniterästangon käyttö saattaa kaksinkertaistaa karbonatisoituneen halkeilemattoman ja halkeilleen betonirakenteen käyttöiän verrattuna tavalliseen betoniterästangon käyttöön. Kloridipitoisessa halkeilemattomassa betonissa käyttöikä kuumasinkittyä betoniterästankoa käytettäessä on 3−5-kertainen verrattuna tavallisen betoniterästangon käyttöön. Käyttöiän pidentyminen perustuu kuumasinkityn betoniterästangon kriittiseen vesiliukoisten kloridien pitoisuuteen 1.0–1.5 wt%$_{CEM}$, joka on olennaisesti korkeampi kuin tavallisen betoniterästangon kriittinen vesiliukoisten kloridien pitoisuus 0.3–0.4 wt%$_{CEM}$.

Asiasanat   kuumasinkitty betoniraudoite, halkeaman leveys, korroosiomekanismit, käyttöikä

ISBN (painettu) 978-952-248-167-2	ISSN (painettu) 1797-4836
ISBN (pdf) 978-952-248-168-9	ISSN (pdf) 1797-4844
Kieli Englanti	Sivumäärä 161 s.+ liit. 16 s.

Julkaisija   TKK Rakenne- ja rakennustuotantotekniikan laitos

Painetun väitöskirjan jakelu   TKK Rakenne- ja rakennustuotantotekniikan laitos

☒ Luettavissa verkossa osoitteessa http://lib.tkk.fi/Diss/

ACKNOWLEDGMENTS

ABBREVIATIONS AND NOTATIONS

AD	Anderson-Darling goodness-of-fit test value	[-]
AFm	Monosulphate	
BSE	Backscattered Electron Detector	
CaHZn	Calcium hydroxozincate	
CSE	Copper/copper sulphate half-cell electrode	
CH	Calcium Hydroxide	
CSH	Calcium Silicate Hydrate	
Corr. Area	Sum of all the corroded area per the measuring range of GECOR6	[%]
EDS	Energy-Dispersive Spectrometer	
ESEM	Environmental Scanning Electron Microscope	
HPC	High-performance concrete	
ITZ	Interfacial transition zone	
KS	Kolmogorov-Smirnov goodness-of-fit test value	[-]
RH	Relative humidity	[%]
$RI(x_i)$	Relative significance of factor i	[-]
A_{gt}	Percentage elongation after failure	[%]
A_{10}	Percentage total elongation at maximum force	[%]
C_1	Surface chloride content	[wt%$_{CEM}$]
C_{cr}	Critical chloride content	[wt%$_{CEM}$]
D_c	Chloride diffusion coefficient of concrete	[mm^2/a]
D_{cr}	Diffusion coefficient of the crack with respect to carbon dioxide	[mm^2/a]
D_{ccr}	Diffusion coefficient of the crack with respect to chloride ions	[mm^2/a]
D_e	Diffusion coefficient of the concrete with respect to carbon dioxide	[mm^2/a]
E_{corr}	Corrosion potential	[mV]
F	Faraday's constant = 96487	[C/mol]
F	Cumulative distribution function	[-]
I_{corr}	Corrosion current	[μA/cm^2]
L	Location parameter in Weibull and Gamma distribution	[-]
M	Atomic weight	[g/mol]
P	Probability	[-]
P -%	Phosphorus content of steel reinforcement bar	[%]
R	Resistivity of concrete	[kΩ·cm]
R^2	Correlation factor	[-]
R_m	Tensile strength	[N/mm^2]
$R_{p0.2}$	Elongation limit 0.2%	[N/mm^2]
S_{crack}	Length of the corroded area along the reinforcing steel surface at the crack	[mm]
Si -%	Silicon content of steel reinforcement bar	[%]
Si_e	Silicon equivalent of steel reinforcement bar	[%]
S_K	Number of variable combinations	[-]
S_{pr}	Projective area of transversal ribs	[mm^2]
T	Temperature	[°C]
V	Coefficient of variation	[-]

a	Length between transversal ribs	[mm]
c	Thickness of the concrete cover	[mm]
c_{carb}	Coefficient of carbonation	[mm/a^{½}]
d	Nominal bar diameter	[mm]
d	Thickness of zinc coating	[μm]
d_{cr}	Carbonation depth at a crack	[mm]
f	Density distribution function	[-]
f_{cm}	Concrete strength	[MPa]
f_R	Relative rib area	[-]
$f_{R,min}$	Minimum permitted relative rib area	[-]
h	Height of the rib	[mm]
i_{corr}	Corrosion current	[μA/cm^2]
k	Coefficient	
k	Summing term	[-]
k_{cl}	Coefficient of critical chloride content	[mm/$\sqrt{a}$]
k_e	Circumstantial factor	[-]
k_s	Coefficient of the rate of corrosion in uncracked carbonated concrete for ordinary steel reinforcement bars	[μm/$\sqrt{a}$]
k_x	Coefficient of relative rib area	[-]
k_1	Coefficient of the rate of corrosion in uncracked and cracked carbonated concrete for hot-dip galvanised reinforcement bars	[μm/$\sqrt{a}$]
k_1	Coefficient of the rate of corrosion in uncracked and cracked chloride-contaminated concrete for hot-dip galvanised reinforcement bars	[μm/$\sqrt{a}$]
k_2	Coefficient of the rate of corrosion in cracked carbonated and chloride-contaminated concrete for ordinary steel reinforcement bars	[μm/$\sqrt{a}$]
m	Mean value	[-]
m	Mode parameter in Extreme value distribution (Type 1)	[-]
n	Exponent of time	[-]
n	Number of measurements or variables	[-]
n	Number of measured beams or cylinders	[-]
p	Chi-Square goodness-of-fit test value	[-]
p_r	Protective pore ratio	[-]
r	Deterioration rate	
r_s	Rate of corrosion in uncracked carbonated and chloride-contaminated concrete for ordinary steel reinforcement bars	[μm/a]
r_1	Rate of corrosion in uncracked and cracked carbonated concrete for hot-dip galvanised reinforcement bars	[μm/a]
r_1	Rate of corrosion in uncracked and cracked chloride-contaminated concrete for hot-dip galvanised reinforcement bars	[μm/a]
r_2	Rate of corrosion in cracked carbonated and chloride-contaminated concrete for ordinary steel reinforcement bars	[μm/a]
s	Standard deviation	[-]
s	Corrosion depth	[μm]
s	Deterioration depth or grade	
s_{max}	Maximum deterioration depth or grade allowed	
s_{max}	Maximum permitted corrosion depth of a reinforcement	[μm]
t	Time (in years)	[a]
t_0	Initiation time	[a]

t_1	Propagation time for zinc coating	[a]
t_2	Propagation time for ordinary steel reinforcement bars	[a]
t_L	Service life of reinforced concrete structure	[a]
t_{Ltarg}	Target service life	[a]
$t_{\phi=5\%}$	Service life with a 5% probability of damage	[a]
$t_{\phi=10\%}$	Service life with a 10% probability of damage	[a]
v_{corr}	Rate of corrosion	[μm/a]
w	Crack width	[mm]
w/b	Water-to-binder ratio of concrete	[-]
w/c	Water-to-cement ratio of concrete	[-]
x	Loss of bar radius attributable to corrosion	[-]
$\bar{x}$	Mean value	[-]
z	Number of electrons transferred per atom	[-]
Γ	Gamma function	
Φ[.]	(0,1)-normal cumulative distribution function	[-]
α	Pitting factor	[-]
α	Shape parameter in Gamma distribution	[-]
α	Scale parameter in Weibull and Extreme value distribution (Type 1)	[-]
α	Shape parameter in Weibull distribution	[-]
α	Angle of slope of transversal ribs	[deg]
$α_{crack}$	Central angle for the width of the corroded area at the surface of the reinforcing steel at the crack	[deg]
β	Drift angle of the rib	[deg]
β	Test parameter for (0,1)-normal cumulative distribution function ø	[-]
β	Scale parameter in Gamma distribution	[-]
β	Shape parameter in Weibull distribution	[-]
δ	Delta phase	
η	Eta phase	
γ	Gamma phase	
Ø	Reinforcement bar diameter	[mm]
ρ	Density of steel	[g/m³]
σ	Standard deviation	[-]
$σ(x_i)$	Standard deviation of variable x_i	[-]
$σ(t_L)$	Standard deviation of service life	[-]
σ(Y)	Standard deviation of lognormal distribution function	[-]
λ	Scale parameter in Weibull distribution	[-]
μ	Mean value	[-]
$μ(t_L)$	Mean value of service life	[-]
$μ(x_i)$	Mean value of service life for variable x_i	[-]
μ(Y)	Mean value of lognormal distribution function	[-]
ν	Coefficient of variation (=σ/μ)	[-]
$ν_i$	Coefficient of variation for factor i	[-]
ζ	Zeta phase	
$∂μ(t_L)/∂x_i$	Partial derivate of service life as for variable x_i	[-]

TABLE OF CONTENTS

1 INTRODUCTION

1.1 Background

The most obvious consequence of the corrosion of steel reinforcements is the deterioration of reinforced concrete, a topic that has been widely studied and reported. Knowledge, especially of the long-term effects of the methods used for increasing the service life of old structures, is inadequate. The lack of basic knowledge of substantial corrosion processes prior to and after maintenance and repair measures is a drawback in structural rehabilitation. This lack of knowledge causes unexpected expenses and even fatal errors when decisions are being made about the methods and time of extending the service life of concrete structures. Restricting the corrosion risk in reinforced concrete structures under outdoor conditions can be ensured with the protection of steel reinforcement bars. Reinforcing steel for concrete can be galvanised by the hot-dipping process. Galvanising has been used since the 1930s for corrosion protection in many types of reinforced concrete structures and elements exposed to a range of environmental conditions[1].

The use of corrosion-protected reinforcing steel increases the service life of structures, but it also produces a need to research its behaviour in concrete. The effect of cracks in concrete on corrosion-protected reinforcing steel is different from the effect on ordinary reinforcing steel. Therefore, different crack widths may have a different effect on the durability of these reinforcing materials as well. A significant factor to be considered when choosing hot-dip galvanised reinforcement bars is the balance between material costs and the additional service life achieved.

1.2 Research problem

The role of the reinforcement bar material in a deteriorated reinforced concrete structure focuses on the strength of the structure. Thus, the load-bearing capacity of the structure depends mostly on the loss of bar section. In that case the research problem focuses on methods that ensure the functioning of the structure in its fulfilled service and ultimate limit state in the long term. Furthermore, as long a service life as possible often requires protective systems. This raises the need to research hot-dip galvanised reinforcement bars as a method for extending service life and to show the benefits of the material. However, the limitations and requirements that are basic elements in using hot-dip galvanised reinforcement bars should be recognised. For instance, the feasibility of using hot-dip galvanised reinforcement bars in concrete façades, bridges, pools, and tunnels may not be taken for granted. Furthermore, the increase in the service life compared to ordinary steel reinforcement bars in carbonated and chloride-contaminated concrete is debatable.

1.3 Aim and objectives of the research

The aim of this study was to research the factors influencing the service life of hot-dip galvanised concrete reinforcements. The objective of the study was to develop an estimation of the service life and to consider the problems in its calculation. Another

---

[1] Yeomans, S.R. (2004). Galvanizing of Steel Reinforcement for Use in Building and Construction.

objective of the study was to concretise the improvement of the service life when hot-dip galvanised steel reinforcement bars are used.

1.4   Research methods

The methodology presented in the literature (Chapter 2) concentrated on factors affecting the durability of hot-dip galvanised reinforcement bars. The study of the literature was focused on the influence of steel material and its deterioration. The main topics include, among others, corrosion mechanisms, mechanical properties, concrete properties, steel properties, the properties of the galvanising method, the formation and structure of the zinc coating, and the properties and reactions of galvanised reinforcements in concrete.

The study of the service life estimation (Chapter 3) was focused on a stochastic method based on the probability of damage, Monte Carlo simulation, and reliability analysis. The definition of service life is based on the assumption that the corrosion products spall the concrete cover, or a maximum permitted corrosion depth is reached.

The study of the laboratory work (Chapter 4) was focused on reinforced concrete beam and cylinder specimens. Durability tests with two concrete and four reinforcement bar types (ordinary steel, hot-dip galvanised steel, weathering (TENCOR), and austenitic stainless steel (grade AISI 304)) are presented. The same cement type (CEM II A 42.5 R) was used. Each measurement in the durability tests was supplementary in the study to the analysis of the long-term properties of hot-dip galvanised reinforcement bars. The methodology of the laboratory work concentrated on finding the probable corrosion mechanisms of hot-dip galvanised reinforcement bars. The rate of corrosion (uniform, decreasing), cracking (pitting corrosion), and thickness of the zinc coating (non-uniform) were the main parameters in the study of the corrosion mechanisms of hot-dip galvanised reinforcement bars. The research results were processed and analysed. With data and statistical parameters (mean value, standard deviation, coefficient of variation), most suitable distribution models with a close fit, and extreme value distribution (Type 1) from electrochemical, crack width, and zinc coating thickness measurements were taken into account. The methodology chosen assisted in the analysis of the reliability of the research results.

The effects of hot-dip galvanised reinforcing steels on the service life of outdoor concrete structures were estimated through calculations that also included sensitivity analysis (Chapter 5). The study of this chapter was focused on discussing the knowledge gathered from Chapters 2, 3, and 4. Finally, conclusions are drawn and recommendations for further research are discussed in Chapter 6.

1.5   Scope of the research

The main studied parameters were the degree of corrosion, crack width, and the thickness of the zinc coating. The research concentrated on hot-dip galvanising as a galvanisation method because it is globally used and accepted technique. This study was focused on the following exposure classes[1]: corrosion caused by carbonation XC1 (dry or permanently wet) or XC4 (cyclic wet and dry), and corrosion caused by chlorides

---

[1] SFS-EN 206-1 (2001). Concrete. Part 1: Specification, Performance, Production and Conformity.

XD2 (wet, rarely dry) and XD3 (cyclic wet and dry). The exposure classes XC4 and XD3 represent the most severe exposure circumstances.

1.6 Thesis contribution

The author has also been an essential contributor to the following publications, which should be considered supplemental to this thesis:

- Sistonen, E. (2001). The Main Corrosion Parameters and their Influence on the Durability of Outdoor Concrete Structures, Licentiate Thesis, Espoo, Finland, TKK, 84 p. + app. 20 p. (in Finnish).
- Sistonen, E., Cwirzen, A., Puttonen J. (2008). Corrosion mechanism of hot-dip galvanised reinforcement bar in cracked concrete, *Corrosion Science*, Vol. **50**, No. 12. pp. 3416-3428.
- Sistonen, E., Huovinen, S. (2005). Improvement in the Durability of Reinforced Outdoor Concrete Structures by Restricting Cracks and Protecting Reinforcement, Nordic Concrete Research - Research Projects 2005, Proceedings Nordic Concrete Research Meeting, XIX Symposium on Nordic Concrete Research & Development - A meeting place for research and practice; Sandefjord, Norway: 12.-15.6.2005, Publication No. 33, pp. 259-261.
- Sistonen, E., Huovinen, S. (2005). The Main Corrosion Parameters and their Influence on the Durability of Outdoor Concrete Structures, Nordic Concrete Research - Research Projects 2005, Proceedings Nordic Concrete Research Meeting, XIX Symposium on Nordic Concrete Research & Development - A meeting place for research and practice; Sandefjord, Norway: 12.-15.6.2005, Publication No. 33, pp. 271-273.
- Sistonen, E., Huovinen, S. (2005). Possibilities of controlling cracks and improving the Durability of Outdoor Reinforced Concrete Structures, Nordic Concrete Research - Research Projects 2005, Proceedings Nordic Concrete Research Meeting, XIX Symposium on Nordic Concrete Research & Development - A meeting place for research and practice; Sandefjord, Norway: 12.-15.6.2005, Publication No. 33, pp. 262-264.
- Sistonen, E., Huovinen, S. (2005). Problems in Service life Modelling of Corroded Outdoor Concrete Structures, Nordic Concrete Research - Research Projects 2005, Proceedings Nordic Concrete Research Meeting, XIX Symposium on Nordic Concrete Research & Development - A meeting place for research and practice; Sandefjord, Norway: 12.-15.6.2005, Publication No. 33, pp. 265-267.
- Sistonen, E., Kari, O-P., Tukiainen, P., Huovinen, S. (2006). Stochastic Method and Monte Carlo Simulation for Predicting Service Life of Hot-Dip Galvanised Reinforcement, 2nd International RILEM Symposium on Advances in Concrete through Science and Engineering, Quebec City, Canada, September 11-13, 2006, RILEM proceedings PRO 51 (editors: Marchand, J., et al.) (Abstract at p. 289 and the paper number 45 is 23 pages on symposium CD-ROM proceedings).
- Sistonen, E., Kari, O-P., Tukiainen, P., Huovinen, S. (2007). The Influence of the Crack Width on the Durability of Different Reinforcement Bar Materials, CONSEC'07, Concrete under severe conditions: Environment and loading, Tours, France, (editors: Toutlemonde et al.) June 4-6, 2007. pp. 419-428.
- Sistonen, E., Peltola, S. (2005). Quality Specifications for Hot-Dip Galvanised Reinforcement to Ensure the Target Service Life, Nordic Concrete Research - Research Projects 2005, Proceedings Nordic Concrete Research Meeting, XIX Symposium on Nordic Concrete Research & Development - A meeting place for research and practice; Sandefjord, Norway: 12.-15.6.2005, Publication No. 33, pp. 133-134.
- Sistonen, E., Tukiainen, P. (2005). The Influence of Rebar Material on the Durability of Outdoor Reinforced Concrete Structures, Nordic Concrete Research - Research Projects 2005, Proceedings Nordic Concrete Research Meeting, XIX Symposium on Nordic Concrete Research & Development - A meeting place for research and practice; Sandefjord, Norway: 12.-15.6.2005, Publication No. 33, pp. 268-270.
- Sistonen, E., Tukiainen, P., Huovinen, S. (2005). Bonding of Hot Dip Galvanised Reinforcement in Concrete, Nordic Concrete Research; Publication No. 34, 2/2005, The Nordic Concrete Federation, Oslo, 2005, pp 1-14.
- Sistonen, E., Tukiainen, P., Laitala, M., Huovinen, S. (2000). Restricting Corrosion Risk in Reinforced Concrete Structures under Outdoor Conditions, Espoo, Finland, TKK-TRT-111, 141 p. + app. 47 p. (in Finnish).

- Sistonen, E., Tukiainen, P., Peltola, S., Kari, O-P., Huovinen, S. (2006). Service Life and Quality Specifications for Hot-Dip Galvanised Reinforcement, European Symposium on Service Life and Serviceability of Concrete Structures, ESCS-2006, Proceedings, Helsinki, Finland, June 12-14, 2006, pp. 395-400.
- Sistonen, E., Tukiainen, P., Peltola, S., Skriko, S., Huovinen, S. (2002). Restricting Corrosion Risk in Reinforced Concrete Structures under Outdoor Conditions – Part II, Espoo, Finland, TKK-TRT-121, 212 p. + app. 101 p. (in Finnish).

2 FACTORS AFFECTING THE DURABILITY OF HOT-DIP GALVANISED REINFORCEMENT BARS

The experience gathered after several years shows that zinc delays the propagation of the corrosion process in aggressive circumstances. Furthermore, galvanisation reduces the cracking and spalling of the concrete cover and rust damage formed on the surface of the structure and caused by reinforcement corrosion[1]. Galvanised reinforcement bars are more resistant against failures such as too thin a concrete cover, insufficient compacting of the concrete, and poor curing than ordinary steel. A zinc coating protects reinforcement bars before concreting and also protruding reinforcement bars[2]. The rate of corrosion of zinc in carbonated concrete is low and zinc is substantially more resistant against chloride attack than ordinary steel. The main reason for this is that zinc-coated steel in concrete remains passivated to a pH level of about 9.5. However, the severity of the corrosive environment, the quality of the concrete, and the internal structure of the zinc layer have an effect on the corrosion of a zinc coating[3]. Furthermore, zinc itself does not prevent corrosion but reduces it.

2.1 Influence of steel material

Hot-dip galvanising involves the immersion of cleaned and non-heated steel in a bath of molten zinc at about 440-470 ºC, allowing a metallurgical reaction to occur between the steel and the zinc. This reaction produces a coating on the steel made up of a series of iron-zinc alloy phases (gamma (γ), delta (δ), and zeta (ζ)), which grow from the steel-zinc interface with a phase of eta (η) on the outer surface (Fig. 1). The thickness of the zinc coating depends, among other factors, on the dipping temperature, dipping time (typically between 1.5 and five minutes), and the chemical composition of the steel. The contents of carbon, manganese, phosphorus, and especially silicon in the steel have a significant effect on the structure of the zinc coating that is formed. As the content of silicon in the steel increases, the thickness of the zinc coating (especially the eta (η) phase) increases and the iron content of the zinc phases also tends to increase. The thickness of the zinc coating can be controlled by changing the dipping time. It is not possible to achieve an exact thickness of the zinc coating by controlling the dipping time if the content of silicon in the steel is not appropriate (see Chapter 2.1.2) for the thickness of the zinc coating that is formed.[4,5]

---

[1] Yeomans, S.R. (1993). Coated Steel Reinforcement in Concrete Part 1.
[2] Yeomans, S.R. (1994). A Conceptual Model for the Corrosion of Galvanized Reinforcement in Concrete.
[3] Yeomans, S.R. (2004). Galvanizing of Steel Reinforcement for Use in Building and Construction.
[4] Yeomans, S.R. (2004). Galvanizing of Steel Reinforcement for Use in Building and Construction.
[5] Galvanizers' Association of Australia (1999). After-Fabrication Hot Dip Galvanizing.

(η) Eta phase 99.97% Zn, 0.03% Fe, Average hardness 70 DNP	
(ζ) Zeta phase 94.2-93.3% Zn, 5.8-6.7% Fe, Average hardness 180 DNP	
(δ) Delta phase 93-89% Zn, 7-11% Fe, Average hardness 245 DNP	
(γ) Gamma phase 79-72% Zn, 21-28% Fe, Average hardness 350 DNP	
Steel, Average hardness 160 DNP	
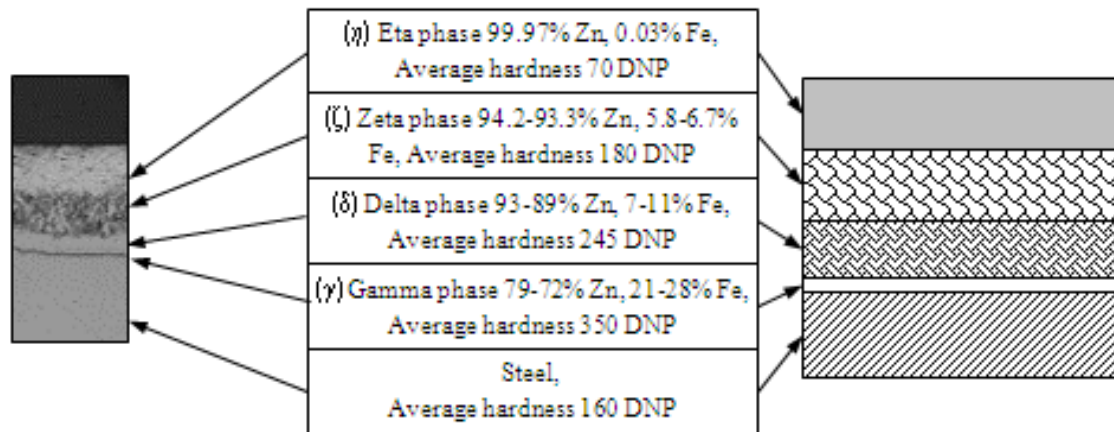
Fig. 1.   Cross-section of typical hot-dip galvanised zinc coating with relative proportions of different phases.

Depending on the manufacturing process and the chemical composition of the steel, the zinc coating does not necessarily always include the above-mentioned phases. In some cases the zinc coating may consist of only one phase. The variation in the microstructure of the zinc coating does not have much significance for corrosion resistance; the most important property regarding corrosion in protection is the thickness of the zinc coating[1] and, especially, the proportion of the eta (η) phase in the total thickness. Furthermore[2], the thickness of the eta (η) phase should be at least 10 μm and the total thickness 60-100 μm. The zinc coating can be homogeneous and uniform.

2.1.1   Thickness and formation of zinc coating

The thicker the zinc coating of the reinforcement bar is, the longer the protective effect of the zinc coating lasts. However, increasing the thickness of the zinc coating also creates problems by reducing the bond between the reinforcement bar and the concrete[3]. The thicker the coating is, the more easily the zinc coating cracks and spalls. A zinc coating thickness of approximately 100-150 μm and, especially, a high proportion of the tough eta (η) phase substantially improves the bending properties. Furthermore[4], a limit of 200 μm is often recommended as an absolute maximum for the thickness of the zinc coating. Additionally, the thickness of the eta (η) phase should be considered. A zinc coating with no eta (η) phase at all offers notably weaker corrosion protection in concrete than a zinc coating with the eta (η) phase[5]. The adhesion of the zinc coating can be determined, for instance, by causing the coating to deteriorate with a stout knife (by cutting, prying, scraping, or notching) or by using the so-called applied hammer test to an exactly specified part of the rib (rebound pendulum with impact series).[6] Very thick layers also change the profile of the reinforcement bar and thus reduce the bond with the concrete[7]. However, a chemical bond is not expected to be significant,

---

[1] Yeomans, S.R. (2004). Galvanized Steel in Reinforced Concrete.
[2] Andrade, C. et al. (1992). Protection Systems for Reinforcement.
[3] Andrade, C. et al. (1995). Coating Protection for Reinforcement.
[4] Andrade, C. et al. (1992). Protection Systems for Reinforcement.
[5] Maahn, E., Sorensen, B. (1996). Influence of Microstructure on the Corrosion Properties of Hot-dip Galvanized Reinforcement in Concrete.
[6] ASTM A-153-82 (1987). Standard Specification for Zinc Coating (Hot-Dip) on Iron and Steel Hardware.
[7] Andrade, C. et al. (1995). Coating Protection for Reinforcement.

depending predominantly on the thickness of the eta (η) phase[1]. The primary factor to minimise fractures and lamels in bending would be a uniform and relatively thin layer in which the proportion of the tough eta (η) phase would also be high[2]. In the case of bending the bond between the steel and the zinc coating is a secondary factor.

2.1.2   Factors influencing the thickness and formation of zinc coating

The factors influencing the thickness, the formation of the phases, and the formation of the zinc coating are primarily the bath temperature, dipping time, cooling rate, and steel properties, especially the content of silicon in the steel. The process is complicated. With a normal temperature area between 440 °C and 470 °C, the speed of the steel-zinc reaction does not change remarkably and it is possible to achieve all the phases. The shape and the thickness of the galvanised piece have a great influence on the dipping time. The dipping time of pieces that are difficult to handle (for instance massive structural members) can be as much as ten minutes. If a reinforcement bar lifted from the zinc bath cools slowly, i.e. in air, the eta (η) phase may yet react with the steel and transform to zeta (ζ) phase. However, the microstructure can be varied; it depends upon the cooling rate[3]. The minimum thickness of the zinc layer is determined by the cross-sectional area of the reinforcement bar. The thicker the reinforcement bar is, the thicker the zinc coating, which is due to the heating time of the steel. Furthermore, the surface roughness of the steel reinforcement bars as a result of surface hardening influences the thickness of the zinc coating. As the roughness increases, the thickness of the zinc coating increases. One reason for this is that a rough steel surface as obtained by grit blasting, course grinding etc., prior to pickling gives a thicker coating than a surface that is obtained by pickling alone[4]. [5,6]

The chemical composition of the reinforcement bar has an influence on the formation of the zinc coating. Most grades of reinforcing steels can be galvanised, but reactive components of steel such as silicon (Si) and phosphorus (P) can influence the quality of hot-dip galvanisation. The interaction of zinc, iron, and silicon plays a significant role in achieving galvanisation circumstances such that molten zinc would react continuously at the same velocity as steel, despite the growing zinc layer. The silicon content in the steel should be approximately 0.12-0.20%. In that case it is possible to achieve the normal layer thickness (app. 50-300 μm[7]) with all zinc phases[8]. As the silicon content in the steel is 0.04-0.12%, the thickness of the zinc coating increases significantly; this depends on the dipping time. This phenomenon is called the Sandelin effect[9] (Fig. 2). The reactivity of zinc and steel is also high with a silicon content in the steel above approximately 0.25%. In that case, the alloyed layers can be significantly thicker and the eta (η) phase may be missing totally[10]. The phosphorus content in the steel increases

[1] Yeomans, S.R. (2004). Galvanized Steel in Reinforced Concrete.
[2] Yeomans, S.R. (1998). Corrosion of the Zinc Alloy Coating in Galvanized Reinforced Concrete.
[3] Marder, A.R. (2000). The metallurgy of zinc-coated steel.
[4] EN ISO 1461 (1999). Hot dip galvanized coatings on fabricated iron and steel articles – Specifications and test methods.
[5] Andrade, C. et al. (1995). Coating Protection for Reinforcement.
[6] Yeomans, S.R. (2004). Galvanized Steel in Reinforced Concrete.
[7] Andrade, C. et al. (1995). Coating Protection for Reinforcement.
[8] Porter, F. (1991). Zinc Handbook, Properties, Processing and Use in Design.
[9] Foct, J. et al. (1993). How does Silicon lead the Kinetics of the Galvanizing Reaction to lose its solid-solid Character.
[10] Andrade, C. et al. (1995). Coating Protection for Reinforcement.

the growth rate of the alloyed layers. It reduces the formation of the delta (δ) phase and increases the formation of the zeta (ζ) and eta (η) phases, whereas the gamma (γ) phase becomes discontinuous[1].

According to an ASTM standard[2], steel that is going to be hot-dip galvanised should be chemically suitable for metal coatings complying with the following requirements: carbon below 0.25 per cent, silicon below 0.04 per cent or between 0.15 and 0.22 per cent, phosphorus below 0.04 per cent, and manganese below 1.3 per cent.
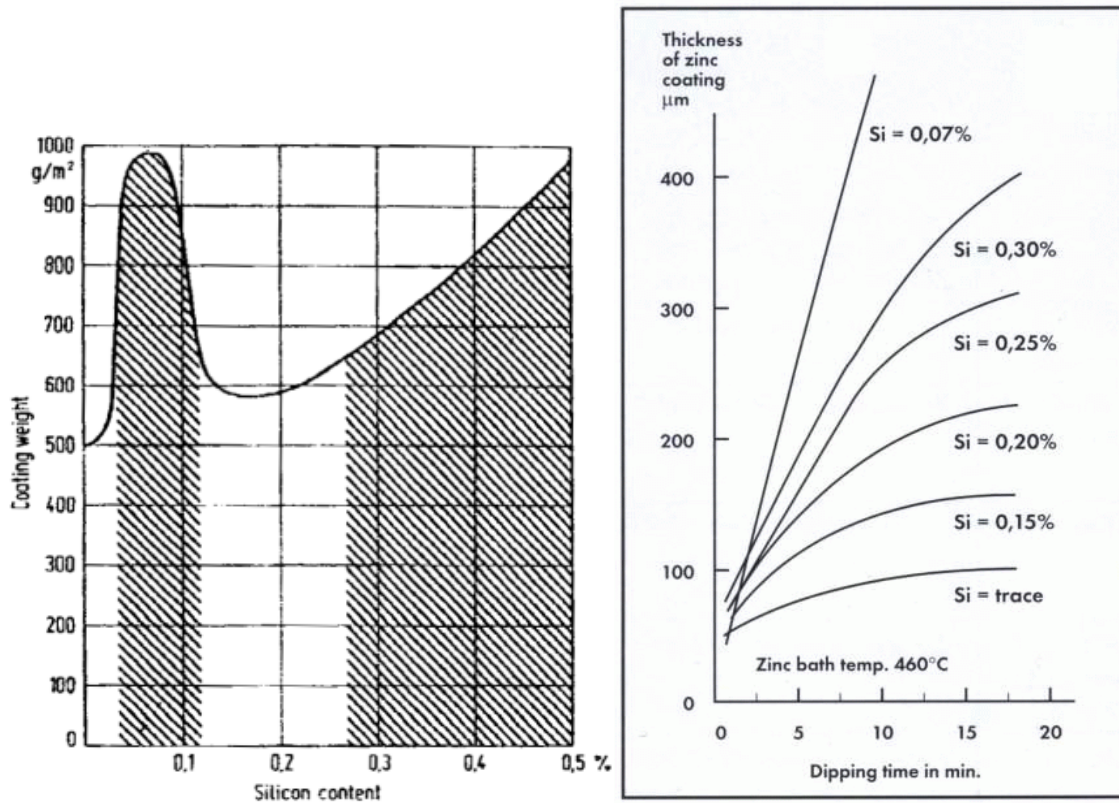
Fig. 2.   Left: Effect of silicon of steel on zinc coating weight. Right: Relationship between dipping time and thickness of zinc coating in steels with different contents of silicon.

Aluminium is probably the most important alloying element added to the hot-dip galvanising bath, with different levels required in order to produce different properties in the bath[3]. The standard practice involves the use of about 0.15 to 0.19% of aluminium. With low Al additions (galvanised < 1%) the inhibition layer may break down. The outbursts which nucleate at the substrate grain boundaries are shown in Fig. 3[4,5].

The addition of nickel to the zinc bath reduces the thicknesses of the alloyed layers, but keeps the eta (η) phase[6]. With the addition of nickel to the zinc bath, the significance of

[1] Porter, F. (1991). Zinc Handbook, Properties, Processing and Use in Design.
[2] ASTM A385 (2003). Standard Practice for Providing High Quality Zinc Coatings.
[3] Marder, A.R. (2000). The Metallurgy of Zinc-coated Steel.
[4] Hisamatsu, Y. (1989). Science and Technology of Zinc and Zinc Alloy Coated Sheet Steel.
[5] Nishimoto, A. et al. (1986). Effects of Surface Microstructure and Chemical Composition of Steels on Formation of Fe-Zn Compounds during continuous Galvanizing.
[6] Alonso, C. et al. (2000). The Addition of Ni to Improve the Corrosion Resistance of Galvanized Reinforcement.

the content of silicon in the steel and the length of the steel dipping time for the thickness of the zinc coating decreases. The Sandelin peak smoothens linearly with a nickel content in the zinc bath of 0.1% to a silicon content in the steel of 0.2% (Fig. 4).[1,2] Nickel makes the alloy layers thinner, but does not reduce the proportion of the eta (η) phase[3]. The analysis of the silicon content of the cast steel only gives an indication of the amount of free silicon in the reaction at the surface of the steel reinforcement bar. The positive effect of the addition of nickel disappears with a nickel content in the zinc bath of 0.2%. In the author's opinion, the essential factor in the addition of nickel to the zinc bath is the better zinc coating quality rather than the lower zinc coating thickness because of its mechanical and durability properties. The effect of the phosphorus content in steel with nickel-rich zinc has been little studied in the literature.
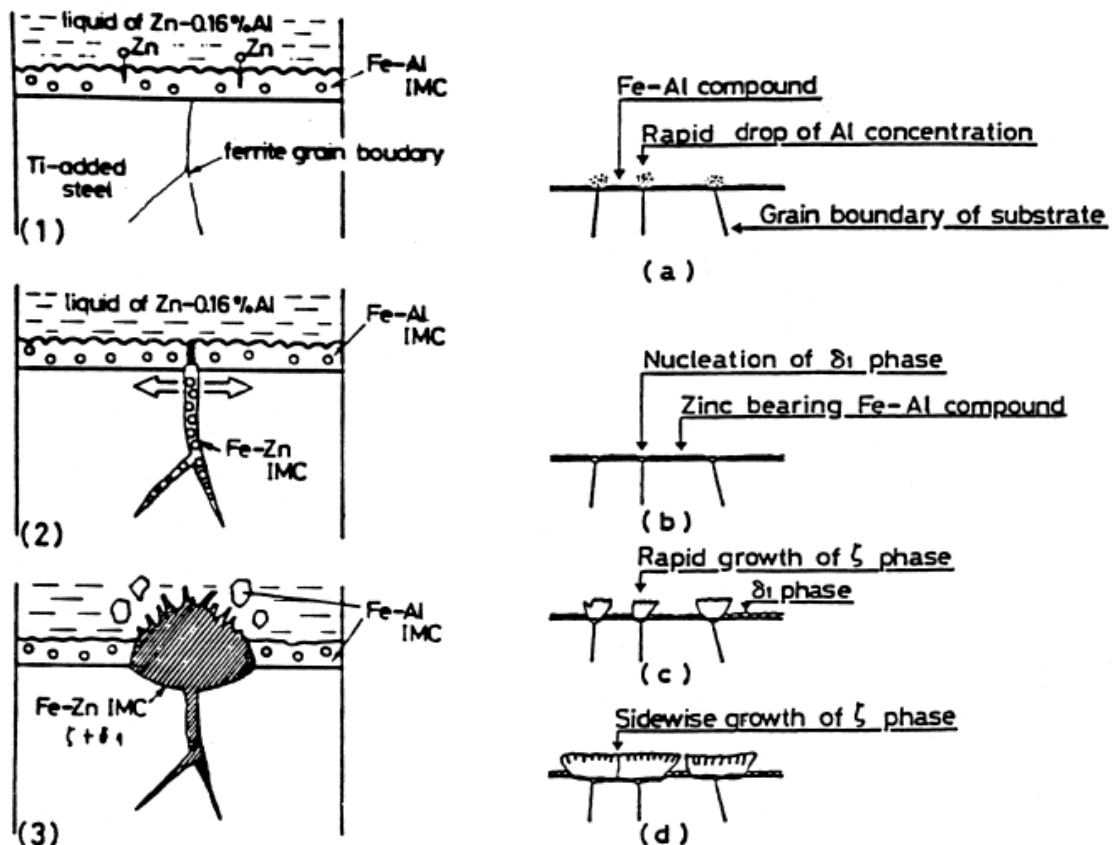
Fig. 3.   Left: Schematic diagram showing the Fe-Zn outburst growth behaviour. Right: Schematic diagram of the formation of Fe-Zn phase growth at substrate grain boundaries.

[1] Reumont, G. et al. (1998). Thermodynamic study of the galvanizing process in a Zn–0.1%Ni bath.

[2] Notowidjojo, B.D. et al. (1989). Possible Source of Dross Formation in Zinc-0.1% Nickel Galvanizing Process.

[3] Alonso, C. et al. (2000). The Addition of Ni to Improve the Corrosion Resistance of Galvanized Reinforcement.
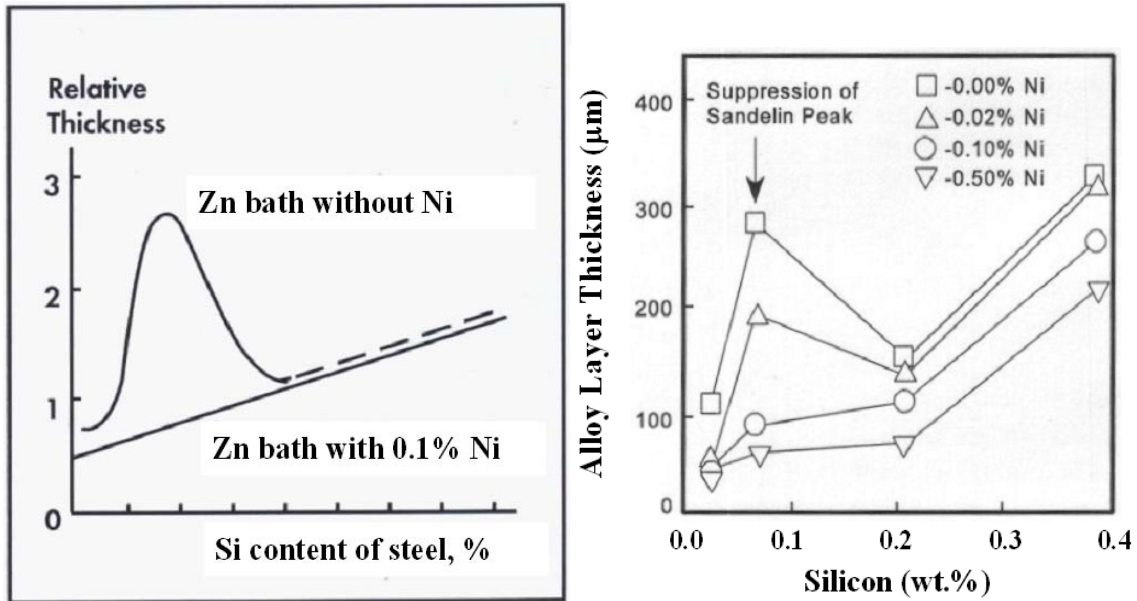
Fig. 4.   Effect of nickel in zinc bath on zinc coating thickness.

The silicon equivalent, Si_e, which is used with the content of the silicon-zinc coating thickness curves (position on the Sandelin curve), can be determined with Equation (1)[1]:

$$Si_e = Si \text{ -\%} + 2.5 \times P \text{ -\%}, \qquad\qquad (1)$$

where Si_e is the silicon equivalent of the steel reinforcement bar [%],
                    Si -%   is the silicon content of the steel reinforcement bar [%], and
                    P -%   is the phosphorus content of the steel reinforcement bar [%].

When nickel is not added to the zinc bath, the silicon equivalent is stated as 0.25% for structural steel. For instance, with Si equal to 0.17% and P equal to 0.03%, Si_e is equal to 0.25%, which is in the acceptable area (see Fig. 2). It should be noted that usually chemical components are within some range (for instance ± 0.05%). This should be taken into account when choosing the chemical components of the steel. An increase in the nickel content or the preheating of steel reinforcement bars (approximately 400 ºC) can make it possible to use higher silicon and phosphorus contents in the steel. The same applies for the situation where steel reinforcement bars are not required to be bent after hot-dip galvanising. In that case, the negative effect of the thicker zinc coating in bonding that is possibly achieved has to be taken into account separately.[2]

2.2   Protection mechanisms of zinc coating

Zinc is an amphoteric metal and reacts with both acids and strong alkalis. The zinc reaction is most intense with pH values below 6 or over 13. With pH values 6-13 the corrosion of zinc is slow as the corrosion products that form passivate the surface of the zinc. Zinc protects a steel reinforcement bar against corrosion in two ways. The zinc coating acts as physical protection by preventing aggressive materials from penetrating into the steel surface. In order to have a protective action, a durable passive layer should be formed in the steel surface. If the passive layer does not form, the zinc coating corrodes quickly. In that case the duration of the protective action of the zinc coating

---

[1] Porter, F. (1991). Zinc Handbook, Properties, Processing and Use in Design.
[2] Porter, F. (1991). Zinc Handbook, Properties, Processing and Use in Design.

depends on the thickness and structure of the zinc coating. If the zinc coating has deteriorated as a result of non-uniform corrosion, differences in the thicknesses of the original coating, or porosity to such a degree that the coating is completely lost from small areas of the bar surface, the remaining zinc cathodically protects the uncoated spots as the rate of corrosion of the zinc increases. In cathodic protection (Fig. 5) zinc compounds dissolve from the zinc coating and migrate to the cathode (uncoated steel area), where they deposit and protect the steel. At first steel corrodes in the damaged spot but gradually light grey spots occur which cover the damaged area. The thickness of the zinc coating and conductivity of the electrolyte have an effect on the size of the damaged areas that the zinc can protect cathodically. It has been estimated[1] that a zinc layer can protect and repair cathodically local cracks in the zinc coating of steel reinforcement bars that are up to 3 mm wide.
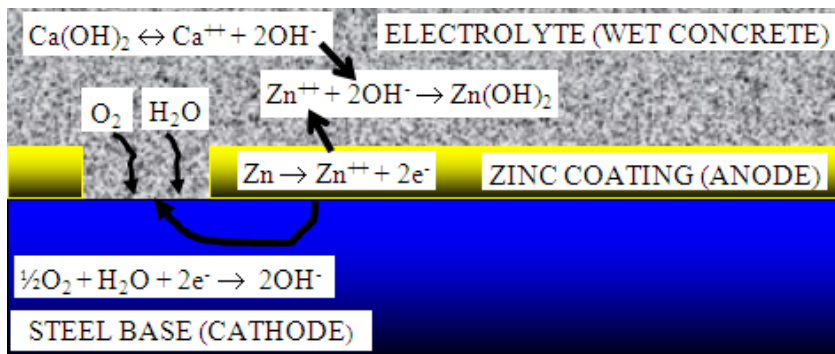
Fig. 5.   *Cathodic protection of zinc coating in carbonated concrete.*

Reaction equations in cathodic protection are presented in Fig. 5. In some cases zinc does not provide cathodic protection in chloride-contaminated concrete[2]. In that case strong pitting corrosion takes place and the small cathode changes to a small anode related to a large cathode. The activity of the cathodic protection depends on several factors, not least the conductivity of the concrete electrolyte. In pitting corrosion, the rate of corrosion of galvanised steel is lower than with ordinary steel. This is caused by the zinc coating surrounded the pit, which is a poor cathode. Thus, it slows the effect of the autocatalytic mechanism for ordinary steel. On the other hand, in concrete containing chloride no cathodic protection was observed[3]. In that case, after the local corrosion of the zinc, strong pitting corrosion took place. In general, when a zinc coating is passive, it cannot offer active protection for steel and the rate of corrosion does not decrease in unprotected areas. It can be assumed that after the full dissolution of a zinc coating the chloride content in the concrete is much higher than the threshold value for ordinary steel. In that case the rate of corrosion for ordinary steel is very severe.

Yeomans[4] has concluded that cutting surfaces ought to be patched. Cut surfaces and wider cracks in hot-dip galvanised reinforcement bars form a substantial cathode area. Thus, it is reasonable to patch these by painting them or with spray galvanisation. In the case of copious electrolyte[5], for instance in sea water, the gap in the zinc coating can

[1] Andrade, C. et al. (1992). Protection Systems for Reinforcement.
[2] Andrade, C. et al. (1995). Coating Protection for Reinforcement.
[3] Nürnberger, U. (2000). Supplementary Corrosion Protection of Reinforcing Steel.
[4] Yeomans, S.R. (1987). Galvanized Steel Reinforcement in Concrete.
[5] Porter, F. (1991). Zinc Handbook, Properties, Processing and Use in Design.

theoretically even be 5-10 mm. Porter[1] specifies that in the atmosphere the fully protected gap may be 1 μm or less if there is little deposited moisture and if the gap is pure and hence of low conductivity. The rate of corrosion of zinc in sacrificial protection is proportional to the ratio of the zinc and the uncoated steel area, and the corrosion current per unit of zinc area, which in turn is related to the electrical conductivity of the electrolyte[2]. The deciding factor in corrosion is not so much the quantity of the potential difference as the electrical conductivity of the electrolyte[3].

2.2.1   The formation of the passive layer of the galvanised reinforcement bar

The passive layer of the galvanised reinforcement bar can be found before concreting if the bar is chromated in a chromate bath or oxidation of the galvanised reinforcement bar is adequate. Usually, galvanised products are chromated to avoid the formation of white rust and the evolution of hydrogen between the zinc and the cement matrix, which may reduce the bond of the bar in the concrete. The corrosion resistance of galvanised reinforcement bars can be increased with chromating by lengthening the initiation time to active corrosion.

Chromating can be performed in two ways. Chromates of either concrete or pore water generate the formation of a passive layer or bars can be chromated in a water chromate bath (minimum 32 °C). The latter approach is suitable when the chromate content is low and it is not desired to add chromates to the concrete mix.[4] Nowadays the use of chromates is not suitable, for health reasons. However, it is still in use, for instance in South Africa[5].

The thickness and protection properties of the zinc-iron layers depend on the composition of the chromate solution used, its pH value, the temperature, the quality of the coating, and the state of the surface. On the basis of the ASTM A767 standard,[6] zinc-coated steel bars should be chromated. Reinforcement bars can be chromated immediately after galvanising by dipping the bars into a solution with a temperature of at least 32 °C for a minimum of 20 seconds. The temperature of the bars immediately after galvanising is about 450-470 ºC. However, bars are usually cooled before chromating treatment. A suitable solution is a water solution of 0.2% sodium dichromate (anion, $Na_2Cr_2O_7$) or a minimum of 0.2% chromic acid (CrO_3). If the bars are at an ambient temperature processing is the same as described, except that a 0.5-1.0% concentration of sulphuric acid (H_2SO_4) has to be added as an activator of the chromate solution. In this case there are no requirements for the temperature of the solution[7]. A zinc chromate film ($ZnCrO_4$) is formed on the surface of the zinc-coated steel bar when galvanised reinforcement bars are chromated after a zinc bath[8].

In fresh concrete chromate ions are oxidative inhibitors which are themselves being reduced. As the chromate ions are reduced, hydrogen ions are not reduced to hydrogen

---

[1] Porter, F. (1991). Zinc Handbook, Properties, Processing and Use in Design.
[2] Porter, F. (1991). Zinc Handbook, Properties, Processing and Use in Design.
[3] Porter, F. (1991). Zinc Handbook, Properties, Processing and Use in Design.
[4] Andrade, C. et al. (1992). Protection Systems for Reinforcement.
[5] http://www.hdgasa.org.za/ (12.04.2009).
[6] ASTM A767 / A767M-00b (2000). Standard Specification for Zinc-Coated (Galvanized) Steel Bars for Concrete Reinforcement.
[7] Andrade, C. et al. (1992). Protection Systems for Reinforcement.
[8] Yeomans, S.R. (1994). Coated Steel Reinforcement in Concrete Part 2.

gas. Thus, hydrogen gas is not formed. A sodium chromate content (cation, Na_2CrO_4) of 70 ppm in the concrete mix effectively prohibits the formation of hydrogen gas on the surface of the zinc-coated steel bar[1]. If there are chromates in the cement or they are added to the pore water, a passive film consisting of zinc chromate ($ZnCrO_4$) and chromic oxide (Cr_2O_3) is formed[2]. If the chromate content is too low the evolution of hydrogen may take place. In that case[3] the inadequate passive layer that forms is a solution of zinc chromate ($ZnCrO_4$), chromic oxide (Cr_2O_3), and calcium hydroxozincate (Ca (Zn (OH) $_3$)$_2$ · $2H_2O$). However, chromating or oxidation of the galvanised reinforcement bar may have a positive effect on passivation if the chromate content of the cement is too low.

Treadaway concluded that chromating substantially increased corrosion durability in chloride attacks[4]. Short et al. concluded that chromating essentially increased the corrosion resistance of the surface of a zinc coating[5]. Furthermore, chromating increases the bond between zinc-coated steel bars and concrete, which is most probably the result of the passivating effect of the reactions that generate hydrogen[6]. In that case, the bond to the concrete can be even better than with an ordinary steel bar[7].

If the galvanised reinforcement bar is not chromated, the storage conditions, chromate content, pH value, and chloride content of the concrete mix have an effect on the composition and structure of the passive layer. The formation of the passive layer has to be formed in the presence of the aggressive ions and the protective effect is weak if the concrete mix includes chlorides. In that case with high pH value, it is likely a lower chloride content will be sufficient to initiate the corrosion. However, oxidation of the galvanised reinforcement bar may have a positive effect on passivation if chlorides are added to the concrete mix. When the galvanised coating first comes into contact with fresh concrete and is initially passivated, about 10 μm of zinc is dissolved from the eta (η) phase of the coating. The coating remains in this condition for extended periods of time, provided that the conditions in the concrete do not change significantly. In such circumstances, very little further metal loss will occur until the zinc is depassivated and active corrosion commences.[8,9,10]

The zinc coating reacts with the pore solution of the alkaline concrete. In fresh concrete the galvanised coating first dissolves quite rapidly. Dissoluted zinc corrosion products form a stable protecting passive layer. The further corrosion of the zinc is reduced to a very low rate. If the pH value of the pore solution of the concrete is below 13.2 for the first few hours after casting, a protective passive layer is formed on the surface of the zinc coating. When the pH value of the pore solution is from 12.2 ± 0.1 to 13.2 ± 0.1 this passive layer is thin and a tight layer of calcium hydroxozincate (CaHZn) forms on the surface of the zinc coating. An increase in the pH value of the pore solution of the

---

[1] Corderoy, D.J.H., Herzog, H. (1980). Passivation of Galvanized Reinforcement by Inhibitor Anions.
[2] Yeomans, S.R. (1994). Coated Steel Reinforcement in Concrete Part 2.
[3] Corderoy, D.J.H., Herzog, H. (1980). Passivation of Galvanized Reinforcement by Inhibitor Anions.
[4] Treadaway, K.W.J. et al. (1980). Durability of Galvanized Steel in Concrete.
[5] Short, N.R. et al. (1994). Corrosion Behaviour of Zinc Alloy Coated Steel in Hardened Cement Pastes.
[6] Sarja, A. et al. (1984). Zinc-coated Concrete Reinforcement.
[7] Andrade, C. et al. (1992). Protection Systems for Reinforcement.
[8] Andrade, C. et al. (1995). Coating Protection for Reinforcement.
[9] Yeomans, S.R. (1998). Corrosion of the Zinc Alloy Coating in Galvanized Reinforced Concrete.
[10] Yeomans, S.R. (2004). Galvanizing of Steel Reinforcement for Use in Building and Construction.

concrete after the formation of the passive layer does not cause deterioration of a passive layer that has already formed.[1,2]

The dissolution of zinc decreases significantly as the calcium hydroxozincate layer passivates the zinc coating. If the thickness is not homogeneous, the coating must have sufficient eta (η) phase to avoid the formation of the passivating layer on the alloyed layers. Above the threshold value[3] at about pH equal to 13.2 ± 0.1 during the few first hours after casting the zinc corrosion products (ZnO, $Zn(OH)_2$) are large crystals, which are not able to effectively protect the zinc layer. In that case the protective passive layer does not form onto the surface of the zinc and the zinc coating dissolves quickly in an active state. The formation of zinc oxide and zincates and the simultaneous evolution of hydrogen reduce the adhesive bond at an early stage. Furthermore, the formation of zinc oxide and zincates delays the setting and reduces the early strength of the concrete close to the bar. This could delay the stripping of the formwork by several days.

Andrade et al.[4] concluded that through further reactions the zincates disappear, evidently binding to the hydration products. Then the strength of the concrete close to the coating surface increases. Therefore the bond strength is time-dependent, increasing with time. At the end, the setting of the zincates in the concrete might result in an even stronger bond than with ungalvanised bars.

The reaction of zinc salts forms calcium hydroxozincate Ca (Zn (OH) $_3)_2 \cdot 2H_2O$, which covers the zinc surface even after a longer period of exposure. Thus, the corrosion resistance of galvanised steel depends significantly on the alkalinity of the pore solution of the concrete, especially when the bars are not chromated or the fresh concrete does not include chromates. The alkalinity of the pore solution depends on the chemical composition of the cement. The composition of the cement has the following effects on the corrosion resistance of the bar:[5]

− as the amount of water-soluble alkalis increases, the pH value of the pore solution also increases. In this case the zinc coating dissolves more quickly;
− as the SO_3 content increases, the solubility of alkalis (Na_2O, K_2O) in the pore water decreases. In this case the zinc coating dissolves more slowly;
− as the K_2O/Na_2O molar ratio (water-soluble K_2O and water-soluble Na_2O) increases, the zinc coating dissolves more quickly.

2.2.2 The corrosion resistance of galvanised steel in fresh concrete

The corrosion resistance of steel is mainly based on the passivation phenomenon, in which a tight oxide or hydroxide layer is formed on the surface of the steel. The passive layer may almost prevent the dissolution of the metal, in which case the corrosion current decreases substantially. The structure of the passive layer can be either crystalline or amorphous (non-crystalline). Amorphous structures have a random orientation, whereas crystalline structures form a highly ordered repeating pattern. In the reaction of fresh concrete and zinc the most important phases are the reaction of the

---

[1] Andrade, C. et al. (1992). Protection Systems for Reinforcement.
[2] Yeomans, S.R. (2004). Galvanized Steel in Reinforced Concrete.
[3] Yeomans, S.R. (2004). Galvanized Steel in Reinforced Concrete.
[4] Andrade, C. et al. (1992). Protection Systems for Reinforcement.
[5] Proverbio, E. et al. (1998). Long Term Exposure Tests on Galvanized Steel in Different Concrete Types.

zinc and calcium hydroxide, the passivation of the zinc surfaces, and the evolution of hydrogen.

The chemical equations of the corrosion of zinc in strongly alkaline (App. 13.2-14) concrete are as follows:

Anode reaction $\quad$ $Zn\,(s) + 4OH^- \rightarrow Zn\,(OH)_4^{2-} + 2e^-$, $\qquad$ (2)

Cathode reaction $\quad$ $2H_2O + 2e^- \rightarrow H_2\,(g)\uparrow + 2OH^-$, $\qquad$ (3)

Total reaction $\quad$ $Zn\,(s) + 2OH^- + 2H_2O \rightarrow Zn\,(OH)_4^{2-} + H_2\,(g)\uparrow[1]$. (4)
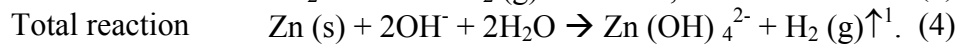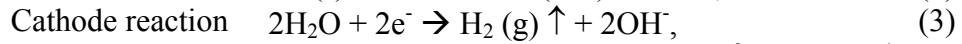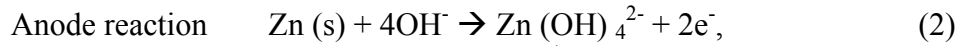
Zinc is immediately converted into calcium hydroxozincate[2], which forms a tight barrier layer on the zinc surface:

$$2Zn + Ca\,(OH)_2 + 6H_2O \rightarrow Ca\,[Zn\,(OH)_3]_2 \cdot 2H_2O + 2H_2\uparrow[3]. \qquad (5)$$
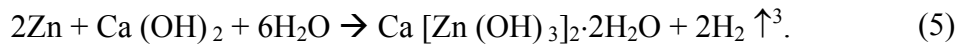
Furthermore, the formation of dissolved zincate and liberation of hydrogen gas in concrete is possible:

$$Zn + 2OH^- \rightarrow ZnO_2^{2-} + H_2\uparrow[4]. \qquad (6)$$

Zincate further reacts with water and forms zinc hydroxide, which is slightly soluble in water:

$$ZnO_2^{2-} + 2\,H_2O \rightarrow Zn\,(OH)_2 + 2OH^-. \qquad (7)$$

The type and stability of the reaction products that form in the reaction of corrosion of zinc depend on the pH value and the composition of the fresh concrete. The pH value of concrete (12-14) is high right after curing, depending on the composition and hydration rate of the cement. The alkalinity depends on freely soluble potassium and sodium salts and calcium hydroxide forming in the hydration of the cement. For a short period after mixing the cement and water the pore water of the concrete is saturated with $Ca\,(OH)_2$ (pH 12.6)[5]. After a few days the $Ca\,(OH)_2$ content decreases but the other substances, such as NaOH and KOH, maintain the high pH value[6]. In these solutions of fresh concrete the concentration of Ca^{2+} - ions decreases as the pH increases[7]. With a slightly lower pH, which is typical in the early stages of the hydration, the solution becomes

---

[1] Vinka, T.-G., Becker, M. (1998). Corrosion of Galvanised Steel in Concrete.
[2] Yeomans, S.R. (1987). Galvanized Steel Reinforcement in Concrete.
[3] Andrade, C. et al. (1995). Coating Protection for Reinforcement.
[4] Sarja, A. et al. (1984). Zinc-coated Concrete Reinforcement.
[5] Alonso, C. et al. (2000). The Addition of Ni to Improve the Corrosion Resistance of Galvanized Reinforcement.
[6] Andrade. C. et al. (1983). Relation Between the Alkali Content of Cements and the Corrosion Rates of the Galvanized Reinforcements.
[7] Alonso, C. et al. (2000). The Addition of Ni to Improve the Corrosion Resistance of Galvanized Reinforcement.

saturated with Ca^{2+} - ions. The presence of calcium ions is essential for developing a passive zinc layer in alkaline material[1].

In the later stages of hydration silica cement consumes calcium hydroxide, in which case the pH of the hardened concrete decreases. Additionally, blast-furnace slag and fly ash cement have a rather lower influence but one of the same kind. However, Andersson et al.[2] concluded that the pH (13.4) of a pore solution of fly ash concrete after ten months of exposure was the same as with Portland cement concrete, although the calcium content was only one sixth. When the pH value decreases after curing zinc is transferred to the passive area, but as a result of the reduced calcium hydroxide content the formation of the passive layer is endangered. However, the lower pH value reduces the evolution of hydrogen. The low water-to-binder ratio also shortens the period of the evolution of hydrogen[3].

Additionally, the size of the zincate crystals has a conclusive significance on the formation of the passive layer. When the pH value increases the size of the crystals also increases: above a pH value of 13.2 ± 0.1[4] corrosion products appear as single crystals which are not able to fully cover the surface. The reason for this is that at pH values above 13.2, the concentration of Ca^{2+} - ions in solution is depleted. The zinc surface does not passivate due to the lack of Ca^{2+} - ions and the zinc continues to actively corrode and may completely dissolve in a short period of time[5]. Thus, it is primary for the durability of zinc coating to lower pH value of concrete under 13.2. Alonso et al.[6] concluded that the addition of nickel to the zinc bath has a reducing effect on the zinc reactivity and evolution of hydrogen in alkaline circumstances. In that case the zincate crystals have a smaller size and thereby they can better cover and protect the zinc coating. If a passive layer of calcium hydroxozincate $Ca\,(Zn\,(OH)_3)_2 \cdot 2H_2O$ has formed, its stability does not change any more if the pH later rises[7]. However, the zinc passivation process is a complex reaction depending on several factors and it is not yet fully understood. There is contradictory information on zinc passivation in the literature. In the author's opinion, the variation between the different research results probably depends on the various cement compositions around the world.

In high-alkali cement the rate of corrosion of hot-dip galvanised reinforcement bars can be as much as over tenfold compared with the rate in low-alkali cement[8]. The rate of corrosion changes exponentially as the pH value increases from 12 to 14. Above a pH value for concrete of 13 the rate of corrosion increases significantly[9]. Andrade et al.[10] concluded that a uniform and tight passive layer forms on the surface of the galvanised

---

[1] Alonso, C. et al. (2000). The Addition of Ni to Improve the Corrosion Resistance of Galvanized Reinforcement.

[2] Andersson, K. et al. (1989). Chemical Composition of Cement Pore Solutions.

[3] Fagerlund, G. (1990), Durability of Concrete Structures, Summary Review.

[4] Andrade, C. et al. (1995). Coating Protection for Reinforcement.

[5] Andrade, et al. (2004). Electrochemical Aspects of Galvanized Reinforcement Corrosion.

[6] Alonso, C. et al. (2000). The Addition of Ni to Improve the Corrosion Resistance of Galvanized Reinforcement.

[7] Alonso, C. et al. (2000). The Addition of Ni to Improve the Corrosion Resistance of Galvanized Reinforcement.

[8] Andrade, C. et al. (1995). Coating Protection for Reinforcement.

[9] Andrade. C. et al. (1983). Relation between the Alkali Content of Cements and the Corrosion Rates of the Galvanized Reinforcements.

[10] Andrade. C. et al. (1985). Advances in the Study of the Corrosion of Galvanized Reinforcements Embedded in Concrete.

steel if the cement used is low-alkaline (App. 12.5-13.2). The reactions between the zinc and alkaline concrete end as the concrete hardens. However, the halting of the reaction does not indicate the formation of the passive layer. Additionally, the presence of chlorides in the fresh concrete interrupts the formation of the passive layer. The zinc is more unstable at higher pH values. If there is a high pH value, it is most probable that a lower chloride content will be sufficient to initiate the corrosion[1].

2.2.3   Influence of hydrogen evolution

Carbonation and detrimental substances such as water, oxygen, and chlorides propagate faster in porous concrete. However, it has been proposed that crack formation in concrete is avoided as the corrosion products of zinc are able to expand into the hydrogen pores. Several opinions on the evolution of hydrogen are expressed in the literature. Alonso et al.[2] state that the evolution of hydrogen begins shortly after the contact between the zinc and the alkaline matter. Other sources of information give pH limits $(11…13.2 \pm 0.1)$[3] below which hydrogen is not formed. Hydrogen gas is formed more easily by the reaction of a zinc-iron alloy (mainly zeta (ζ) phase) surface than with eta (η) phase. Thus, the rate of corrosion of the zinc is also higher in the absence of an eta (η) phase[4]. If the zinc surface has oxidised before concreting or hot-dip galvanised pieces are chromated[5], the reaction leading to the evolution of hydrogen is prevented and the absence of an eta (η) phase does not have any significance regarding the rate of corrosion.

Chromates act as inhibitors in concrete[6]. Corderoy et al.[7] state that the formation of hydrogen stops almost completely, as the chromate ions reduce, instead of the water. With a pH value of approximately 12.5 chromium trioxide (CrO_3) reduces as chromium oxide (Cr_2O_3). In this case a passive layer is formed that includes zinc chromate, chromium oxide, and also possibly zinc hydroxide. The reaction is not known exactly. The durability of a water-soluble chromate layer after cleansing, transport, storage, and installation exposed to rain is very uncertain. Furthermore, Yeomans[8,9] states that the durability of the chromate layer of galvanised reinforcement bars cannot be ensured for longer than some weeks or months. Because of their water-solubility and low durability, chromated bars should be used as soon as possible after chromating.

It is easy to devastate organic acids. The passivating effect of organic acids via atmospheric passivation is based on the formation of a tight salt layer on the surface of the zinc. Hydrochloric and sulphuric acid are already used in the galvanisation process. Thus, there is a basis for using these acids in the passivation of the zinc coating and preventing the evolution of hydrogen.

---

[1] Andrade, C. et al. (1995). Coating Protection for Reinforcement.
[2] Alonso, C. et al. (2000). The Addition of Ni to Improve the Corrosion Resistance of Galvanized Reinforcement.
[3] Andrade, C. et al. (1995). Coating Protection for Reinforcement.
[4] Vinka, T.-G., Becker, M. (1998). Corrosion of Galvanised Steel in Concrete.
[5] Yeomans, S.R. (1993). Coated Steel Reinforcement in Concrete.
[6] Andrade, C. et al. (1995). Coating Protection for Reinforcement.
[7] Corderoy, D.J.H., Herzog, H. (1978). Passivation of Galvanized Reinforcement by Inhibitor Anions.
[8] Yeomans, S.R. (1987). Galvanized Steel Reinforcement in Concrete.
[9] Yeomans, S.R. (1993). Coated Steel Reinforcement in Concrete.

Simultaneous corrosion and passivation in galvanised steel causes the evolution of hydrogen along the surface of the reinforcement bar. As soon as a zinc coating is subjected to contact with alkaline media, severe hydrogen evolution takes place. However, it decreases uniformly as a function of time when the CaHZn layer forms. In circumstances without chlorides the time during which hydrogen evolves is approximately 1-2 hours. In chloride-contaminated circumstances, on the other hand, despite a decrease in the pH value of capillary water, the duration of the evolution of the hydrogen may be several hours. Furthermore, the duration of the evolution of the hydrogen depends primarily on the chromium and alkali content of the cement.[1]

With suitable concrete properties the amount of hydrogen evolving and level of corrosion of zinc in fresh concrete could be reduced. This research result was also found by the author[2]. The effect of water-to-binder ratio and the strength of concrete on the hydrogen evolution can be noticed in Fig. 6. The relevant factors are, for instance, the cement type used having a low pH value, the concrete mix proportions, the use of rapid-hardening concrete, a low water-to-binder ratio, and the use of low-alkaline binders. The exact pH value does not have a direct correlation with the evolution of hydrogen and rate of corrosion because the critical pH value also depends on the composition of the cement (C_3A/C_3S, w/c, and the amount of soluble alkalis)[3]. However, the pH value has an essential significance compared to other factors.

The pH of concrete can be reduced by adding silica, fly ash, or blast furnace slag as blend components. However, when the above-mentioned blend components are used, the formation of the passive layer may abort as the amount of free calcium hydroxide decreases. Furthermore, the durability of the reinforced concrete structure may be lower.[4]

Concrete	Concrete

Steel	Steel
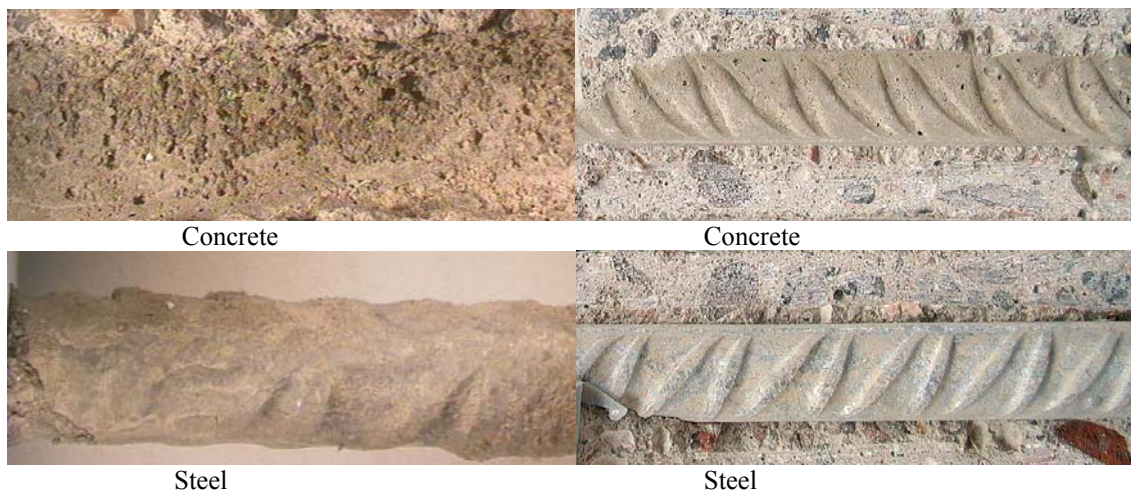
Fig. 6.   Left: Not possible to identify rib geometry and major hydrogen evolution (w/b = 0.95; f_c = 25 MPa; four weeks' passivation; sheltered from rain; weldable hot-rolled ribbed steel reinforcement bar, A500HW). Right: No degradation of rib geometry and low level of hydrogen evolution (w/c = 0.46; f_c = 45 MPa; four weeks' passivation; exposed to rain; weldable hot-rolled ribbed steel reinforcement bar, A500HW).

---

[1] Yeomans, S.R. (2004). Galvanized Steel in Reinforced Concrete.
[2] Sistonen, E. et al. (2006). Service Life and Quality Specifications for Hot-Dip Galvanised Reinforcement.
[3] Arliguie, G. (2001). Performance of Galvanized Rebar.
[4] Arliguie, G. (2001). Performance of Galvanized Rebar.

Shortening the storage time and reducing the evolution of hydrogen and the porosity caused by it can be affected by the choice of materials, so that the final result would be acceptable. Properties of the concrete such as the pH value, the amount of free calcium hydroxide, the water-to-binder ratio, compactness, ductility, binder, differences in alkalinity between different cement types, etc. can have a dominating effect on hydrogen evolution and porosity. Furthermore, the use of low-alkaline concretes and rapid-hardening cements is recommended in order to shorten the time for the zinc reaction and evolution of hydrogen. No exact limit values can be given.[1]

One significant factor in the effect of the evolution of hydrogen on the durability of galvanised reinforcement bars is the possible migration of corrosion products into the hydrogen pores. This factor has a positive effect on the corrosion of steel, but a negative effect, for instance, on frost durability and chloride resistance. Furthermore, deterioration parameters such as frost damage, chloride diffusion, and reinforcement corrosion have an interactive effect on the service life of hot-dip galvanised reinforced concrete structures contaminated by chlorides. In the author's opinion, the influence of the evolution of hydrogen can be handled as a secondary phenomenon with quality requirements and the zinc coating protected in alkaline media.

2.2.4 Zinc in hardened concrete

As a result of the alkalinity of the concrete a corrosion-protected oxide layer forms on the surface of ordinary steel. The layer disappears as a result of the carbonation of the concrete or chloride attack. The concrete cover protects both zinc and ordinary reinforcing steel from the detrimental effects of air contamination. As the concrete carbonates as a result of the action of carbon dioxide, the pH value decreases from approximately 12.5-14.0 to approximately 8.0-8.5. As the pH value of the concrete decreases below 11.5[2] the corrosion of ordinary steel becomes possible if the other conditions for corrosion to take place are fulfilled.

Zinc-coated reinforcement bars are more durable in carbonated concrete than ordinary steel reinforcement bars because zinc is passive through a much wider pH area, approximately up to a pH value of 9.5 for the concrete[3]. The corrosion of zinc continues until the concrete has almost fully carbonated to the level of the steel reinforcement bar. Poor workmanship resulting in variable concrete quality and a possible reduced cover thickness of concrete are less dangerous with zinc-coated reinforcement bars than ordinary steel ones[4]. On the other hand, if the passivation process of the zinc coating fails, the porous layer formed by the hydrogen bubbles makes it possible for carbon dioxide and detrimental material to penetrate to the level of the steel reinforcement bars. In this case the active corrosion stage may be reached earlier. However, the thickness of the porous layer may be insignificant compared to the thickness of the concrete cover.

---

[1] Sistonen, E. et al. (2006). Service Life and Quality Specifications for Hot-Dip Galvanised Reinforcement.
[2] Yeomans, S.R. (1993). Coated Steel Reinforcement in Concrete.
[3] Yeomans, S.R. (1993). Coated Steel Reinforcement in Concrete.
[4] Andrade, C. et al. (1995). Coating Protection for Reinforcement.

2.3 Influence of deterioration

2.3.1 Experimental measurements

Corrosion resistance can be researched with measurements of the corrosion potential, the corrosion current, and the resistivity of the concrete. The corrosion potential (E_{corr}) and corrosion current (I_{corr}) have a correlation, but there is significant variation between different research results[1]. The same phenomenon is also found with both the correlation of the corrosion potential (E_{corr}) and the resistivity of concrete (R) and the correlation of the corrosion current (I_{corr}) and the resistivity of concrete (R). On the basis of Faraday's law and the density of zinc, the corrosion current of zinc (eta (η) phase) I_{corr} [$\mu A/cm^2$] can be converted to the rate of corrosion of zinc (eta (η) phase) v_{corr} [$\mu m/a$] as follows:

$$1 \ \mu A/cm^2 = 15.0 \ \mu m/a. \tag{8}$$

With iron-zinc alloy the conversion factor is lower than with the eta (η) phase (Equation (8)). With ordinary steel corrosion a current of $1 \ \mu A/cm^2$ corresponds to a rate of corrosion of 11.6 $\mu m/a$. The state of corrosion based on the corrosion current is shown in Table 1. The resistivity of the concrete depends, among other factors, on the moisture content and pore structure of the concrete. The resistivity of dry concrete has been measured up to $10^6 \ k\Omega cm$ and that of water-saturated concrete $10 \ k\Omega cm$. The electrolyte needed for corrosion is not present in dry concrete[2]. The values of the resistivity of concrete (R) state the moisture content of the concrete, which give conditions for possible corrosion and approximate rate of corrosion when the steel is actively corroding. The range of resistivity of the concrete and the possible state of corrosion is shown in Table 2.

Table 1. *State of corrosion based on corrosion current measured in laboratory and field conditions[3].*

Corrosion current [$\mu A/cm^2$]	Rate of corrosion of zinc coating [$\mu m/a$]	State of corrosion
< 0.1	< 1.5	Passive
0.1 – 0.5	1.5 – 7.5	Low
0.5 – 1	7.5 – 15	Moderate
> 1	> 15	High

Table 2. *The range of resistivity of the concrete and the possible state of corrosion with normal Portland and blended cement[4].*

Resistivity of concrete [$k\Omega cm$]	State of corrosion
> 100 – 200	Cannot distinguish between active and passive steel
50 – 100	Low rate of corrosion
10 – 50	Moderate to high rate of corrosion where steel is active
< 10	Resistivity is not the controlling parameter (Severe)

The reaction process between fresh concrete and reinforcement bars and the state of corrosion of steel in hardened concrete can be measured with corrosion potential. So-

---

[1] Andrade, C., Alonso, C. (2001). On-Site Measurements of Corrosion Rate of Reinforcements.
[2] Locke, C.E. (1986). Corrosion of Steel in Portland Cement Concrete: Fundamental Studies.
[3] Andrade, C., Alonso, C. (2001). On-Site Measurements of Corrosion Rate of Reinforcements.
[4] Andrade, C., Alonso, C. (2001). On-Site Measurements of Corrosion Rate of Reinforcements.

called Pourbaix diagrams[1] represent the electrochemical state of corrosion of metals in pH-potential coordinates (parts of Pourbaix diagrams are measured empirically). Metal passivation can be estimated with them.

The corrosion potential can be considered as the potential difference between the surface of the reinforcement bar (zinc in this case) and the electrolyte, expressed in mV. Because this potential cannot be measured in practice, the potential difference between a reference electrode in contact with the electrolyte and with the reinforcement bar is measured. When the electrode potential of the reference electrode is known and stable, the potential difference between the reinforcement bar and the concrete can be calculated.[2]

2.3.2   Corrosion products of galvanised reinforcement bars in concrete

There is some disagreement about the composition and inconvenience of the corrosion products of a galvanised reinforcement bar. The main corrosion product of zinc, zinc oxide (ZnO), occupies 1.5 times the volume of the original zinc[3,4]. However, the volume of zinc oxide is approximately 1/3 less[5] than the volume of the corrosion products of ordinary steel. Corrosion products are friable, loose, and powdery minerals. The products are able to migrate away from the bar and into the adjacent porous concrete matrix, where they fill small voids and micro-cracks[6,7]. In that case the local tensile stresses in the concrete are also lower and zinc corrosion products do not exactly cause the concrete cover to deteriorate. Furthermore, the strengthened concrete may form a barrier layer which decreases the penetration of detrimental material (CO_2, water, oxygen, and chlorides). Additionally, the zinc coating delays the time to cracking and the spalling forces in the concrete are smaller[8].

In practice the corrosion products formed on the surface of the steel cause major changes in the mutual noble-mindedness order of metals. Additionally, the noble-mindedness of different phases in the zinc coating can largely differ from the noble-mindedness of the original chemical element. In an alkaline material like concrete, alloyed iron-zinc layers are probably less corrosion-resistant than the eta (η) phase.[9] In moderate acid circumstances, for instance in air, the opposite is true[10].

Yeomans concluded that the zinc corrosion product in chloride-contaminated concrete is the mineral form of zinc oxide (ZnO). Zinc chloride oxygen compounds were not found. Yeomans proposed as a corrosion mechanism a partial dissolution of the galvanised coating and a plume of zinc-rich corrosion product migrating into the cement matrix. Furthermore, zinc-rich corrosion products were found in the reinforcement bar/binder matrix, as well as in the bulk matrix. As the zinc corroded, holes and tunnels were

---

[1] Pourbaix, M. (1963). Atlas of Electrochemical Equilibria in Aqueous Solutions.
[2] Camitz, G., Pettersson, K. (1989). Corrosion Protection of Steel in Concrete - Stage 1, Cathodic Corrosion Protection of Steel Reinforcement in Concrete - the Literature Review.
[3] Yeomans, S.R. (2004). Galvanized Steel in Reinforced Concrete.
[4] Porter, F. (1991). Zinc Handbook, Properties, Processing and Use in Design.
[5] Yeomans, S.R. (1993). Coated Steel Reinforcement in Concrete.
[6] Hoke, J.H. et al. (1981). Cracking of Reinforced Concrete.
[7] Yeomans, S.R. (1993). Coated Steel Reinforcement in Concrete.
[8] Yeomans, S.R. (1998), Corrosion of the Zinc Alloy Coating in Galvanized Reinforced Concrete.
[9] Alonso, C. et al. (2000). The Addition of Ni to Improve the Corrosion Resistance of Galvanized Reinforcement.
[10] Porter, F. (1991). Zinc Handbook, Properties, Processing and Use in Design.

formed in the zinc phases. Some of them filled up with a mix of hydration and corrosion products. The distance of the migration from the bar varies considerably. However, there is evidence that corrosion products can migrate as far as 0.5 mm from the bar, clearly far beyond the interfacial transition zone (ITZ) between the bar and matrix[1]. Thus, it is possible that with filled voids the corrosion products can form some kind of matrix that reduces permeability. This protective layer could both increase the bond between the steel and concrete matrix and reduce the diffusion of aggressive compounds into the zinc coating. On the other hand, the frost resistance may decrease, in the author's opinion.

Proverbio & Meloni observed that after the eta (η) phase fully dissolved and the zeta (ζ) phase started to corrode, the surface of the zinc coating was surrounded by a crystalline compound of calcium hydroxozincate (CaHZn) and zinc oxide (ZnO). When the corrosion reached the gamma (γ) phase, the corrosion products detected were iron chloride hydroxide, zinc oxide (ZnO), and hydroxide ($Zn(OH)_2$) crystals.[2]

According to Hime & Machin's studies[3], the zinc corrosion product as a result of chloride attack is a compound of zinc hydroxychloride ($Zn_5(OH)_8 Cl_2 \cdot H_2O$). This compound occupies 3.6 times the volume of the original zinc. Thus, it causes almost the same expansion as many iron corrosion products. Shimada studied the corrosion resistance of galvanised steel exposed to sea water. The rate of corrosion of the zinc coating was substantially slower compared with the rate of corrosion of ordinary steel[4]. However, the lower rate of corrosion did not prevent the cracking of the concrete cover as a result of spalling corrosion products. Thus, the benefit of the galvanising was questionable. Treadaway concluded in his research that galvanised steel reduced the spalling of the concrete cover if the chloride content is less than 0.96% of chlorides by weight of cement[5]. However, the benefit was marginal. When the chloride content reached 1.9% of chlorides by weight of cement, the zinc coating no longer influenced the intensity of the existing cracks in the concrete cover. In Treadaway's tests chlorides were added to fresh concrete.

The influence of the consistency of the concrete on the formation of zinc corrosion products has not been researched enough. The main corrosion products reported are:

- Zincite (Zinc oxide), ZnO (powdery products, cement paste, fresh concrete, carbonated concrete, and chloride-contaminated concrete);
- Zinc hydroxide (Wulfingite), $Zn(OH)_2$ (cathode reaction (after cracking), fresh concrete, carbonated concrete, and chloride-contaminated concrete);
- Zinc hydroxychloride (Simonkolleite: Zn (OH) Cl), $Zn_5(OH)_8Cl_2) \cdot H_2O$ (spalling products, chloride-contaminated concrete).[6]

---

[1] Yeomans, S.R. (1998). Corrosion of the Zinc Alloy Coating in Galvanized Reinforcement.
[2] Proverbio, E. et al. (1998). Long Term Exposure Tests on Galvanized Steel in Different Concrete Types.
[3] Hime, W.G., Machin, M. (1993). Performance Variances of Galvanized Steel in Mortar and Concrete.
[4] Shimada, H., Nishi, S. (1983). Sea Water Corrosion Attack on Concrete Blocks Embedding Zinc Galvanized Steel Rebars.
[5] Treadaway, K.W.J. (1989). Durability of Corrosion Resisting Steels in Concrete.
[6] Belaïd, F. et al. (2001). Corrosion Products of Galvanized Rebars Embedded in Chloride-Contaminated Concrete.

2.3.3   Durability of galvanised reinforcement bars in concrete

Several approximate values of the rate of corrosion of galvanised reinforcement bars in concrete have been presented[1]. The temperature, the moisture and chloride content, and the carbonisation of the concrete, among others, have a significant effect on the rate of corrosion. Zinc dissolves more quickly than ordinary steel in uncarbonated concrete, but the rate of corrosion is low, approximately 1.5 μm/a. In the same circumstances the rate of corrosion for ordinary steel[2] is approximately 1.0 μm/a. Therefore, in some circumstances the zinc coating may be fully dissolved before the carbonisation layer reaches the reinforcement bar.

The carbonation of concrete reduces the pH of the pore solution[3] to 8-8.5. The rate of corrosion of the zinc coating depends on the pH of the pore solution surrounding the galvanised reinforcement bar. The rate of corrosion of the zinc coating increases as the pH of the pore solution decreases. On the basis of laboratory tests it is approximately 3 μm/a in carbonated concrete. On the basis of the same laboratory tests, the rate of corrosion of ordinary steel is much higher[4], app. 22.5 μm/a. In some cases the rate of corrosion of the zinc coating may decrease during the carbonation of the concrete (Fig. 7, left). In principle, it is possible to study the actively corroding zinc phase and when the dissolution of the phase starts (Fig. 7, right). However, it is a requirement that the smooth thick zinc layer corrodes uniformly.
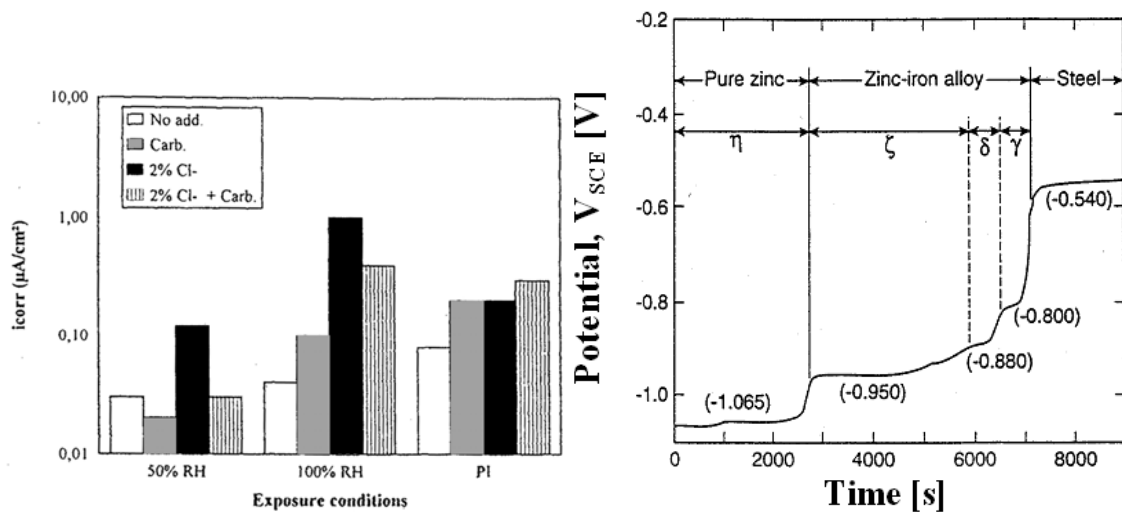
Fig. 7.   *Left: Effect of the exposure conditions (carbonation and Cl⁻ ions) on the rate of corrosion of galvanised reinforcement bars in cement mortar after one year of exposure under the same conditions (1 μA/cm² ≈ 15 μm/a, PI means partially immersed)[5]. Right: Dependence between alloy layer and corrosion potential of galvanised reinforcement bar[6].*

Research results[7] show that the rate of corrosion of galvanised steel is not substantially higher and is also lower in carbonated concrete than in alkaline concrete. Galvanised reinforcement bars are appropriate for use when the carbonisation causes corrosion in

[1] Yeomans, S.R. (2004). Galvanized Steel in Reinforced Concrete.

[2] Andrade, C. et al. (1992). Protection Systems for Reinforcement.

[3] Bentur, A. et al. (1997). Steel Corrosion in Concrete: Fundamentals and Civil Engineering Practice.

[4] Andrade, C. et al. (1992). Protection Systems for Reinforcement.

[5] Ramirez, E. et al. (1996). The Protective Efficiency of Galvanizing Against Corrosion of Steel in Mortar and in Ca (OH)₂ Saturated Solutions Containing Chlorides.

[6] Yeomans, S.R. (1993). Coated Steel Reinforcement in Concrete Part 2.

[7] Yeomans, S.R. (2004). Galvanized Steel in Reinforced Concrete.

ordinary steel. There are good results for the use of galvanised reinforcement bars in façade elements[1]. Service life properties are emphasised, along with the increased propagation time (Fig. 8). The service life of a cracked concrete hot-dip galvanised reinforcement bar can be increased if the corrosion products do not cause critical spalling forces compared to an ordinary steel reinforcement bar.[2,3]
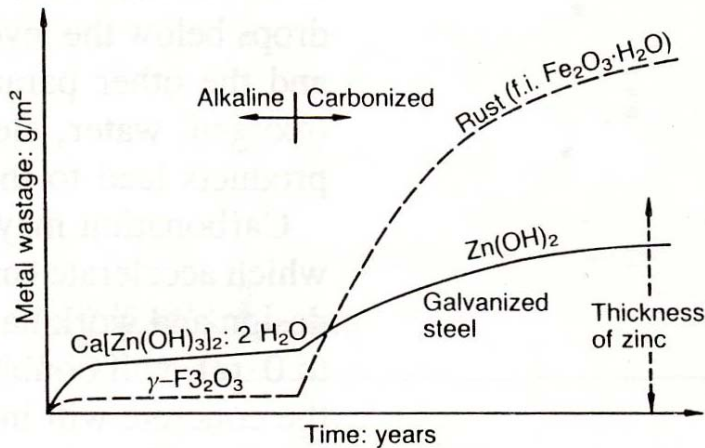
Fig. 8.   *Corrosion of ordinary and hot-dip galvanised reinforcement bars in carbonated concrete (initiation and propagation period).*

The research results on the corrosion resistance of galvanised steel in chloride-contaminated concrete are contradictory[4]. This controversy is lower in carbonated concrete. A reason for this controversy is the arrangement of an unequivocal testing procedure. For example, zinc wastage as a function of the chloride content has been tested in the laboratory with low concrete cover and a high water-to-binder ratio, which cannot be compared with real concrete structures. Furthermore, there exist some discrepancies between the test electrolyte actually generated in the concrete's pore solution and the simulated electrolyte used in the laboratory (saturated limewater)[5].

It is significant for the durability of galvanised steel whether chlorides are added to the mix or penetrate later from outside. The formation of the passive film of the zinc coating is disturbed if chlorides are added to the fresh concrete. The rate of corrosion of galvanised reinforcement bars depends very substantially on the chloride content and state of the surface of the galvanised reinforcement bar[6]. On the basis of Fig. 9, the rate of corrosion of a galvanised reinforcement bar is higher than that of an ordinary steel bar in uncarbonated cement mortar. However, the rate of corrosion of ordinary steel increases substantially with a rather low chloride content. Additionally, the rate of corrosion of galvanised reinforcement bars increases with a higher chloride content.

---

[1] Broomfield, J.P. (1997). Corrosion of Steel in Concrete.

[2] Rostam, S. (2002). Service Life Design of Concrete Structures - A Challenge to Designers as well as to Owners.

[3] Nürnberger, U. (2000). Supplementary Corrosion Protection of Reinforcing Steel.

[4] Andrade, C. et al. (1992). Protection Systems for Reinforcement.

[5] Ghosh, R. et al. (2007). Kinetics, Mechanism and Characterisation of passive Film formed on Hot Dip Galvanized Coating exposed in simulated Concrete Pore Solution.

[6] Andrade, C. et al. (1992). Protection Systems for Reinforcement.
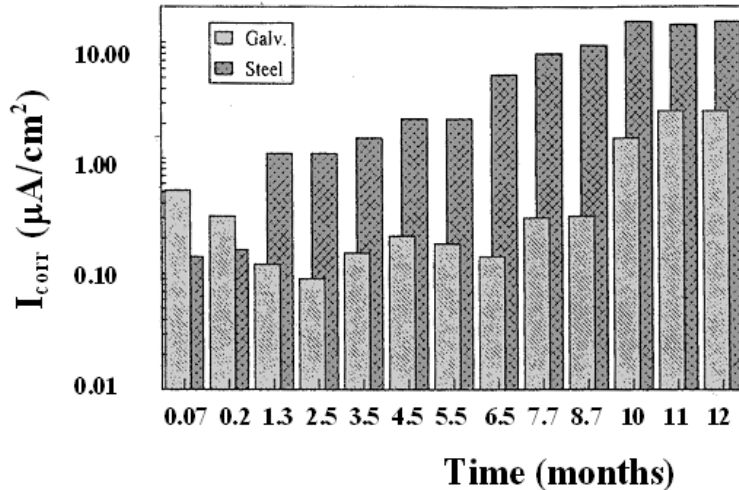
Fig. 9. *Variation in the rate of corrosion for ordinary and galvanised steel embedded in cement mortar. Specimens were partially immersed in artificial sea water and contained no chlorides[1]. (Note the rate of corrosion difference; galvanised steel: 1 $\mu A/cm^2 \approx 15$ $\mu m/a$, ordinary steel: 1 $\mu A/cm^2 \approx 12$ $\mu m/a$.)*

On the basis of the research results achieved by Treadaway,[2] the rate of corrosion of galvanised reinforcement bars as a function of the chloride content is presented in Fig. 10. The rates of corrosion are calculated from mass loss measurements. Those measurements were made at exposures of 1-9.5 years. Some specimens spalled before the mass loss measurements. The calculated rates of corrosion represent mean values. Thus, it was not noticed whether specimens were cracked or uncracked. The chlorides were added to fresh concrete during casting, which has an effect on the research results. On the basis of Treadaway's research results, there was a significant variation in the rate of the corrosion values of galvanised reinforcement bars. Other research results[3,4] support the rate of corrosion values presented by Treadaway. It should be noticed that pitting corrosion in chloride-contaminated concrete may be a multiple in comparison with the mean rate of corrosion.

---

[1] Ramirez, E. et al. (1996). The Protective Efficiency of Galvanizing Against Corrosion of Steel in Mortar and in Ca(OH)$_2$ Saturated Solutions Containing Chlorides.

[2] Treadaway, K.W.J. (1989). Durability of Corrosion Resisting Steels in Concrete.

[3] Bentur, A. et al. (1997). Steel Corrosion in Concrete: Fundamentals and Civil Engineering Practice.

[4] Ramirez, E. et al. (1996). The Protective Efficiency of Galvanizing Against Corrosion of Steel in Mortar and in Ca (OH)$_2$ Saturated Solutions Containing Chlorides.
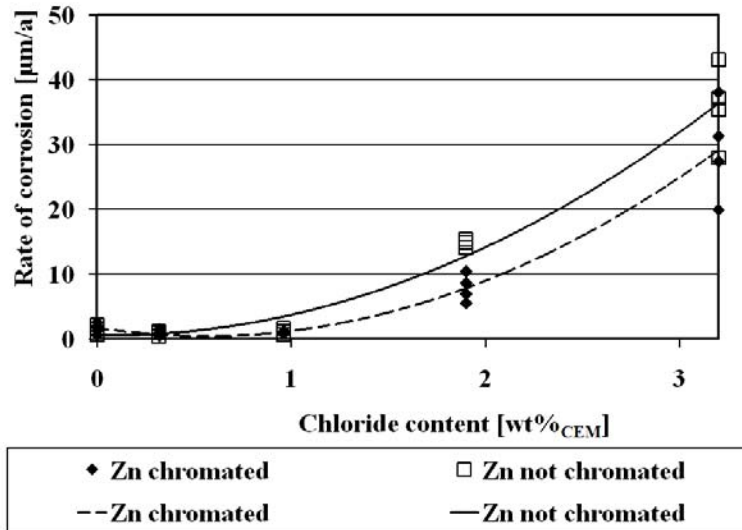
Fig. 10.   *Rate of corrosion of galvanised reinforcement bar in chloride-contaminated concrete.*

Shimada et al. researched the corrosion resistance of galvanised and chromated reinforcement bars and ordinary steel bars exposed to sea water[1]. The pitting corrosion was measured. After five years of exposure the maximum value for the pit was 3.3 mm in ordinary steel and 1.9 mm in galvanised steel. Thus, the zinc coating significantly slowed the initiation of corrosion. However, the rate of corrosion increased after the full dissolution of the zinc layer. It is clear that the critical chloride threshold of galvanised steel is higher than that of ordinary steel. For instance, under identical exposure conditions, the galvanised reinforcement resisted chloride levels in concrete at least 2.5 times higher than was the case for ordinary steel and delayed the time to the onset of corrosion of the underlying steel by a period some 4-5 times longer[2,3].

The density of a barrier layer of calcium hydroxozincate (CaHZn) and the microstructure of the residual zinc coating define the chloride resistance of galvanised steel when chlorides penetrate from outside into the concrete. Then the protective film has already formed. In that case the chloride resistance is quite good.[4]

The measured threshold value[5,6] for galvanised steel is 1.0-1.5% of water-soluble chlorides per weight of cement. Then, the propagation of corrosion in the zinc phases takes place. At content of chloride 1.0-1.5% of chlorides per weight of cement, with ordinary steel reinforcement bars the concrete structure may crack or spall in the propagation state. The threshold value for ordinary steel is approximately 0.3-0.4% of water-soluble chlorides per weight of cement[7]. The threshold value is lower in carbonated concrete compared with non-carbonated concrete, because of the reduced alkalinity of the concrete. Then the carbonation of concrete releases chloride ions bound

---

[1] Shimada, H., Nishi, S. (1983). Sea Water Corrosion Attack on Concrete Blocks Embedding Zinc Galvanized Steel Rebars.

[2] Yeomans S.R. (1994). Performance of black, galvanized, and epoxy-coated reinforcing steel in chloride-contaminated concrete.

[3] Bautista, A., Gonzalez, J.A. (1996). Analysis of the Protective Efficiency of Galvanizing Against Corrosion of Reinforcements Embedded in Chloride Contaminated Concrete.

[4] Andrade, C. et al. (1995). Coating Protection for Reinforcement.

[5] Bertolini, L. et al. (2004). Corrosion of Steel in Concrete – Prevention, Diagnosis, Repair.

[6] Andrade, C. et al. (1992). Protection Systems for Reinforcement.

[7] Angst, U. et al. (2007). Critical chloride content - State of the Art.

into the cement paste to diffuse deeper into the structure. Furthermore, the low amount of bound chlorides in the carbonated concrete affects on the lower threshold value.

Calcium aluminates (AC_3) and ferrite aluminates (AFC_4) react with chlorides. The rate of corrosion depends on the total amount of AC_3 and AFC_4 and the alkali content of the cement at higher pH values[1]. The use of high-performance concrete (HPC) together with galvanised steel will substantially delay chloride ion-induced corrosion[2]. Maldonado et al.[3] researched hot-dip zinc-coated and plain steel reinforcement bars with four different water-to-binder ratios. Experimental work was done with cylindrical samples submitted to immersion and dry periods under natural conditions at a coastal site in the Gulf of Mexico. They concluded that corrosion behaviour depends strongly on the concrete design. The corrosion of galvanised steel is negligible in concrete with a water-to-binder ratio of 0.4 and 0.5, after 421 days of exposure, while in concrete with w/c ratios of 0.6 and 0.7, corrosion initiates during the first days of exposure and is very high after about 200 days.

Because of the higher chloride threshold value and decreasing rate of corrosion in carbonated cracks, galvanised reinforcement bars have better corrosion protection properties in cracked concrete compared with ordinary steel reinforcement bars. The following observations have been made in the research results of galvanised and chromated steels in concrete.

Okamura et al.[4] concluded that a zinc coating reduced the extent of corrosion in salt exposure (3% salt solution sprayed daily) compared with ordinary steel. The basis of the research results was visual measurements after one year of exposure. Red rust was found on the ordinary steel bars near the tip of each crack in the concrete, while little such rusting was observed on the galvanised bars. Thus, using galvanised bars, the durability of a concrete member with a crack width of 0.3 mm was the same as that of an ordinary steel reinforcement bar in concrete with a crack width of 0.2 mm.

Fratesi et al.[5] investigated the performance of galvanised steel embedded in cracked concrete immersed in sea water. While the thickness of the zinc coating was progressively reduced in the cracked area, sometimes exposing the underlying steel, no iron corrosion products were observed. This supported the view that zinc cathodically protects adjacent areas of exposed steel. Where an attack on the zinc was observed, a thick white compact deposit of calcium hydroxozincate (CaHZn) was present.

Swamy's[6] research results showed excellent corrosion resistance of galvanised and chromated bars in cracked concrete exposed to sea water with sufficient concrete cover. In accelerated laboratory cyclic wetting and drying tests, after two years of exposure less than 10% of the bar surface was affected by pitting corrosion with a concrete cover of 40 mm and 70 mm. Additionally, with all cover depths of 20 mm to 70 mm, a white rust formation was observed covering a major part of the bar surface outside the red rust

---

[1] Nürnberger, U. (2000). Supplementary Corrosion Protection of Reinforcing Steel.
[2] Gowripalan, N., Mohamed, H.M. (1998). Chloride-Ion Induced Corrosion of Galvanized and Ordinary Steel Reinforcement in High-Performance Concrete.
[3] Maldonado, L. et al. (2006). Corrosion of zinc-coated reinforcing bars in tropical humid marine environments.
[4] Okamura, H. & Hisamatsu, Y. (1976). Effect of Use of Galvanized Steel on the Durability of Reinforced Concrete.
[5] Fratesi, R. et al. (1996). The Influence of Steel Galvanization on Rebars Behaviour in Concrete.
[6] Swamy, R.N. (1990). Resistance to Chlorides of Galvanized Rebars.

formation. Thus, the zinc layer was corroded. However, it is significant that the corroded area with a zinc coating after two years of exposure was slightly more than 70% with a cover depth of 20 mm. On the other hand, the corroded area with ordinary steel was app. 75% with a cover depth of 70 mm; red rust was also observed in the artificial cracks (the crack widths varied between 0.11 mm and 0.25 mm with an increase in the cover depth). With the cover depths of 20 mm and 40 mm the bars were covered with rust throughout. However, pitting corrosion was generally observed in the cracks. In that case, the depth of the pits in ordinary steel with all cover depths was more than 2 mm (maximum value 2.73 mm with a cover depth of 20 mm). The depths of the pits in galvanised steel with cover depths of 20 mm, 40 mm, and 70 mm were 2.02 mm, 1.08 mm, and 1.00 mm, respectively. However, most pits with a cover depth of 40 mm had a depth of less than 0.5 mm and those with a cover depth of 70 mm even less than that.

Thus, the research results suggest that the protective and corrosion-reducing efficiency of the zinc coating is obvious if a cover of sufficient depth is provided. A cover depth of 20 mm may not be sufficient in cases of severe exposure, even for galvanised steel, despite smaller crack widths than with thicker cover depths.

2.3.4   Galvanic couple

When zinc and steel are connected in an electrolyte, an electrochemical galvanic couple forms as a result of the potential difference. Zinc is a more electronegative metal than steel. Thus, zinc is an anode in electrochemical corrosion and the steel does not corrode. The corrosion of a zinc coating may be very severe in galvanic corrosion.[1] This type of corrosion is presented schematically in Fig. 11. The same electrochemical phenomenon which causes cathodic protection is also the basis for galvanic corrosion if the ratio of the zinc and steel surface area is small enough or the electrolyte is appropriate. The properties of the steel and alloy surface forming the passivity layer influence the probability of galvanic corrosion. The cathodic rate of corrosion in the steel surface may be low or passive, despite the existence of the galvanic couple. Passivity depends on, among other factors, the electrolyte and may reach wide potential areas[2]. Local deterioration of the passivity film, for instance as a result of chlorides, reaches the galvanic couple and accelerates local corrosion. The manner of fixing to a connection point has an effect on galvanic corrosion. Different composition areas are generated when steel is welded. The weld metal mixes gradually with connectable steel. The heat effect changes the base steel properties. Thus, there may be anodic and cathodic areas in the joint[3].

[1] Galvanizers' Association of Australia (1999). After-Fabrication Hot Dip Galvanizing.
[2] Baboian, R. (1976). Electrochemical Techniques for Predicting Galvanic Corrosion.
[3] Compton, K.G., Turley, J.A. (1976). Electrochemical Examination of Fused Joints between Metals.
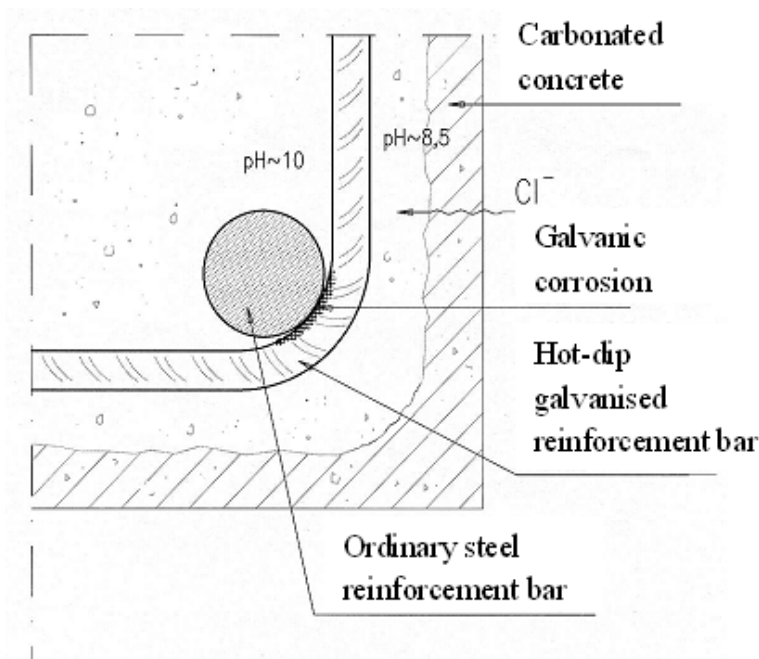
Fig. 11.   *Galvanic corrosion of zinc coating in chloride-contaminated and carbonated concrete.*

Steel and alloy are compared only individually with each other in galvanic series. In fact, better estimates of galvanic corrosion are reached in comparison with different couples of steel[1]. In cracks of the zinc coating reaching the steel, the galvanic couple is formed in the presence of the electrolyte. Additionally, potential differences may exist between different phases.

The Australian guide allows ordinary steel reinforcement bars to be connected with hot-dip galvanised steel bars in the parts of the structure where galvanising is used to provide a high degree of corrosion protection[2]. On the basis of the guide, ordinary steel reinforcement bars can induce only highly localised sacrificial protection in the galvanised bars they are in contact with. As a result, the effect on the service life of the hot-dip galvanised bars which are in contact is negligible. According to Andrare et al.,[3] in alkaline concrete an ordinary steel bar in contact with a hot-dip galvanised steel bar tends to accelerate the rate of corrosion of zinc and the risk of detrimental effects as a result of the galvanic contact remains. Thus, the connecting of hot-dip galvanised and ordinary steel bars in concrete is not recommended. Additionally, the service life of the zinc coating is shortened by galvanic corrosion. The difference compared to the Australian guide is probably due to neutrality aspects.

2.4   Influence of particular properties

Hot-dip galvanised reinforcement bars may corrode more than ordinary steel in the non-carbonated zone, but the rate of corrosion as a whole is considered to be insignificantly low in many cases and corrosion is not often taken into account in service life planning. Furthermore, in fresh concrete the porosity and thus non-homogeneity surrounding the hot-dip galvanised reinforcement bar as a result of the reaction of the evolution of

---

[1] Mansfeld, F., Kenkel, J.V. (1976). Laboratory Studies of Galvanic Corrosion of Aluminum Alloys.
[2] Galvanizers' Association of Australia (1999). After-Fabrication Hot Dip Galvanizing.
[3] Andrade, C. et al. (1995). Coating Protection for Reinforcement.

hydrogen from the zinc and cement paste is not taken into account in service life calculation.[1]

Hot-dip galvanised reinforcement bars are considered to be a very effective way to increase service life in carbonated concrete. This is partly based on the hypothesis that zinc corrosion products are more minor than with ordinary steel, and would not cause critical spalling forces in the concrete cover[2]. In service life planning the above-mentioned case can be taken into account, for instance in specifications for quality requirements.

2.4.1   Quality of hot-dip galvanised reinforcements

The main issue of hot-dip galvanising[3] is the quality of the coating. It should be uniform, irrespective of the diameter, length, shape (whether bent or straight), or the silicon and phosphorus content of the steel reinforcement bars. Obviously, the silicon and phosphorus content has to be within some limits. The thickness of the coating should be equal between the ribs and on top of the ribs, as well as at both ends of the bar. Care should be taken when placing the bars into the rack. There should be sufficient support for bars with smaller diameters. The dimensions should be taken into account in the dipping time. A visual estimation of the quality of the coating, in particular of the profile, is suggested. For example, the sharpness of the ribs can be seen with the naked eye, especially when compared with an uncoated steel reinforcement bar. Supplementary to visual estimation, magnetic zinc coating thickness measurement, transverse rib, and thin section studies are suggested.

In concrete, contact with other metals and other types of zinc coatings should be avoided because of the risk of galvanic corrosion. Care should be taken when handling the reinforcement so as not to damage the zinc coating. During storage stagnant water on the reinforcement should be avoided, because of the danger of the formation of zinc oxide (ZnO). Quality specifications for zinc coatings are, for instance, the target silicon content of the steel reinforcement bar, Si equal to 0.15%, the target phosphorus content of the steel reinforcement bar, P equal to 0.020%, the target value for the [Si-% + $2.5 \times$P-%] content of steel reinforcement bar, 0.20%, the properties of the galvanising method, and the formation and structure of the zinc coating. The quality of the zinc coating is usually better with larger bar diameters. The galvanising method may not be suitable for achieving a uniform coating. The addition of nickel may improve the quality of the coating. The chromate treatment is not long-lasting. Alternatives to chromating are the use of outside storage or treatment with oxalic acid.

An article[4] discusses in detail the material properties of steel reinforcement bars which are to be galvanised, the special recommendations for galvanisation, the zinc coating, the bending and cutting of galvanised reinforcements, their intermediate storage, specifications for the reinforcements and concrete, the transportation of hot-dip galvanised reinforcements, and their handling on the building site. In addition to the physical requirements and the stipulated criteria for acceptance, certain inspections and

---

[1] Yeomans, S.R. (2004). Galvanized Steel in Reinforced Concrete.

[2] Yeomans, S.R. (2004). Galvanizing of Steel Reinforcement for Use in Building and Construction.

[3] Sistonen, E., Peltola, S. (2005). Quality Specifications for Hot-Dip Galvanised Reinforcement to Ensure the Target Service Life.

[4] Sistonen, E. et al. (2006). Service Life and Quality Specifications for Hot-Dip Galvanised Reinforcement.

measurements, careful logging and recording of all data, and traceable details of every step in the process are imperative. The conclusion reached in the article is that there are several factors that should be ensured for the end product to be reliable.

For galvanised products, documentation should be received with particulars of the reinforcing bars (e.g. smelting analysis), the hot-dip galvanising plant, the lot of reinforcements delivered, the hot-dipping conditions (length or duration of dipping, nickel content, etc.), the test results of the hot-dip galvanised reinforcements, analysis of the zinc coating, the time of the hot-dipping, the standards or directions complied with, an assurance that the zinc coating and the hot-dip galvanised reinforcements fulfil the requirements, and the name and the code of the inspection office (if relevant). This means that certain changes and modifications are needed in the planning directions and provisions. Quality standards must also be laid down for hot-dip galvanised reinforcements to ensure that the special features and practical requirements of hot-dip galvanised reinforcements are recognised.

2.4.2   Guidance of design

Quality requirements from the point of view of service life are summarised in the project research report[1] and briefly presented and discussed below. These requirements comply with the research results obtained in the dissertation. The careful choice of the above-mentioned parameters and correct site practice are the basis of a long service life. It goes without saying that site practice should be precise and it should be monitored. The influence of ageing is not always a priority from the point of view of service life. For instance, a bond in concrete does not necessarily weaken as a function of ageing.

Quality requirements for hot-dip galvanised reinforcement bars

Requirements for reinforcement bars

The optimum value for the silicon equivalent of a steel reinforcement bar (Si-% + 2.5 × P-%) is 0.20%. That equivalent value ensures the quality of the zinc coating. The limit value (product analysis) of the silicon content is between 0.13% and 0.60% and the maximum phosphorus content allowed is 0.07% for the hot-rolled steel bar that was studied[2]. The maximum silicon content allowed (product analysis) is 0.65% and the phosphorus content 0.07% for the cold-worked steel bar that was studied[3]. Thus, the required equivalent value limits the use of several ordinary steel reinforcement bars manufactured nowadays.

Requirements for hot-dip galvanising

The dipping time of ordinary steel reinforcement bars should be brief (approximately three minutes). Ordinary steel reinforcement bars with different bar diameters should be dipped in zinc separately. That was noticed during the research work. The uniform quality of the thickness of the zinc coating in different sections of hot-dip galvanised reinforcement bars can be ensured with reverse dipping.

---

[1] Sistonen, E. et al. (2002). Restricting Corrosion Risk in Reinforced Concrete Structures under Outdoor Conditions – Part II.
[2] SFS 1215 (1996). Reinforcing steels. Weldable Hot Rolled Ribbed Steel Bars A500HW.
[3] SFS 1257 (1996). Reinforcing steels. Cold Worked Ribbed Steel Bars B500K.

Requirements for zinc coating

The same classification criterion for the zinc coating should be used for hot-dip galvanised reinforcement bars, whether or not they are bent before dipping (Table 3). The mean value for the thickness of the zinc coating should be 100-200 μm and the tolerance in different sections of the bar 75-225 μm as a result of, for instance, mechanical properties. In the author's opinion, hot-dip galvanised reinforcement bars with a diameter less than 12 mm are not suitable for use as main reinforcements, mainly because the distance between the transversal ribs is too low and leads to low-quality rib geometry. This was noticed during the research work.

Table 3.   Classification criteria in visual inspection.

Classification criterion	Number of instances of damage [pc/m]	Note
3	2	Rib geometry and uniform quality of hot-dip galvanised reinforcement bar is good
2	5	Degradation of rib geometry and occurrence of zinc uptake
1	10	Rib geometry clearly lowered by zinc uptake
0 (Rejected)	>10	Rib geometry with low quality and significant zinc uptake

Hot-dip galvanised main reinforcement bars delivered to building sites are not allowed to include defects with a surface area of more than 50 mm^2. Defects with a surface area of less than 25 mm^2 and the total number of defects shown in Table 3 can be allowed on the basis of the cathodic protection system. Defects with a surface area of 25-50 mm^2 and the total number of defects shown in Table 3 should be repaired with zinc-rich paint or the protective effect of the concrete cover should be improved. The depth of the damage to the zinc coating is more critical than observed surface damage such as abrasion.

Requirements for bending and cutting

Main reinforcement bars should be galvanised before bending. Stirrups, hooks, and loops should be bent before hot galvanising. In bending the critical area of the zinc coating is between the ribs and in the sloping part of the rib. This was noticed during the research work. Hot-dip galvanised bent main reinforcement bars delivered to building sites are not allowed to include in the bent area single fractures and lamels with a surface area greater than the upper limit value presented in Table 4. Single fractures and lamels with a surface area smaller than the lower limit value presented in Table 4 and the total number of fractures, lamels and damage shown in Table 3 can be allowed on the basis of the cathodic protection system. Single fractures and lamels with a surface area between the lower and upper limit values presented in Table 4 and the total number of fractures, lamels, and damage shown in Table 3 should be repaired with zinc-rich paint or the protective effect of the concrete cover should be improved. It should be noted that the values presented in Table 4 correspond to a fracture approximately 0.5-2.0 mm wide. Thus, the values are conservative compared to the cathodic protection potential presented in Chapter 2.2.

Hot-dip galvanised cut main reinforcement bars in a cut area with a surface area larger than 25 mm^2 (reinforcement bar diameter, Ø > 5 mm) should be repaired with zinc-rich

paint or the protective effect of the concrete cover should be improved. The depth of the damage to the zinc coating is more critical than observed surface damage such as abrasion.

Table 4. *Classification of fractures and lamels of zinc coating in bent section of main reinforcement [mm²].*

Reinforcement bar diameter, Ø [mm]	Lower limit value for surface area of single fracture or lamel, A_{damage} [mm²]	Upper limit value for surface area of single fracture or lamel, A_{damage} [mm²]
< 9	25	30
9…16	30	40
> 16	40	50

The minimum bending radius for hot-dip galvanised bent main reinforcement bars should be at least the same as the minimum bending radius for ordinary bent main reinforcement bars presented in the Finnish concrete code[1] (Section 4.2.3.2). This requirement is on the safe side compared to the limit values presented in Chapter 2.4.4. In the author's opinion, production logistics demand the use of the same values that an ordinary steel reinforcement bar has.

Special requirements for hot-dip galvanised reinforcement bars and concrete mix

The bond strength of hot-dip galvanised reinforcement bars should be at least the same as the bond strength of ordinary steel reinforcement bars presented in the Finnish concrete code[2] (Section 2.2) with three slip values. The slip values considered are of 0.01 mm, 0.1 mm, and 1.0 mm, corresponding to the stress (approximately 100 MPa, 200 MPa, and maximum strength respectively) measured from the unloaded end. The requirements are applied from the specifications of RILEM[3]. In the author's opinion, this requirement is possible to achieve and is also noted in Chapter 2.4.3. The rib geometry and the roughness of the zinc coating and hydrogen pores in the area under study affect the bond strength achieved. Lifting loops are not allowed to galvanise. The use of a lower water-to-binder ratio than stated in the Finnish concrete code[4] to shorten the time for zinc reaction and the evolution of hydrogen is required, irrespective of the exposure class. This was noted during the research work. However, the need for further research is obvious in order to find suitable concrete mixes for use with hot-dip galvanised reinforcement bars.

Requirements for intermediate storage

The passivation of zinc coatings for hot-dip galvanised reinforcement bars is achieved with outside storage within four to eight weeks if the requirements for the hot-dip galvanised reinforcement bars and the concrete mix are fulfilled. This was noticed during the research work. The storage of hot-dip galvanised main reinforcement bars, can be allowed on the basis of the cathodic protection system, if provided defects with a surface area less than 25 mm² and the total number of defects shown in Table 3.

The storage of hot-dip galvanised bent main reinforcement bars, can be allowed on the basis of the cathodic protection system, if provided within the bent length single

---

[1] By 50 (2004). Concrete Code 2004.
[2] By 50 (2004). Concrete Code 2004.
[3] RILEM TC (1994). RC 6 Bond Test for Reinforcement Steel. 2. Pull-out Test, 1983.
[4] By 50 (2004). Concrete Code 2004.

fractures and lamels with a surface area less than the lower limit value shown in Table 4 and the total number of fractures, lamels, and damage shown in Table 3.

Requirements for transportation on building sites

Damage and abrasion of hot-dip galvanised reinforcement bars should be avoided to minimise shifting and handling and the use of metallised tools. The installation of hot-dip galvanised reinforcement bars should only be performed with zinc binding wire and secondary reinforcements. In the author's opinion, in this case the probability of galvanic corrosion may be low but it should be estimated and taken into account in planning of galvanised reinforcement embedded in concrete.

2.4.3   Bonding of hot-dip galvanised reinforcement bars

Bonding is formed by adhesion, friction, and mechanical bonding. Adhesion is based on the capillary and adhesion forces between the concrete and steel. Friction bonding is based on the friction and shear resistance between the roughness of the steel surface and the cement stone. Since the reinforcement most commonly used is ribbed, in the service limit state adhesion and friction play important roles, and they mainly affect lighter loads and smaller slips. As the bar slips further in the friction phase, the ribs gradually begin to act in the ultimate limit state as cracks are stabilised. Mechanical bonding is based on the ribbed geometry of the steel reinforcement bar, which is evaluated by considering the relative rib area, f_R, and the angle of slope of the transversal ribs, α. The relative rib area, f_R, is a parameter which takes account of the height and distance between the transversal ribs. It is the ratio between the projected rib area and the cylindrical surface area of one rib space.[1] The relative rib area increases if the rib height increases or the number of ribs per unit of length increases. The relative rib area, f_R, is calculated as follows:

$$f_R = \frac{\sum S_{PR}}{\pi \cdot d \cdot a},$$

(9)

where d is the nominal bar diameter [mm],
         a is the length between transversal ribs [mm], and
         S_{PR} is the projective area of transversal ribs [mm^2] (Fig. 12).

---

[1] Jokela, J. (1986), Dimensioning of strain or deformation-controlled reinforced concrete beams.
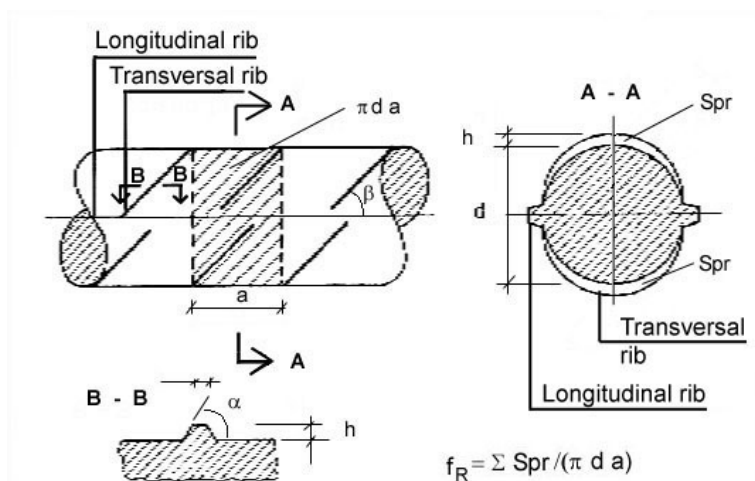
Fig. 12.   *Definition of relative rib area, f_R.*

Slipping and fracturing can occur in two ways, depending on the properties of the concrete and the geometry of the steel reinforcement bar. For instance, typical values involve a nominal bar diameter d equal to 12 mm, and rib height h equal to 0.90 mm, the length between transversal ribs a_{min} equal to 7.2 mm (a_{min} equal to 8h) and a_{max} equal to 7.50 mm[1]. Furthermore, the angle of slope of the transversal ribs α equal to 40...90°, and the drift angle of the rib β equal to 45…80°. If the ribs are high and situated close to one another, ruptures occur in the cylindrical plane at the outermost edges of the ribs. If the ribs are lower or apart from one another, ruptures occur behind the ribs, where the hardened cement paste will be pulverised and the concrete broken in a wedge-shaped formation.[2] This mechanical failure based on a wedge action between two ribs is desired before the pull-out of the bar. In the literature the results obtained for the bonding of galvanised bars are very contradictory[3,4,5,6]. The prevailing tendency, however, is that galvanising does not generally reduce the bond in concrete, and in the case of passivated zinc the results can be even better than with uncoated steel. The results do not merely depend on the quality of the coating and the geometry of the bars: the properties of concrete play a significant role as well.

One aspect of bonding between hot-dip galvanised reinforcement bars and concrete is the reaction of the zinc with fresh concrete, resulting in hydrogen gas. Hydrogen pores and zincates reduce the adhesion forces of initial bonding. Hydrogen pores also have an effect by reducing the friction bond in the contact area of the hardened cement paste near the surface of the bars[7,8]. In addition, if the strength of concrete is reduced, the hardened cement paste will be pulverised more easily. Chromates are used to passivate zinc and to prevent the formation of hydrogen, but unfortunately the durability of the chromating during storage is uncertain. Furthermore, chromates may cause allergic reactions or cancer (chromium (VI))[9] in workers, and therefore other means of

---

[1] SFS 1257 (1996). Reinforcing steels. Cold worked ribbed steel bars B500K.
[2] Jokela, J. (1986). Dimensioning of strain or deformation-controlled reinforced concrete beams.
[3] Proverbio, E. et al. (1998). Long Term Exposure Tests on Galvanized Steel in Different Concrete Types.
[4] Concrete Institute of Australia (1984). The Use of Galvanized Reinforcement in Concrete.
[5] Sarja, A. et al. (1984). Zinc-coated Concrete Reinforcement.
[6] Andrade, C. et al. (1995). Coating Protection for Reinforcement.
[7] Proverbio, E. et al. (1998). Long Term Exposure Tests on Galvanized Steel in Different Concrete Types.
[8] Andrade, C. et al. (1995). Coating Protection for Reinforcement.
[9] Aubriet, F. et al. (2000). Studies on Alkali and Alkaline Earth Chromate by Time-of-flight Laser Microprobe Mass Spectrometry and Fourier Transform Ion Cyclotron Resonance Mass Spectrometry.

passivating zinc are being researched. At low slip values (lower stress in steel) the evolution of hydrogen has greater significance. At higher slip values (higher stress in steel) the evolution of hydrogen does not have significance, because the bonding property of the rib of the hot-dip galvanised reinforcement bar is emphasised (the mechanical bonding of the ribs).

On the basis of large-scale bond tests[1] it appears that hot-dip galvanisation does not significantly weaken the bond if passivation has succeeded. Sarja et al.[2] and Andrade et al.[3] concluded that the bond of chromated and hot-dip galvanised reinforcement bars corresponds to the bond of ordinary steel. However, on the basis of Building Research Establishment[4], the slip at 150 MPa was 0.1 mm with an ordinary ribbed steel reinforcement bar. The same slip occurred at 160 MPa with a hot-dip galvanised reinforcement bar and at 190 MPa with a chromated and hot-dip galvanised reinforcement bar. Furthermore, the University of California[5] concluded that the bond of a hot-dip galvanised reinforcement bar was the same as or better than with an ordinary steel reinforcement bar in different circumstances. The slips of different reinforcing steel types at 150 MPa, 200 MPa, 250 MPa, and maximum stress[6] are presented in Fig. 13. There is a slight correlation between the slip and the relative rib area for all values. The result is probably mainly due to a non-uniform zinc coating, which smoothed the reinforcement bar geometry.

Hot-dip galvanising changed the geometry of the reinforcement bars by smoothing the ribs and reducing their height, thus affecting the bonding between the reinforcement bar and the concrete. In most cases galvanising had an adverse effect on the bonding between the reinforcement bar and the concrete. It can be seen in Fig. 13 (top left) that the slip is not dependent on the relative rib area with values over 0.04. In all cases the slip plays an important role on the relative rib area with values below 0.04. Actually, these measurement values consisted of those bars with approximately 50 per cent of the minimum allowed relative rib area, $f_{R,min}$[7].

The angle of slope diminishes with zinc drops gathering between the ribs at the corners. The effect of galvanising on the relative rib area is not as straightforward; this can be seen from the test results. Obviously, the ribs become wider. If the projected rib area becomes larger, the relative rib area will be enlarged as well. On the other hand, the relative rib area is reduced with the growing diameter, and the rib height possibly becomes lower: the coating is thicker between the ribs than on top of them. Furthermore, under mechanical loading the bond between the zinc-coated reinforcement bar and the concrete is weaker lower with thicker zinc coatings.

The emphasis should be on the quality of the coating. It should be uniform, regardless of the diameter, length, shape (whether bent or straight), or silicon content of the bars. The thickness of the coating should be equal between the ribs and on the top of the ribs as well as at both ends of the bar, so that the smoothing and reduction in the height of the ribs can be avoided.

[1] Concrete Institute of Australia (1984). The Use of Galvanized Reinforcement in Concrete.
[2] Sarja, A. et al. (1984). Zinc-coated Concrete Reinforcement.
[3] Andrade, C. et al. (1995). Coating Protection for Reinforcement.
[4] Yeomans, S.R. (2004). Galvanizing of Steel Reinforcement for Use in Building and Construction.
[5] Yeomans, S.R. (2004). Galvanizing of Steel Reinforcement for Use in Building and Construction.
[6] Sistonen, E. et al. (2005). Bonding of Hot Dip Galvanised Reinforcement in Concrete.
[7] SFS 1257 (1996). Reinforcing steels. Cold worked ribbed steel bars B500K.
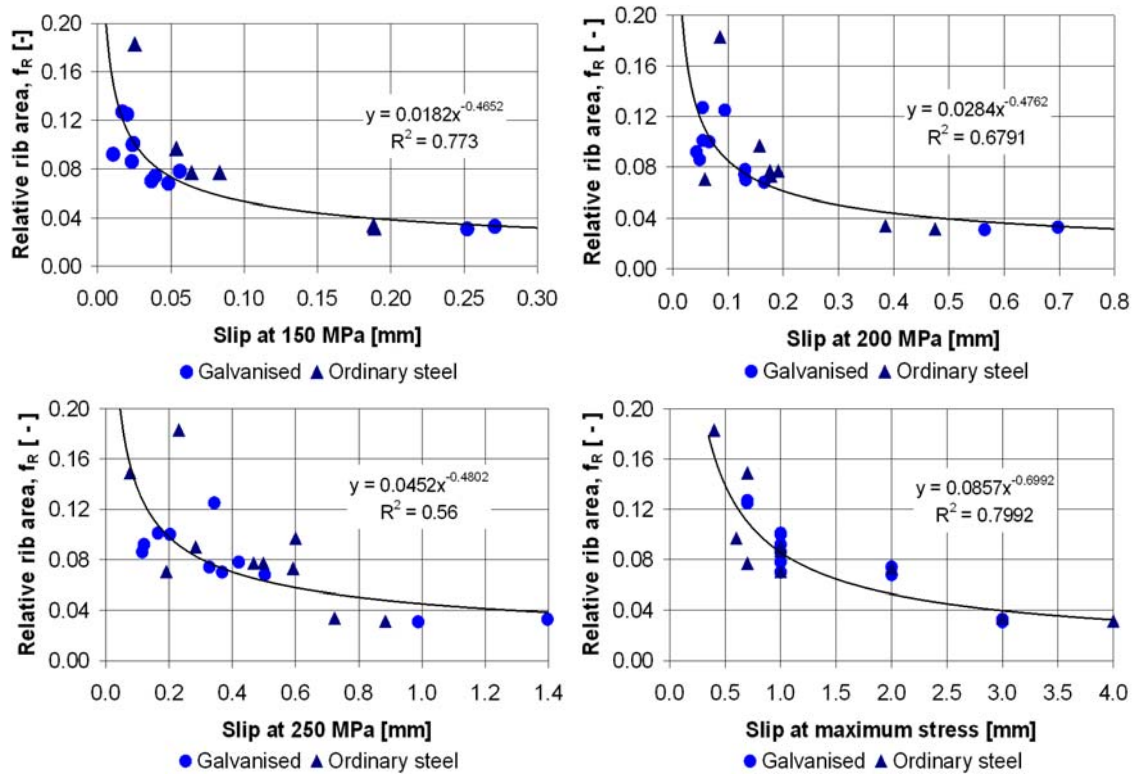
Fig. 13.   Slip at 150, 200, and 200 MPa and maximum stress – relative rib area, average.

Belaïd et al. found that a galvanised coating affects the porous structure of the interfacial transition zone (ITZ) with the surrounding cement paste[1]. However, it was observed[2] that the main parameters for bonding were the quality of the concrete and the zinc coating. Andrade et al.[3] present a series of tests that compare the bond of deformed bare steel reinforcement bars with galvanised ones, exposed for up to 10 years to a chloride environment in natural sea water (Mediterranean). The results showed that galvanised reinforcement bars maintained bond characteristics throughout the test period, with values much higher than the minimum requirements of RILEM[4]. Furthermore, comparing the results of the bare steel bars to those of the galvanised ones, the bond strength was greater in the galvanised ones than in the bare ones. The addition of an H_2 inhibitor or the use of cements with a high alkali content has proved to be irrelevant in the long term.

It is possible to choose the steel reinforcement bar and the concrete in such a way that the bonding of the hot-dip galvanised reinforcement in concrete is as good as the bonding with an ordinary steel reinforcement. This clause is used in the German technical approval, which permits the same admissible bond stresses to be applied for both coated and uncoated bars[5]. This technical approval is on the same acceptance level as the German code and is given mainly for newly developed products. Thus, in some ways the design of hot-dip galvanised concrete structures may be similar to the design of concrete structures reinforced with ordinary steel. The effect of hydrogen pores on

[1] Belaïd, F. et al. (2001). Porous structure of the ITZ around galvanized and ordinary steel reinforcements.
[2] Sistonen, E. et al. (2005). Bonding of Hot Dip Galvanised Reinforcement in Concrete.
[3] Andrade, C. et al. (2001). Tests on Bond of Galvanized Rebar and Concrete Cured in Seawater.
[4] RILEM TC (1994). RC 6 Bond Test for Reinforcement Steel. 2. Pull-out Test, 1983.
[5] Yeomans, S.R. (2004). Galvanized Steel in Reinforced Concrete.

bonding may be temporary because it is possible that CaHZn crystals act as bridges between the steel surface and the concrete and improve the adhesion of the bars. This compensates for possible degradation of the bond resulting from hydrogen pores[1].

2.4.4   Bending of hot-dip galvanised reinforcement bars

The coating could fracture during bending as a result of being thick and non-uniform (Fig. 14). If there is a thinner zinc coating in fractured areas, the coating may be completely lost from the bar surface earlier, which may lead to a reduction in the durability of a reinforced concrete structure. The intensity and width of the fractures and lamels formed are clearly related to the bending radius and angle, reinforcement bar diameter, and thickness of the zinc coating. Therefore it is advisable that bending is carried out prior to galvanising when small bending mandrels are used (stirrups).

Fig. 14.   Bent specimens after three years of storage outdoors[2].

The bending radius, the formation and the structure of the zinc coating, and the thickness of different phases are factors which, among others, influence the success of bending. The maximum value suggested[3] for the thickness of the zinc coating is approximately 200 µm (approximately 1400 g/m²). The thicker the zinc coating is, the more sensitive it is when being bent. The eta (η) phase is the most ductile compared with the other phases, and good bending properties require the existence of an eta (η) phase. Fractures and lamels caused by the bending of hot-dip galvanised reinforcement bars have the same direction as the transversal ribs. Fractures often begin at the thickest point of the zinc layer, i.e. the root of the rib. The more uniform the zinc coating, the greater the proportion of the eta (η) phase in its coating, and the less influence the thickness of the zinc coating will have on the number of fractures and lamels that appear.

The minimum bending radius for hot-dip galvanised reinforcement bars has not been defined in Finland. Australian[4] standard AS 3600 recommends a minimum bending radius for hot-dip galvanised reinforcement bars. In Table 5 the minimum bending

---

[1] Yeomans, S.R. (2004). Galvanized Steel in Reinforced Concrete.
[2] Sistonen, E. et al. (2006). Service Life and Quality Specifications for Hot-Dip Galvanised Reinforcement.
[3] Andrade, C. et al. (1995). Coating Protection for Reinforcement.
[4] Galvanizers' Association of Australia (1999). After-Fabrication Hot Dip Galvanizing.

radius to minimise fractures and lamels of the zinc coating is shown. The limit values presented in ASTM A767[1] are very similar to the values presented in AS 3600.

Table 5.   *Minimum bending radius for hot-dip galvanised reinforcement bars, based on Australian standard AS 3600.*

Reinforcement bar diameter, Ø [mm]	Minimum bending radius
≤ 16	$5 \times Ø$
> 16	$8 \times Ø$

Sarja et al.[2] noticed that a zinc coating of a stirrup of ordinary steel reinforcement bars fractured when the bending radius was $3 \times Ø$ and the $5 \times Ø$. With a bending radius of $10 \times Ø$, the zinc coating did not fracture. Fractures resulting from bending can be avoided when the bending is carried out prior to galvanising. In that case strain ageing may be the problem. Additionally, the costs of the zinc coating process rise and the geometry of the reinforcement bar changes. The most positive property of the preliminary bending of the bars is that the patching of the cut spots is avoided.

Strain age embrittlement is caused by the cold-working of steels, mainly those with a low carbon content, followed by ageing at temperatures less than 600 °C or by the hot-working of steels below 600 °C[3]. The cold-working (bending) of structural steels thicker than 6 mm should be avoided, if the item will subsequently be subjected after hot-dip galvanising to ultimate tensile stress[4]. If cold-working cannot be avoided, an embrittlement test based on ASTM A143 can be used[5]. Warming the steel to a temperature of 650 °C before galvanising relieves the stresses formed in the steel. Steels susceptible to embrittlement should be bent with a smooth mandrel at a minimum bending radius of $3 \times Ø$[6].

For practical reasons, bending can normally be carried out after galvanising because the transportation and processing of bundles of straight bars is easier and more economical[7]. In the author's opinion main reinforcement bars may be bent after galvanising and stirrups, ties, and hooks prior to galvanising.

2.4.5   The repair of structures reinforced with hot-dip galvanised reinforcement bars

The sprayed coating can be made by melting zinc powder or zinc wire with a flame or electric arc and spraying the melted drops with air or gas onto the grit-blasted surface of the steel. The zinc bonds mechanically with the reinforcement bar. The coating is porous but the pores soon fill up with zinc corrosion products. After that the coating is compact. The corrosion product, zinc oxide (ZnO), does not prohibit the electronic continuity and contact of the coating with the reinforcement bar. Thus, the cathodic

---

[1] ASTM A767/A767M-00b (2000). Standard Specification for Zinc-Coated (Galvanized) Steel Bars for Concrete Reinforcement.
[2] Sarja, A. et al. (1984). Zinc-coated Concrete Reinforcement.
[3] Galvanizers' Association of Australia (1999). After-Fabrication Hot Dip Galvanizing.
[4] Galvanizers' Association of Australia (1999). After-Fabrication Hot Dip Galvanizing.
[5] ASTM A143/A143M-03 (2004). Standard Practice for Safeguarding Against Embrittlement of Hot-Dip Galvanized Structural Steel Products and Procedure for Detecting Embrittlement.
[6] Galvanizers' Association of Australia (1999). After-Fabrication Hot Dip Galvanizing.
[7] Yeomans, S.R. (2004). Galvanized Steel in Reinforced Concrete.

protection is active[1]. The local dissolution of the zinc coating, for instance in the deteriorated part of the zinc, is presented schematically in Fig. 5.

In cathodic protection the steel in areas where the zinc coating is fully dissolved does not corrode. The prerequisite for this is that the ratio between the zinc and the steel surface area is large. In repairing cathodic protection the corrosion products of the zinc coating migrate to the damaged part of the coating. The poorly soluble and least conductive compounds gather on the surface of the steel, reducing the corrosion reaction. However, the zinc coating deteriorates in cathodic protection.

Zinc-rich paint allows moderate cathodic protection for the reinforcement bar if the zinc content of the dry paintwork is at least 92 wt%. The painting also bonds mechanically with the reinforcement bar. With both zinc-rich paint and spray galvanising good mechanical resistance and corrosion durability can be achieved, though not as good as with hot-dip galvanising. The abrasion resistance is worse with zinc-rich paint than with spray galvanising. Zinc-rich paint and spray galvanising are applied to patches of corrosion, welding, and mechanical damage (cut surfaces, bending cracks, and bruises) in the zinc coating of hot-dip galvanised reinforcement bars. According to Porter[2], when repairing with zinc-rich paint, the thickness of the zinc coating ought to be approximately 50% thicker than the thickness of the original coating so that the coating serves sufficiently. Yeomans[3] states that a zinc coating thickness of 100 μm is adequate for repaired areas. Detailed specifications can be found from the references[4,5].

Electrochemical repairing methods are very unsafe for concrete structures reinforced with galvanised reinforcement bars. In this case strong peak corrosion of the galvanised reinforcement bars may occur. The company NCT, which owns the patent for electrochemical realkalisation and chloride removal from concrete in general (NORCURE®), does not recommend the use of these methods in structures reinforced with galvanised reinforcement bars[6].

A zinc coating corrodes faster if galvanised and ordinary steel reinforcement bars are situated in the same structure. The reason for this is galvanic corrosion. Pfeifer et al. noticed that the rate of corrosion in the decks of chloride-contaminated bridges was very low when both the upper and lower surfaces of the decks were reinforced with galvanised mesh reinforcement. When the galvanised mesh reinforcement was used in the upper surface of the decks and ordinary mesh reinforcement in their lower surfaces, the rate of corrosion of the zinc increased significantly[7]. Furthermore, the rate of corrosion of the zinc increased when the galvanised mesh reinforcement in the upper surface of a deck with a high chloride content was connected with an ordinary mesh reinforcement in the lower surface of a deck with a low chloride content. In that case the galvanised mesh reinforcement functioned as a sacrificial anode. Because of this, ordinary steel and galvanised reinforcement bars should be electrically isolated, at least from each other, if they are used in the same structure.

[1] Porter, F. (1991). Zinc Handbook, Properties, Processing and Use in Design.
[2] Porter, F. (1991). Zinc Handbook, Properties, Processing and Use in Design.
[3] Yeomans, S.R. (1987). Galvanized Steel Reinforcement in Concrete.
[4] Sarja, A. et al. (1984). Zinc-coated Concrete Reinforcement.
[5] Porter, F. (1991). Zinc Handbook, Properties, Processing and Use in Design.
[6] Broomfield, J.P. (1997). Corrosion of Steel in Concrete.
[7] Pfeifer, D.W. et al. (1987). Protective Systems for New Prestressed and Substructure Concrete.

2.4.6   Other properties of hot-dip galvanised reinforcement bars

Hot-dip galvanising does not have a significant effect on the static strength values of hot-rolled steels. The strength of cold-worked steel reinforcement bars, on the other hand, can decrease slightly as a result of hot-dip galvanising[1], which is due to a rise in temperature during hot-dip galvanising. The zinc coating is durable against abrasion: it withstands transportation, storage, and impacts and friction during the production of the reinforcement bars, so that, remarkably, the zinc coating does not get broken[2]. However, moving the bars should be performed by lifting, not by pulling. During the installation and compacting of concrete abrasions may form, which cause local deterioration of the zinc coating. Thus, hot-dip galvanised reinforcement bars should be handled carefully and during installation binding should be used so that the reinforcement is supported and no excessive abrasions appear.

Hot-dip galvanised reinforcement bars do not corrode in warm and wet storage circumstances where ordinary steel reinforcement bars would corrode. Furthermore, the zinc coating protects reinforcement bars against corrosion during storage and in the structure before concreting. Furthermore, hot-dip galvanised reinforcement bars are cleaner and easier to handle than ordinary steel reinforcement bars. Atmospheric oxygen forms a zinc oxide (ZnO) film, but it soon transforms to zinc hydroxide ($Zn(OH)_2$) as a result of outdoor moisture or water and further to alkaline zinc carbonate[3], $4ZnCO_3 \cdot 3Zn(OH)_2 \cdot H_2O$, and other alkaline zinc salts as a result of atmospheric carbon dioxide and chemical air pollutants. Zinc carbonate is compact, well attached to its base, and almost insoluble in water. Thus, it protects the zinc well. The duration of the wetness, relative humidity, and temperature influence the time taken for zinc carbonate to form. It may vary from a few weeks to several months.

If the supply of air to the surface of the zinc is restricted, and the subsequent formation of a zinc carbonate ($ZnCO_3$) layer cannot take place, very severe corrosion continues further and it forms so-called white rust, with a hundred-fold volume compared with the zinc volume[4]. To avoid white rust galvanised reinforcement bars should be stored in an airy place and either sheltered from rain or, if outdoors, in such a way that water can easily run off the surfaces, and all the surfaces should be well ventilated.

The bending radii used in main reinforcement bars are so large $(12\text{-}17 \times \varnothing)$[5] that the zinc coating usually survives the bending without fractures and lamels. The cutting of galvanised reinforcement bars can be performed quite normally on the construction site. However, the cutting surfaces are so large that the cathodic protection of zinc does not protect them. Zinc-coated reinforcement bars can be welded with the same methods as used in the welding of ordinary steel reinforcement bars. However, the zinc coating influences the welding. Thus, some changes in the welding process need to be made. For instance, the rate of welding should be reduced. Furthermore, ventilation should be ensured because gas is formed during the welding. The gas includes zinc oxide (ZnO), which is insanitary. If large deteriorated areas are formed in the zinc coating during welding, the damage should be patched with zinc-rich paint.[6]

---

[1] Sarja, A. et al. (1984). Zinc-coated Concrete Reinforcement.
[2] Sarja, A. et al. (1984). Zinc-coated Concrete Reinforcement.
[3] Porter, F. (1991). Zinc Handbook, Properties, Processing and Use in Design.
[4] Porter, F. (1991). Zinc Handbook, Properties, Processing and Use in Design.
[5] By 50 (2004). Concrete Code 2004.
[6] Andrade, C. et al. (1992). Protection Systems for Reinforcement.

On the basis of exposure to corrosion, the thinner coating of concrete in the cracked area exposes the steel more rapidly. In that case the uncoated part of the steel and the eta (η) phase can form a galvanic couple and accelerate the corrosion of the zinc. On the other hand, Sarja et al. noticed [1] that cracks in the zinc coating had no exact effect on corrosion. In that case the formation of lighter zinc oxide (ZnO) took place in the galvanised reinforcement bar, which clogged the fracture in the zinc coating by preventing local corrosion in the steel. However, it is obvious that fractures in the zinc coating still pose a risk for durability.

2.5   Summary

The literature study revealed that several factors have an influence on the thickness and formation of the zinc coating and the formation of the passive layer on hot-dip galvanised reinforcement bars, which are linked to the durability and service life of hot-dip galvanised reinforcement bars.

Certain research results are found as commonly accepted criteria to ensure the good quality of the zinc coating. These are, for instance, limits on the silicon, phosphorus, and manganese content in the steel and the nickel content in the zinc bath. With small reinforcement bar diameters the zinc coating could be non-uniform, despite the bath properties. Furthermore, accepted criteria to predict service life and to ensure the durability of hot-dip galvanised reinforcement bars in alkaline media are, for instance, limits on the pH values of the pore solution in carbonated concrete. There are contradictory opinions concerning the service life in chloride-contaminated concrete. Furthermore, there are contradictory opinions concerning the protection and corrosion mechanisms of hot-dip galvanised reinforcement bars.

More detailed research work should be performed to find techniques for achieving optimum thickness and formation of the zinc coating, suitable material parameters, optimum treatments after zinc baths, and concrete mixtures used in different exposure classes. Furthermore, the service life of hot-dip galvanised reinforcement bars in bent areas and the effect of natural passivation sheltered from rain or exposed to rain should be studied more precisely. In particular, detailed information concerning the threshold value of galvanised steel in chloride-contaminated concrete is needed. Additionally, more studies concerning the durability of hot-dip galvanised reinforcement bars in chloride-contaminated and cracked concrete should be performed. In the Finnish concrete code[2] no special requirements concerning hot-dip galvanised reinforcement bars (for instance the chemical composition of the steel) are presented.

---

[1] Sarja, A. et al. (1984). Zinc-coated Concrete Reinforcement.
[2] By 50 (2004). Concrete Code 2004.

3   SERVICE LIFE EVALUATION OF HOT-DIP GALVANISED REINFORCEMENT BARS

The objective is to present the factors influencing the service life evaluation of hot-dip galvanised concrete reinforcements. Service life estimation is developed and the problems in calculation are considered. In service life studies for both carbonated and chloride-contaminated concretes, the basis for classification is the uniform or decreasing rate of the corrosion of reinforcement bars. The same applies to intact and cracked concrete. A stochastic method based on the probability of damage, Monte Carlo simulation, and reliability analyses are used. Standard deviation and distribution functions used in service life calculation are presented in Appendix A.

3.1   General

The service life of hot-dip galvanised reinforcement bars can be divided into three sections: the initiation time, the propagation time for the zinc coating, and the propagation time for an ordinary steel reinforcement bar. The deterministic formulae used are calculated as follows:

$$t_L = t_0 + t_1 + t_2, \tag{10}$$

where t_L is the service life of a reinforced concrete structure [a],

                 t_0 is the initiation time [a],

                 t_1 is the propagation time for the zinc coating [a], and

                 t_2 is the propagation time for an ordinary steel reinforcement bar [a].[1,2]

In the equation t_0 is the time when the state of the corrosion of the zinc coating is insignificant (passive state), t_1 is the time when the state of the corrosion of the zinc coating is from low to high (active state), and t_2 is the time when the state of the corrosion of an ordinary steel reinforcement bar is from low to high (active state). The propagation time t_2 begins after the zinc coating has corroded totally, and ends when the corrosion products spall the concrete cover or the maximum permitted corrosion depth is reached. The principle used in calculating the service life of hot-dip galvanised reinforcement bars is shown in Fig. 15. In the equation it is accepted that the level of confidence in an old structure decreases. The target service life t_{Ltarg} means the service life required for a reinforced concrete structure imposed by general rules, the client or the owner of the structure[3].

---

[1] Bertolini, L. et al. (2004). Corrosion of Steel in Concrete: Prevention, Diagnosis, Repair.
[2] Yeomans, S.R. (2004). Galvanized Steel Reinforcement in Concrete.
[3] Sarja, A., Vesikari, E. (1996). Durability Design of Concrete Structures.
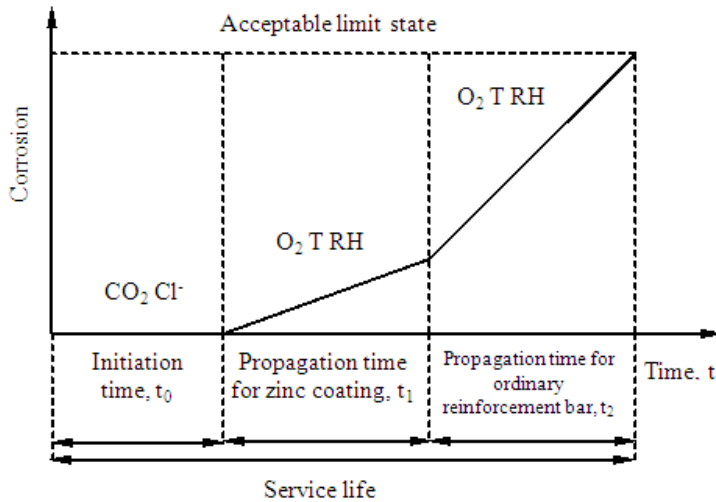
Fig. 15.   *The principle used in calculating the service life of hot-dip galvanised reinforcement bars.
The final limit state for the service life is the time after which the corrosion products spall
the concrete cover, or the maximum allowed corrosion depth is reached.*

Based on Fig. 15, explanations and alternatives of the service life evaluation are
presented in the following. In general, deterioration phenomena comply with the simple
mathematical model[1]:

$$ s = k \cdot t^n \text{,} \tag{11} $$

where s is the deterioration depth or grade,
               k is the coefficient,
               t is the deterioration time [a], and
               n is the exponent of time [-].

The exponent of time is equal to one if the deterioration is uniform. In the case of the
accelerated deterioration the exponent of time is greater than one. If the deterioration is
decreasing the exponent of time is less than one. As k is assumed to be constant the first
derivate of Equation (11) gives for the rate of deterioration:

$$ r = n \cdot k \cdot t^{n-1} \text{,} \tag{12} $$

where r is the deterioration rate,
               k is the coefficient,
               t is the deterioration time [a], and
               n is the exponent of time [-].

Obtained from Equation (11) by marking s equal to s_{max}, and t equal to t_L the service life
of a reinforced concrete structure can be expressed as follows:

$$ t_L = \left(\frac{s_{max}}{k} \right)^{\frac{1}{n}} \text{,} \tag{13} $$

---

[1] Clifton, J.R., Pommersheim, J.M., (1992). Methods for Predicting the remaining service life of concrete
in structures.

where t_L is the service life of a reinforced concrete structure [a],

s_{max} is the maximum deterioration depth or grade allowed,

k is the coefficient, and

n is the exponent of time [-].

In the case of carbonation, based on Fick's law, the exponent of time is equal to 0.5. Adapted from Equation (13) by marking s_{max} equal to c, k equal to c_{carb}, and t_L equal to t_0 the initiation time of corrosion in carbonated uncracked concrete can be expressed as follows:

$$t_0 = \left(\frac{c}{c_{carb}}\right)^2 , \tag{14}$$

where t_0 is the initiation time [a],

c is the thickness of the concrete cover [mm], and

c_{carb} is the coefficient of carbonation $[mm/(a)^{\frac{1}{2}}]$.

In the case of chloride attack, based on Fick's law, the exponent of time is equal to 0.5. Adapted from Equation (13) by marking s_{max} equal to c, k equal to k_{cl}, and t_L equal to t_0 the initiation time of corrosion in chloride-contaminated uncracked concrete can be expressed as follows:

$$t_0 = \left(\frac{c}{k_{cl}}\right)^2 , \tag{15}$$

where t_0 is the initiation time [a],

c is the thickness of the concrete cover [mm], and

k_{cl} is the coefficient of the critical chloride content $[mm/(a)^{\frac{1}{2}}]$.

The initiation time of corrosion at crack in carbonated concrete can be expressed as[1]:

$$t_0 = \frac{1}{4} \cdot \frac{c^4}{w^2 \cdot c_{carb}^2} \cdot \left(\frac{D_e}{D_{cr}}\right)^2 , \tag{16}$$

where t_0 is the initiation time [a],

c is the thickness of the concrete cover [mm],

w is the crack width [mm],

c_{carb} is the coefficient of carbonation $[mm/(a)^{\frac{1}{2}}]$,

D_e is the diffusion coefficient of the concrete with respect to carbon dioxide $[mm^2/a]$, and

D_{cr} is the diffusion coefficient of the crack with respect to carbon dioxide $[mm^2/a]$.

An approximate estimate of the carbonation depth from the equation (16) at a crack can be presented as follows[2]:

---

[1] Schieβl, P. (1976). Regarding the Question of maximum Crack Width and the required Concrete Cover in Reinforced Concrete Structures paying particular Attention to the Carbonation of the Concrete.
[2] Vesikari, E. (1981). Corrosion of Reinforcing Steels at Cracks in Concrete.

$$d_{cr} = 50 \cdot \sqrt{w} \cdot \sqrt[4]{t} \ , \qquad (17)$$

where d_{cr} is the carbonation depth at a crack [mm],
           w   is the crack width [mm], and
           t   is the time [a].

Corrosion of steel can be assumed to initiate a crack when the top of the carbonated zone reaches the steel. Thus, the initiation time of corrosion from Equation (17) is obtained:

$$t_0 = \left(\frac{c}{50 \cdot \sqrt{w}} \right)^4 \ , \qquad (18)$$

where t_0 is the initiation time [a],
           c   is the thickness of the concrete cover [mm], and
           w   is the crack width [mm].

The initiation time of corrosion at crack in chloride-contaminated concrete can be expressed as[1]:

$$t_0 = \frac{7^2}{12^2} \cdot \frac{c^4}{w^2 \cdot k_{cl}^2 \cdot \left(1 - \sqrt{\dfrac{C_{cr}}{C_1}} \right)^2} \cdot \left(\frac{D_c}{D_{ccr}} \right)^2 \ , \qquad (19)$$

where t_0 is the initiation time [a],
           c   is the thickness of the concrete cover [mm],
           w   is the crack width [mm],
           k_{cl} is the coefficient of the critical chloride content [mm/(a)^{½}],
           C_{cr} is the critical chloride content [wt%$_{CEM}$],
           C_1 is the surface chloride content [wt%$_{CEM}$],
           D_c is the chloride diffusion coefficient of the concrete [mm^2/a], and
           D_{ccr} is the diffusion coefficient of the crack with respect to chloride ions [mm^2/a].

In the case of uniform rate of corrosion for the zinc coating, the exponent of time is equal to one. Adapted from Equation (13) by marking s_{max} equal to d, k equal to r_1, and t_L equal to t_1 the propagation time for the zinc coating in uncracked and cracked carbonated or chloride-contaminated concrete can be expressed as follows:

$$t_1 = \left(\frac{d}{r_1} \right) \ , \qquad (20)$$

where t_1 is the propagation time for the zinc coating [a],
           d   is the thickness of zinc coating [μm], and
           r_1 is the rate of corrosion [μm/a].

---

[1] Vesikari, E. (2009). Carbonation and Chloride Penetration in Concrete - with Special Objective of Service Life Modelling by the Factor Approach.

In the case of decreasing rate of corrosion for the zinc coating, the exponent of time is equal to 0.5. Adapted from Equation (13) by marking s_{max} equal to d, k equal to k_1, and t_L equal to t_1 the propagation time for the zinc coating in uncracked and cracked carbonated or chloride-contaminated concrete can be expressed as follows:

$$t_1 = \left(\frac{d}{k_1} \right)^2 ,$$

(21)

where t_1 is the propagation time for the zinc coating [a],

           d   is the thickness of zinc coating [μm], and

           k_1 is the coefficient of the rate of corrosion [μm/(a)$^{1/2}$].

In uniform corrosion, the metal loss occurs at essentially the same rate over the entire surface of the metal. With a decreasing rate of corrosion the thicker rust layer reduces oxygen diffusion. The corrosion depth during the propagation time, where the corrosion products spall the concrete cover, is calculated as follows[1]:

$$s = \frac{80 \cdot c}{\text{ø}} ,$$

(22)

where   s   is the corrosion depth [μm],

           c   is the thickness of the concrete cover [mm], and

           ø   is the diameter of the reinforcement bar [mm].

The equation is based on laboratory studies and theoretical analyses. The coefficient of 80 μm as a unit in the calculation formula is a simplification based on empirical study.

In the case of uniform rate of corrosion for an ordinary steel reinforcement bar, the exponent of time is equal to one. Adapted from Equation (13) by marking s_{max} equal to s (Equation (22)), k equal to r_s, and t_L equal to t_2 the propagation time for an ordinary steel reinforcement bar in uncracked carbonated or chloride-contaminated concrete can be expressed as follows:

$$t_2 = \left(\frac{80 \cdot c}{r_s \cdot \text{ø}} \right) ,$$

(23)

where t_2 is the propagation time for an ordinary steel reinforcement bar [a],

           c   is the thickness of the concrete cover [mm],

           r_s is the rate of corrosion [μm/a], and

           ø   is the diameter of the reinforcement bar [mm].

In the case of decreasing rate of corrosion for an ordinary steel reinforcement bar, the exponent of time is equal to 0.5. Adapted from Equation (13) by marking s_{max} equal to s (Equation (22)), k equal to k_s, and t_L equal to t_2 the propagation time for an ordinary

---

[1] Siemens, A. et al. (1985). Durability of Buildings: a Reliability Analysis.

steel reinforcement bar in uncracked carbonated or chloride-contaminated concrete can be expressed as follows:

$$t_2 = \left(\frac{80 \cdot c}{k_s \cdot \o} \right)^2 , \qquad (24)$$

where
t_2 is the propagation time for an ordinary steel reinforcement bar [a],

c is the thickness of the concrete cover [mm],

k_s is the coefficient of the rate of corrosion [$\mu m/(a)^{1/2}$], and

$\o$ is the diameter of the reinforcement bar [mm].

In the case of uniform rate of corrosion for an ordinary steel reinforcement bar, the exponent of time is equal to one. Adapted from Equation (13) by marking k equal to r_2, and t_L equal to t_2 the propagation time for an ordinary steel reinforcement bar in cracked carbonated or chloride-contaminated concrete can be expressed as follows:

$$t_2 = \left(\frac{s_{max}}{r_2} \right) , \qquad (25)$$

where
t_2 is the propagation time for an ordinary steel reinforcement bar [a],

s_{max} is the maximum permitted corrosion depth of a reinforcement [μm], and

r_2 is the rate of corrosion [$\mu m/a$].

In the case of decreasing rate of corrosion for an ordinary steel reinforcement bar, the exponent of time is equal to 0.5. Adapted from Equation (13) by marking k equal to k_2, and t_L equal to t_2 the propagation time for an ordinary steel reinforcement bar in cracked carbonated or chloride-contaminated concrete can be expressed as follows:

$$t_2 = \left(\frac{s_{max}}{k_2} \right)^2 , \qquad (26)$$

where
t_2 is the propagation time for an ordinary steel reinforcement bar [a],

s_{max} is the maximum permitted corrosion depth of a reinforcement [μm], and

k_2 is the coefficient of the rate of corrosion [$\mu m/(a)^{1/2}$].

The deterministic formulae used in the calculation of the service life are presented in Table 6. The magnitudes of the symbols are presented in Table 8, Table 9, Table 10, Table 11, and Table 12.[1,2,3,1,2,3,4]

---

[1] Vesikari, E. (1988). Service Life of Concrete Structures with regard to Corrosion of Reinforcement.
[2] Siemens, A. et al. (1985). Durability of Buildings: a Reliability Analysis.
[3] Schieβl, P. (1976). Regarding the Question of maximum Crack Width and the required Concrete Cover in Reinforced Concrete Structures paying particular Attention to the Carbonation of the Concrete.

Table 6. *Deterministic formulae used in calculation of the service life of hot-dip galvanised reinforcement bars. The symbol $\mu(t_L)$ represents the mean service life value.*

	Carbonated uncracked concrete[5,6,7,8,9]	Carbonated cracked concrete[10,11,12,13]
Uniform rate of corrosion	$\mu(t_L) = \left(\dfrac{c}{c_{carb}}\right)^2 + \left(\dfrac{d}{r_1}\right) + \left(\dfrac{80 \cdot c}{r_s \cdot \o}\right)$	$\mu(t_L) = \left(\dfrac{k_x}{w}\right)^2 \cdot \left(\dfrac{c}{50}\right)^4 + \left(\dfrac{k_x \cdot d}{r_1}\right) + \left(\dfrac{k_x \cdot s_{max}}{r_2}\right)$
Decreasing rate of corrosion	$\mu(t_L) = \left(\dfrac{c}{c_{carb}}\right)^2 + \left(\dfrac{d}{k_1}\right)^2 + \left(\dfrac{80 \cdot c}{k_s \cdot \o}\right)^2$	$\mu(t_L) = \left(\dfrac{k_x}{w}\right)^2 \cdot \left(\dfrac{c}{50}\right)^4 + \left(\dfrac{k_x \cdot d}{k_1}\right)^2 + \left(\dfrac{k_x \cdot s_{max}}{k_2}\right)^2$
	Chloride-contaminated uncracked concrete[14,15,16]	Chloride-contaminated cracked concrete[17,18,19,20]
Uniform rate of corrosion	$\mu(t_L) = \left(\dfrac{c}{k_{cl}}\right)^2 + \left(\dfrac{d}{r_1}\right) + \left(\dfrac{80 \cdot c}{r_s \cdot \o}\right)$	$\mu(t_L) = \left(\dfrac{k_x}{w}\right)^2 \cdot \left(\dfrac{c}{50}\right)^4 + \left(\dfrac{k_x \cdot d}{r_1}\right) + \left(\dfrac{k_x \cdot s_{max}}{r_2}\right)$
Decreasing rate of corrosion	$\mu(t_L) = \left(\dfrac{c}{k_{cl}}\right)^2 + \left(\dfrac{d}{k_1}\right)^2 + \left(\dfrac{80 \cdot c}{k_s \cdot \o}\right)^2$	$\mu(t_L) = \left(\dfrac{k_x}{w}\right)^2 \cdot \left(\dfrac{c}{50}\right)^4 + \left(\dfrac{k_x \cdot d}{k_1}\right)^2 + \left(\dfrac{k_x \cdot s_{max}}{k_2}\right)^2$

In the case of uniform rate of corrosion the exponent of time presented in this study is equal to one. As rate of corrosion is decreasing the exponent of time is stated as 0.5. The initiation time at carbonated uncracked concrete is assumed to be the same for the

[1] Vesikari, E. (1981). Corrosion of Reinforcing Steels at Cracks in Concrete.

[2] Sistonen, E. et al. (2006). Stochastic Method and Monte Carlo Simulation for Predicting Service Life of Hot-Dip Galvanised Reinforcement.

[3] Sistonen, E. et al. (2000). Restricting Corrosion Risk in Reinforced Concrete Structures under Outdoor Conditions.

[4] Sistonen, E. et al. (2002). Restricting Corrosion Risk in Reinforced Concrete Structures under Outdoor Conditions – Part II.

[5] Vesikari, E. (1988). Service Life of Concrete Structures with regard to Corrosion of Reinforcement.

[6] Siemens, A. et al. (1985). Durability of Buildings: a Reliability Analysis.

[7] Sistonen, E. et al. (2006). Stochastic Method and Monte Carlo Simulation for Predicting Service Life of Hot-Dip Galvanised Reinforcement.

[8] Sistonen, E. et al. (2000). Restricting Corrosion Risk in Reinforced Concrete Structures under Outdoor Conditions.

[9] Sistonen, E. et al. (2002). Restricting Corrosion Risk in Reinforced Concrete Structures under Outdoor Conditions – Part II.

[10] Schießl, P. (1976). Regarding the Question of maximum Crack Width and the required Concrete Cover in Reinforced Concrete Structures paying particular Attention to the Carbonation of the Concrete.

[11] Vesikari, E. (1981). Corrosion of Reinforcing Steels at Cracks in Concrete.

[12] Sistonen, E., et al. (2006). Stochastic Method and Monte Carlo Simulation for Predicting Service Life of Hot-Dip Galvanised Reinforcement.

[13] Sistonen, E. et al. (2002). Restricting Corrosion Risk in Reinforced Concrete Structures under Outdoor Conditions – Part II.

[14] Siemens, A. et al. (1985). Durability of Buildings: a Reliability Analysis.

[15] Sistonen, E. et al. (2006). Stochastic Method and Monte Carlo Simulation for Predicting Service Life of Hot-Dip Galvanised Reinforcement.

[16] Sistonen, E. et al. (2002). Restricting Corrosion Risk in Reinforced Concrete Structures under Outdoor Conditions – Part II.

[17] Schießl, P. (1976). Regarding the Question of maximum Crack Width and the required Concrete Cover in Reinforced Concrete Structures paying particular Attention to the Carbonation of the Concrete.

[18] Vesikari, E. (1981). Corrosion of Reinforcing Steels at Cracks in Concrete.

[19] Sistonen, E. et al. (2006). Stochastic Method and Monte Carlo Simulation for Predicting Service Life of Hot-Dip Galvanised Reinforcement.

[20] Sistonen, E. et al. (2002). Restricting Corrosion Risk in Reinforced Concrete Structures under Outdoor Conditions – Part II.

studied reinforcement bar types. To be exact, there are differences between different reinforcement bar types (see Chapter 2.2.4). However, the used simplification is relevant for the comparative analysis.

The simplified Equation (18) is used in this study also at cracked chloride-contaminated concrete for the initiation time. It should be pointed out that the coefficient of the critical chloride content, the critical chloride content, and the surface chloride content affect the usability of the used model in a different way than the coefficient of carbonation (cf. Equation (16) and Equation (19)). For instance, the coefficient of the critical chloride content depends on the reinforcement bar type. Furthermore, diffusion properties are different. However, in many cases the initiation time is shorter in chloride-contaminated than in carbonated concrete. Thus, the used simplification is relevant for the comparative analysis. On the basis of the possibility to control cracks by means of the rib geometry of reinforcement, and thus improve the durability of outdoor reinforced concrete structures, coefficient of relative rib area k_x is added to the service life estimation (Table 6)[1].

Concrete carbonation can be estimated with an empirical model,[2] which is based on the water-to-binder ratio of concrete and obeys a basic square root assumption of carbonation ($x = A + B \cdot \sqrt{t}$). The empirical model developed takes into account the effects of mineral admixtures as well. The model is given thus:

$$x = 3 \cdot \left(\frac{w}{b} - 0.25\right) \cdot (1 + 0.02 \cdot k - 0.045 \cdot s) + \frac{\frac{10.8}{1.6 - \frac{w}{b}} - 8 + 0.3 \cdot (a - 2) + 0.03 \cdot s + 0.022 \cdot k}{1.05 - 0.01 \cdot s - 0.0022 \cdot k} \cdot \sqrt{t_0}, \tag{27}$$

where   x   is the carbonation depth [mm],
         w/b   is the water-to-binder ratio of concrete [-],
         k   is the proportion of blast furnace slag in the cement [%],
         a   is the amount of the air in the concrete, and
         t_0 is the initiation time [a].

The model is based on a test series with different concretes exposed to natural outdoor carbonation sheltered from rain. The coefficient of carbonation in the model is calculated as follows:

$$c_{carb} = \frac{k_e \cdot x}{\sqrt{t_0}}, \tag{28}$$

where c_{carb} is the coefficient of carbonation [mm/(a)$^{1/2}$],
         k_e is the circumstantial factor [-],
         x   is the carbonation depth [mm], and
         t_0 is the initiation time [a].

The circumstantial factor is 1.0 for structures sheltered from rain and 0.5 for structures exposed to rain. The model is used in this study in the case of Monte Carlo simulation

---

[1] Sistonen, E. et al. (2005). Possibilities of Controlling Cracks and Improving the Durability of Outdoor Reinforced Concrete Structures.
[2] Matala, S. (1991). Calculation methods of service life.

and reliability analyses. Obtained from Equation (11) by marking k equal to k_s, t equal to t_2, and n equal to 0.5, the corrosion depth is calculated as follows:

$$s = k_s \cdot \sqrt{t_2} \quad , \tag{29}$$

where
s   is the corrosion depth [μm],
k_s is the coefficient of the rate of corrosion [μm/(a)$^{1/2}$], and
t_2 is the propagation time [a].

As k_s is assumed to be constant the first derivate of Equation (29) gives the equivalent value for the rate of corrosion:

$$r_s = \frac{k_s}{2 \cdot \sqrt{t_2}} \quad , \tag{30}$$

where
r_s is the uniform rate of corrosion [μm/a],
k_s is the coefficient of the rate of corrosion [μm/(a)$^{1/2}$], and
t_2 is the propagation time [a].

Obtained from Equation (12) by marking r equal to r_s, k equal to k_s, t equal to t_2, and n equal to 0.5, gives also the Equation (30). Calculated correspondence between the uniform rate of corrosion r_s and the coefficient of the rate of corrosion k_s (assumed constant) as a function of propagation time t_2 is shown in Fig. 16.
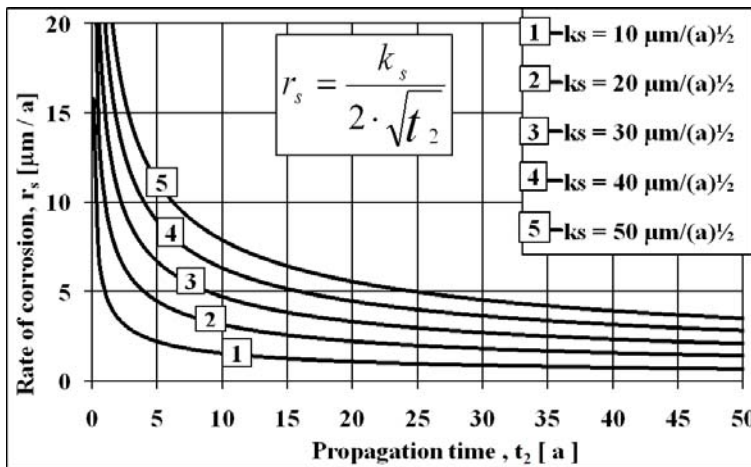
Fig. 16.   *The rate of corrosion r_s as a function of the coefficient of the rate of corrosion k_s and propagation time t_2.*

It should be noted that Equation (30) can not be combined together with Equation (29) and Equation (22) and further compare it with the uniform rate of corrosion because the exponent of time, n equal to one in the uniform rate of corrosion differs from the exponent of time, n equal to 0.5 in the decreasing rate of corrosion. Furthermore, the coefficient k_s has different status in Equation (29) and Equation (30). The corrosion depth s as a function of the thickness of the concrete cover c and the diameter of the reinforcement bar Ø is shown in Fig. 17.
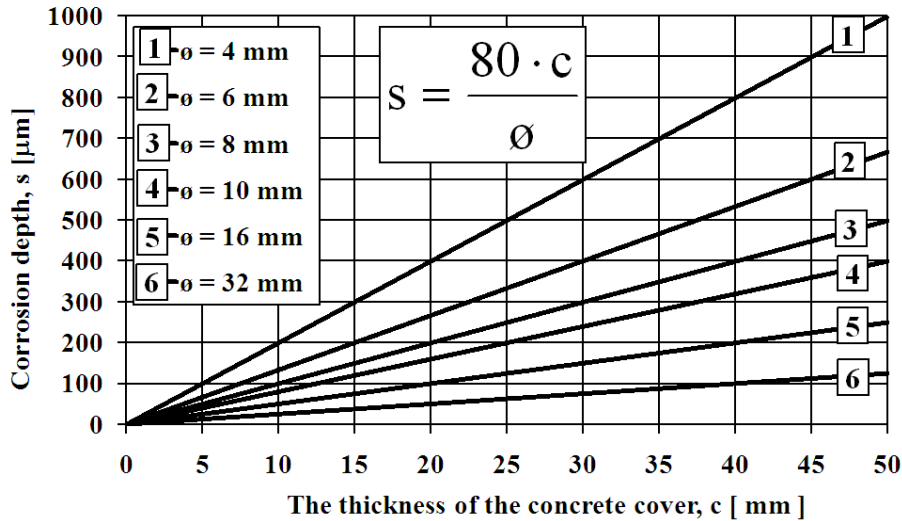
Fig. 17.   *Corrosion depth s as a function of the thickness of the concrete cover c and reinforcement bar diameter Ø.*

The chloride diffusion coefficient of concrete at the time of initiation is calculated as follows[1]:

$$D_c = 0.6 \cdot (55 - f_{cm})^2 + 15 \,, \tag{31}$$

where D_c is the chloride diffusion coefficient of the concrete [mm^2/a], and

                 f_{cm} is the cubic (10cm×10cm×10cm) compressive strength of the concrete [MPa].

The equation is not valid for concrete strength values above 55 MPa. The initiation time in chloride-contaminated uncracked concrete is calculated as follows[2]:

$$t_0 = \frac{1}{12 \cdot D_c} \cdot \left(\frac{c}{1 - \sqrt{\dfrac{C_{cr}}{C_1}}} \right)^2 , \tag{32}$$

where t_0 is the initiation time [a],

                 D_c is the chloride diffusion coefficient of the concrete [mm^2/a],

                 c is the thickness of the concrete cover [mm],

                 C_{cr} is the critical chloride content [wt%$_{CEM}$], and

                 C_1 is the surface chloride content [wt%$_{CEM}$].

Equation (32) is based on the basic error-function assumption derived from Fick's diffusion theory. The calculation formula is a simplified parabola function. After adding the initiation time from Equation (15) to Equation (32), the coefficient of the critical chloride content is calculated as follows:

---

[1] Finnish Association of Civil Engineers (1995). RIL 183-4.9-1995. Service Life of Construction Materials and Structures. Methods of Appraisal.
[2] Vesikari, E. (1988). Service Life of Concrete Structures with regard to Corrosion of Reinforcement.

$$k_{cl} = \sqrt{12 \cdot D_c} \cdot \left(1 - \sqrt{\frac{C_{cr}}{C_1}} \right), \tag{33}$$

where

	k_{cl}	is the coefficient of the critical chloride content $[mm/(a)^{1/2}]$,
	D_c	is the chloride diffusion coefficient of concrete $[mm^2/a]$,
	C_{cr}	is the critical chloride content $[wt\%_{CEM}]$, and
	C_1	is the surface chloride content $[wt\%_{CEM}]$.

The coefficient of critical water-soluble chloride content C_{cr} with different reinforcement bar materials is presented[1,2,3,4] in Table 7. The assumption of the ratio of weight of concrete to the weight of cement is six. It should be pointed out that the ratio depends on the concrete mix proportion. Values are specified for concrete specimens to which chlorides were added during the casting process. Carbonation has a decreasing effect on the coefficient of the critical chloride content, which is not catered for in the table. Lower values than those presented in the table provide the coefficients of critical chloride content for carbonated chloride-contaminated concrete.

Table 7.   The critical water-soluble chloride content with different reinforcement bar types (C_{cr}) in uncarbonated concrete.

Reinforcement bar	wt% (Cl⁻) weight of cement	wt% (Cl⁻) weight of concrete
Ordinary steel reinforcement bar	0.3 - 0.4	0.05 - 0.07
Weathering steel reinforcement bar (TENCOR)	0.3 - 0.4	0.05 - 0.07
Hot-dip galvanised steel reinforcement bar	1.0 - 1.5	0.17 - 0.25
Austenitic stainless steel reinforcement bar	3.0 - 4.0	0.50 - 0.67

The coefficient of the critical chloride content k_{cl}, as a function of the chloride diffusion coefficient of concrete D_c, the critical chloride content C_{cr}, concrete strength f_{cm}, and the surface chloride content C_1 are shown in Fig. 18. The corrosion parameters used in the service life calculation are presented in Table 8, Table 9, Table 10, Table 11, and Table 12. The corrosion depth is related to a loss of section of the reinforcing steels.[5,6,7,8,9]

[1] Hausmann, D.A. (1967). Steel Corrosion in Concrete: How Does It Occur?

[2] Collepardi, M. (2000). Ordinary and Long-Term Durability of Reinforced Concrete Structures.

[3] Treadaway, K.W.J. (1989). Durability of Corrosion Resisting Steels in Concrete.

[4] Sistonen, E. et al. (2002). Restricting Corrosion Risk in Reinforced Concrete Structures under Outdoor Conditions – Part II.

[5] Siemens, A. et al. (1985). Durability of Buildings: a Reliability Analysis.

[6] Vesikari, E. (1988). Service Life of Concrete Structures with regard to Corrosion of Reinforcement.

[7] Bertolini, L. et al. (2004). Corrosion of Steel in Concrete – Prevention, Diagnosis, Repair.

[8] Andrade, C. et al. (1992). Protection Systems for Reinforcement.

[9] Angst, U. et al. (2007). Critical chloride content - State of the Art.
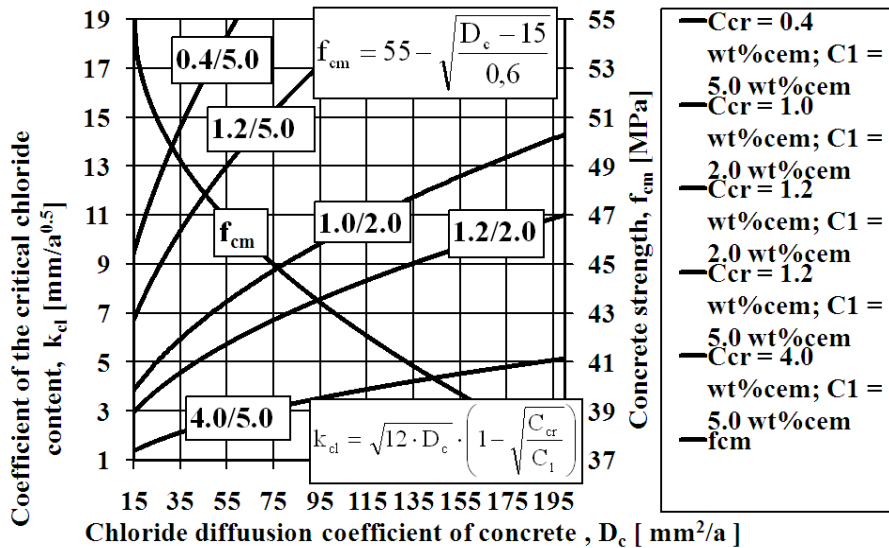
Fig. 18.   *The coefficient of the critical chloride content k_{cl} as a function of the chloride diffusion coefficient of concrete D_c, the critical chloride content C_{cr}, concrete strength f_{cm}, and the surface chloride content C_l.*

The values of the coefficient of variation in Table 8, Table 9, Table 10, Table 11, and Table 12 are evaluated with the literature used[1,2,3,4,5] and with expert estimation by the author. For instance, the aggregate size, curing time, and type of cement influence the coefficient of variation for the thickness of the concrete cover, coefficient of carbonation, and the coefficient of the critical chloride content. The reason for the coefficient of variation used for the reinforcement bar diameter and coefficient of relative rib area is that in a condition survey the exact bar diameter and type cannot reliably be proved without destructive studies. On the basis of factors presented in Chapter 2, the coefficient of variation used for the thickness of the zinc coating can be substantiated. The coefficient of variation for the crack width and the maximum allowed corrosion depth of the reinforcement bar can be justified by the differences and difficulties involved in the measurement. The assumption for the mean value of the maximum corrosion depth of a reinforcement allowed in the cracked concrete is that the migration of the corrosion products is possible from the concrete structure. The reason for the value used for the coefficient of the variation for the rate of corrosion and coefficient of the rate of corrosion is that they represent long-term values, including seasonal variation. The rate of corrosion and coefficient of the rate of corrosion in uncracked or cracked carbonated concrete for austenitic stainless steel reinforcement bars are assumed to be nil. The reason for this is that these circumstances are too mild for the above-mentioned reinforcement bar type to corrode.

---

[1] Finnish Association of Civil Engineers (1995). RIL 183-4.9-1995. Service Life of Construction Materials and Structures. Methods of Appraisal.
[2] Sarja, A., Vesikari, E. (1996). Durability Design of Concrete Structures.
[3] Vesikari, E. (1988). Service Life of Concrete Structures with regard to Corrosion of Reinforcement.
[4] Sarja, A. (2006). European Symposium on Service Life and Serviceability of Concrete Structures, ESCS-2006.
[5] Sarja, A. (2000). Integrated Life-Cycle Design of Materials and Structures, ILCDES 2000.

Table 8.   *Corrosion parameters (basic values).*

| Parameter | Symbol | Mean value | | | Coefficient of variation, ν [-] |
		Typical value	Range for typical value	Unit	
The thickness of the concrete cover	c	30	5…50	mm	0.25
Coefficient of carbonation	c_{carb}	2.5	1…7	mm/(a)$^{1/2}$	0.25
Reinforcement bar diameter	Ø	12	4…32	mm	0.15
Thickness of zinc coating	d	200	50…275	µm	0.25
Crack width	w	0.2	0.1…0.7	mm	0.25
Coefficient of relative rib area	k_x	1.0	0.8…1.2	-	0.15
Maximum corrosion depth of reinforcement allowed	s_{max}	500	100..1000	µm	0.25
The coefficient of the critical chloride content	k_{cl}	3	1…15	mm/(a)$^{1/2}$	0.25

Table 9.   *Corrosion parameters (carbonated uncracked concrete).*

| Parameter | Symbol | Mean value | | | Coefficient of variation, ν [-] |
		Typical value	Range for typical value	Unit	
Rate of corrosion in uncracked carbonated concrete [hot-dip galvanised reinforcement]	r_1	3	1…10	µm/a	0.40
Rate of corrosion in uncracked carbonated concrete [ordinary steel reinforcement]	r_s	8	1…50	µm/a	0.40
Rate of corrosion in uncracked carbonated concrete [weathering steel reinforcement]	r_s	5	1…50	µm/a	0.40
Coefficient of the rate of corrosion in uncracked carbonated concrete [galvanised reinforcement]	k_1	14	10…30	µm/(a)$^{1/2}$	0.40
Coefficient of the rate of corrosion in uncracked carbonated concrete [ordinary reinforcement]	k_s	17	10…30	µm/(a)$^{1/2}$	0.40
Coefficient of the rate of corrosion in uncracked carbonated concrete [weathering reinforcement]	k_s	15	10…30	µm/(a)$^{1/2}$	0.40

Table 10.   *Corrosion parameters (carbonated cracked concrete).*

| Parameter | Symbol | Mean value | | | Coefficient of variation, ν [-] |
		Typical value	Range for typical value	Unit	
Rate of corrosion in cracked carbonated concrete [hot-dip galvanised reinforcement]	r_1	5	1…10	μm/a	0.40
Rate of corrosion in cracked carbonated concrete [ordinary steel reinforcement]	r_2	10	5…15	μm/a	0.40
Rate of corrosion in cracked carbonated concrete [weathering steel reinforcement]	r_2	8	5…15	μm/a	0.40
Coefficient of the rate of corrosion in cracked carbonated concrete [galvanised reinforcement]	k_1	30	10…60	μm/(a)$^{1/2}$	0.40
Coefficient of the rate of corrosion in cracked carbonated concrete [ordinary reinforcement]	k_2	40	10…60	μm/(a)$^{1/2}$	0.40
Coefficient of the rate of corrosion in cracked carbonated concrete [weathering reinforcement]	k_2	35	10…60	μm/(a)$^{1/2}$	0.40

Table 11.   *Corrosion parameters (chloride-contaminated uncracked concrete).*

Parameter	Symbol	Mean value Typical value	Range for typical value	Unit	Coefficient of variation, ν [-]
Rate of corrosion in uncracked chloride-contaminated concrete [hot-dip galvanised reinforcement]	r_1	20	5…50	$\mu m/a$	0.40
Rate of corrosion in uncracked chloride-contaminated concrete [ordinary steel reinforcement]	r_s	50	10…100	$\mu m/a$	0.40
Rate of corrosion in uncracked chloride-contaminated concrete [weathering steel reinforcement]	r_s	30	10…100	$\mu m/a$	0.40
Rate of corrosion in uncracked chloride-contaminated concrete [austenitic stainless steel reinforcement]	r_s	5	1…10	$\mu m/a$	0.40
Coefficient of the rate of corrosion in uncracked chloride-contaminated concrete [hot-dip galvanised reinforcement]	k_1	50	20…110	$\mu m/(a)^{1/2}$	0.40
Coefficient of the rate of corrosion in uncracked chloride-contaminated concrete [ordinary steel reinforcement]	k_s	75	20…110	$\mu m/(a)^{1/2}$	0.40
Coefficient of the rate of corrosion in uncracked chloride-contaminated concrete [weathering steel reinforcement]	k_s	60	20…110	$\mu m/(a)^{1/2}$	0.40
Coefficient of the rate of corrosion in uncracked chloride-contaminated concrete [austenitic stainless steel reinforcement]	k_s	10	1…50	$\mu m/(a)^{1/2}$	0.40

Table 12.   Corrosion parameters (chloride contaminated cracked concrete).

| Parameter | Symbol | Mean value | | | Coefficient of variation, ν [-] |
		Typical value	Range for typical value	Unit	
Rate of corrosion in cracked chloride-contaminated concrete [hot-dip galvanised reinforcement]	r_1	30	10…110	$\mu m/a$	0.40
Rate of corrosion in cracked chloride-contaminated concrete [ordinary steel reinforcement]	r_2	60	10…110	$\mu m/a$	0.40
Rate of corrosion in cracked chloride-contaminated concrete [weathering steel reinforcement]	r_2	40	10…110	$\mu m/a$	0.40
Rate of corrosion in cracked chloride-contaminated concrete [austenitic stainless steel reinforcement]	r_2	10	1…50	$\mu m/a$	0.40
Coefficient of the rate of corrosion in cracked chloride-contaminated concrete [hot-dip galvanised reinforcement]	k_1	75	10…110	$\mu m/(a)^{\frac{1}{2}}$	0.40
Coefficient of the rate of corrosion in cracked chloride-contaminated concrete [ordinary steel reinforcement]	k_2	90	10…110	$\mu m/(a)^{\frac{1}{2}}$	0.40
Coefficient of the rate of corrosion in cracked chloride-contaminated concrete [weathering steel reinforcement]	k_2	80	10…110	$\mu m/(a)^{\frac{1}{2}}$	0.40
Coefficient of the rate of corrosion in cracked chloride-contaminated concrete [austenitic stainless steel reinforcement]	k_2	20	1…50	$\mu m/(a)^{\frac{1}{2}}$	0.40

3.2   Stochastic method based on probability of damage

This section concerns a parametric study that includes the deterministic service life formulae presented in Table 8, Table 9, Table 10, Table 11, and Table 12. The service life nomograph[1,2,3] for hot-dip galvanised reinforcement bars in carbonated uncracked concrete with a deterioration probability of 5% is presented in Fig. 19 (uniform rate of corrosion). The relative significance of the corrosion parameters (influence on maximum error) for hot-dip galvanised reinforcement bars as a function of the rate of corrosion r_s in carbonated uncracked concrete is shown in Fig. 20 (uniform rate of corrosion). The service life nomograph for hot-dip galvanised reinforcement bars in carbonated uncracked concrete with a deterioration probability of 5% is presented in Fig. 21 (decreasing rate of corrosion). The relative significance of the corrosion parameters for hot-dip galvanised reinforcement bars as a function of the coefficient of

---

[1] Sistonen, E. et al. (2006). Stochastic Method and Monte Carlo Simulation for Predicting Service Life of Hot-Dip Galvanised Reinforcement.

[2] Sistonen, E. et al. (2005). Problems in Service Life Modelling of corroded Outdoor Concrete Structures.

[3] Sistonen, E. et al. (2005). Possibilities of Controlling Cracks and Improving the Durability of Outdoor Reinforced Concrete Structures.

the rate of corrosion k_s in carbonated uncracked concrete is shown in Fig. 22 (decreasing rate of corrosion).

The service life nomograph for hot-dip galvanised reinforcement bars in carbonated uncracked concrete with a deterioration probability of 5% is presented in Fig. 23 (decreasing rate of corrosion). The service life nomograph for hot-dip galvanised reinforcement bars in carbonated cracked concrete with a deterioration probability of 5% is presented in Fig. 24 (uniform rate of corrosion). As can be seen in Fig. 20, the thickness of the concrete cover c, the coefficient of carbonation c_{carb}, and the rate of corrosion of hot-dip galvanised reinforcement bars r_l are the most significant parameters when the values of the rate of corrosion are high.

As can be seen in Fig. 22, the thickness of the concrete cover c, the coefficient of the rate of corrosion of hot-dip galvanised reinforcement bars k_1, and the coefficient of carbonation c_{carb} are the most significant parameters when the values of the coefficient of the rate of corrosion k_s are high. The service life nomograph for hot-dip galvanised reinforcement bars in chloride-contaminated uncracked concrete with a deterioration probability of 5% is presented in Fig. 25 (uniform rate of corrosion). The service life nomograph for hot-dip galvanised reinforcement bars in chloride-contaminated uncracked concrete with a deterioration probability of 5% is presented in Fig. 26 (decreasing rate of corrosion).

Fig. 19.   *The coefficient of carbonation c_{carb} as a function of the target service life and the rate of corrosion of a hot-dip galvanised reinforcement bar r_1 with a 5% probability of damage.*

Fig. 20.   *The relative significance of corrosion parameters as a function of the rate of corrosion of an ordinary steel reinforcement bar r_s in carbonated uncracked concrete.*
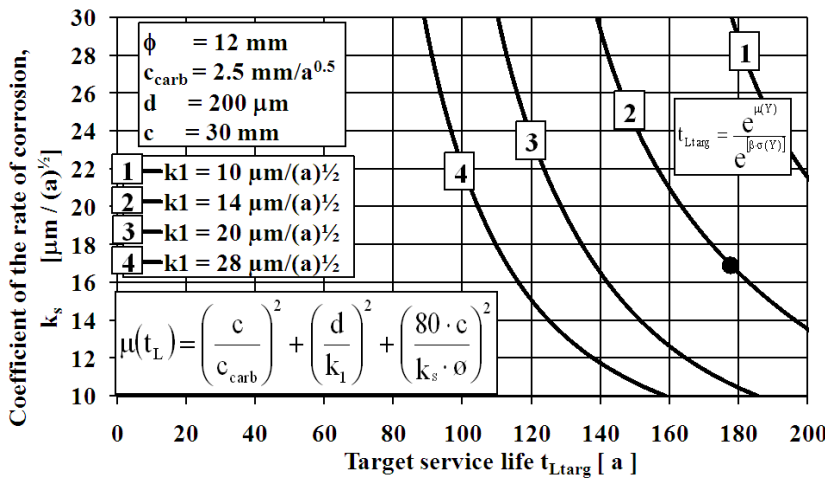
Fig. 21.   *The coefficient of the rate of corrosion of an ordinary steel reinforcement bar k_s as a function of the target service life and the coefficient of the rate of corrosion of a hot-dip galvanised reinforcement bar k_1 with a 5% probability of damage.*
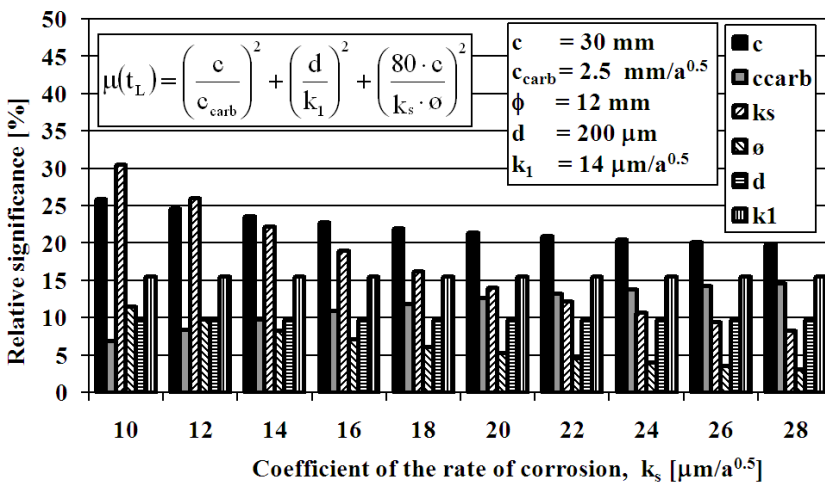
Fig. 22.   *The relative significance of corrosion parameters as a function of the coefficient of the rate of corrosion of the ordinary steel reinforcement bar k_s in carbonated uncracked concrete.*
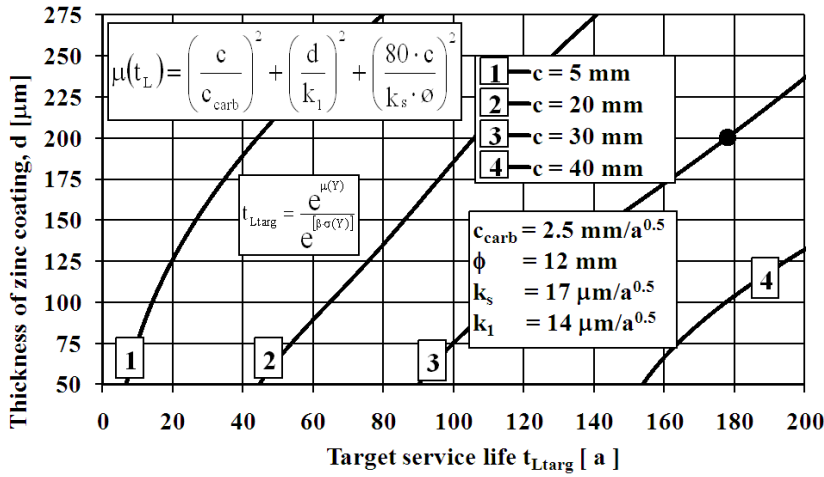
Fig. 23.   *Zinc coating thickness d as a function of the target service life and the thickness of the concrete cover c with a 5% probability of damage.*
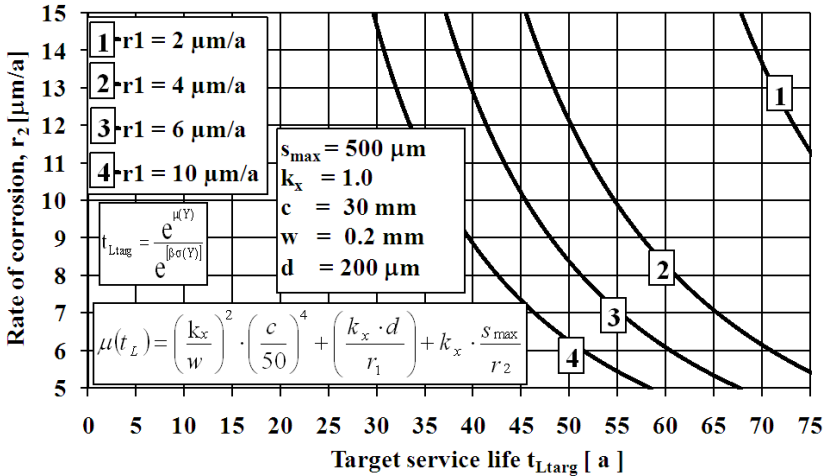
Fig. 24.   *Rate of corrosion of an ordinary steel reinforcement bar r₂ as a function of the target service life and rate of corrosion of a hot-dip galvanised reinforcement bar r₁ with a 5% probability of damage.*
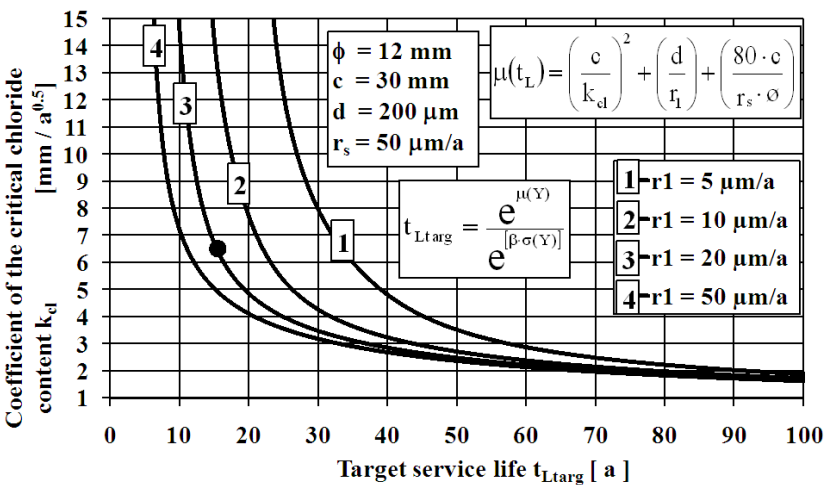
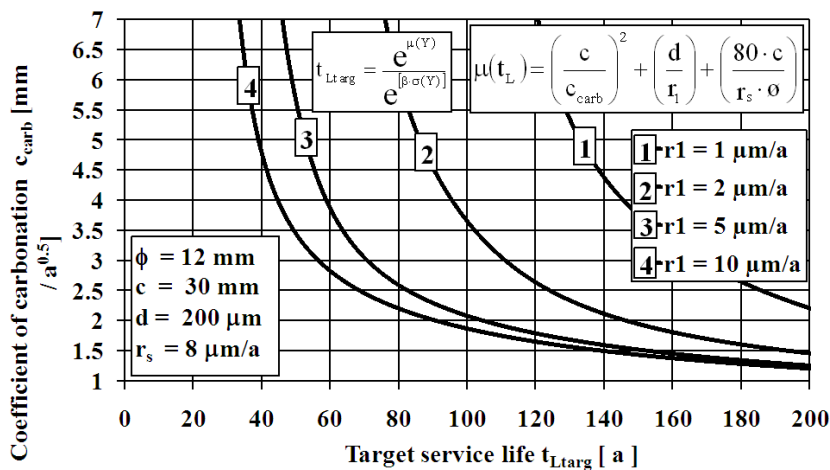Fig. 25.   *The coefficient of the critical content of chloride k_{cl} as a function of the target service life and the rate of corrosion of a hot-dip galvanised reinforcement bar r₁ with a 5% probability of damage.*
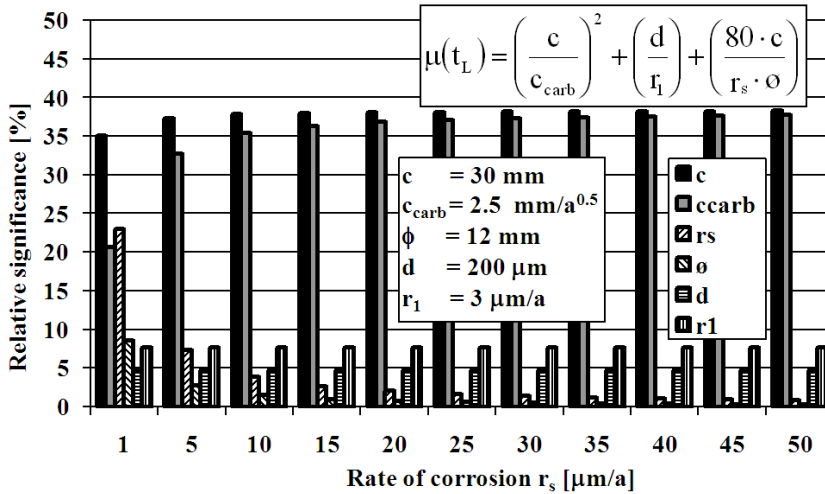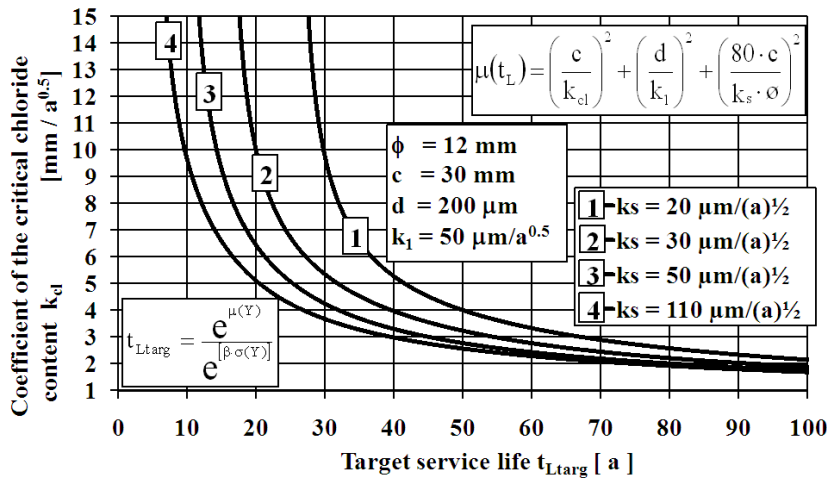
Fig. 26. *The coefficient of the critical chloride content k_{cl} as a function of the target service life and the coefficient of the rate of corrosion of an ordinary steel reinforcement bar k_s with a 5% probability of damage.*

Service life nomographs can be a practical method, for instance, in conducting a life cycle analysis and in the design process. A potential difficulty may arise in choosing the values of parameters appropriate to the specific circumstances in question. For example, based partly on the Delphi method, the estimates of the rates of corrosion given in the literature differ greatly from one another and are a possible source of error. The Delphi method is a systematic, interactive forecasting method which relies on a panel of independent experts. Recommendations for distribution models and values for the probability of deterioration can be included in building codes, but in practical design special attention should be paid to those measures and solutions which are deemed rational, for instance, in terms of life cycle economics, rather than to higher estimates of service life as such.[1]

Unreliability and difficulties in the interpretation can arise when a simplified service life calculation is used. The relative significance determined by using a random number generator or a stochastic method will give an idea of the corrosion parameters that contribute most effectively to extending the service life. In stochastic estimation, the most suitable deterministic formulae might be the ones that are of a power of three at the most. That depends on the study being performed[2]. The analysis showed that as a result of the high power of the parameter the absolute value of a partial derivate has a significance influence on the maximum error. Because of possible sources of error in service life calculation, it is recommended that priority is given to determining which of the parameters are the most significant in view of the target service life instead of relying on the estimates as such. All in all, the guiding principle in investigating deterioration, like any other physical phenomenon, should be that the stochastic service life estimation models scientifically used accounts adequately for its object.[3]

In carbonated intact concrete the significance of hot-dip galvanising increases on the service life when the rate of corrosion r_1 is less than or equal to 5 µm/a, and the coefficient of the rate of corrosion k_1 is less than or equal to 15 µm/a$^{\frac{1}{2}}$. Respectively, in

---

[1] Sistonen, E. et al. (2005). The Influence of Rebar Material on the Durability of Outdoor Reinforced Concrete Structures.

[2] Sistonen, E., (2001). The Main Corrosion Parameters and their Influence on the Durability of Outdoor Concrete Structures.

[3] Sistonen, E. et al. (2005). Problems in Service life Modelling of Corroded Outdoor Concrete Structures.

cracked carbonated concrete the significance of hot-dip galvanising increases when the rate of corrosion r_1 is less than or equal to 6 µm/a, and the coefficient of the rate of corrosion k_1 is less than or equal to 30 µm/a$^{1/2}$. The service life will be extended considerably when the crack width w is less than or equal to 0.2 mm and the maximum permitted corroded depth s_{max} is greater than or equal to 300 µm. The service life of a hot-dip galvanised reinforcement bar in cracked carbonated concrete will be extended considerably if the corrosion products do not cause significant spalling forces.[1,2]

In chloride-contaminated concrete the significance of hot-dip galvanising increases on the service life when the critical chloride content coefficient k_{cl} is less than or equal to 6 mm/a$^{1/2}$. Respectively, in chloride-contaminated uncracked concrete the significance of hot-dip galvanising also increases when the rate of corrosion r_1 is less than or equal to 15 µm/a, and the coefficient of the rate of corrosion k_1 is less than or equal to 50 µm/a$^{1/2}$.[3,4] Furthermore, in chloride-contaminated cracked concrete the significance of hot-dip galvanising increases on the service life when the rate of corrosion r_1 is less than or equal to 20 µm/a, and the coefficient of the rate of corrosion k_1 is less than or equal to 50 µm/a$^{1/2}$.

3.3 Stochastic method based on Monte Carlo simulation

The Monte Carlo simulation of hot-dip galvanised reinforcement bars, which includes the deterministic service life formulae presented in Table 8, Table 9, Table 10, and Table 11, is presented here with two examples: carbonated uncracked concrete (decreasing rate of corrosion) and chloride-contaminated uncracked concrete (uniform rate of corrosion)[5]. The study was made to analyse the effect of the distribution parameters on the service life of a concrete structure. In a Chi-Square test the fit for the coefficient of the determination of the distribution function is high when p is greater than or equal to 0.5. The mean values of the parameters used are the same as those presented in Table 8, Table 9, Table 10, and Table 11. The distribution parameters and probability distribution models differ from Table 8, Table 9, Table 10, and Table 11. That was done for sensitivity analysis purposes, for instance the effect of the standard deviation of the service life.

3.3.1 Carbonated uncracked concrete (decreasing rate of corrosion)

Table 13 and Fig. 27 present the values used and the relative significance of the corrosion parameters calculated with the Monte Carlo method. In this example, for a concrete structure subjected to carbonation, the coefficients chosen for the rate of corrosion correspond to a uniform rate of corrosion of a hot-dip galvanised reinforcement bar r_1 of 1.0 µm/a and a uniform rate of corrosion of an ordinary steel reinforcement bar r_s of 1.4 µm/a (Fig. 16).

[1] Sistonen, E. et al. (2005). The Main Corrosion Parameters and their Influence on the Durability of Outdoor Concrete Structures.
[2] Sistonen, E. et al. (2006). Stochastic Method and Monte Carlo Simulation for Predicting Service Life of Hot-Dip Galvanised Reinforcement.
[3] Sistonen, E. et al. (2005). The Main Corrosion Parameters and their Influence on the Durability of Outdoor Concrete Structures.
[4] Sistonen, E. et al. (2006). Stochastic Method and Monte Carlo Simulation for Predicting Service Life of Hot-Dip Galvanised Reinforcement.
[5] Sistonen, E. et al. (2006). Stochastic Method and Monte Carlo Simulation for Predicting Service Life of Hot-Dip Galvanised Reinforcement.

Table 13.   Corrosion parameters used in Monte Carlo simulation.

Parameter	Symbol	Mean value	Distribution parameter	Unit	Probability distribution	Relative significance [%]
The thickness of the concrete cover	c	30	L = 26 $\alpha = 4$ $\beta = 2$	mm	Weibull	16.4
Coefficient of carbonation	c_{carb}	2.5	L = 1.6 $\alpha = 1$ $\beta = 3$	$mm/(a)^{1/2}$	Weibull	18.8
Thickness of zinc coating	d	200	m = 200 s = 19	μm	Lognormal	23.8
Coefficient of the rate of corrosion of hot-dip galvanised reinforcement bar	k_1	14	m = 13; $\alpha = 1$	$\mu m/(a)^{1/2}$	Extreme value (Type 1)	18.1
Coefficient of the rate of corrosion of ordinary steel reinforcement bar	k_s	17	m = 16; $\alpha = 2$	$\mu m/(a)^{1/2}$	Extreme value (Type 1)	18.6
The diameter of a reinforcement bar	$\emptyset$	12	m = 12 s = 1	mm	Normal	4.4

The thickness of the concrete cover, c [mm]

Coefficient of carbonation, c_{carb} $[mm/(a)^{1/2}]$

Thickness of zinc coating, d [μm]

Coefficient of the rate of corrosion of hot-dip galvanised reinforcement bar, k_1 $[\mu m/(a)^{1/2}]$

Coefficient of the rate of corrosion of ordinary steel reinforcement bar, k_s $[\mu m/(a)^{1/2}]$

The diameter of a reinforcement bar, $\emptyset$ [mm]

Fig. 27.   Distribution of corrosion parameters.

The results of the Monte Carlo simulation are shown in Fig. 28 and Table 14. As compared with the stochastic method based on the probability of damage, service life estimates approximately 202 years longer are obtained with a 5% probability of damage. The reference value is marked with (●) in Fig. 21 and Fig. 23. This difference can be attributed to the fact that the standard deviation of the service life in the

simulation ($\sigma(t_L) \approx 90$ a) is smaller than in the stochastic method based on the probability of damage ($\sigma(t_L) \approx 276$ a).

Fig. 28.   *Probability density and cumulative distribution function: a fit of Gamma distribution [p = 0.34]). The horizontal axes indicate the time that has passed (in years).*

Table 14.   *Mean value of the service life and fit of Gamma distribution with a 5% and 10% probability of damage*

Initiation time	Propagation time for zinc coating	Propagation time for ordinary steel reinforcement bar	Mean value of the service life	A fit of Gamma distribution with a 5% probability of damage	A fit of Gamma distribution with a 10% probability of damage
t_0	t_1	t_2	t_L	$t_\phi = 5\%$	$t_\phi = 10\%$
[a]	[a]	[a]	[a]	[a]	[a]
144	204	138	486	379	405

It should be noticed that the values for the coefficient of the rate of corrosion used in Table 13 are extreme values. The reason for this is that in the case of a decreasing rate of corrosion a conservative hypothesis should be used. Furthermore, the values shown in Table 13 are assumed to be long-term mean values including seasonal variation.

3.3.2   Chloride-contaminated uncracked concrete (uniform rate of corrosion)

Table 15 and Fig. 29 present the values used and the relative significance of the corrosion parameters calculated with the Monte Carlo method. In this example, for a concrete structure subjected to chloride attack, the chloride diffusion coefficient of concrete D_c is 67 mm^2/a. It is calculated from these parameters: the surface chloride content C_1 is 2 wt%$_{CEM}$ (sea water, concrete structure in the Baltic Sea), the critical chloride content C_{cr} is 1.2 wt%$_{CEM}$ (hot-dip galvanised reinforcement bar, Table 7), and the concrete strength f_{cm} is 46 MPa.

Table 15.   Corrosion parameters used in Monte Carlo simulation.

Parameter	Symbol	Mean value	Distribution parameter	Unit	Probability distribution	Relative significance [%]
The thickness of the concrete cover	c	30	$m = 30$ $s = 4$	mm	Lognormal	90
The coefficient of the critical chloride content	k_{cl}	6.5	$L = 5.6$ $\alpha = 1$ $\beta = 4$	mm/(a)^{½}	Weibull	6.2
Thickness of zinc coating	d	200	$m = 200$ $s = 19$	µm	Lognormal	1.9
Rate of corrosion of hot-dip galvanised reinforcement bar	r_1	20	$L = 17.4$ $\alpha = 3$ $\beta = 2$	µm/a	Weibull	1.2
Rate of corrosion of ordinary steel reinforcement bar	r_s	50	$m = 50$ $s = 5$	µm/a	Lognormal	0.5
The diameter of a reinforcement bar	$\varnothing$	12	$m = 12$ $s = 1$	mm	Normal	0.2

The thickness of the concrete cover, c [mm]

The coefficient of the critical chloride content, k_{cl} [mm/(a)^{½}]

Thickness of zinc coating, d [µm]

Rate of corrosion of hot-dip galvanised reinforcement bar, r_1, [µm/a]

Rate of corrosion of ordinary steel reinforcement bar, r_s [µm/a]

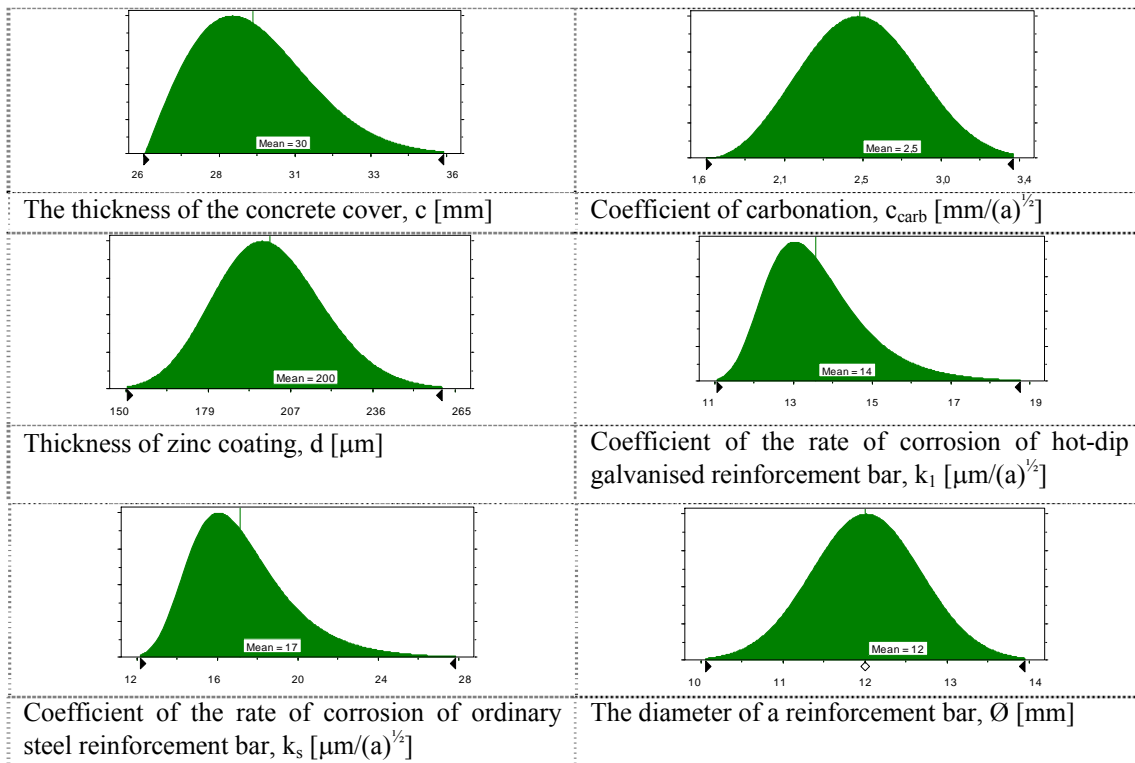The diameter of a reinforcement bar, $\varnothing$ [mm]
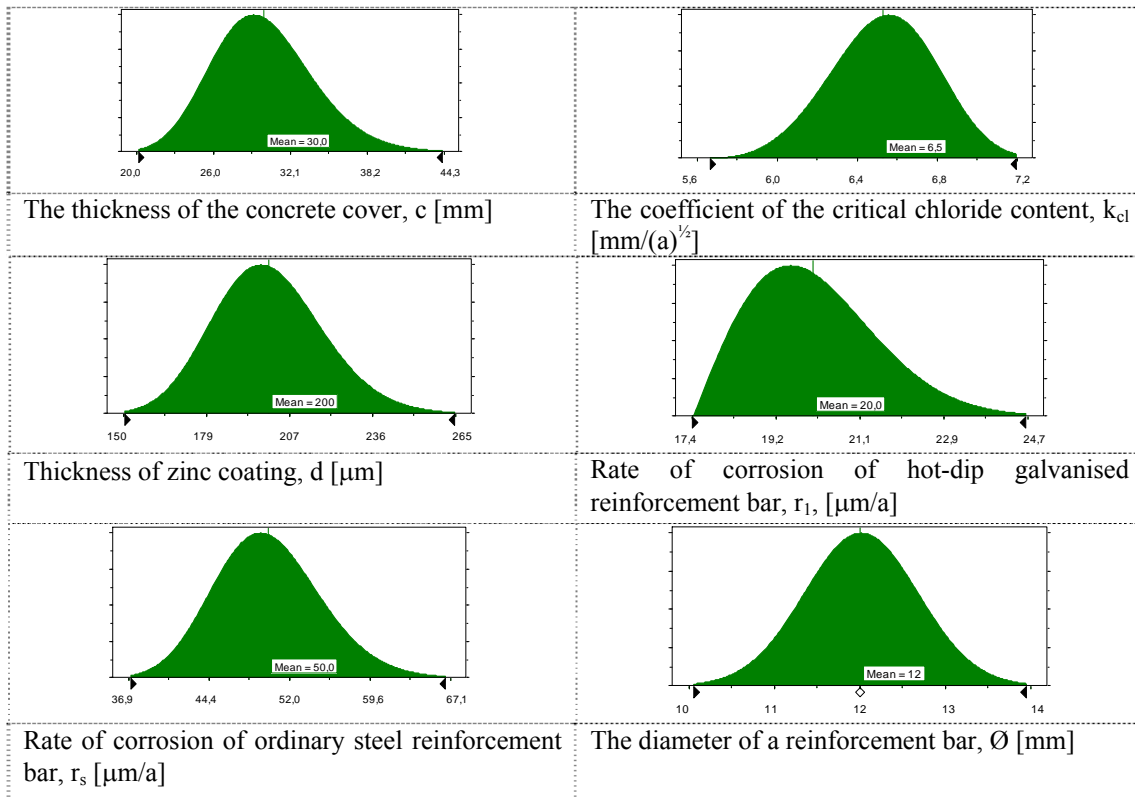
Fig. 29.   Distribution of corrosion parameters.

The results of the Monte Carlo simulation are shown in Fig. 30 and Table 16. If compared with the stochastic method based on the probability of damage, service life estimates approximately 11 years longer are obtained with a 5% probability of damage. The reference value is marked with (●) in Fig. 25. This difference can be attributed to the fact that the deviation of the service life is smaller in the simulation ($\sigma(t_L) \approx 7$ a) than in the stochastic method based on the probability of damage ($\sigma(t_L) \approx 17$ a).
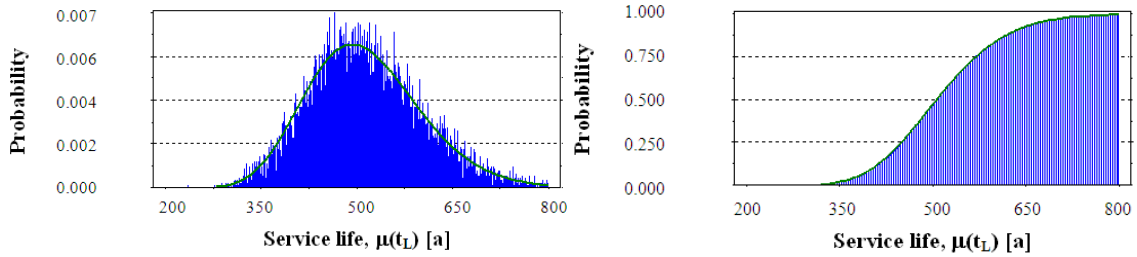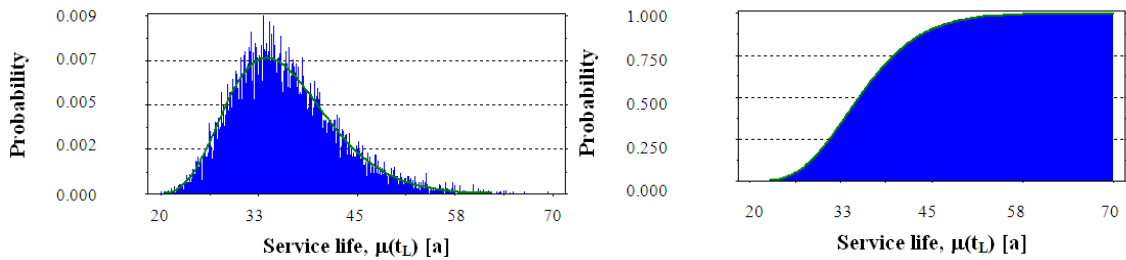
Fig. 30.   Probability density and cumulative distribution function: a fit of Gamma distribution [p = 0.57]). The horizontal axes indicate the time that has passed (in years).

Table 16.   Mean value of the service life and a fit of Gamma distribution with a 5% and 10% probability of damage.

Initiation time	Propagation time for zinc coating	Propagation time for ordinary steel reinforcement bar	Mean value of the service life	A fit of Gamma distribution with a 5% probability of damage	A fit of Gamma distribution with a 10% probability of damage
t_0	t_1	t_2	t_L	$t_\phi = 5\%$	$t_\phi = 10\%$
[a]	[a]	[a]	[a]	[a]	[a]
21	10	4	35	26	28

It should be noticed that the values for the rate of corrosion used in Table 15 are not extreme values. The reason for this is that in the case of a uniform rate of corrosion the use of a conservative hypothesis is not necessary. Furthermore, the values shown in Table 15 are assumed to be long-term mean values including seasonal variation.

3.4   Reliability analysis

For both carbonated and chloride-contaminated concrete, the basis of the division is the uniform or decreasing rate of corrosion of the type of steel reinforcement bar in question. The same applies to intact and cracked concrete. In service life design, the appropriate formula for describing corrosion ought to be chosen individually, depending on the type of structure. Unfortunately, there are no generally applicable rules for making this decision. Nonetheless, as the design is always carried out according to particular criteria, it might be advisable to provide some tentative guidelines in building codes. The uniform rate of corrosion may be mainly applicable to façades, the decreasing rate of corrosion to cases where corrosion products remain on the surface of a steel reinforcement bar, e.g. massive bridge structures. For a cracked concrete structure, the most relevant factors to be considered in choosing between these alternatives are the crack width, moisture conditions, and the location of a corroded steel reinforcement bar in the structure. The main problems in service life estimation are as follows:

1. the reliability of the distribution of parameters in a deterministic formula (a lack of sufficient statistical data);
2. the accuracy of the distribution function chosen to describe a deterministic model;

3. a deterministic formula may take account of only one deterioration mechanism; a probability of damage needs to be chosen that will ensure that the deterioration probability of the formula is sufficiently low.[1,2]

The reliability of service life evaluation is mainly dependent on the adequacy of the deterministic formula and the chosen distribution model, as well as on the availability of trustworthy statistical data. The problem with simplified formulae is that they take into account neither the simultaneous occurrence of several deterioration mechanisms nor the influence of the interaction of different mechanisms on durability. A service life design that relies on simplified formulae with a sufficiently low probability of damage is seemingly straightforward, but may not describe the deterioration accurately and may also give rise to misinterpretations if improperly applied.[3]

The service life of hot-dip galvanised reinforcement bars in carbonated uncracked concrete can be divided into: the initiation time t_0; the propagation time for the zinc coating t_1; the propagation time for an ordinary steel reinforcement bar t_2, and the target service life t_L with the Weibull and lognormal distribution functions[4] as presented in Fig. 31. The corrosion parameter values used are presented in Table 8 and Table 9. Three significant aspects can be noticed in the figure. With a low probability of damage (for instance 5%) the target service life t_L with the Weibull and lognormal distribution function will be longer than that calculated with the superposition principle ($t_0 + t_1 + t_2$). The reason for this lies in set theory. When the different parts of the service life are combined with a stochastic method, the distribution is overlapped (see Table 17) in the calculation process ($t_0 \cup t_1 \cup t_2$).[5] Thus, with a 5% probability of damage, the target service life t_L is approximately 22 years longer calculated with the lognormal distribution function and approximately 24 years longer calculated with the Weibull distribution function compared to the superposition principle ($t_0 + t_1 + t_2$). The longest estimation of the service life with a 5% probability of damage is reached when the lognormal distribution function is used for the initiation time t_0, the propagation time for the zinc coating t_1, and the propagation time for an ordinary steel reinforcement bar t_2 and they are combined stochastically (target service life 102 years). The shortest estimation of the service life with a 5% probability of damage is reached when the Weibull distribution function is used for the initiation time t_0, the propagation time for the zinc coating t_1, and the propagation time for an ordinary steel reinforcement bar t_2 and they are combined stochastically with the superposition principle ($t_0 + t_1 + t_2$) (target service life 47 years). In this example, the maximal difference between the estimations of the service life is approximately 55 years. The other approximations calculated are between those extreme values. Thus, it is significant which distribution or calculation method (combination) is used[6].

---

[1] Sistonen, E. et al. (2006). Stochastic Method and Monte Carlo Simulation for Predicting Service Life of Hot-Dip Galvanised Reinforcement.
[2] Sistonen, E. et al. (2005). Problems in Service life Modelling of Corroded Outdoor Concrete Structures.
[3] Sistonen, E. et al. (2005). The Influence of Rebar Material on the Durability of Outdoor Reinforced Concrete Structures.
[4] Sistonen, E. (2001). The Main Corrosion Parameters and their Influence on the Durability of Outdoor Concrete Structures.
[5] Schneider, J. (1997). Introduction to Safety and Reliability of Structures.
[6] Høyland, A. et al. (1993). System Reliability Theory. Models and Statistical Methods.
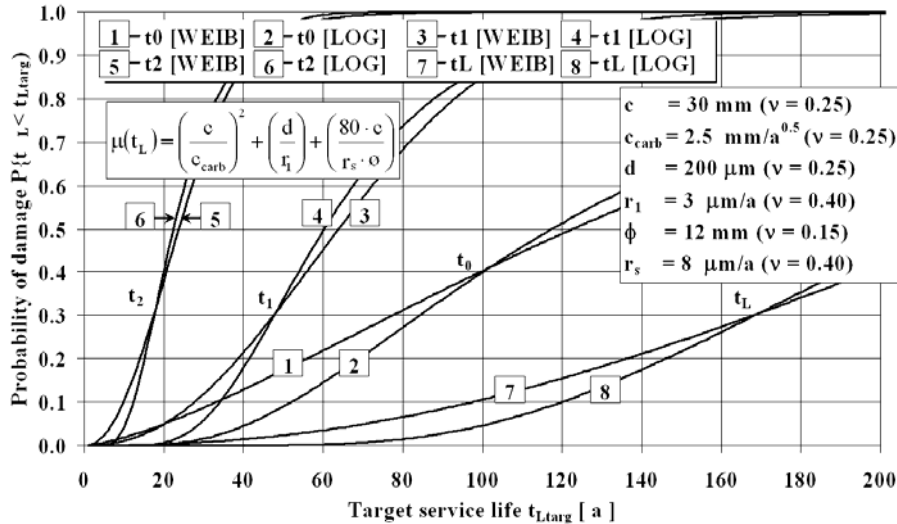
Fig. 31.   *Service life based on steel corrosion, carbonation of uncracked concrete, initiation time t_0, propagation time for zinc coating t_1, propagation time for ordinary steel reinforcement bar t_2, and target service life t_{Ltarg}: Weibull and lognormal distribution.*

Table 17.   *Target service life with Weibull and lognormal distribution probability function (probability of damage 5%).*

$\mu(t_i)$ [a]	Weibull	Lognormal	Lognormal - Weibull	Lognormal/Weibull
$\mu(t_0)$ [a]	20	41	21	2.05
$\mu(t_1)$ [a]	20	29	9	1.45
$\mu(t_2)$ [a]	7	10	3	1.43
$\mu(t_0)+\mu(t_1)+\mu(t_2)$ [a]	47	80	33	1.70
$\mu(t_L)$ [a]	71	102	31	1.44
$\mu(t_L)-(\mu(t_0)+\mu(t_1)+\mu(t_2))$ [a]	24	22	55	2.17
$\mu(t_L)/(\mu(t_0)+\mu(t_1)+\mu(t_2))$ [a]	1.51	1.28	9	1.13

Differences between the values estimated for the service life with a low probability of damage (5-15%) measured with the Weibull and the lognormal distribution function can be seen in Table 17. The 5% probability of damage measured with the lognormal distribution function corresponds to a 10-15% probability of damage measured with the Weibull distribution function. In many cases, when the stochastic lognormal and the Weibull distribution functions are compared, the following rough estimate can be found: the service life measured with the stochastic lognormal distribution function with a 5% probability of damage corresponds to the service life with the stochastic Weibull distribution function with a 10-20% probability of damage [Log (5%) $\approx$ Weib (10-20%)].

On the basis of field studies of concrete façades, the depth of the concrete cover measurement data with the fit of three different distribution functions (Gamma, Lognormal, Weibull) have been presented[1]. It is not problematic to find an appropriate fit of distribution function, as can be found in the study. There should be adequate measurement data and coefficient of the determination of the distribution function to

---

[1] Pentti, M. (1999). The Accuracy of the Extent-of-Corrosion Estimate Based on the Sampling of Carbonation and Cover Depths of Reinforced Concrete Facade Panels.

perform reliability analysis. The appropriate fit of distribution function may change in different façades and parts of them. In the case of adequate measurement data, the distribution function should be chosen according to the closest fit. Otherwise conservatively emphasised functions should be used.

3.5 Summary

On the basis of the service life evaluation, the study presented the factors which extend the service life of a structure most effectively with respect to each corrosion parameter. The emphasis was laid on the use of galvanised reinforcement bars, including cracking. The limit values that considerably extend the service life were presented, including cracking. The effects of galvanised reinforcement bars on the service life of outdoor concrete structures were estimated through calculations. A stochastic method and Monte Carlo simulation were used in the study.[1]

When a stochastic evaluation is used in service life calculations, the results are heavily influenced by the hypotheses made about the deviation of the parameters, as well as by the chosen probability of damage. Moreover, in the model for chloride-induced reinforcement corrosion, the coefficient of the critical chloride content used for the type of steel reinforcement bar in question plays an important role. Owing to problems in measurement and a lack of sufficient statistical data, it is difficult to choose annual mean values for rates of corrosion in a way that the dependency of the values of environmental conditions of different steel types will be correctly described. This obviously affects the reliability of service life calculation. By means of Monte Carlo simulation, approximated distributions for parameters can be determined. The fits of distribution used in the study were lognormal, Gamma, and extreme value (Type 1) distributions. The final fit of distribution is influenced by the deviation of the corrosion parameters. Nevertheless, combined with stochastic evaluation, simulation is a useful tool in assessing the adequacy of a model and service life estimates that have been obtained.[2,3,4]

---

[1] Sistonen, E. et al. (2005). The Main Corrosion Parameters and their Influence on the Durability of Outdoor Concrete Structures.

[2] Sistonen, E. et al. (2005). Improvement in the Durability of Reinforced Outdoor Concrete Structures by Restricting Cracks and Protecting Reinforcement.

[3] Sistonen, E. et al. (2005). The Influence of Rebar Material on the Durability of Outdoor Reinforced Concrete Structures.

[4] Sistonen, E. et al. (2006). Stochastic Method and Monte Carlo Simulation for Predicting Service Life of Hot-Dip Galvanised Reinforcement.

4 DURABILITY TESTS

4.1 Objective and materials

The objective is to define the influence of the reinforcement bar material and crack width on the durability of outdoor reinforced concrete structures, especially for hot-dip galvanised reinforcing steels. Studies were done in order to estimate the extent of the corrosion after five and seven years of exposure and to determine the probable corrosion mechanisms. The exposure conditions of concrete façade elements and bridge structures were simulated in the laboratory work.

Four types of reinforcement bars were used; ordinary steel, hot-dip galvanised steel, weathering steel (TENCOR), and austenitic stainless steel (grade AISI 304). Different types of ordinary steel reinforcement bars were used for reference purposes. The reinforcement bar diameters used in the laboratory study represented the diameters for typical hooks and edge reinforcements of the structures being studied. Furthermore, the size and mechanical properties of the specimens influenced the selected reinforcement bar diameters. A detailed description of the reinforcement bars used is given in Table 18.

Table 18.   Reinforcement bar types.

Code	Reinforcement bar type	Remark	Reinforcement bar diameter, Ø [mm]
A500HW/Ø8	Finnish weldable hot-rolled ribbed steel bar	Reference reinforcement bar for hot-dip galvanised reinforcement bar	8
A500HW/ Ø8/ZN	Finnish weldable hot-rolled ribbed steel bar	Hot-dip galvanised reinforcement bar	8
B500K/Ø8	Finnish cold-worked ribbed steel bar	Reference reinforcement bar for hot-dip galvanised reinforcement bar	8
B500K/Ø8/ZN	Finnish cold-worked ribbed steel bar	Hot-dip galvanised reinforcement bar	8
B500K/Ø7	Finnish cold-worked ribbed steel bar	Reference reinforcement bar for austenitic stainless steel reinforcement bar	7
B600KX/Ø7	Finnish austenitic stainless ribbed steel bar	Austenitic stainless steel reinforcement bar	7
A500HW/Ø12	Finnish weldable hot-rolled ribbed steel bar	Reference reinforcement bar for weathering steel reinforcement bar	12
TENCOR/Ø12	Finnish weathering ribbed steel bar	Weathering steel reinforcement bar	12

The Rapid Portland cement type CEM II/A-LL 42.5 R produced by Finnsementti Oy (Ltd.) was used to produce the test specimens. The modified naphthalene formaldehyde poly-condensate based superplasticiser YLEIS-PARMIX® was used. The aggregates were mainly granite. A total of 243 beams with dimensions of 100×80-100×700-815 mm^3 and 336 cylinders with dimensions of Ø43.6mm×200mm were cast. Two of the beam specimens were unreinforced. The reinforcement bar diameters are shown in Table 18. Because of the different diameters, the height and the length of the beams were different in order to get a similar ultimate limit state. That made it possible to gain

different crack widths in the specimens. Furthermore, the specimens were exposed under the same conditions as those which, it was presumed, would cause the bars to yield. The concrete cover of the reinforcement was 5 mm in the case of the beam specimens and approximately 15-19 mm in the case of the cylinder specimens. The concrete for the beam specimens was ordered from Lohja Rudus Oy (Ltd.). The concrete for the cylinder specimens was made in the laboratory. The mix proportions are shown in Table 19 and Table 20, while the hardened concrete properties and air content of the fresh mix are shown in Table 21. The chemical composition of the cement is shown in Table 22. The water-to-binder ratio was either 0.46 or 0.7 and the corresponding 28-day compressive strength was 47.3 MPa and 38.1 MPa.

Protective pore ratio of the hardened concrete for the beam specimens were measured with six samples according to standard SFS 4475[1]. Mean value for protective pore ratio p_r was equal to 0.30 and standard deviation was 0.01. The result fulfilled the old requirements for exposure class E3b (difficult circumstances, chloride attack, and freezing and thawing stress) which were 0.25[2]. It should be noted that the requirements for protective pore ratio are not included in concrete code of Finland any more[3]. As a result of the geometry, the maximum aggregate size was limited to 5 mm in the case of the cylinder specimens and to 8 mm for the beam specimens. Air-entrained concrete was used to produce the beam specimens. One cement type was used. The water-to-binder ratio and concrete quality were variables which were not studied.

Table 19.   *Mix proportions of concrete.*

Test concrete	Cement [kg/m^3]	Water [kg/m^3]	W/C ratio [-]	Aggregates [kg/m^3]	Superplasticiser [kg/m^3]	Concrete/Cement ratio [-]
Beam	428	195	0.46	1610	5.1	5.23
Cylinder	350	245	0.70	1661	-	6.45

Table 20.   *Mix proportions of aggregates [kg/m^3].*

Test concrete	Filler	#0.1-0.6 mm	#0.5-1.2 mm	#1-2 mm	#2-5 mm	#0-8 mm (coarse)	#0-8 mm (fine)
Beam	-	-	-	-	-	1524	86
Cylinder	149.5	216	149.5	382	764	-	-

Table 21.   *Fresh and hardened concrete properties.*

Test concrete	Air content [vol%]	7-day compressive strength [MPa] cubes 15cm×15cm×15cm	28-day compressive strength [MPa] cubes 15cm×15cm×15cm
Beam	4.1*	39.2	47.3
Cylinder	1.4	-	38.1

* measured from hardened concrete in spacing factor analysis after five and a half years of exposure

[1] SFS 4475 (1988). Concrete. Frost resistance. Protective pore ratio.
[2] By 32 (1992). Durability Guideline and Service Life Dimensioning of Concrete Structures.
[3] By 50 (2004). Concrete Code 2004.

Table 22.   The chemical composition of the cement, according to the producer.

Constituent	Clinker analysis [wt%]	Constituent	Mineral composition [wt%]
CaO	66	C_3S	71
SiO_2	21	C_2S	7
Fe_2O_3	2.7	C_3A	9
Al_2O_3	5.2	$C_4(A;F)$	8
MgO	3.2	Others	5
SO_3	0.2		
Others	1.7		

All the specimens were removed from the moulds seven days after casting. Thereafter, the cylinder specimens were stored for 14-21 days in a climate chamber (22 °C, 45% RH) whereas the beam specimens were stored in a hall with T ≈ 20 °C and RH ≈ 40% until the age of 14 days. After curing, artificial cracks were made in the concrete specimens. The cracks in the beam specimens were made by three-point bending and in the cylinder specimens by a two-point tensile strength test so that the bars yielded with different loads. The cracks were mainly situated in the middle of the beam specimens and constantly distributed in the case of the cylinder specimens. The corrosion specimens were exposed to accelerated carbonation in the chamber, in which the atmosphere contained approximately 4-10 vol% CO_2, and had 60% RH and temperature T equal to 22 °C. The cylinder specimens were carbonated for ten weeks and the beam specimens for around three months. As a result of the higher water-to-binder ratio of the cylinder specimens their permeability was higher than that of the beam specimens, which resulted in the full carbonation of the cylinder specimens after ten weeks of exposure. Thereafter the specimens were subjected to wetting and drying cycles using either a 10 wt% sodium chloride solution (6 wt% Cl^-) or pure tap water. Approximately half of the specimens were exposed to tap water and half of the specimens to the sodium chloride solution.

The wetting and drying cycles of the beam specimens with the tap water simulated the exposure conditions of underwater parts of bridges (exposure class XC1). The wetting and drying cycles of the cylinder specimens with the tap water simulated the exposure conditions of concrete façade elements exposed to rain (exposure class XC4). The wetting and drying cycles of the beam specimens with the sodium chloride solution simulated the exposure conditions of the concrete structures stressed by industrial waters with chlorides or swimming pools (exposure class XD2). The wetting and drying cycles of the cylinder specimens with the sodium chloride solution simulated the exposure conditions of the edge beams of bridge structures (exposure class XD3). The testing arrangements are shown in Fig. 32. The wetting and drying cycles are described in Chapter 4.3.7. The containers of the beam and cylinder specimens were covered with a plastic sheet. The duration of the wetting and drying cycles was different for the beam and cylinder specimens and is shown in Table 23. Longer cycles were used in the case of the cylinder specimens because of the thickness of their concrete cover and the water-to-binder ratio. Described wetting and drying cycles correspond to exposure classes presented in SFS-EN 206-1[1]: The beam and cylinder specimens were placed vertically because it was technically reasonable. That may have had an influence on the test results, because the structure of the capillary pores was different from that of the real

---

[1] SFS-EN 206-1 (2001). Concrete. Part 1: Specification, Performance, Production and Conformity.

structure experimentally simulated. However, in a comparative study this factor concerns all the specimens.

Fig. 32.   Testing arrangements for beam (left) and cylinder (right) specimens.

Table 23.   Wetting and drying cycles.

Test concrete	Wetting [days]	Drying [days]	Length of one full cycle [days]	Total number of cycles
Beam	0.5	0.5	1	app. 1900
Cylinder	7	7	14	app. 190

4.2   Experimental set-up

The studies included the determination of the carbonation depth and average chloride content, thin section analysis, spacing factor analysis, and the measurement of the pH values, electrochemical properties, crack width, and moisture condition. Furthermore, optical microscopy and ESEM (environmental scanning electron microscope) studies were performed. Each measurement in the durability tests was needed in the study to analyse the long-term properties of hot-dip galvanised reinforcement bars.

4.2.1   Carbonation depth

The main harmful effect of carbonation is the reduced alkalinity of concrete, which makes possible the onset of the corrosion of the reinforcement. According to PrEN 13295[1] a concentration of 1 vol% CO_2 in air after 56 days in the cabinet develops the same reaction products with hydrated cement as a normal atmosphere at 0.03 vol% CO_2. This statement may need further research on chemical analysis of cement paste (for instance using X-ray diffraction (XRD), Scanning electron microscopy (SEM), and Thermogravimetric analysis (TGA)). Furthermore, in this study accelerated carbonation has an effect on the different reaction products of hydrated cement and on the reliability of the corrosion of the reinforcement bar. However, accelerated carbonation is actually the only way to neutralise the concrete cover of a reinforcement bar within a limited time. The carbonation depth was determined in cracked and uncracked areas using a 1 vol% phenolphthalein solution prior to and after the corrosion tests. This solution was produced by Reagena Oy (Ltd.). The carbonation depth for the beam and cylinder specimens before the corrosion tests, and also outdoors in natural carbonation, sheltered from rain and exposed to rain or snow, was determined from separate concrete prisms with dimensions of $50 \times 50 \times 150$ mm³. The carbonation depth of the beam specimens

---

[1] PrEN 13295 (2003). Products and Systems for the Protection and Repair of Concrete Structures.

after five years of exposure was determined with broken beam specimens during visual examination, likewise for the cylinder specimens after seven years of exposure. The carbonation depth was determined by breaking a piece off from the sample. With pH indicator sprayed onto the freshly broken surface, it was possible to measure the carbonation depth after a few minutes. The edges of the broken surface were omitted from the measurements. The reason for this is that greater depths of carbonation occur in the corner areas of the specimen, where carbon dioxide can penetrate from two sides at once[1].

4.2.2   Average chloride content

The water-soluble chloride content was determined for the beams by the method described in the ASTM C1218[2]. The procedure included drilling cores with a diameter of 50 mm, followed by sawing them into 5-mm-thick slides, which enabled the chloride profile to be determined. The cores from the beam specimens were drilled perpendicularly to the reinforcement bar. The cores did not include the reinforcement bar itself and the distance from the nearest crack was at least 25 mm; see Fig. 33. The drilling and slicing of the cores were performed with water. Each slide corresponded to a certain depth measured from the surface. In the last steps the slides were crushed and pulverised and the chloride content was determined by potentiometric titration using a Piston Burette TITRONIC Basic titration apparatus with a pH/mV/Temperature Orion 420A meter and an Orion 9617BN probe.

The chloride content of the tap water and sodium chloride solution was determined by potentiometric titration and also by using an HDS 1024 Handheld Digital TDS/Salt-Meter for control purposes. This Salt Manager is produced by DYS Daeyoon Scale Industrial Co., Ltd. The sodium chloride content can be measured with the apparatus in a few seconds. The measurement is based on electrical conductivity. Furthermore, the chloride content of the solution can be measured by evaporation. However, the use of the Salt Manager was justified by the speed of the measurement compared to evaporation.
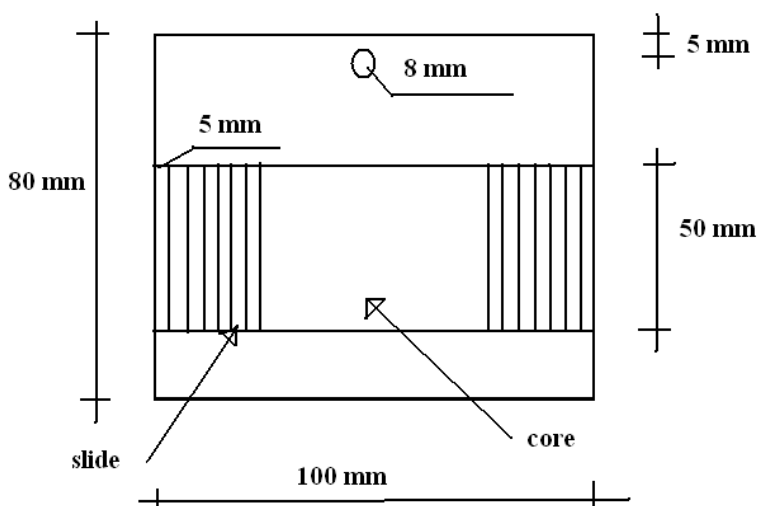

Fig. 33.   Schematic drilling position for cores from the beam specimens.

---

[1] PrEN 13295 (2003). Products and Systems for the Protection and Repair of Concrete Structures.
[2] ASTM C1218/C1218M-99 (1999). Standard Test Method for Water-Soluble Chloride in Mortar and Concrete.

The determination of the acid-soluble chloride content is also widely used. However, that does not describe the right critical chloride content that propagates the corrosion of the reinforcement bar. Thus, it is reasonable in this study to determine the water-soluble chloride content.

Some chlorides may be washed away from the sample during the drilling and sliding procedure. This may need further research. However, it is very typical to drill the sample with water from the structure during a condition survey. One possibility is to drill the bigger sample with water and to drill or grind the smaller sample from the bigger sample without using water. Furthermore, the sliding of the sample is almost impossible without water for technical, noise, and dust reasons.

Another way to measure the water-soluble chloride content is to grind a powdered sample from the surface of the drilled concrete specimen. That can be made with special profile grinding equipment. However, for achieving the chloride content as a function of the depth from the concrete surface, more samples are needed to determine that profile from the total chloride content of the powdered samples. Two grinded samples from the unreinforced beam specimens after 5.7 years of exposure without using water were analysed to compare the test results with drilled and slided samples using water.

Accurate potentiometric titration to measure the chloride content of the solution cannot be compensated with the use of the Salt Manager. However, it is a fast way to map the state of the chloride content of the solution and the accuracy is fairly good. The content of the sodium chloride solution, leached corrosion products of the tap water or the solution, and the temperature of the aggressive liquid are among the factors that affect the reliability of the measurement results.

4.2.3   Thin section and spacing factor analysis

Thin section analysis was performed on the beam and cylinder specimens exposed to tap water and the sodium chloride solution. Furthermore, spacing factor analysis was performed on a beam specimen exposed to the sodium chloride solution. The thin section analysis was determined by using a method described in the ASTM C856[1]. The spacing factor analysis was determined by using a method described in the VTT TEST R003-00 (ASTM C457)[2]. Olympus SZ3060 stereo microscopy and Nikon E400 POL polarisation microscopy were used in the study. Those measurements were carried out in cracked and uncracked areas of the beam and cylinder specimens. The analyses were performed after five and half years of exposure for one beam specimen exposed to tap water and one beam specimen exposed to the sodium chloride solution. Likewise, analyses were performed after seven years of exposure for one cylinder specimen exposed to tap water and one cylinder specimen exposed to the sodium chloride solution. The analyses were performed by WSP TutkimusKORTES Oy (Ltd.)[3,4]. With thin section and spacing factor analysis the possible ways in which concrete samples deteriorate can be estimated and, especially in this study, the extent of the corrosion. The accuracy and the applicability of the measurement in this study are better than for

---

[1] ASTM C856-04 (2004). Standard Practice for Petrographic Examination of Hardened Concrete.
[2] ASTM C457-98 (1998). Standard Test Method for Microscopical Determination of Parameters of the Air-Void System in Hardened Concrete.
[3] WSP TutkimusKORTES Oy (Ltd.) (2006). Research report 6462/06.
[4] WSP TutkimusKORTES Oy (Ltd.) (2007). Research report 7300/07.

instance the determination of the frost resistance of hardened concrete, thanks to the beneficial technical image analysis.

4.2.4 The measurement of the pH values

The pH values were determined for tap water and the sodium chloride solution during the wetting and drying exposure. The pH value was determined with a pH/mV/Temperature Orion 420A meter, Orion 9617BN probe, and pH paper. With these measurements a possible leaching of OH⁻ ions to the water can be noticed, and the pH values in the cracks and a possible increase in the pH value during the exposure test can be estimated. That may have an effect on the corrosion of the reinforcement bar.

These measurements of the pH values were completed with the accurate measurement of the carbonation depth with phenolphthalein solution to determine the neutralisation of the concrete cover. It is a fast way to estimate the state of corrosion of the reinforcement bar. The pH meter has better accuracy than pH paper but lower than chemical analysis. Leached corrosion products of the tap water or the solution and the temperature of the aggressive liquid are among the factors that affect the reliability of the measurement results.

4.2.5 Electrochemical measurements

The rate of corrosion, corrosion potential, and the resistivity of concrete were determined[1,2,3] using a GECOR6 unit produced by GEOCISA. The measured corrosion current i_{corr} ($\mu A/cm^2$) was converted to the rate of corrosion v_{corr} ($\mu m/a$) by employing Faraday's law[4]:

$$\frac{\Delta x}{\Delta t} = \frac{M}{z \cdot F \cdot \rho} \cdot i_{corr},$$
(34)

where
- x is the corrosion penetration, i.e. the loss of bar radius attributable to corrosion [10^{-8}m],
- t is the time [s],
- M is the atomic weight [g/mol],
- z is the number of electrons transferred per atom [-],
- F is Faraday's constant = 96487 [C/mol],
- ρ is the density of the steel = 7.85 [g/cm³], and
- i_{corr} is the corrosion current [$\mu A/cm^2$].

In the determination of the rate of corrosion, the correction factors based on Faraday's law were as follows: 11.6 for ordinary steel; 15 for galvanised steel; 10.3[5] for austenitic stainless steel, and 11.3 for weathering steel reinforcement bars. Atomic weight, the numbers of electrons transferred per atom, and the density of the material have an effect on the calculated correlation factors. In conjunction with the polarisation measurements,

---

[1] Andrade, C. et al. (2004). Recommendations of RILEM TC-154-EMC.
[2] Luping, T. (2002). Calibration of the Electrochemical Methods for the Corrosion Rate Measurement of Steel in Concrete.
[3] Boyd, W.K., Tripler, A.B. (1968). Corrosion of Reinforced Steel Bars in Concrete.
[4] Sykes, J.M. (1995). Electrochemical Studies on Steel in Concrete.
[5] Sandoval-Jabalera, R. et al. (2006). Electrochemical Behaviour of 1018, 304 and 800 Alloys in Synthetic Wastewater.

the half-cell potential and resistivity (see Chapter 2.3.1) measurements of the concrete specimens were performed during evaporation. In order to enhance the stability of the values the specimens were damp. A copper/copper sulphate half-cell (CSE) was used as a reference electrode. The diameter of the electrode was 10.5 cm. The electrodes were placed longitudinally to the reinforcement bar. All specimens were kept horizontal during the measurements. The electrochemical measurement technique used is adequate for a comparative study in the testing arrangements selected.

4.2.6　Crack width measurements

Crack width measurements were determined using optical microscope produced by Maxta Ltd. Three measurement points on the beam specimens were selected after six months of exposure and four measurement points after five years of exposure, with uniform distribution. Other cracks observed in the beam specimen were also measured, but the largest crack was used for the analysis. Eight measurement points on the cylinder specimens were selected within measuring range after seven years of exposure. Crack widths were not measured on the cylinder specimens after three months of exposure. The possible clogging of the cracks was processed as uncracked concrete. The results of the crack width measurements were combined with the results of the electrochemical measurements. The clogging of the cracks and changes in the people taking the measurements are among the factors affecting the reliability of the measurement results. The crack width measurement technique used is adequate for comparative study in the selected testing arrangements.

4.2.7　The measurement of the moisture conditions of the reinforced concrete specimens

The measurements of the moisture conditions were determined for the beam and cylinder specimens exposed to tap water and the sodium chloride solution. The moisture conditions were determined using a Squirrel logger with a Vaisala Oy (Ltd.) HMP 44 temperature and relative humidity probe. The measurement point was situated near a cracked area of concrete, where the concrete cover was approximately 28 mm. The containers of the beam specimens had been covered with a plastic sheet since the tests began. The plastic sheet reduced the evaporation. Meanwhile, the containers of the cylinder specimens were covered with a plastic sheet after 1.8 years of exposure. The reason for the difference in the testing conditions is that the cylinder specimens had to be moved from their original position because of the renovation of the laboratory. Thus, the harmonisation in the testing conditions compared to the beam specimens was reasonable.

With the measurements of the moisture conditions it is possible to estimate the extent of the corrosion. As a result of the gauging technique it was not possible to measure the moisture conditions of the concrete of the beam and cylinder specimens near the reinforcement bar. However, the technique used made it possible to estimate the effect of wetting and drying cycles on moisture conditions.

4.2.8　The optical microscopic examination of the reinforced concrete specimens

The reliability of the electrochemical and other measurements can be ensured with destructive studies. After one year of exposure 16 beam specimens were broken and

after five years of exposure 34 beam specimens were broken. Those 34 beam specimens were used for tensile tests of the reinforcement bars after optical microscopic examination, and were used as references for the reinforcement bars of the cylinder specimens. This was justified by the lower rate of deterioration of the reinforcement bars of the beam specimens compared to the reinforcement bars of the cylinder specimens.

The cylinder specimens were broken five times: after 0.2 year, one year, two years, five years, and seven years of exposure. Each time 16 cylinder specimens were broken, except that the last time 65 cylinder specimens were broken for tensile tests of the reinforcement bars after optical microscopic examination.

The selection criteria for the specimens for the destructive studies were typical values of electrochemical measurements, carbonation depth, and crack width. Furthermore, half of the beam specimens broken after five years of exposure displayed remarkably greater crack width values.

The beam specimens were sawn by diamond cutting into 10-mm-thick concrete pieces longitudinal to the reinforcement bar. The rest of the concrete was broken mechanically. The reinforcement bars were removed with an angle grinder and a steel cutter. The cylinder specimens were also sawn by diamond cutting, but only by splitting them longitudinally to the reinforcement bar. The broken beam and cylinder specimens and removed reinforcement bars were photographed and the microscopic examination was performed using Leica WILD MZ8 marked optical microscopy with a JVC KY-F55B marked camera. The microscopic examination was performed on the broken beam specimens and reinforcement bars removed after five years of exposure and the broken cylinder specimens and reinforcement bars removed after seven years of exposure.

4.2.9   The microscopic examination of the zinc layer of the reinforcement bars of the specimens

The microscopic examination of the zinc layer of the reinforcement bars of the specimens was performed using optical microscopy and ESEM, Electro scan E3, combined with an Energy Dispersive Spectrometer (EDS) and Backscattered Electron Detector (BSE). The acceleration voltage was kept at 20 keV. The working distance was around 13 mm. The vacuum pressure was set at around 5 torr (1 torr equal to 133.322 Pa) for BSE image acquisition and 2 torr while the EDS spectra were being acquired. The EDS spectra were processed using a standardless quantitative analysis. The beam and cylinder specimens for the ESEM studies were cores drilled at a distance of approximately 15 mm from the cracked area of the concrete. The water was removed by the alcohol exchange technique and the specimens were impregnated under a vacuum with a low-viscosity resin. The impregnated specimens were ground and polished using a diamond spray, with a grain size from 9 to 0.25 μm. All the images were taken in the backscattered electron mode, which allowed the main hydration phases to be identified according to the procedure described by Scrivener[1]. The ESEM-EDS spot analyses were performed on the same polished specimens and the location of the electron beam was determined on the basis of the BSE images. The measurement technique used is suitable for the estimation of the extent of the corrosion.

---

[1] Scrivener, K.L. (2004). Backscattered Electron Imaging of Cementitious Microstructures: Understanding and Quantification.

4.3 Test results

4.3.1 Carbonation depth

The test results showed that the carbonation of the concrete of the entire cross-section of the beam specimens occurred only in the cracks, whereas the cross-sections of cylinder specimens were fully carbonated. The carbonation depth of the beam specimens in uncracked concrete exceeded the thickness of the concrete cover, which was 5 mm. The carbonation depth of the beam specimens in uncracked concrete, and also in cracked concrete longitudinally to the reinforcement bars, increased by approximately 1 mm during the wetting and drying exposure. The realkalisation was not measured in this study. The carbonation depth of the beam specimens did not go beyond the rear surface of the bars in all cases. That may have an effect on the non-uniform and partly one-sided corrosion.

Accelerated carbonation affects the chemical composition of concrete. Furthermore, the microstructure of the capillary pores may change. This causes the state of the moisture round the reinforcement bar to vary. However, this factor has the same effect on all the reinforcement bar types studied. Specimens with varying carbon dioxide content may corrode differently. However, that was not recognised in the study. The average value and standard deviation of the carbonation depth, and the numbers of measured samples of the beam specimens, are shown in Table 24. An example of the carbonation depth measurement is presented in Fig. 34. The measurement points shown in Fig. 34 are as follows: uncracked concrete near the cracked area (1); in cracked concrete longitudinally to the crack (2), and in cracked concrete longitudinally to the reinforcement bar (3). As can be seen in Fig. 34, the cracked concrete longitudinal to the crack was fully carbonated, whereas the rear of the reinforcement bar is not carbonated (discoloured by the indicator solution).

Table 24. *Average value and standard deviation of the carbonation depth and numbers of measured samples of the beam specimens before exposure and after five years of exposure.*

Reinforcement Bar type	Ordinary steel	Hot-dip galvanised steel	Weathering steel (TENCOR)	Austenitic stainless steel
Number of measured samples [-]	8[a] 8[b]	4[a] 4[b]	2[a] 2[b]	2[a] 2[b]
Carbonation depth	(Mean value / Standard deviation) [mm]			
Beam specimen in tap water	(12 / 3)[a] (13 / 3)[b]	(11 / 2)[a] (12 / 2)[b]	(9 / 1)[a] (10 / 1)[b]	(11 / 4)[a] (12 / 1)[b]
Beam specimen in NaCl solution	(11 / 2)[a] (13 / 3)[b]	(10 / 0)[a] (12 / 2)[b]	(10 / 0)[a] (12 / 1)[b]	(10 / 0)[a] (11 / 1)[b]

[a] before exposure
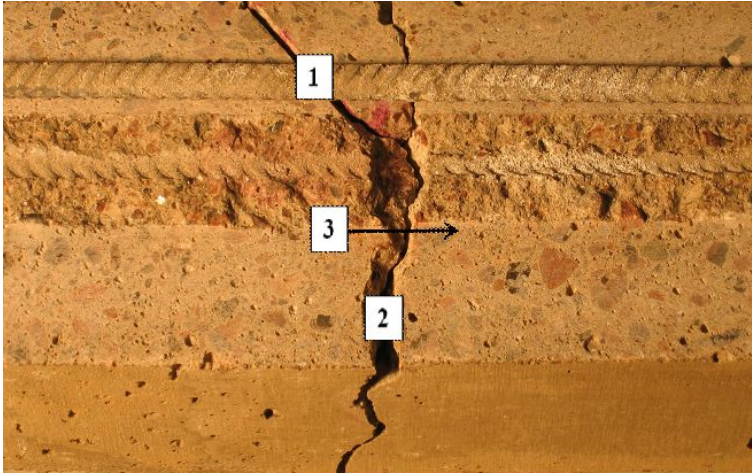[b] after five years of exposure

Fig. 34. *Carbonation depth measurement of hot-dip galvanised reinforcement beam specimen after five years of exposure to tap water (Finnish cold-worked ribbed steel reinforcement bar B500K/Ø8/Zn, crack width w = 0.15 mm).*

The measured carbonation depth for beam specimens outdoors in natural carbonation after seven years of exposure sheltered from rain was, on average, 2.8 mm (c_{carb} equal to 1.0 mm/a$^{1/2}$) and for those exposed to rain 1.3 mm (c_{carb} equal to 0.5 mm/a$^{1/2}$). The carbonation of the beam specimens during the durability tests (Table 24) corresponds to the natural carbonation of specimens exposed to rain. This is logical, as a result of their having the same high moisture content.

The carbonation depth for the cylinder specimens outdoors in natural carbonation after seven years of exposure sheltered from rain was, on average, 6.3 mm (c_{carb} equal to 2.4 mm/a$^{1/2}$) and for those exposed to rain 2.5 mm (c_{carb} equal to 0.9 mm/a$^{1/2}$). It should be noted that the coefficients of carbonation were calculated from Equation (28) as follows: $c_{carb} / k_e = x / \sqrt{t_0}$. Furthermore, the exposure time outdoors in natural carbonation represents the initiation time. The carbonation depth values exposed to rain are lower than half than those sheltered from rain. Thus, the circumstantial factor k_e equal to 0.5 for concrete exposed to rain is a rough estimation in Equation (28).

The carbonation depth values under outdoor conditions for the beam and cylinder specimens exposed to rain were the same as those measured after two years of exposure. The reason for this may be that the concrete prisms are fully saturated in their surfaces. In future specimens exposed to rain may not be attacked by carbonation in uncracked concrete. The calculated values of the coefficient of carbonation for the beam and cylinder specimens correspond to the mix proportions of the concrete used (see Table 19, Equation (27), and Equation (28)). The carbonation depth measurements in natural carbonation completed the conclusion that the specimens in the durability tests were carbonated deeply enough to achieve an active state of corrosion.

4.3.2 Average chloride content

The test results revealed the same maximum chloride content of around 1.1 wt%$_{CEM}$ in the outer layer when measured after one and five years of exposure. A significantly higher chloride content, exceeding 1.6 wt%$_{CEM}$, was measured in the internal zone located more than 10 mm from the surface after five years of exposure. These results might indicate the leaching of chloride off the binder matrix during the wetting and drying cycles, a process which could be further enhanced by the existing cracks. The

water-soluble chloride content was determined only in the beam specimens and the results obtained are shown in Fig. 35. The average value and standard deviation of the chloride, and the numbers of measured samples at the different depths, are shown in Table 25. The measurements were made from different beam specimens.
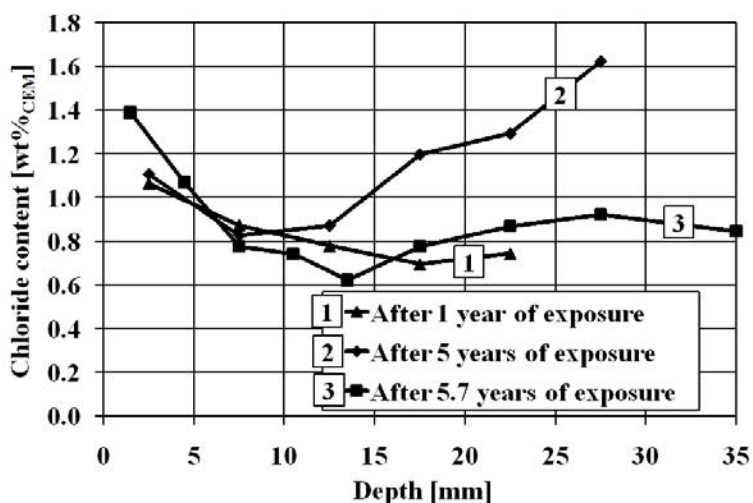
Fig. 35.   *Average water-soluble chloride content (wt%$_{CEM}$) of the beam specimens measured after one year, after five years and after 5.7 years of exposure.*

Table 25.   *Average value and standard deviation of the water-soluble chloride content (wt%$_{CEM}$) and numbers of measured samples of the beam specimens measured at the different depths after one year and after five years of exposure.*

Depth [mm]	0-5	5-10	10-15	15-20	20-25	25-30
Number of measured samples [-]	2[a] 7[b]	2[a] 6[b]	2[a] 6[b]	2[a] 8[b]	2[a] 5[b]	- 2[b]
Chloride content	(Mean value / Standard deviation) [wt%$_{CEM}$]					
Beam specimen in NaCl solution	(1.07 / 0.12)[a] (1.11 / 0.11)[b]	(0.88 / 0.15)[a] (0.83 / 0.12)[b]	(0.78 / 0.13)[a] (0.87 / 0.17)[b]	(0.70 / 0.01)[a] (1.20 / 0.32)[b]	(0.75 / 0.11)[a] (1.29 / 0.13)[b]	- (1.63/0.01)[b]

[a] after one year of exposure
[b] after five years of exposure

The test results of two grinded samples from the unreinforced beam specimens after 5.7 years of exposure without using water showed no significant difference around the reinforcement bar as compared the test results with drilled and slided samples using water. It was noticed that the chloride content were little higher on bottom of the beam than top of the beam specimen. Reason for this may be in different capillary properties of the concrete along the beam specimen. The results obtained are shown in Fig. 35. The average value and standard deviation of the chloride, and the numbers of measured samples at the different depths, are shown in Table 26. The measurements were made from different beam specimens.

The standard deviation of the water-soluble chloride content with grinded samples is lower than with drilled and slided samples, excluding the surface layer. In the case of drilled samples the surface layer was exposed to water a longer time than deeper in the sample. Furthermore, wetting and drying of the beam specimens affect the chloride ingress deeper in the sample. These factors may be some explanations for the differences of the research results obtained between drilled and slided samples and grinded samples.

Table 26. *Average value and standard deviation of the water-soluble chloride content (wt%$_{CEM}$) and numbers of measured samples of the unreinforced beam specimens measured at the different depths after 5.7 years of exposure.*

Depth [mm]	0-3	3-6	6-9	9-12	12-15	15-20	20-25	25-30	30-40
Number of measured samples [-]	2	2	2	2	2	2	2	2	2
Mean value [wt%$_{CEM}$]	1.39	1.07	0.78	0.74	0.62	0.78	0.87	0.92	0.85
Standard deviation [wt%$_{CEM}$]	0.42	0.00	0.02	0.20	0.03	0.02	0.07	0.19	0.02

Only tap water was added to the sodium chloride solution before the solution was changed. The basis for this was because chlorides do not wear off during evaporation. The solution was changed after 4.8 years of exposure in the case of the beam specimen and after 8.6 years of exposure in the case of the cylinder specimen. Because of a low chloride content value, a solution with the same chloride content was added to the sodium chloride solution after the solution had been changed in the case of the beam specimens. The reason for this is that chlorides penetrated into the concrete and crystallised into the concrete surface at the level of the water. Another reason could be the flowing of the solution from the pipe joints of the container used in the case of the beam specimens. The leaching of corrosion products into the tap water and sodium chloride solution during exposure may have had an influence on the test results. The results of the chloride content of the tap water and sodium chloride solution during exposure are shown in Table 27 and Table 28.

Table 27. *Average chloride content (wt% Cl⁻) of different solutions of beam specimens.*

Duration of exposure, [a]	0	1.2	3.4	4.8	4.8	5.3
Beam specimen in tap water	-	-	-	0.05	0.05	0.05
Beam specimen in NaCl solution	6*	4.4[x]	1.1[x]	1[a]	6[b]	6

* estimated value (not measured)
[x] potentiometric titration
[a] before changing the solution
[b] after changing the solution

Table 28. *Average chloride content of (wt% Cl⁻) of different solutions of cylinder specimens.*

Duration of exposure, [a]	0	1.8	4.4	7.2	8.6	8.6
Cylinder specimen in tap water	-	-	-	0.03	-	0.02
Cylinder specimen in NaCl solution	4*	6[b,*]	5.6[x]	5.5	5.4[a]	6[b,*]

* estimated value (not measured)
[x] potentiometric titration
[a] before changing the solution
[b] after changing the solution

4.3.3   Thin section and spacing factor analysis

In the case of the beam specimen exposed to tap water, carbonation shrinkage and drying shrinkage associated with concrete was not significant[1]. The hydration of the binder matrix was uniform and very little unhydrated cement appeared. It was recognised from the beam specimen exposed to sodium chloride solution that a great deal of harmful ettringite crystallised into the protective pores, because the concrete sample was continuously wet. Crystallisation by ettringite was not noticed in the microscopic cracks. To judge from the pore structure and the results of the spacing factor analysis, the concrete samples were not frost-resistant in moisture loading.

Probably as a result of the hot-dipping of the steel, the composition or structure of the concrete of the cylinder specimen exposed to tap water was different. The reason for this could be the evolution of hydrogen in the fresh concrete. The surface crack was probably plastic and it was consistent with the aggregates. Binder matrix carbonated through the sample. The state of corrosion of the hot-dip galvanised steel was high and the corrosion products of the cylinder specimen exposed to the sodium chloride solution were spread into the concrete through micro-cracks and fractures, which significantly reduced the durability of the concrete. The reason for this is that cracking increases moisture and chloride ingress and in that way increases the deterioration of the concrete. Close to the steel iron hydroxides penetrated strongly into the concrete, which was noticed from the dark red colour of the concrete and cracks in it. The results of the thin section analysis are presented in Table 29, Fig. 36, and Fig. 37. The results of the spacing factor analysis are presented in Table 30.

The determination of the frost resistance of hardened concrete, thin section and spacing factor analysis for the non-exposed beam and cylinder specimens were not made. In stead, one non-exposed beam and one non-exposed cylinder specimen was broken and studied visually. The evolution of hydrogen was noticed. Furthermore, hardened concrete properties were measured and reported in Chapter 4.1.

On the basis of the thin section analysis four deterioration types were found: ettringite reaction, the carbonation of concrete, chloride diffusion, and reinforcement corrosion. The interaction of these deterioration types may additionally reduce the service life of hot-dip galvanised reinforcement bars. This phenomenon is not included in this study.

---

[1] WSP TutkimusKORTES Oy (Ltd.) (2006). Research report 6462/06.
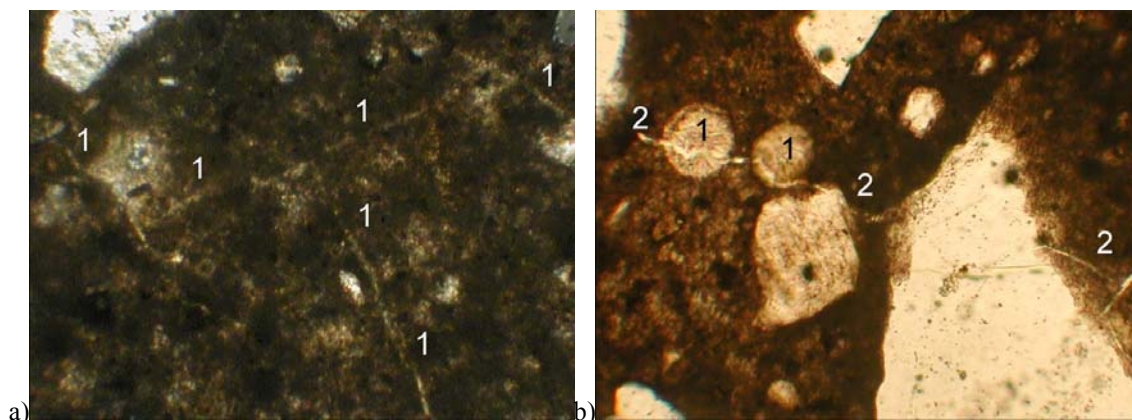
Fig. 36. *Thin section analysis for beam specimens. a) Specimen exposed to tap water. In the concrete a small amount of nets of microscopic cracks appear (1) filled with carbonate. The width of Figures a and b in the horizontal direction is 0.5 mm. b) Specimen exposed to sodium chloride solution. Voids expired by ettringite (1) have microscopic cracks (2) in places, which is probably a result of the pressure from crystallisation.*
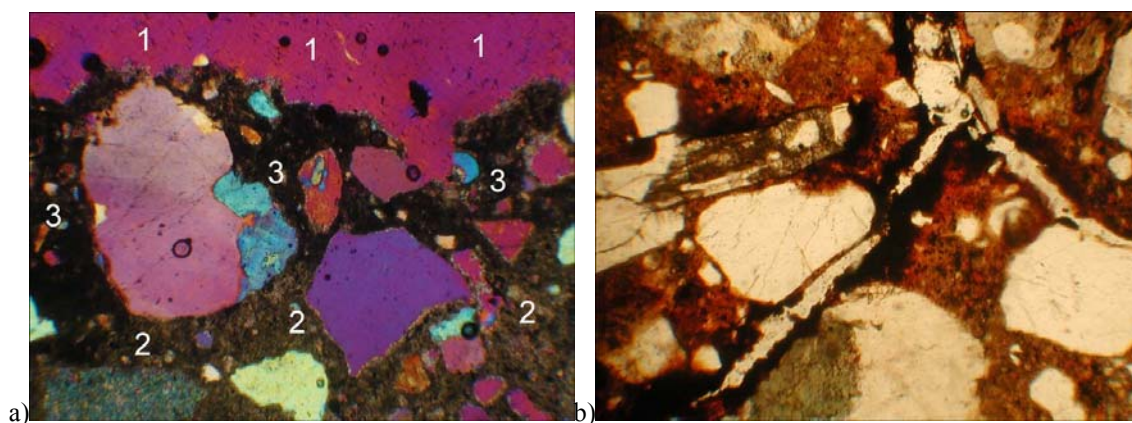
Fig. 37. *Thin section analysis for cylinder specimens. a) Specimen exposed to tap water. Carbonation of the binder matrix (3) is different in its porosity in the interfacial area of the mechanically removed reinforcement bar (1) and concrete (2). b) Specimen exposed to sodium chloride solution. The width of Figures a, and b in a horizontal direction is 1.5 mm.*

Table 29. *Thin section analysis.*

Specimen type	Reinforcement bar type	Condition of concrete	Mean carbonation [mm]	Frost resistance/ Pore fillers	Frost weathering*
Beam specimen in tap water	Hot-dip galvanised steel	satisfactory	19	insufficient, often healed up, ettringite	0
Beam specimen in NaCl solution	Ordinary steel	satisfactory	17	none/often healed up, ettringite	0
Cylinder specimen in tap water	Hot-dip galvanised steel	satisfactory	Through	no/no	0
Cylinder specimen in NaCl solution	Hot-dip galvanised steel	adequate	Through	no/no	0

* Frost weathering described by scale 0…4; 0 = no weathering, 1 = minor, 2 = nascent, 3 = moderate, 4 = high

Table 30.   Spacing factor analysis.

Specimen type	Reinforcement bar type	Total air content [%]	Air content of protective pores [%]	Specific surface of protective pores [mm^2/mm^3]	Spacing factor [mm]
Beam specimen in NaCl solution	Ordinary steel	8.4	4.1	11	0.40*

* spacing factor fulfils frost resistance requirements with values <0.20-0.27 depending on planned service life and exposure class[1]

4.3.4   The measurement of the pH values

According to the determined pH values of the tap water and sodium chloride solution of the beam specimens, the OH^{-} ions dissolved in the tap water and sodium chloride solution. The results show the leaching of some alkalis into the solution. That is seen in the increase of the pH values of the tap water and sodium chloride solution of the beam specimens as a function of time. The measured pH values of the tap water and sodium chloride solution of the beam specimens are presented in Table 31.

It should be emphasized that pH values in the tap water or sodium chloride solution is a result of slow calcium leaching in the carbonated concrete. The leached calcium can be carbonated further by carbon dioxide in the air. Therefore, the measured pH values are just a very rough indication of alkali leaching.

Table 31.   The results of the pH values of different solutions of beam specimens.

Duration of exposure [years]	0	0.2	4.8	4.8	5.3
Tap water	7.6	9.3	8.5	8.5	8.8
NaCl solution	7.6	-	8.5[a]	7.7[b]	8.0

[a] before changing the solution
[b] after changing the solution

The pH values of the tap water and sodium chloride solution of the cylinder specimens were not measured at the begin of the wetting and drying exposure, but the determined pH value of the tap water and sodium chloride solution of the beam specimens presented in Table 31 can be used as reference value.

The pH values of the tap water and sodium chloride solution of the cylinder specimens were measured after seven years of exposure with pH paper. The pH values obtained for the tap water and sodium chloride solution of the cylinder specimens ranged from 7.4 to 7.7 in the case of the sodium chloride solution and from 6.9 to 7.2 in that of tap water. This refers to the fact that the increase in the pH values did not occur in the solutions of the cylinder specimens. Thus, this factor does not reduce the corrosion of the reinforcement bar.

The pH of the carbonated concrete of the beam and cylinder specimens was not measured but the carbonation depth was measured with phenolphthalein solution. According to the carbonation test results, the reinforcement bars were actively corroded. Presumably, the pH value in the cracks is equal to that in the surrounding aggressive liquid. The concrete was doubtless neutralised in the crack.

---

[1] By 50 (2004). Concrete Code 2004.

4.3.5 Electrochemical measurements

The electrochemical measurements of the beam specimens were performed after approximately six months and approximately five years of exposure. The electrochemical measurements of the cylinder specimens were performed after approximately three months and approximately seven years of exposure. The measured values for the corrosion potential and resistivity of concrete are reported elsewhere[1,2]. The results obtained revealed that the highest corrosion value rates were recorded for the ordinary steel exposed to the sodium chloride solution and the lowest values for the austenitic stainless steel exposed to tap water. The rates of corrosion were calculated according to the corrosion current values and are shown in Fig. 38 and Table 32. The state of corrosion[3] based on the rate of corrosion is shown in Table 33. The corrosion potential values are shown in Fig. 39 and Fig. 40 the resistivity of concrete values are shown in Fig. 41 and Fig. 42. The state of corrosion[4] based on the resistivity of the concrete is shown in Table 34. A comparison of the reinforcement bars used based on the coefficient of variation is presented in Chapter 4.4.3. The number of measurements and number of measured cylinder and beam specimens are shown in Appendix C.
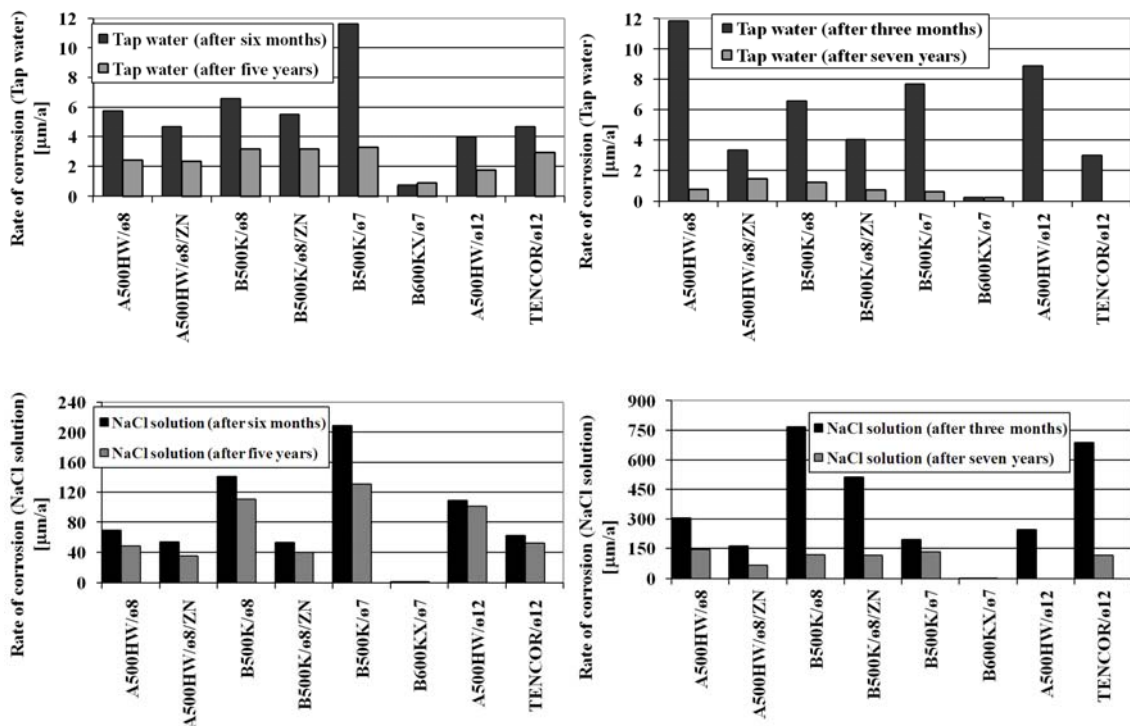
Fig. 38.   *Rate of corrosion of the beam (left) and cylinder (right) specimens exposed to tap water (upper) and sodium chloride solution (lower).*

It should be noted that it was not possible to perform electrochemical measurements for the cylinder specimens of the steel reinforcement bar types A500HW/Ø12 and TENCOR exposed to tap water and the steel reinforcement bar type A500HW/Ø12

---

[1] Sistonen, E. et al. (2006). Stochastic Method and Monte Carlo Simulation for Predicting Service Life of Hot-Dip Galvanised Reinforcement.

[2] Sistonen, E. et al. (2007). The Influence of the Crack Width on the Durability of different Reinforcement Bar Materials.

[3] Andrade, C., Alonso, C. (2001). On-Site Measurements of Corrosion Rate of Reinforcements.

[4] Andrade, C., Alonso, C. (2001). On-Site Measurements of Corrosion Rate of Reinforcements.

exposed to the sodium chloride solution. The reason for this lies in the severity of the deterioration of the specimens.

Table 32. *Average value and standard deviation for the rate of corrosion for beam and cylinder specimens exposed to tap water and sodium chloride solution.*

Rate of corrosion, v_{corr}	(Mean value / Standard deviation) [µm/a]			
Reinforcement Bar type	Ordinary steel	Hot-dip galvanised steel	Weathering (TENCOR) steel	Austenitic stainless steel
Beam specimen in tap water	$(7.2 / 5.0)^a$ $(2.7 / 1.1)^b$	$(5.2 / 2.2)^a$ $(2.7 / 1.0)^b$	$(5.4 / 4.0)^a$ $(2.9 / 1.9)^b$	$(0.7 / 0.2)^a$ $(0.8 / 0.2)^b$
Beam specimen in NaCl solution	$(128.7 / 89.7)^a$ $(95.0 / 68.1)^b$	$(55.6 / 55.3)^a$ $(36.7 / 21.6)^b$	$(60.6 / 42.0)^a$ $(50.4 / 36.6)^b$	$(1.5 / 1.0)^a$ $(1.5 / 1.3)^b$
Cylinder specimen in tap water	$(8.4 / 6.5)^c$ $(0.9 / 0.9)^d$	$(3.7 / 2.1)^c$ $(1.1 / 2.6)^d$	$(3.0 / 2.5)^c$ Not measured^d	$(0.3 / 0.2)^c$ $(0.2 / 0.2)^d$
Cylinder specimen in NaCl solution	$(367.9 / 426.4)^c$ $(131.5 / 98.9)^d$	$(336.7 / 557.0)^c$ $(101.6 / 74.2)^d$	$(687.6 / 1006.0)^c$ $(113.3 / 65.9)^d$	$(0.5 / 0.2)^c$ $(2.3 / 2.9)^d$

[a] after six months of exposure
[b] after five years of exposure
[c] after three months of exposure
[d] after seven years of exposure

Table 33. *State of corrosion based on the rate of corrosion for beam and cylinder specimens exposed to tap water and sodium chloride solution.*

Reinforcement Bar type	Ordinary steel	Hot-dip galvanised steel	Weathering steel (TENCOR)	Austenitic stainless steel
Beam specimen in tap water	Moderate^a Low^b	Low^a Low^b	Low^a Low^b	Passive^a Passive^b
Beam specimen in NaCl solution	High^a High^b	High^a High^b	High^a High^b	Low^a Low^b
Cylinder specimen in tap water	Moderate^c Passive^d	Low^c Passive^d	Low^c Not measured^d	Passive^c Passive^d
Cylinder specimen in NaCl solution	High^c High^d	High^c High^d	High^c High^d	Passive^c Low^d

[a] after six months of exposure
[b] after five years of exposure
[c] after three months of exposure
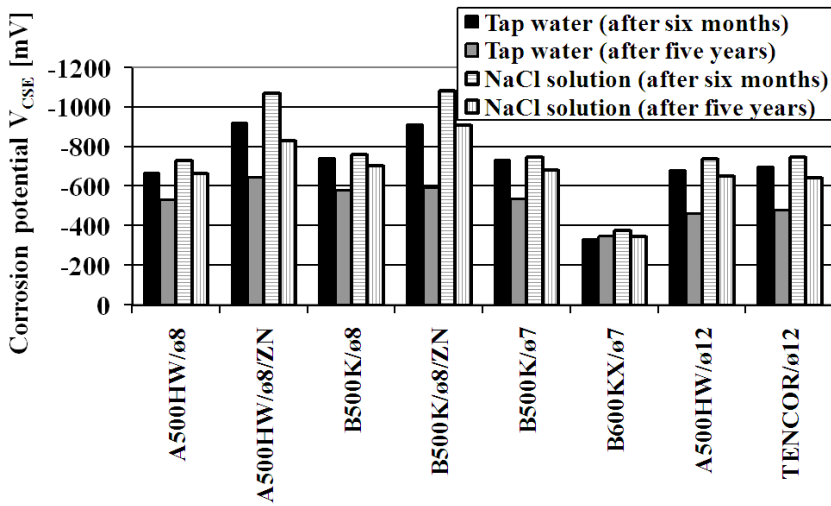[d] after seven years of exposure

Fig. 39.   *Corrosion potential of the beam specimens exposed to tap water and sodium chloride solution.*
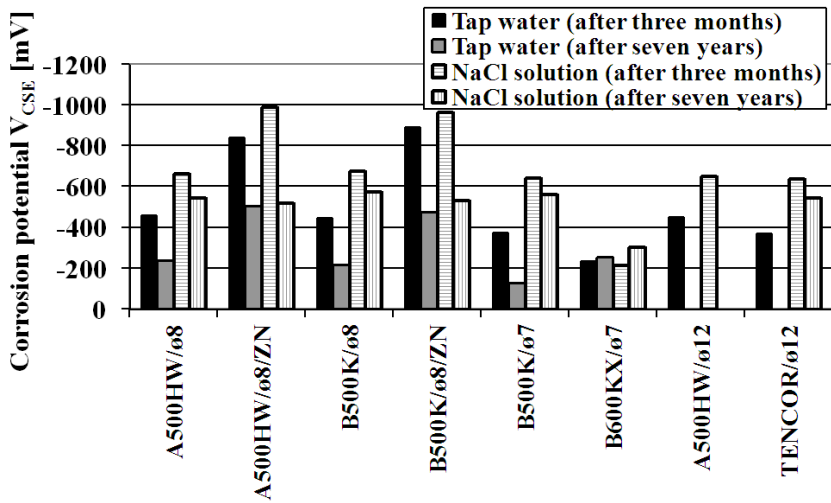

Fig. 40.   *Corrosion potential of the cylinder specimens exposed to tap water and sodium chloride solution.*
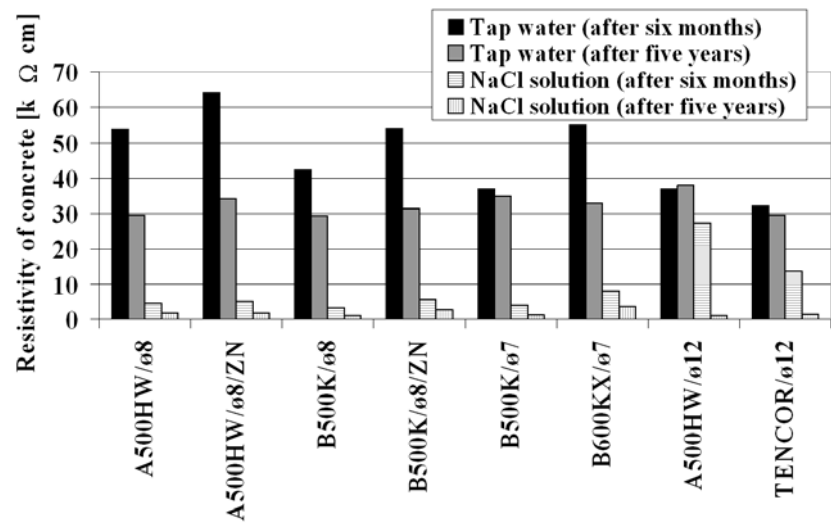

Fig. 41.   *The resistivity of the concrete of the beam specimens exposed to tap water and sodium chloride solution.*
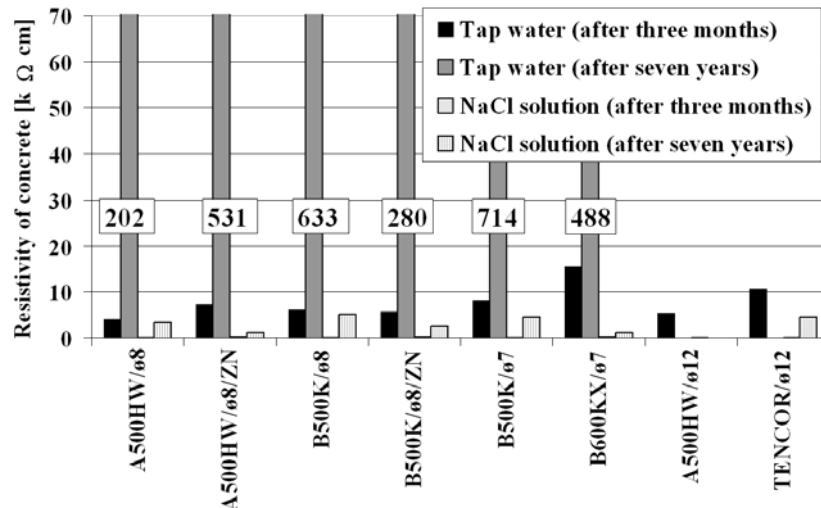
Fig. 42. *The resistivity of the concrete of the cylinder specimens exposed to tap water and sodium chloride solution.*

The resistivity values of the concrete of the cylinder specimens exposed to tap water after seven years of exposure are questionably high. The reason for this may be the measurement technique and measurement errors. Furthermore, the high resistivity of the concrete exposed in the tap water was expected. Due to further leaching and carbonation, no or very little amount of electrically conductive ions was left in the pore solution, resulting in a high resistivity. Thus, these values indicate that active and passive states of corrosion cannot be distinguished from one another.

Table 34. *State of corrosion based on the resistivity of concrete for beam and cylinder specimens exposed to tap water and sodium chloride solution.*

Reinforcement bar type	Ordinary steel	Hot-dip galvanised steel	Weathering steel (TENCOR)	Austenitic stainless Steel
Beam specimen in tap water	Moderate to high[a] Moderate to high[b]	Low[a] Moderate to high[b]	Moderate to high[a] Moderate to high[b]	Low[a] Moderate to high[b]
Beam specimen in NaCl solution	No control parameter[a] No control parameter[b]	No control parameter[a] No control parameter[b]	Moderate to high[a] No control parameter[b]	No control parameter[a] No control parameter[b]
Cylinder specimen in tap water	No control parameter[c] Cannot distinguish between active and passive[d]	No control parameter[c] Cannot distinguish between active and passive[d]	Moderate to high[c] Not measured[d]	Moderate to high[c] Cannot distinguish between active and passive[d]
Cylinder specimen in NaCl solution	No control parameter[c] No control parameter[d]	No control parameter[c] No control parameter[d]	No control parameter[c] No control parameter[d]	No control parameter[c] No control parameter[d]

[a] after six months of exposure
[b] after five years of exposure
[c] after three months of exposure
[d] after seven years of exposure

In addition to the electrochemical measurements, the same beam specimens were used to evaluate the range of corrosion visually. The procedure applied included mechanical opening of the specimens without removing the corrosion products. The following parameters were measured: the length of the corroded area (S_{crack}), the central angle for

the width of the corroded area (α_{crack}), and the sum of all the corroded area (Corr. Area). A total of 32 beam specimens were measured. The corrosion surface areas represent only a local situation and as such cannot be used to evaluate the general condition of the specimens studied. It should be pointed out that the pitting factor α[1] measured from the sum of all the corroded area (α equal to 2.4 - 10.5) were not used in the values of the rate of corrosion. The use of that factor should have led to the unrealistic values of the rate of corrosion when compared to visual and microscopic examination. Thus, results of the electrochemical measurements represent homogeneous corrosion. However, the results obtained correlated well with the thin section analysis and the electrochemical measurement results (Table 33 and Table 34). The results obtained and a definition of these parameters are shown in Table 35.

Table 35.   Corroded area per measuring range of GECOR6 (beam specimens)[2] after five years of exposure.

Reinforcement bar material	Tap water			NaCl solution		
	S_{crack}[a]	α_{crack}[b]	Corr. Area[c]	S_{crack}[a]	α_{crack}[b]	Corr. Area[c]
	[mm]	[deg]	[%]	[mm]	[deg]	[%]
Hot-dip galvanised steel	17	293	13	20	180	10
Ordinary steel[d]	24	244	25	79	191	40
Austenitic stainless steel[d]	0	0	0	0	0	0
Weathering steel (TENCOR)[d]	23	180	42	105	115	32

[a] the length of the corroded area along the reinforcing steel surface at the crack
[b] the central angle for the width of the corroded area at the surface of the reinforcing steel at the crack
[c] the sum of all the corroded area per the measuring range of GECOR6
[d] reference steel reinforcement bar

4.3.6   Crack width measurements

The crack widths of the specimens were measured in the context of the electrochemical measurements (see Chapter 4.3.5). The measured values of the crack widths of the beam specimens are reported elsewhere[3]. The results obtained revealed that the highest crack width values were recorded for the weathering steel exposed to the sodium chloride solution and the lowest values for the austenitic stainless steel exposed to tap water. Examples of the measured cracks are presented in Fig. 43. The figures represent extreme cases of deterioration. Longitudinal corrosion-induced cracking, clogging of the crack (see Chapter 4.4.1), and the migration of corrosion products to the surface of the specimen can be observed in the figures. The same factors were also observed in the cylinder specimens. Crack widths were not measured for the cylinder specimens after three months of exposure. Measured crack width values are shown in Fig. 44 and Fig. 45.

---

[1] Andrade, C. et al. (2004). Recommendations of RILEM TC-154-EMC.
[2] Sistonen, E. et al. (2007). The Influence of the Crack Width on the Durability of different Reinforcement Bar Materials.
[3] Sistonen, E. et al. (2006). Stochastic Method and Monte Carlo Simulation for Predicting Service Life of Hot-Dip Galvanised Reinforcement.
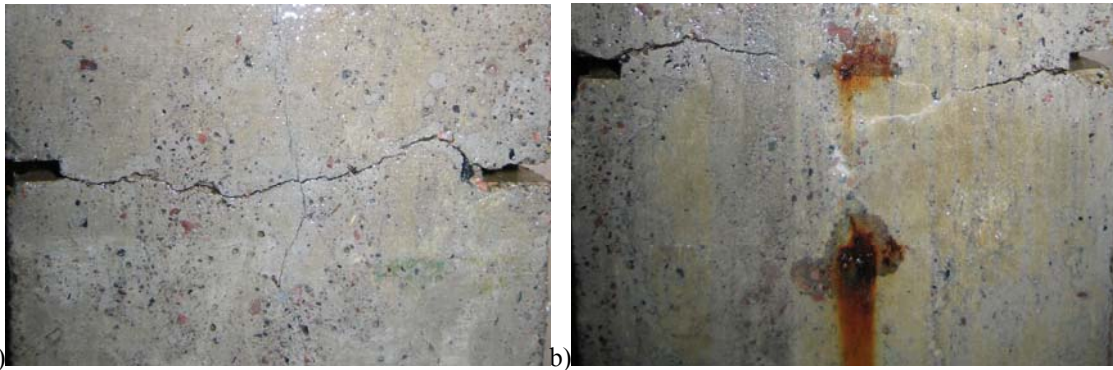
Fig. 43.   *Surface cracks of the beam specimens corroded in sodium chloride solution after five years of exposure. a) Hot-dip galvanised reinforcement bar A500HW/Ø8/Zn (crack width w = 0.39 mm). b) Ordinary steel reinforcement bar B500K/Ø8, crack partly settled (crack width w = 0.41 mm).*
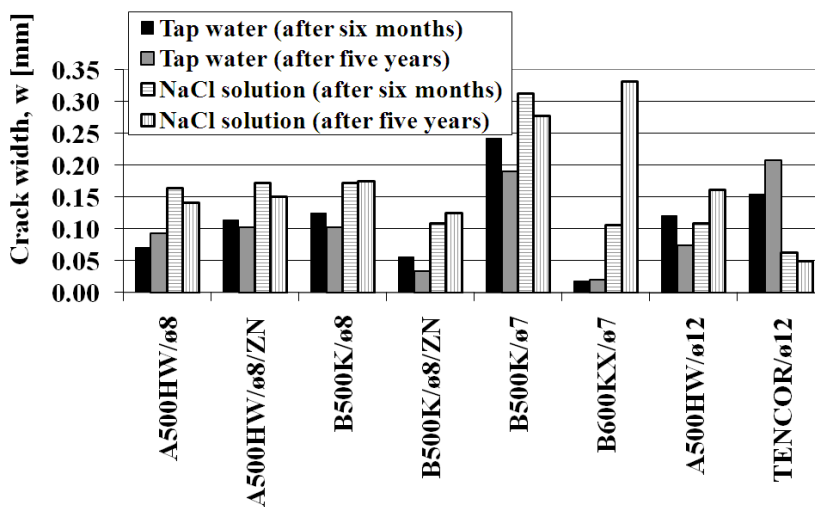
Fig. 44.   *Crack width of the beam specimens exposed to tap water and sodium chloride solution.*
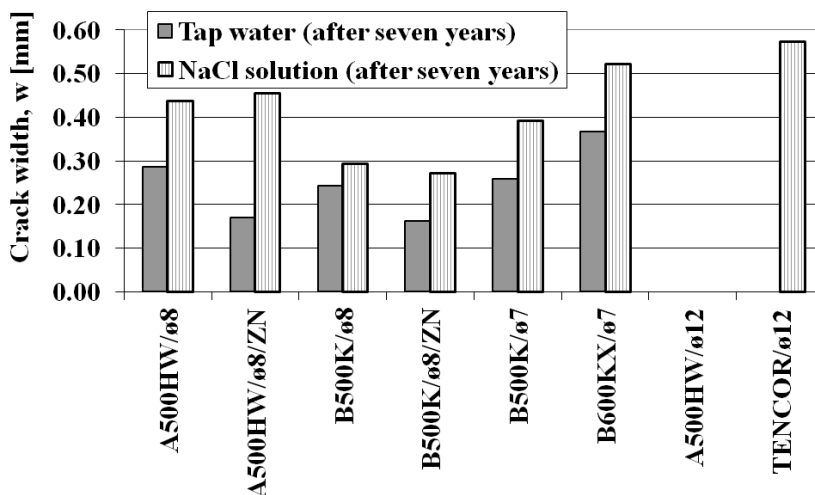
Fig. 45.   *Crack width of the cylinder specimens exposed to tap water and sodium chloride solution.*

The clogging of the cracks for the beam specimens did not indicate reduced crack width values when the results after six months of exposure and five years of exposure were compared, despite the increase in clogging during the durability test. The reason for this is the differences in the arrangements of the measurements for the beam specimens:

different people taking the measurements, number of measurements, and number of measured specimens. For instance, the increase in the crack width values for the steel reinforcement bar type B600KX/Ø7 exposed to the sodium chloride solution can be explained by the above-mentioned reason.

It should be noted that it was not possible to measure the crack widths for the cylinder specimens of the steel reinforcement bar types A500HW/Ø12 and TENCOR exposed to tap water and the steel reinforcement bar type A500HW/Ø12 exposed to the sodium chloride solution. The reason for this lies in the severity of the deterioration of the specimens. A comparison of the reinforcement bars used, based on the coefficient of variation, is presented in Chapter 4.4.3. The number of measurements and the number of measured cylinder and beam specimens are shown in Appendix C.

4.3.7 The measurement of the moisture conditions of the reinforced concrete specimens

The measurements of the moisture conditions for the beam and cylinder specimens exposed to tap water and the sodium chloride solution are presented in Fig. 46, Fig. 47, Fig. 48, Fig. 49, Fig. 50, and Fig. 51. The wetting and drying cycle during the electrochemical and crack width measurements for the cylinder and beam specimens is presented in Fig. 46, and Fig. 47. The wetting and drying cycling procedure for the cylinder specimens functioned as planned. It can be observed that the beam specimens were very wet during the exposure. As a result of the electrochemical and optical microscopy measurements, the wetting and drying cycle for the beam specimens had to be changed. The reason for this is the fact that a lack of oxygen in fully saturated concrete may lead to a very low rate of corrosion. The wetting and drying cycles and the use of the plastic sheet for the beam specimens are presented in Table 36.
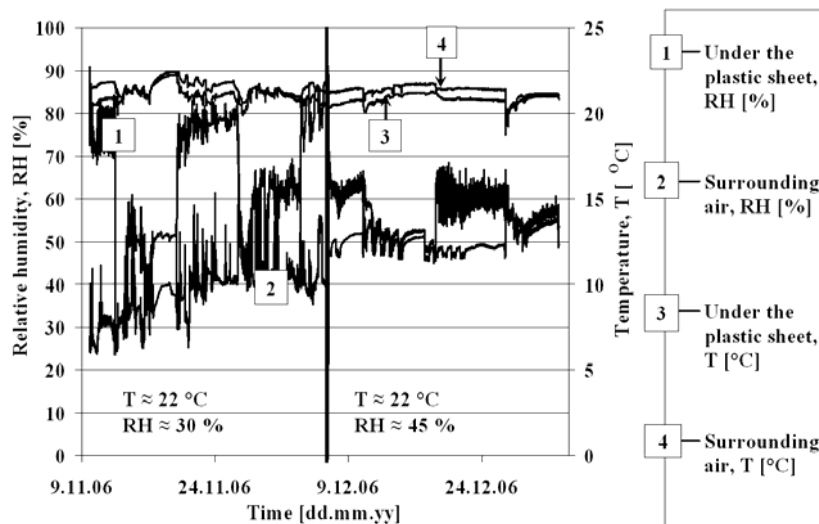
Fig. 46.   Moisture conditions during a short period for cylinder specimens. Length of one full cycle is two weeks (wetting cycle one week; drying cycle one week).

Fig. 47. *Moisture conditions during a short period for beam specimens in uncracked concrete. Length of one full cycle is one day (wetting cycle 0.5 day; drying cycle 0.5 day).*

Table 36. *Wetting and drying cycles for beam specimens.*

Duration of exposure [years]	Wetting [days]	Drying [days]	Length of one full cycle [days]	Plastic sheet to reduce evaporation
0 - 5.6	0.5	0.5	1	x
5.6 - 5.8	3.5	3.5	7	x
5.8 - 6.7	7	7	14	x
6.7 - 7.1	1	27	28	-
> 7.1	7	21	28	-

The change in the wetting and drying cycle did not affect already performed electrochemical and crack width measurements. The length of one full wetting and drying cycle was first changed from one day (Fig. 47) to one week (Fig. 48). That did not substantially change the moisture conditions. Thus, the length of one full cycle was changed from one week (Fig. 48) to two weeks (wetting cycle one week; drying cycle one week) at the same time as the measurements of the moisture conditions during a drying period in the surrounding air were started (Fig. 49). That wetting and drying cycling procedure was not measured, but according to the results presented in Fig. 48, and Fig. 49 the moisture conditions are similar to the results presented in Fig. 47. That corresponds to saturated concrete.
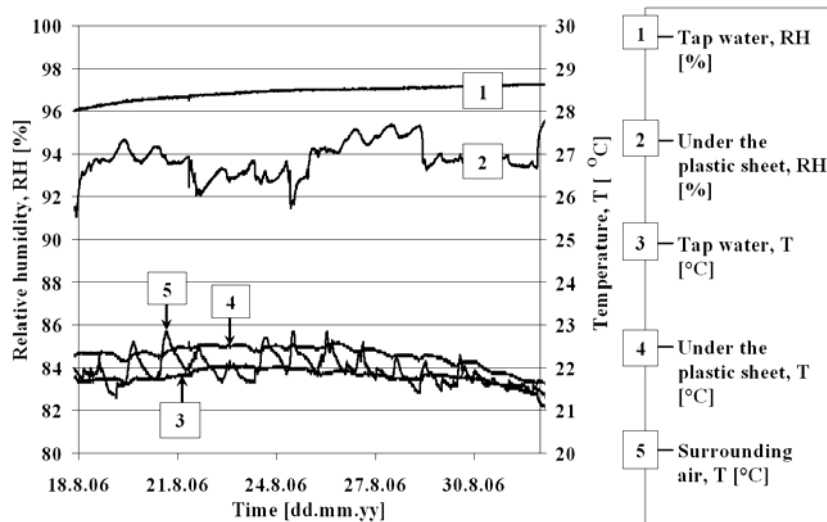
Fig. 48. *Moisture conditions during a short period for beam specimens in uncracked concrete. Length of one full cycle is one week (wetting cycle 3.5 days; drying cycle 3.5 days). There was measurement error in the RH values of the surrounding air.*
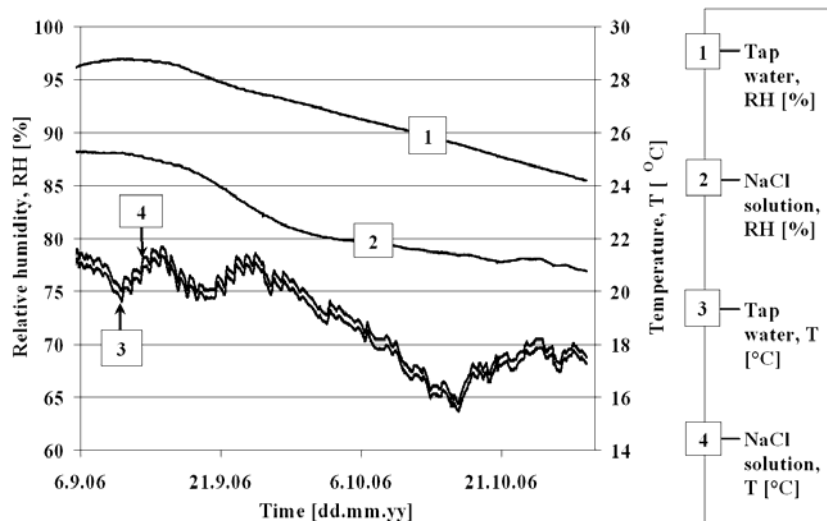
Fig. 49. *Moisture conditions during a drying period in surrounding air for beam specimens in uncracked concrete.*

Due still saturated concrete, the length of one full cycle was changed from two weeks to four weeks (wetting cycle one day; drying cycle 27 days). The plastic sheet that reduced the evaporation from the containers of the beam specimens was removed after the length of one full cycle had been changed to four weeks (see Fig. 50 and Table 36). It was noticed that the wetting cycle of one day was too short (Fig. 50). Finally, the wetting and drying cycling procedure was changed to a wetting cycle of one week and a drying cycle of three weeks (see Fig. 51). It was noticed that the wetting and drying cycle was reasonable for research purposes. The wetting and drying cycle that was experimentally found can be used for further research to measure the rate of corrosion for beam specimens as a function of moisture content.
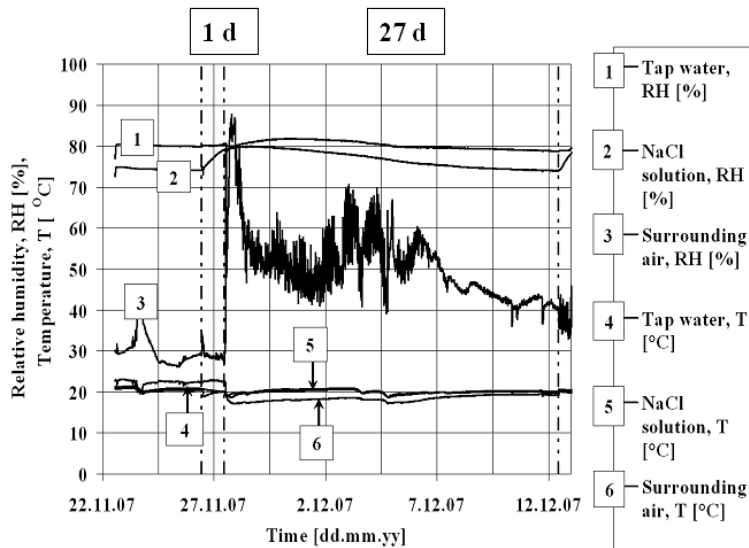
Fig. 50.   *Moisture conditions during a short period for beam specimens in uncracked concrete. Length of one full cycle is four weeks (wetting cycle one day; drying cycle 27 days).*
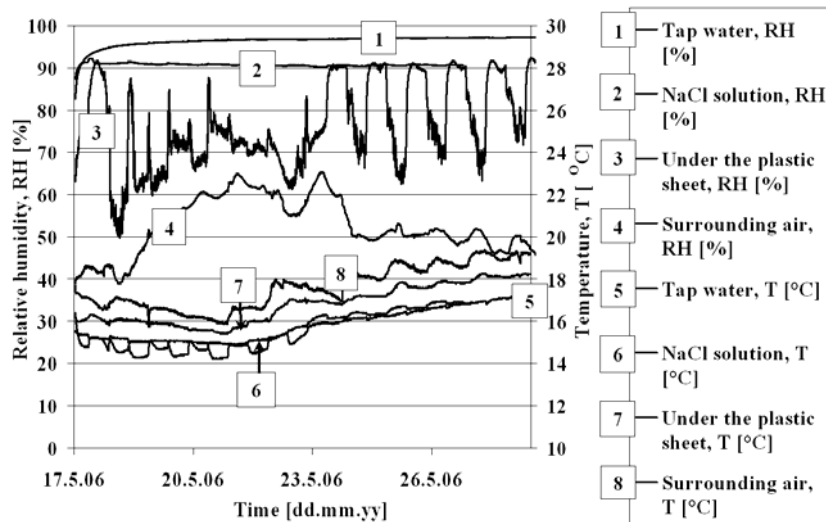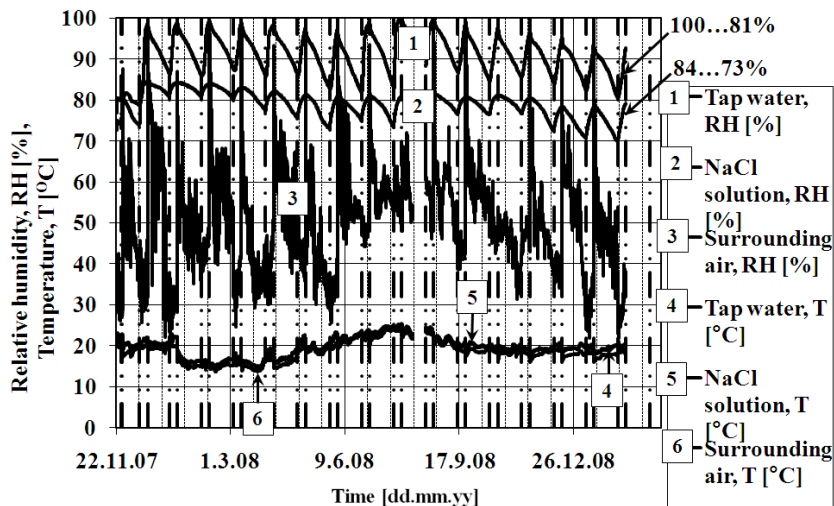

Fig. 51.   *Moisture conditions during a short period for beam specimens in uncracked concrete. Length of one full cycle is four weeks (wetting cycle one week; drying cycle three weeks).*

After the cycling procedure was changed, the wetting and drying cycles of the beam specimens with the tap water simulated the exposure conditions of concrete façade elements exposed to rain (exposure class XC4). After the cycling procedure was changed, the wetting and drying cycles of the beam specimens with the sodium chloride solution simulated the exposure conditions of the edge beams of bridge structures (exposure class XD3). Described wetting and drying cycles correspond to exposure classes presented in SFS-EN 206-1[1].

4.3.8   The optical microscopic examination of the reinforced concrete specimens

The corrosion and protection properties of hot-dip galvanised reinforcements differ from those of other steel reinforcement bar types. It is an interesting phenomenon that a greater amount of visible ferrous corrosion products was found in reinforcements exposed to tap water than in those exposed to the sodium chloride solution.

---

[1] SFS-EN 206-1 (2001). Concrete. Part 1: Specification, Performance, Production and Conformity.

Furthermore, white rust is gathered into a cracked area of the concrete exposed to the sodium chloride solution; see Fig. 52 and Fig. 53. This may indicate effective corrosion protection in chloride-contaminated cracked concrete. In that case zinc corrosion products may migrate amply into the crack. This phenomenon was observed in the crack width measurements, in which the settling of the cracks in hot-dip galvanised reinforcement beam specimens exposed to the sodium chloride solution was greater compared with hot-dip galvanised reinforcement beam specimens exposed to tap water and ordinary steel reinforcement beam specimens exposed to the sodium chloride solution.

The porosity caused by the evolution of hydrogen and the migration of zinc corrosion products into the concrete in the cracked area is shown in Fig. 53. No significant difference was observed between different exposures. The level of hydrogen evolution was higher in the cylinder specimens compared to the beam specimens. The properties of the concrete have an influence on this phenomenon. Longitudinal corrosion-induced cracks in the concrete were not observed in the beam and cylinder specimens exposed to tap water. According to the results of tensile tests, the mechanical properties of hot-dip galvanised reinforcement that were taken from beam specimens after five years of exposure fulfilled the standard requirements in Finland[1,2].

a)   b)
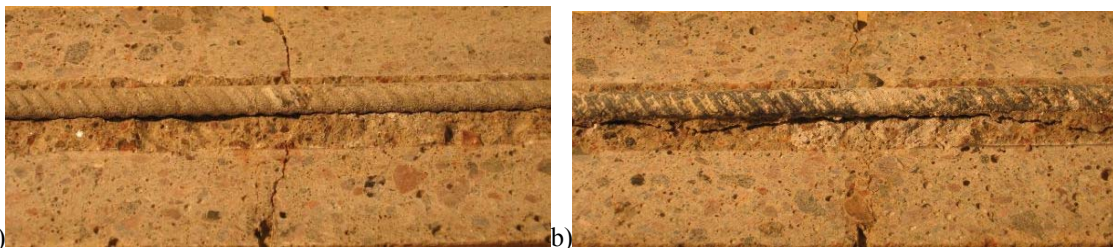
Fig. 52.   a) Corroded hot-dip galvanised reinforcement beam specimen (crack width w = 0.15 mm) after five years of exposure to tap water (Finnish cold-worked ribbed steel reinforcement bar B500K/Ø8) and b) Corroded hot-dip galvanised reinforcement (crack width w = 0.15 mm) after five years of exposure to sodium chloride solution (Finnish cold-worked ribbed steel reinforcement bar B500K/Ø8).

a)   b)
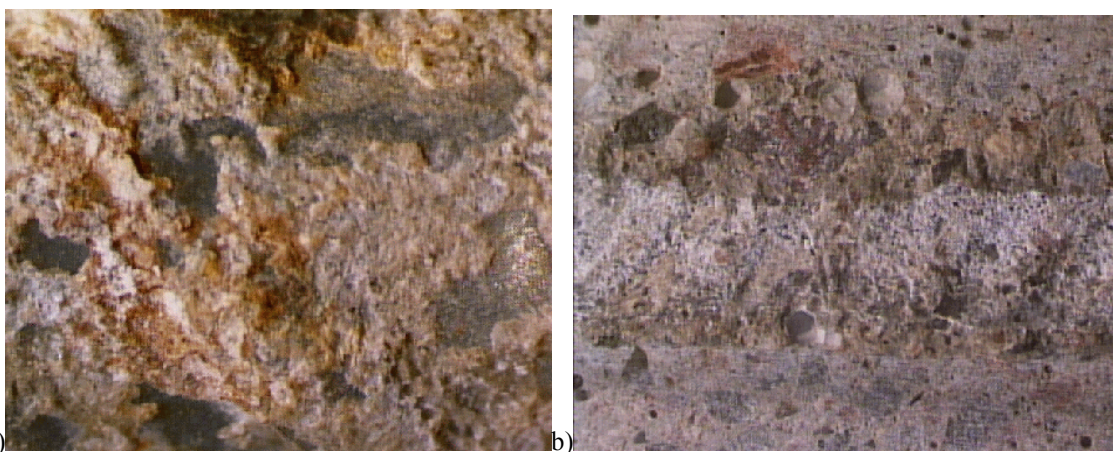
Fig. 53.   Hot-dip galvanised reinforcement bar B500K/Ø8/Zn in cracked area, beam specimen, after five years of exposure. a) Zinc corrosion products on steel surface exposed to tap water, w = 0.15 mm. b) Porosity caused by the evolution of hydrogen and migration of zinc corrosion products into concrete exposed to sodium chloride solution, w = 0.35 mm.

---

[1] SFS 1215 (1996). Reinforcing steels. Weldable hot-rolled ribbed steel bars A500HW.
[2] SFS 1257 (1996). Reinforcing steels. Cold-worked ribbed steel bars B500K.

A comparison between the location or width of the cracks and place of breaking in a tensile test of the corroded cylinder specimens did not indicate a clear correlation. The most corroded areas were often located between cracks or in the upper or lower part of the cylinder specimens. The location did not correlate with crack width, as shown in Fig. 54. The mean values of the crack width (w), elongation limit 0.2% ($R_{p0.2}$), the tensile strength (R_m), the percentage elongation after failure (A_{10}), and the percentage total elongation at maximum force (A_{gt}) are shown in Fig. 54. According to the results of the tensile tests, the mechanical properties of the hot-dip galvanised reinforcement that were taken from cylinder specimens after seven years of exposure did not fulfil the standard requirements in Finland[1,2]. Different moisture conditions between the cracks and cracked area may have had an effect on this phenomenon. Furthermore, the size of the specimens, the longitudinal corrosion-induced cracks, and the deterioration of the chloride-contaminated concrete in the upper part of the specimen had an effect on the steel corrosion. It should be noted that the reinforcement bars were already loaded to their yield limit before the corrosion tests of the beam and cylinder specimens. However, this study focused on comparative research, not on service limit state analysis. Furthermore, there is permanent deformation in the steel which may have opened fractures that accelerate corrosion.
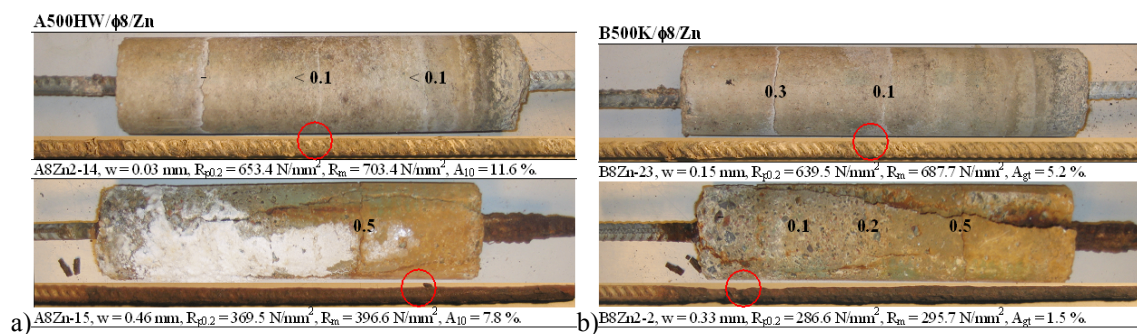
Fig. 54. *Corroded hot-dip galvanised reinforcement cylinder specimen after seven years of exposure to tap water (upper) and sodium chloride solution (lower). a) Hot-dip galvanised reinforcement bar A500HW/Ø8/Zn. b) Hot-dip galvanised reinforcement bar B500K/Ø8/Zn.*

4.3.9 The microscopic examination of the zinc layer of the reinforcement bars of the specimens

The optical microscopy studies of the pristine steel bars before exposure and covered with a zinc layer were performed using resin-impregnated and polished specimens. The analysis revealed the presence of four phases: gamma (γ), delta (δ), zeta (ζ), and eta (η) phases. The gamma (γ) phase is typically a very thin layer covering the ordinary steel. The delta (δ) phase is next to the gamma (γ) phase, followed by the zeta (ζ) and eta (η) phases. The total measured thickness of the zinc coating varied from 62 to 496 μm (see Appendix C) and examples are shown in Fig. 55. Different reinforcement bar diameters (Ø equal to 7 mm, 8 mm, and 12 mm) affect the significant variation in the thickness of the measured zinc coating. Furthermore, the results showed that the thickness of the zinc depends on the location. For example, more zinc was deposited on the slope part of the the rib; see Fig. 55c. Furthermore, two different areas of the delta (δ) phase could be

---

[1] SFS 1215 (1996). Reinforcing steels. Weldable hot-rolled ribbed steel bars A500HW.
[2] SFS 1257 (1996). Reinforcing steels. Cold-worked ribbed steel bars B500K.

distinguished. The inner area appeared to be denser, whereas the outer area consisted of a non-homogeneous and highly porous layer. Local variation in the thicknesses of the phases has an effect on corrosion mechanisms. Visible porous zones (layers) were found in all the specimens investigated. Similar zones have also been found by others[1,2,3,4]. Similar observations were also made during the ESEM-BSE investigation; see Fig. 56.
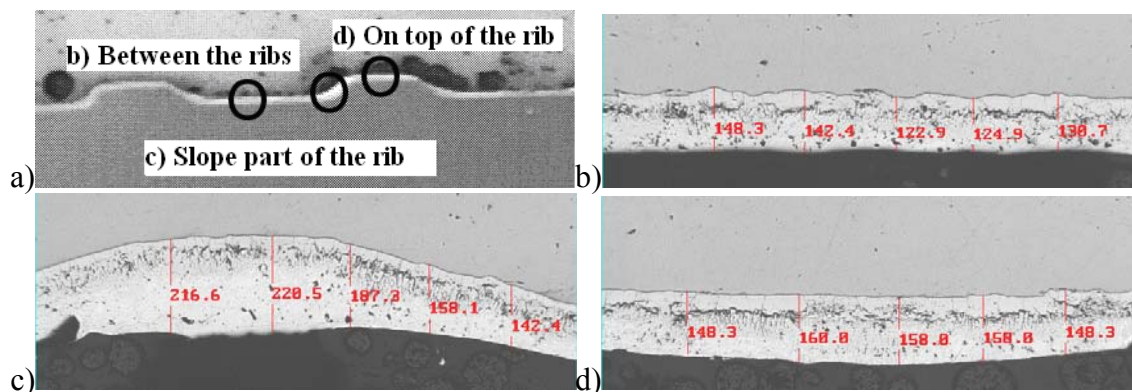
Fig. 55.   *a) Optical microscopy image of a zinc coating on macro level before corrosion tests (Finnish weldable hot-rolled ribbed steel reinforcement bar A500HW/Ø12) and micro level. b) Between the ribs. c) Slope part of the rib. d) On top of the rib. The marked thickness of the zinc coating is expressed in µm. The light part in the micro-level figure is an ordinary steel reinforcement bar.*
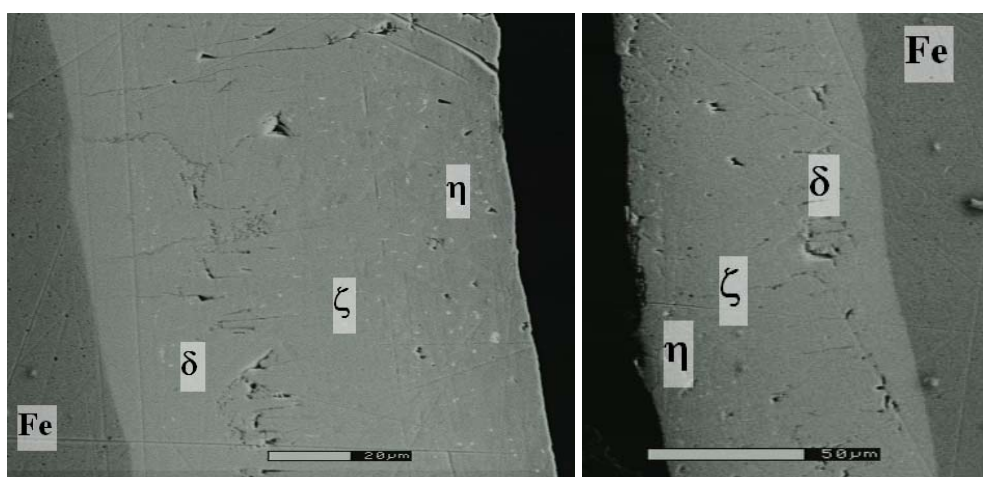
Fig. 56.   *ESEM images of the zinc coating of a pristine non-corroded bar of a Finnish weldable cold-worked ribbed steel bar B500K/ Ø8 before exposure. Iron-zinc alloy phases are marked in the figures. Grid line is 20 µm (left) and 50 µm (right).*

The preparation techniques used for the resin-impregnated and polished specimens preclude the existence of any artefacts which could be associated with the observed porous zones. Despite the use of a type of BSE detector which is known for its directional shadowing, no significant etching was observed between softer and harder materials. See the images in Fig. 57, Fig. 58, and Fig. 59. The ESEM-BSE observations of the deteriorated concrete revealed the existence of cracks in the zinc layer, as well as in the zinc/binder matrix interface. The cracks detected in the zeta (ζ) and eta (η) phases

[1] Bellezze, T. et al. (2006). Corrosion behaviour in Concrete of three differently Galvanized Steel Bars.
[2] Ho-Jong, Lee (2001). Effect of Ni addition in Zinc Bath on Formation of Inhibition Layer during Galvannealing of Hot-dip Galvanized Sheet Steels.
[3] Andrade, C. et al. (2001). Tests on Bond of Galvanized Rebar And Concrete Cured In Seawater.
[4] Andrade, C. et al. (1995). Coating Protection for Reinforcement.

were either longitudinal or perpendicular to the reinforcement bars and could extend into the binder matrix. The cracks within the binder matrix were usually perpendicular to the reinforcement bar.

As shown in Fig. 59, the local dissolution of, most probably, the zeta (ζ) and eta (η) phases was observed. The BSE images of the severely corroded core specimens revealed the existence of virtually untouched zinc layers and a thin Fe layer beneath them. The deeper Fe layers of the reinforcement bars appeared to be fully corroded; see Fig. 60. Furthermore, on the basis of the images obtained several modes of the deterioration of the zinc layer could be distinguished. Fig. 57 shows the local dissolution of, most probably, the zeta (ζ) and eta (η) phases. The second form of deterioration observed is microcracks within the zeta (ζ) and eta (η) phases which extend into the binder matrix; see Fig. 58 and Fig. 59. The last mode of deterioration, shown in Fig. 60, took the form of the extensive corrosion of the steel core beneath the virtually intact zinc layer. Cathodic protection does not act any more in this case. The ESEM analysis of the corroded specimens showed clearly that the corrosion of the steel core occurred deeper under the zinc cover. The corrosion proceeded in all directions, including beneath the zinc layer.
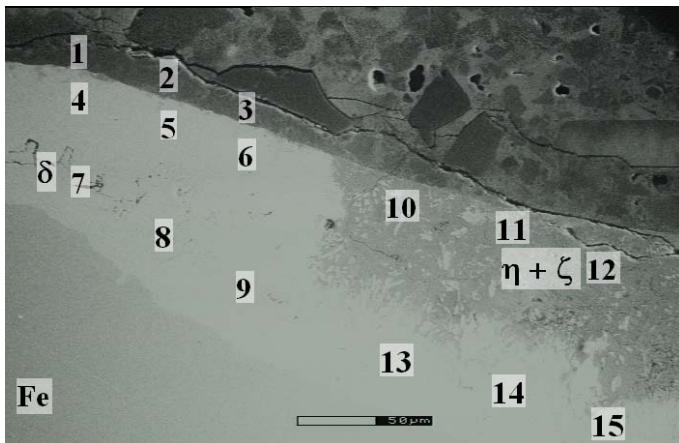
Fig. 57.   *First corrosion mechanism, local dissolution of the eta (η) phase and the zeta (ζ) phase (Hot-dip galvanised reinforcement cylinder specimen, A500HW/Ø8/ZN, tap water, after seven years of exposure). EDS spots in Table 37 are marked in the picture. Grid line is 50 μm.*
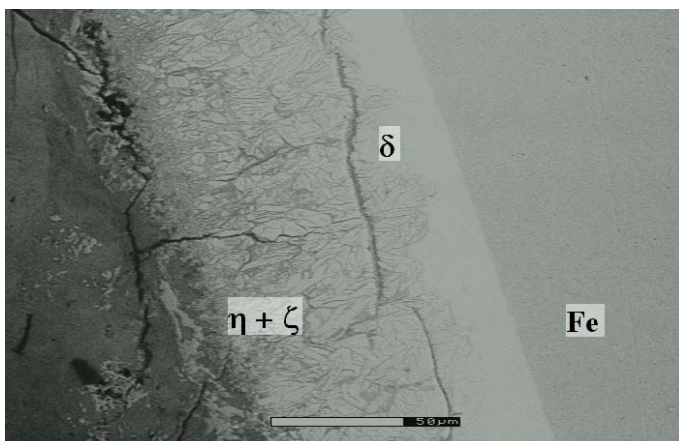
Fig. 58.   *Second corrosion mechanism (zinc separation), local dissolution of the eta (η) and the zeta (ζ) phase, and access to the cracks in the zinc layer (Hot-dip galvanised reinforcement beam specimen, B500K/Ø8/ZN, sodium chloride solution, after five years of exposure). Grid line is 50 μm.*
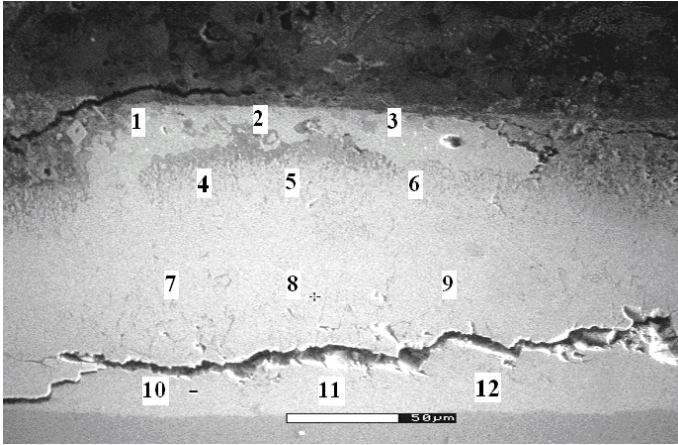
Fig. 59.   *First corrosion mechanism, local dissolution of the eta (η) and the zeta (ζ) phase (Hot-dip galvanised reinforcement beam specimen, B500K/Ø8/ZN, sodium chloride solution, after five years of exposure). The longitudinal crack in the figure is originally from the specimen preparation and results from the sawing. EDS spots in Table 38 are marked in the picture. Grid line is 50 μm.*
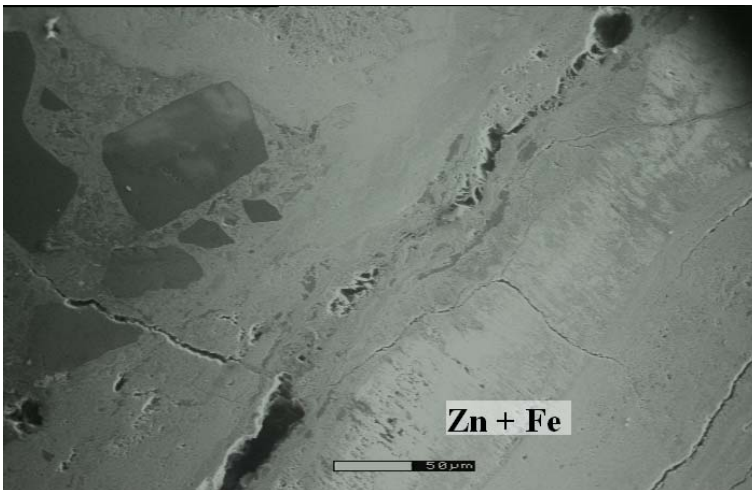
Fig. 60.   *Third corrosion mechanism (zinc and ferrite separation), full dissolution of the eta (η) phase and partial dissolution of the zeta (ζ) phase (Hot-dip galvanised reinforcement cylinder specimen, B500K/Ø8/ZN, sodium chloride solution, after seven years of exposure). Grid line is 50 μm.*

In addition, the EDS spot analysis was performed on the deteriorated specimens exposed either to tap water or the sodium chloride solution. The Ca to Si, (Al+Fe)/Ca, and Zn/Fe atomic ratios were calculated in order to facilitate the recognition of the main hydration phases of the binder matrix. The results obtained are shown in Table 37 and Table 38. The analysed spots are marked by numbers on the BSE images shown in Fig. 57 and Fig. 59. The proportions of (Al+Fe)/Ca to Ca/Si atomic ratios for the beam and cylinder specimens are shown in Fig. 61 and Fig. 62. The limits for the reaction products Calcium Silicate Hydrate (CSH), Calcium Hydroxide, Ca (OH) $_2$ (CH), and monosulphate, Al_2O_3-Fe_2O_3-mono (AFm), are marked in Fig. 61 and Fig. 62[1,2]. Other results are shown in Appendix B. Of the analyses performed, none showed any

---

[1] Taylor, H. et al. (1984). An Electron Microprobe Study of a Mature Cement Paste.
[2] Lachowski, E.E. et al. (1980). Analytical Electron Microscopy of Cement Pastes: II, Pastes of Portland Cements and Clinkers.

indication of CSH, CH, or Afm as the major product. The equipment used and composite material analysed influence this phenomenon and are typical for this case.

Table 37.   EDS spot analysis of Fig. 57 (Hot-dip galvanised reinforcement cylinder specimen, A500HW/Ø8/ZN, tap water, after seven years of exposure).

Spot	Na [%]	Mg [%]	Al [%]	Si [%]	Cl [%]	K [%]	Ca [%]	Mn [%]	Fe [%]	Zn [%]	Ca /Si [-]	(Al+Fe) /Ca [-]	Zn /Fe [-]
1.	0	0	1.06	6.29	0	0.38	30.74	0.46	10.7	50.36	4.9	0.4	4.7
2.	0	0	2.34	9.95	0	0.13	5.27	0.27	6.54	75.51	0.5	1.7	11.5
3.	3.49	0	0.57	8.96	0	0.41	32.38	0.55	7.45	46.2	3.6	0.2	6.2
4.	12.7	0	0	0.39	0	0.16	0.74	0.38	7.63	78	1.9	10.3	10.2
5.	6.54	0	0	0.47	0	0.07	0.65	0.78	4.12	87.37	1.4	6.3	21.2
6.	10.7	0.14	0	0.31	0.05	0.06	0.57	0.59	3.84	83.75	1.8	6.7	21.8
7.	0	0	0	0	0	0	0.51	0.6	12.19	86.7		23.9	7.1
8.	0	0	0	0.26	0	0.18	0.27	0.53	13.17	85.59	1.0	48.8	6.5
9.	0	0	0	0	0	0	0.49	0.59	13	85.93		26.5	6.6
10.	0	0	0	1.33	0	0	1.2	0.47	7.57	89.43	0.9	6.3	11.8
11.	6.11	0	0	1.02	0	0	2.45	0.37	5.72	84.33	2.4	2.3	14.7
12.	0	0	0	0.38	0	0	1.88	0.44	5.68	91.62	4.9	3.0	16.1
13.	0	0	0	0	0	0.09	0.4	0.61	11.87	87.04		29.7	7.3
14.	0	0	0	0	0	0.09	0.4	0.61	11.87	87.04		29.7	7.3
15.	0	0	0	0	0	0.1	0.41	0.48	12.33	86.68		30.1	7.0
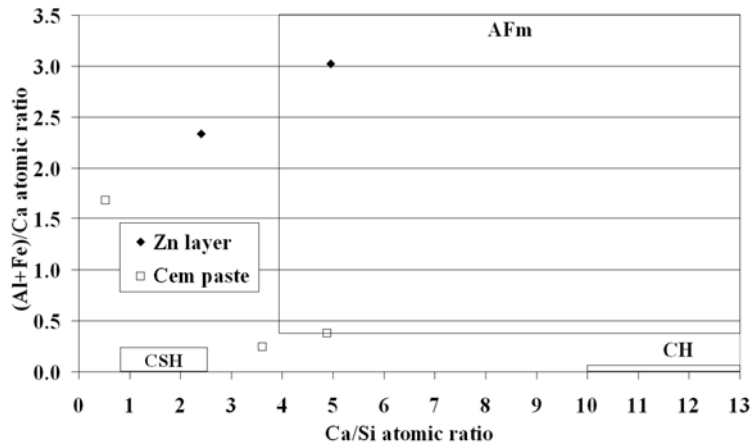
Fig. 61.   Proportions of (Al+Fe)/Ca to Ca/Si atomic ratios for hot-dip galvanised reinforcement cylinder specimen, A500HW/Ø8/ZN, tap water, after seven years of exposure.

Table 38. *EDS spot analysis of Fig. 59 (Hot-dip galvanised reinforcement beam specimen, B500K/Ø8/ZN, sodium chloride solution, after five years of exposure).*

Spot	Na [%]	Mg [%]	Al [%]	Si [%]	Cl [%]	K [%]	Ca [%]	Mn [%]	Fe [%]	Zn [%]	Ca /Si [-]	(Al+Fe) /Ca [-]	Zn /Fe [-]
1.	19.49	0.95	1.19	1.64	1.01	1.1	3.77	1.31	5.52	64.03	2.3	1.8	11.6
2.	14.2	0.88	0.97	1.74	0.97	1.11	4.19	1.57	5.86	68.52	2.4	1.6	11.7
3.	21.57	0	0	0.31	0	0	2.66	0.31	4.79	70.36	8.6	1.8	14.7
4.	12.27	0.81	1.07	1.42	1	1.17	2.26	1.67	9.36	68.98	1.6	4.6	7.4
5.	15.95	0	0	0	0	0.07	1.46	0.69	8.54	73.29		5.8	8.6
6.	7.98	0.81	1.05	1.5	1.01	0.89	2.42	1.68	9.56	73.12	1.6	4.4	7.6
7.	7.98	0.81	1.05	1.5	1.01	0.89	2.42	1.68	9.56	73.12	1.6	4.4	7.6
8.	6.52	0.92	1.13	1.18	0.99	1.15	1.72	1.65	12.5	72.24	1.5	7.9	5.8
9.	8.42	0.93	1.07	1.16	0.77	1.2	1.72	1.74	12.43	70.57	1.5	7.8	5.7
10.	6.61	0.92	1.03	1.13	0.94	1.21	1.33	1.42	21.1	64.31	1.2	16.6	3.0
11.	6.96	0	0	0	0	0	0.6	0.68	25.85	65.91		43.1	2.5
12.*													

* Not done (equipment error)
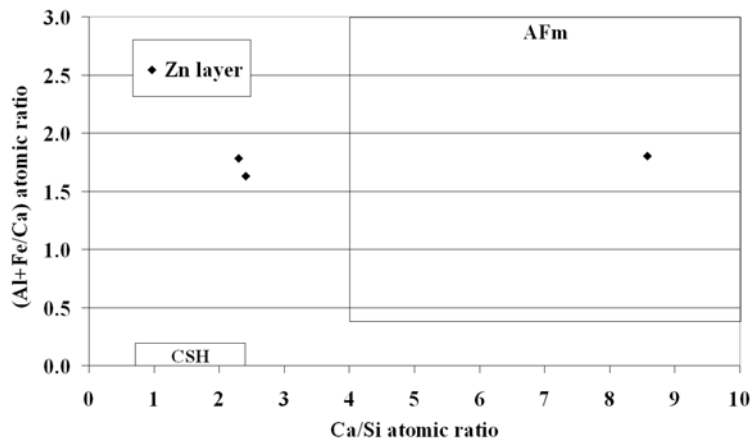
Fig. 62. *Proportions of (Al+Fe)/Ca to Ca/Si atomic ratios for hot-dip galvanised reinforcement beam specimen, B500K/Ø8/ZN, sodium chloride solution, after five years of exposure.*

In general, the results obtained showed an increased amount of Ca ions in the interfacial transition zone (ITZ) between the cement matrix and the reinforcement bars in most of the specimens studied. Some chloride and sodium ions were detected in the beam specimens stored in the sodium chloride solution when the spot analysis was performed in the outer zinc layers and in the binder matrix; see Fig. 59 and Table 38. The amount of the elements detected by the EDS in a certain spot is influenced by the so-called electron beam skirting. As a result of this effect the electrons may originate from an area that is larger than anticipated. Nevertheless, higher Zn/Fe atomic ratios could be observed in the outer layers of the zinc.

4.4 Analysis of the results

4.4.1 Electrochemical and crack width measurements

The present studies showed, as expected, that in general the rate of corrosion, here determined by means of the electrochemical measurements, was significantly higher in the case of chloride-contaminated concretes than carbonated ones. The hot-dip

galvanised steel showed a lower rate of corrosion in comparison with ordinary steel. According to earlier results[1], the recorded corrosion potential values E_{corr} (V_{CSE}) of -750...-900 mV for a hot-dip galvanised steel reinforcement in chloride-contaminated concrete correspond to a high risk of corrosion. At the same time the measured corrosion potential values in carbonated concrete reached more than -700 mV, which, according to the results published earlier, corresponds to a low risk of corrosion. The criteria for the probabilities of corrosion for ordinary steel reinforcement bars[2] cannot be used for different materials of reinforcement bars. No similar criteria for galvanised reinforced bars have previously been published. The same trend was observed in the case of the measured corrosion current values[3]. As presented elsewhere[4], the measured resistivity values of less than 10 kΩ cm for a hot-dip galvanised steel reinforcement bar in chloride-contaminated concrete were not limiting factors with respect to the rate of corrosion. At the same time the measured resistivity values, ranging from 10 kΩ cm to 50 kΩ cm in carbonated concrete, indicated a moderate to high risk of corrosion. The comparison of the measured crack width and rate of corrosion values showed no correlation independently of the exposure duration or type of aggressive liquid; see Fig. 63. Other measured values, such as the corrosion potential, the resistivity of the concrete, and mechanical properties, did not reveal any correlation with the crack width either; see results elsewhere[5].

---

[1] Sistonen, E., Huovinen, S. (2005). The Main Corrosion Parameters and their Influence on the Durability of Outdoor Concrete Structures.

[2] ASTM C 876-91 (1999). Standard Test Method for Half-Cell Potentials of Uncoated Reinforcing Steel in Concrete.

[3] Andrade, C., Alonso, C. (2001). On-Site Measurements of Corrosion Rate of Reinforcements.

[4] Andrade, C. et al. (2000). Recommendations of RILEM TC-154-EMC.

[5] Sistonen, E. et al. (2007). The Influence of the Crack Width on the Durability of different Reinforcement Bar Materials.
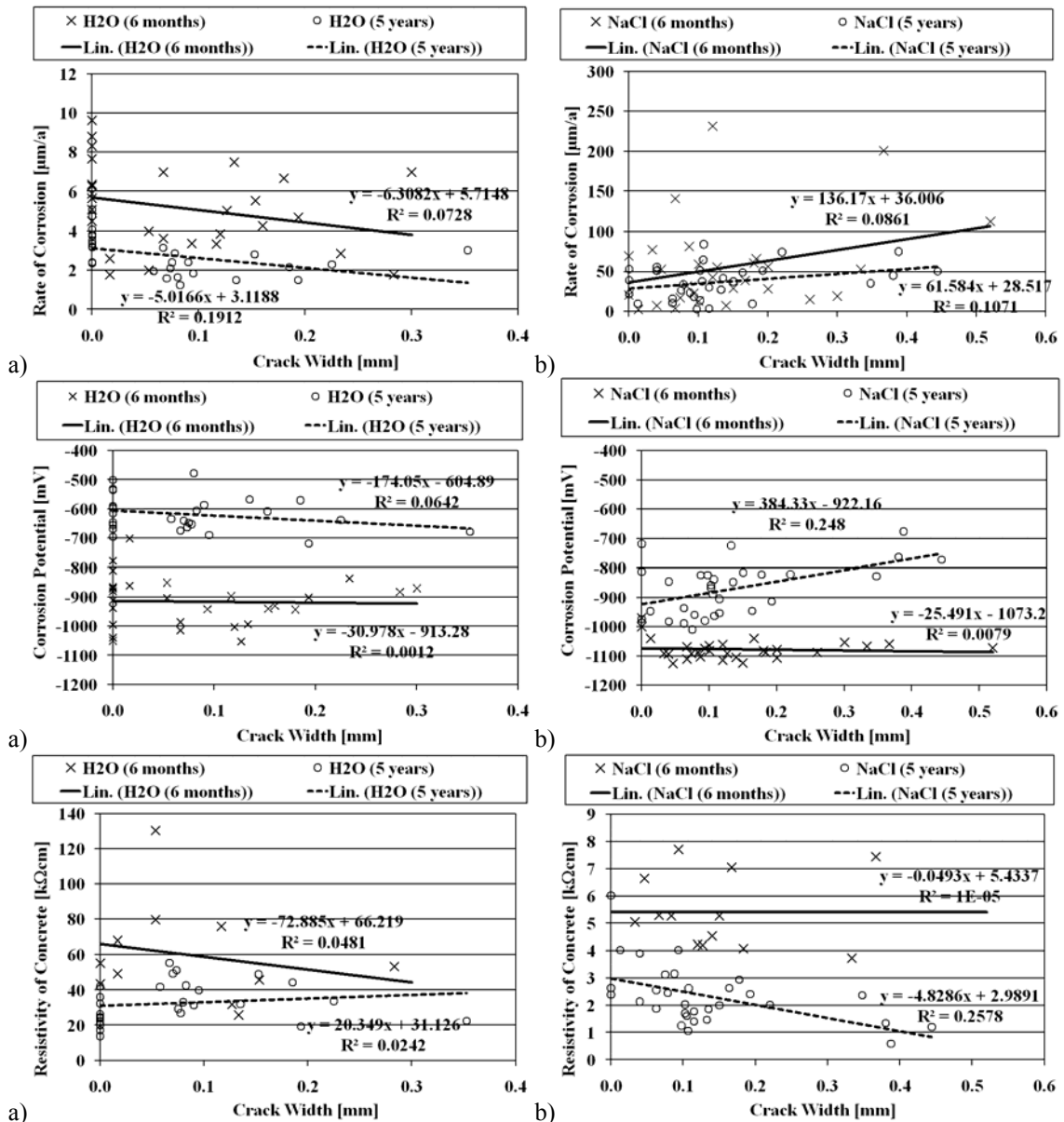
Fig. 63. *Rate of corrosion, corrosion potential, and resistivity of concrete as a function of the crack width for hot-dip galvanised steel reinforcement bars exposed to tap water (a) and sodium chloride solution (b) (beam specimens) after six months and five years of exposure.*

The calculated values for the coefficient of the rate of corrosion k_s (Equation (30)) are shown in Table 39 for the beam and cylinder specimens exposed to tap water and the sodium chloride solution. The values are calculated for the actual propagation time with the rate of corrosion values presented in Table 32. The rate of corrosion is estimated as uniform in Table 32 and decreasing in Table 39. The calculated values for the coefficient of the rate of corrosion k_s for the beam and cylinder specimens exposed to tap water are shown in Fig. 64.

Table 39. *The coefficient of rate of corrosion (k_l or k_s) [$\mu m/(a)^{1/2}$] for beam and cylinder specimens exposed to tap water and sodium chloride solution.*

Reinforcement bar type	Ordinary steel	Hot-dip galvanised steel	Weathering (TENCOR) steel	Austenitic stainless steel
Beam specimen in tap water	11.4[a] 12.1[b]	8.3[a] 12.5[b]	8.8[a] 13.1[b]	1.1[a] 3.6[b]
Beam specimen in NaCl solution	210.2[a] 447.1[b]	86.7[a] 167.9[b]	98.9[a] 231.1[b]	2.5[a] 7.1[b]
Cylinder specimen in tap water	8.8[c] 4.6[d]	3.7[c] 5.8[d]	3.0[c] Not measured[d]	0.3[c] 1.3[d]
Cylinder specimen in NaCl solution	378.3[c] 700.6[d]	336.7[c] 474.0[d]	687.6[c] 603.3[d]	0.5[c] 12.0[d]

[a] after six months of exposure
[b] after five years of exposure
[c] after three months of exposure
[d] after seven years of exposure
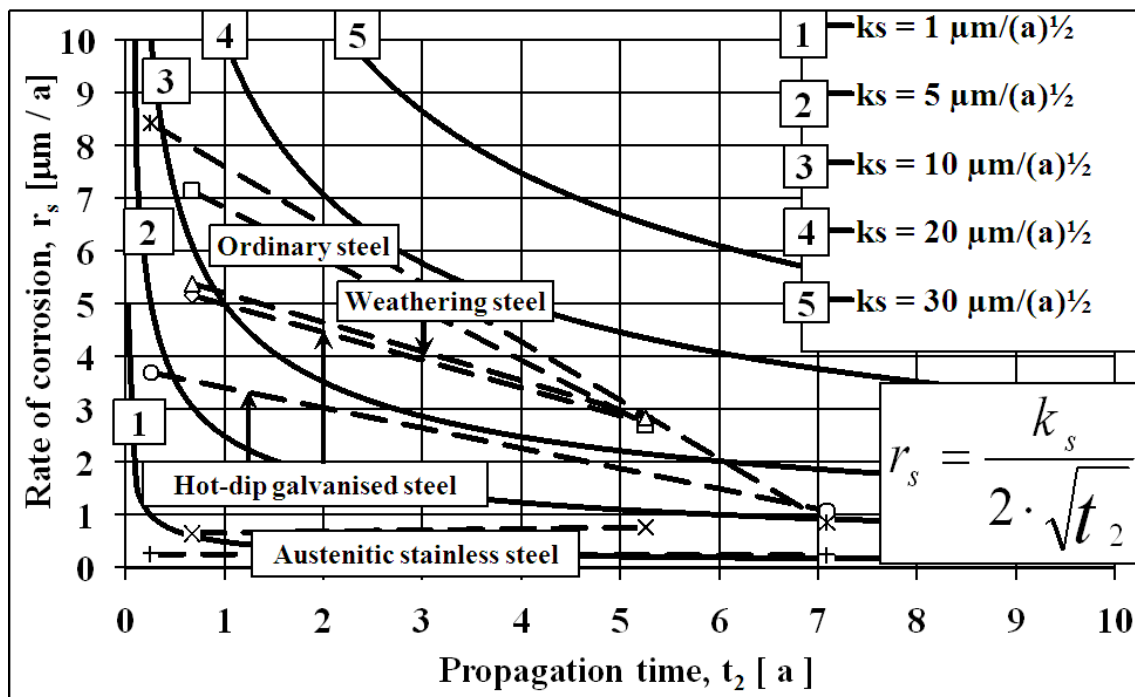
Fig. 64. *The coefficient of rate of corrosion k_s for beam and cylinder specimens exposed to tap water.*

On the basis of Table 39 and Fig. 64 it can be noticed that the rate of corrosion decreased as a function of exposure time. The connection with Table 39 and Fig. 64, and the reason for the statement made partly lies in the estimation of the propagation time. It is significantly longer in the case of decreasing rate of corrosion than in the case of uniform rate of corrosion, especially for beam and cylinder specimens exposed to tap water (see Table 6 and Chapter 5.1). This phenomenon may have a positive effect on improvement of the service life of reinforced concrete structures. The research result was not dependent on the water-to-cement ratio of concrete. It should be pointed out that only one cement type was used in the study. General concrete properties, e.g. diffusivity, have an effect on the rate of corrosion and moisture conditions. Furthermore, the coefficient of the rate of corrosion k_s is not necessarily constant.

Approximated half-cell potential limits for different reinforcement bar materials measured with a copper/copper sulphate half-cell, CSE, were proposed on the basis of the corrosion tests performed, theoretical analyses, and literature (Table 40 and Table 41)[1,2]. One basis for the presented values is the differences in noble-mindedness between the steel reinforcement bars studied. Base metal is stated as having a more negative corrosion potential. Based on the corrosion tests performed with comparison to Pourbaix diagrams[3] corrosion potential values in the carbonated concrete are estimated to be some 100 mV more negative than in chloride-contaminated concrete. The reason for this estimation lies in more probable risk of corrosion in chloride-contaminated concrete than in carbonated concrete. For instance, in chloride-contaminated concrete pitting corrosion may occur with higher pH values of the concrete. It should be pointed out that higher absolute values are more probable in chloride-contaminated concrete than in carbonated concrete as a result of the severity of the exposure. Thus, presented half-cell potential limits are on the safe side compared to the corrosion tests performed. The boundary condition used for the values is the criteria of ASTM C876-91, presented for ordinary steel reinforcement bars in chloride-contaminated concrete[4]. Those criteria were estimated from field measurements of cast-in-place bridge structures in the United States where the concrete was contaminated with chloride. The half-cell potential limits presented for hot-dip galvanised reinforcement bars are based on the iron content of the zinc phases (see Chapter 2.1), earlier measurements found from the literature (see Fig. 7, right), and electrochemical measurements by the author. Half-cell potential limits for austenitic stainless steel reinforcement bars in carbonated concrete are not presented because the state of corrosion is passive in this exposure. This was also noticed by the author when assessing the results of durability tests.

Table 40. *Half-cell potential limits for ordinary, weathering, or austenitic stainless steel reinforcement bar (copper/copper sulphate half-cell, CSE) expressed in mV.*

	Ordinary steel reinforcement bar		Weathering steel reinforcement bar		Austenitic stainless steel reinforcement bar	
State of corrosion	chloride-contaminated concrete*	carbonated concrete	chloride-contaminated concrete	carbonated concrete	chloride-contaminated concrete	carbonated concrete
Low risk of corrosion, < 10%	> -200	> -300	> -150	> -250	> -100	-
Moderate corrosion risk	-200...-350	-300...-450	-150...-300	-250...-400	-100...-250	-
High risk of corrosion, > 90%	-350...-500	-450...-600	-300...-450	-400...-550	-250...-400	-
Severe corrosion risk	< -500	< -600	< -450	< -550	< -400	-

*) ASTM C876-91[5]

[1] Sistonen, E. (2001). The Main Corrosion Parameters and their Influence on the Durability of Outdoor Concrete Structures (in Finnish).

[2] Sistonen, E., Huovinen, S. (2005). The Main Corrosion Parameters and their Influence on the Durability of Outdoor Concrete Structures.

[3] Pourbaix, M. (1963). Atlas of Electrochemical Equilibria in Aqueous Solutions.

[4] ASTM C876-91 (1999). Standard Test Method for Half-Cell Potentials of Uncoated Reinforcing Steel in Concrete.

[5] ASTM C876-91 (1999). Standard Test Method for Half-Cell Potentials of Uncoated Reinforcing Steel in Concrete.

Table 41. *Half-cell potential limits for hot-dip galvanised reinforcement bar, (copper/copper sulphate half-cell, CSE) expressed in mV.*

Phase	Eta (η)		Zeta (ζ)		Delta (δ)		Gamma (γ)	
State of corrosion	chloride-contaminated concrete	carbonated concrete	chloride-contaminated concrete	carbonated concrete	chloride-contaminated concrete	carbonated concrete	chloride-contaminated concrete	carbonated concrete
Low risk of corrosion, < 10%	> -600	>-700	> -500	>-600	> -400	>-500	> -250	>-350
Moderate corrosion risk	-600... -750	-700... -850	-500... -650	-600... -750	-400... -550	-500... -650	-250... -400	-350… -500
High risk of corrosion, > 90%	-750... -900	-850... -1000	-650... -800	-750... -900	-550... -700	-650... -800	-400... -550	-500… -650
Severe corrosion risk	< - 900	<-1000	< - 800	<-900	< - 700	<-800	< - 550	<-650

The corrosion potential E_{corr} (V_{CSE}) for the beam and cylinder specimens exposed to tap water and the sodium chloride solution is shown in Table 42. E_{corr} − log i_{corr} graphs of hot-dip galvanised reinforcement bars for the beam specimens exposed to tap water and the sodium chloride solution are shown in Fig. 65, Fig. 66, Fig. 67, and Fig. 68. E_{corr} − log i_{corr} graphs of hot-dip galvanised reinforcement bars for the cylinder specimens exposed to tap water and the sodium chloride solution are shown in Fig. 69, Fig. 70, Fig. 71, and Fig. 72. Log i_{corr} − R graphs of hot-dip galvanised reinforcement bars for the beam specimens exposed to tap water and the sodium chloride solution are shown in Fig. 73, Fig. 74, Fig. 75, and Fig. 76. Log i_{corr} − R graphs of hot-dip galvanised reinforcement bars for the cylinder specimens exposed to tap water and the sodium chloride solution are shown in Fig. 77, Fig. 78, Fig. 79, and Fig. 80. E_{corr} − R graphs of hot-dip galvanised reinforcement bars for the beam specimens exposed to tap water and the sodium chloride solution are shown in Fig. 81, Fig. 82, Fig. 83, and Fig. 84. E_{corr} − R graphs of hot-dip galvanised reinforcement bars for the cylinder specimens exposed to tap water and the sodium chloride solution are shown in Fig. 85, Fig. 86, Fig. 87, and Fig. 88.

Table 42. *State of corrosion based on the corrosion potential E_{corr} (CSE) for beam and cylinder specimens exposed to tap water and sodium chloride solution.*

Reinforcement bar type	Ordinary steel	Hot-dip galvanised steel	Weathering (TENCOR) steel	Austenitic stainless steel
Beam specimen in tap water	Severe[a] High[b]	High (η)[a] Low (η)[b] Moderate (ζ)[b]	Severe[a] High[b]	Passive[a] Passive[b]
Beam specimen in NaCl solution	Severe[a] Severe[b]	Severe (η)[a] High (η)[b] Severe (ζ)[b]	Severe[a] Severe[b]	High[a] High[b]
Cylinder specimen in tap water	Moderate[c] Low[d]	High (η)[c] Low (η,ζ)[d]	Moderate[c] Not measured[d]	Passive[c] Passive[d]
Cylinder specimen in NaCl solution	Severe[c] Severe[d]	Severe (η)[c] High (γ)[d]	Severe[c] Severe[d]	Moderate[c] High[d]

[a] after six months of exposure
[b] after five years of exposure
[c] after three months of exposure
[d] after seven years of exposure

Fig. 65. *E_{corr} – log i_{corr} graphs of hot-dip galvanised reinforcement bars for the beam specimens exposed to tap water after six months of exposure.*

Fig. 66. *E_{corr} – log i_{corr} graphs of hot-dip galvanised reinforcement bars for the beam specimens exposed to tap water after five years of exposure.*

Fig. 67. E_{corr} − log i_{corr} graphs of hot-dip galvanised reinforcement bars for the beam specimens exposed to sodium chloride solution after six months of exposure.

Fig. 68. E_{corr} − log i_{corr} graphs of hot-dip galvanised reinforcement bars for the beam specimens exposed to sodium chloride solution after five years of exposure.
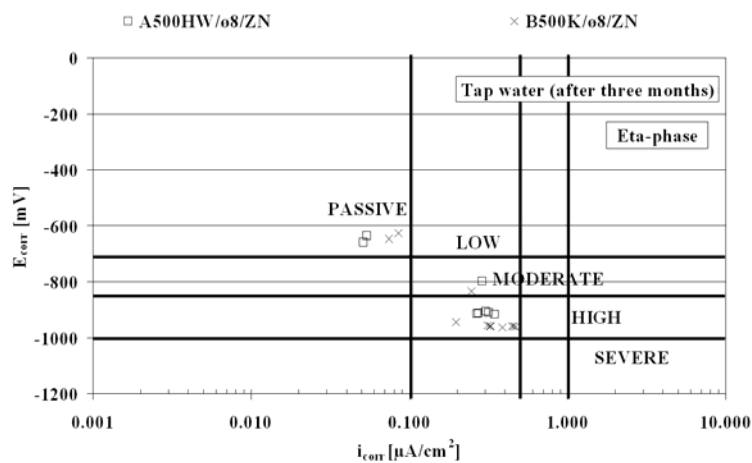
Fig. 69. E_{corr} − log i_{corr} graphs of hot-dip galvanised reinforcement bars for the cylinder specimens exposed to tap water after three months of exposure.
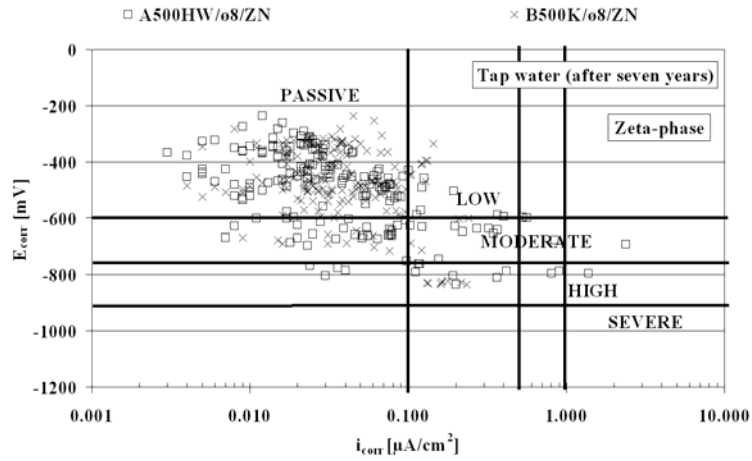
Fig. 70. E_{corr} – log i_{corr} *graphs of hot-dip galvanised reinforcement bars for the cylinder specimens exposed to tap water after seven years of exposure.*
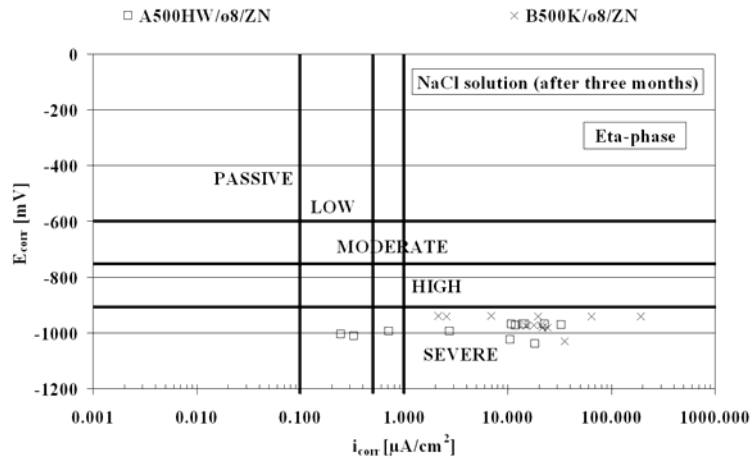
Fig. 71. E_{corr} – log i_{corr} *graphs of hot-dip galvanised reinforcement bars for the cylinder specimens exposed to sodium chloride solution after three months of exposure.*
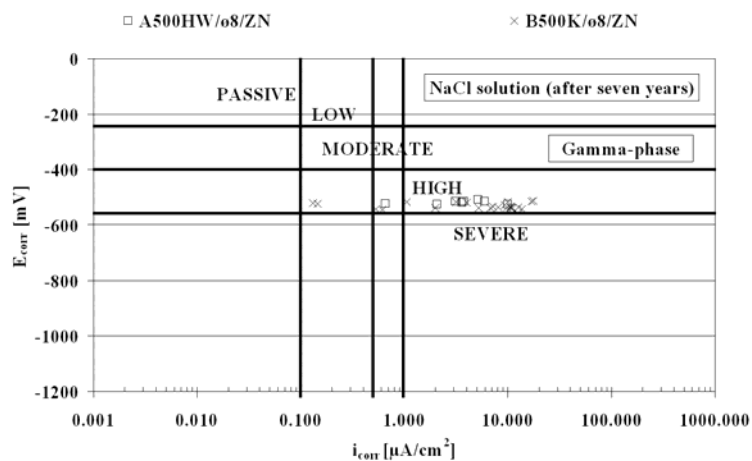
Fig. 72. E_{corr} – log i_{corr} *graphs of hot-dip galvanised reinforcement bars for the cylinder specimens exposed to sodium chloride solution after seven years of exposure.*
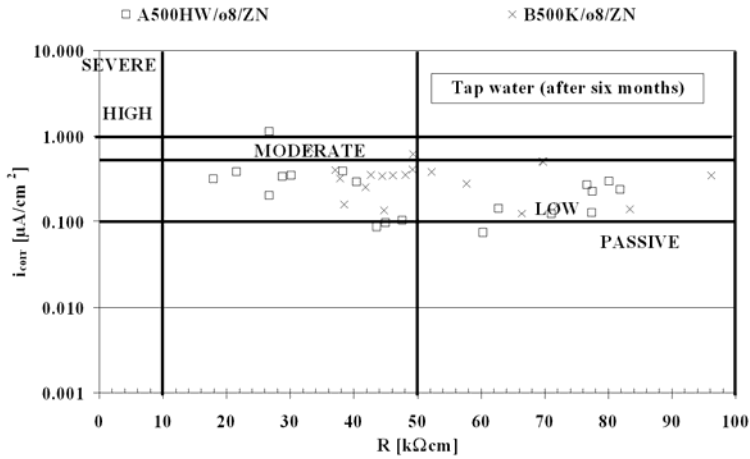
Fig. 73.   *Log i$_{corr}$ – R graphs of hot-dip galvanised reinforcement bars for the beam specimens exposed to tap water after six months of exposure.*
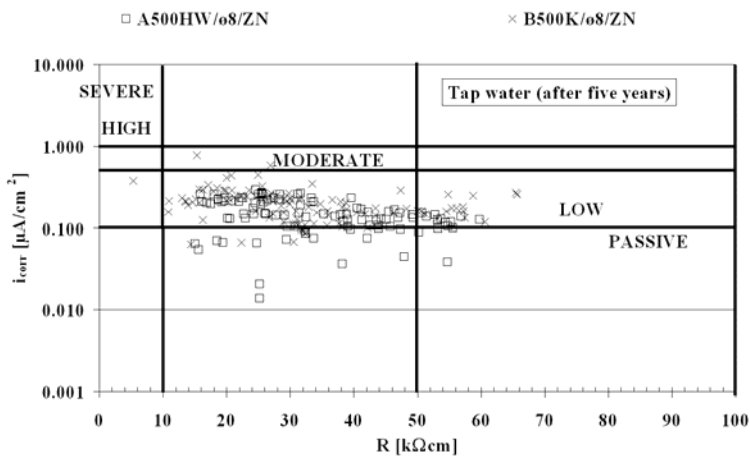
Fig. 74.   *Log i$_{corr}$ – R graphs of hot-dip galvanised reinforcement bars for the beam specimens exposed to tap water after five years of exposure.*
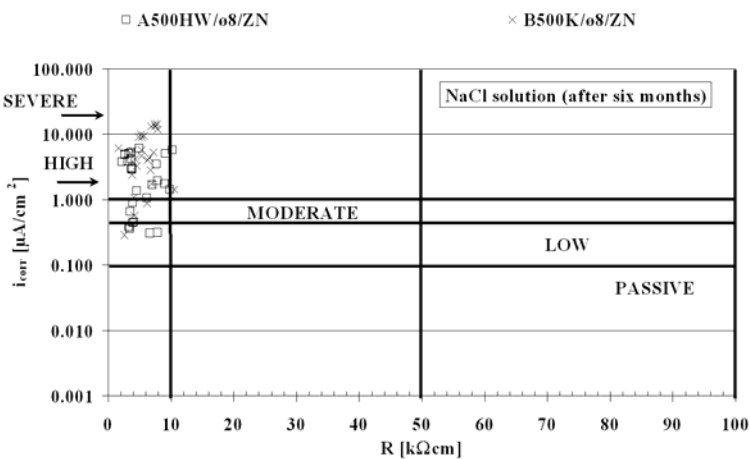
Fig. 75.   *Log i$_{corr}$ – R graphs of hot-dip galvanised reinforcement bars for the beam specimens exposed to sodium chloride solution after six months of exposure.*
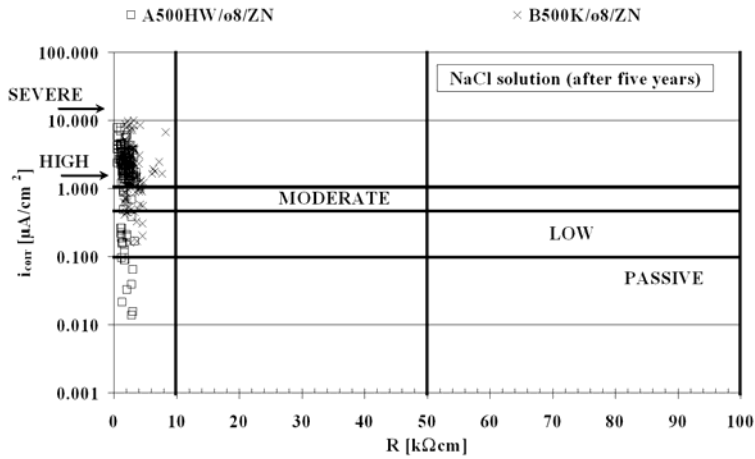
Fig. 76. *Log i_{corr} – R graphs of hot-dip galvanised reinforcement bars for the beam specimens exposed to sodium chloride solution after five years of exposure.*
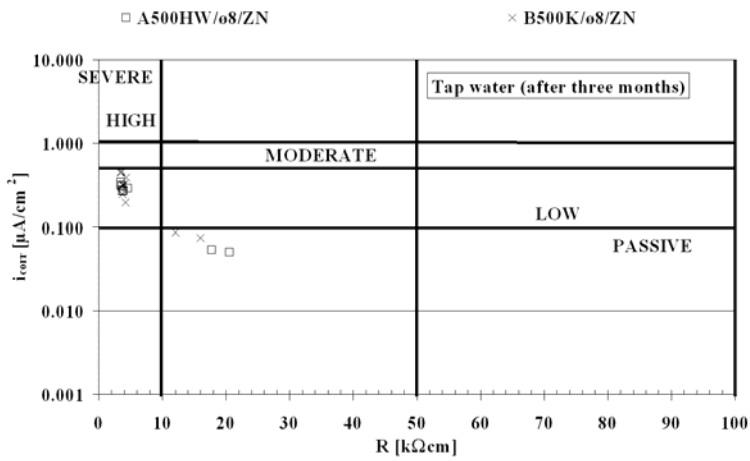
Fig. 77. *Log i_{corr} – R graphs of hot-dip galvanised reinforcement bars for the cylinder specimens exposed to tap water after three months of exposure.*
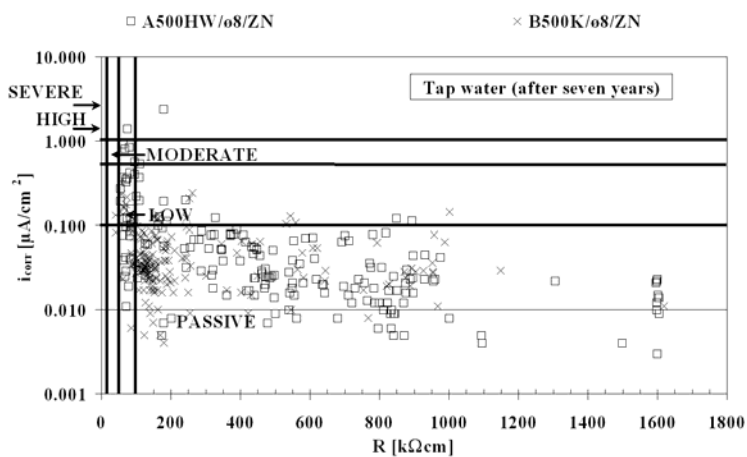
Fig. 78. *Log i_{corr} – R graphs of hot-dip galvanised reinforcement bars for the cylinder specimens exposed to tap water after seven years of exposure.*
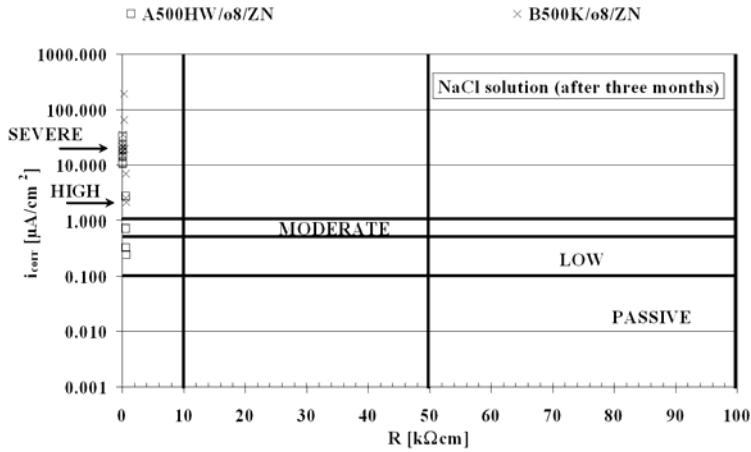
Fig. 79.   *Log i_{corr} – R graphs of hot-dip galvanised reinforcement bars for the cylinder specimens exposed to sodium chloride solution after three months of exposure.*
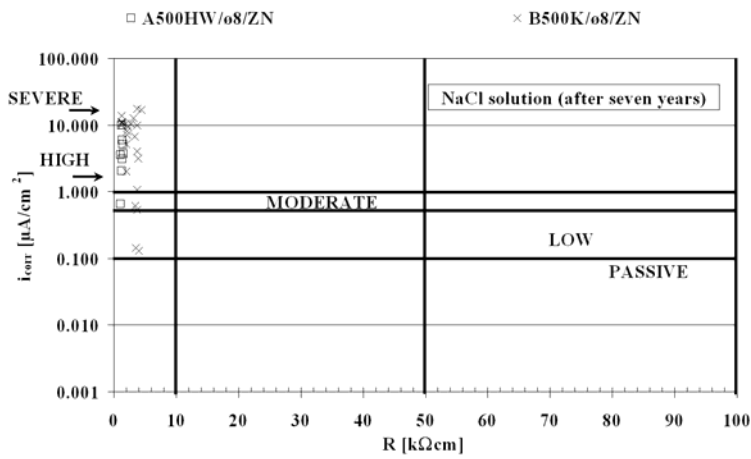
Fig. 80.   *Log i_{corr} – R graphs of hot-dip galvanised reinforcement bars for the cylinder specimens exposed to sodium chloride solution after seven years of exposure.*
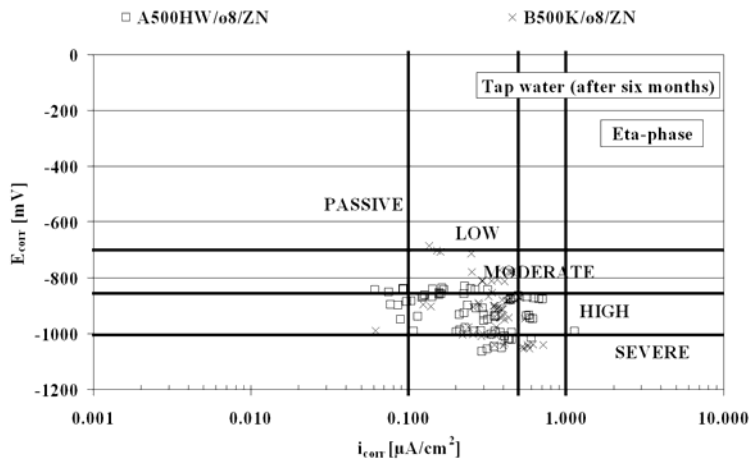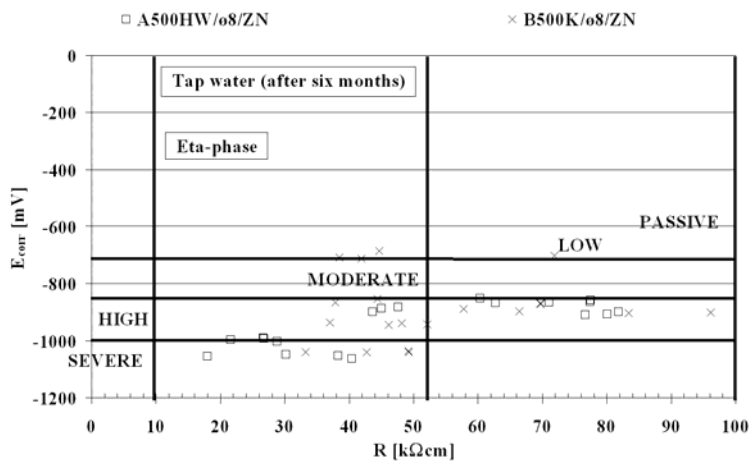

Fig. 81.   *E_{corr} – R graphs of hot-dip galvanised reinforcement bars for the beam specimens exposed to tap water after six months of exposure.*
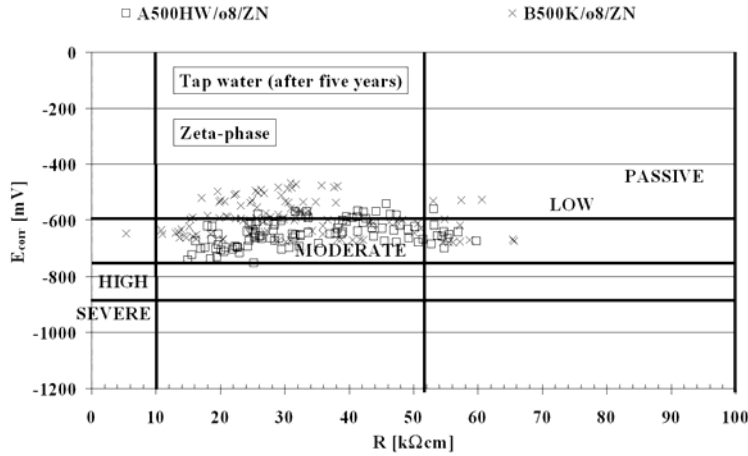
Fig. 82. E_{corr} – R graphs of hot-dip galvanised reinforcement bars for the beam specimens exposed to tap water after five years of exposure.
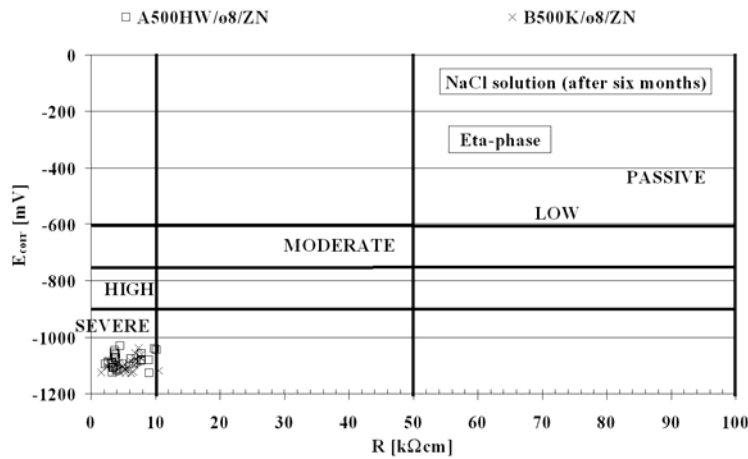
Fig. 83. E_{corr} – R graphs of hot-dip galvanised reinforcement bars for the beam specimens exposed to sodium chloride solution after six months of exposure.
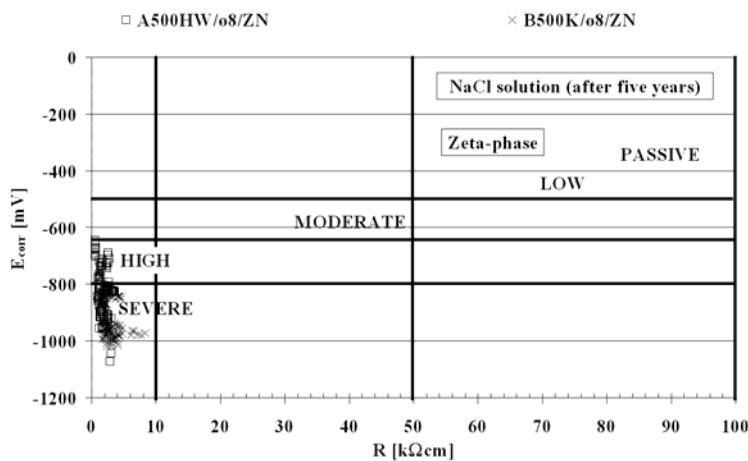
Fig. 84. E_{corr} – R graphs of hot-dip galvanised reinforcement bars for the beam specimens exposed to sodium chloride solution after five years of exposure.
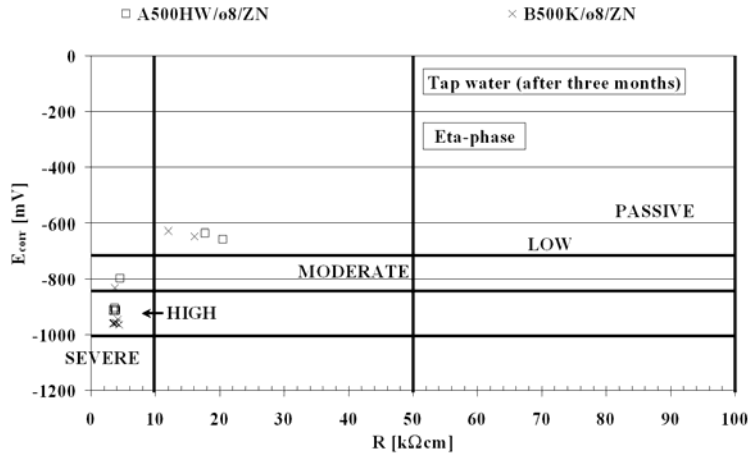
Fig. 85.   *E_{corr} − R graphs of hot-dip galvanised reinforcement bars for the cylinder specimens exposed to tap water after three months of exposure.*
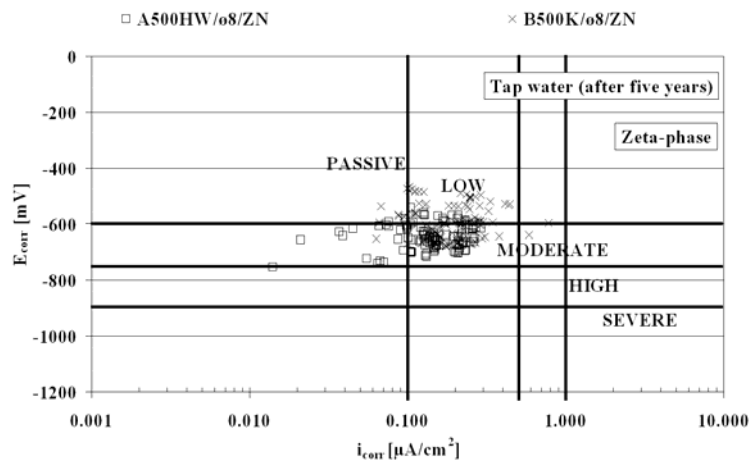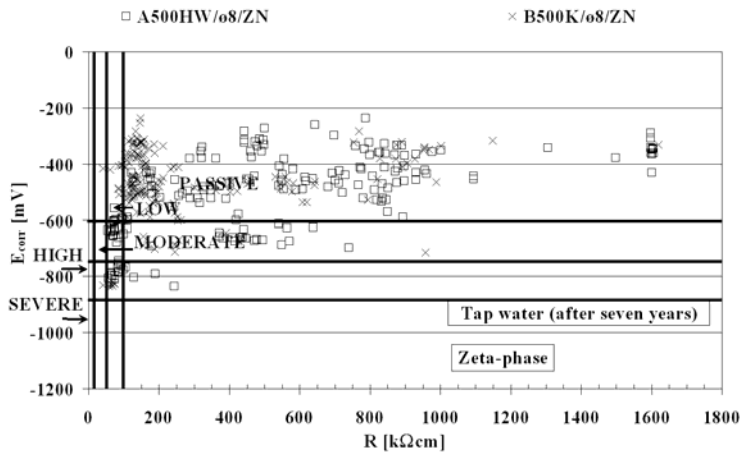

Fig. 86.   *E_{corr} − R graphs of hot-dip galvanised reinforcement bars for the cylinder specimens exposed to tap water after seven years of exposure.*
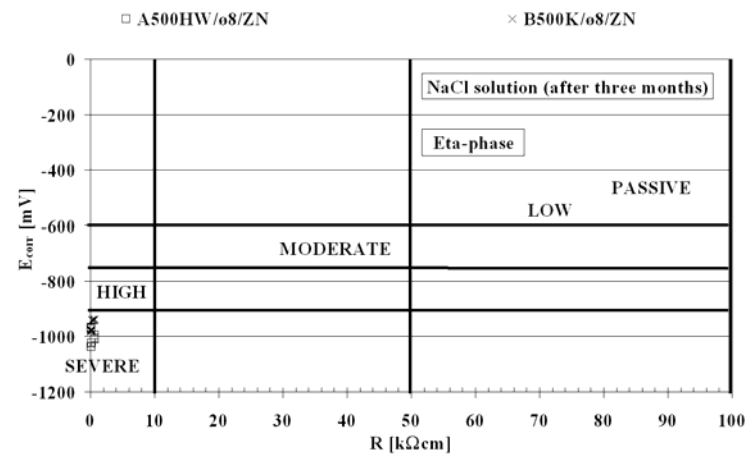
Fig. 87.   *E_{corr} − R graphs of hot-dip galvanised reinforcement bars for the cylinder specimens exposed to sodium chloride solution after three months of exposure.*
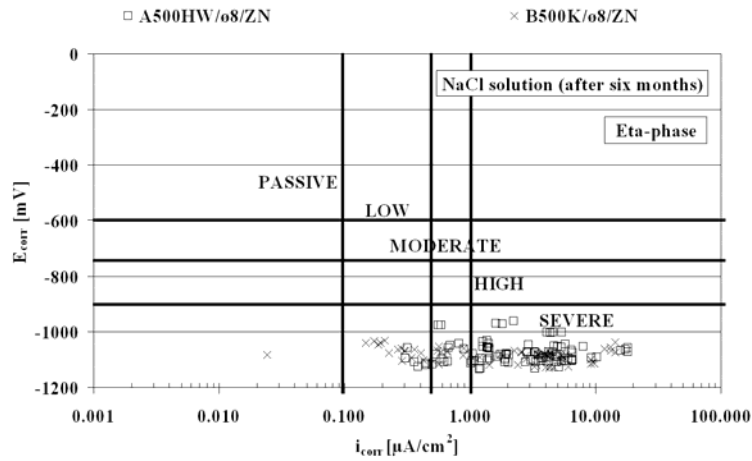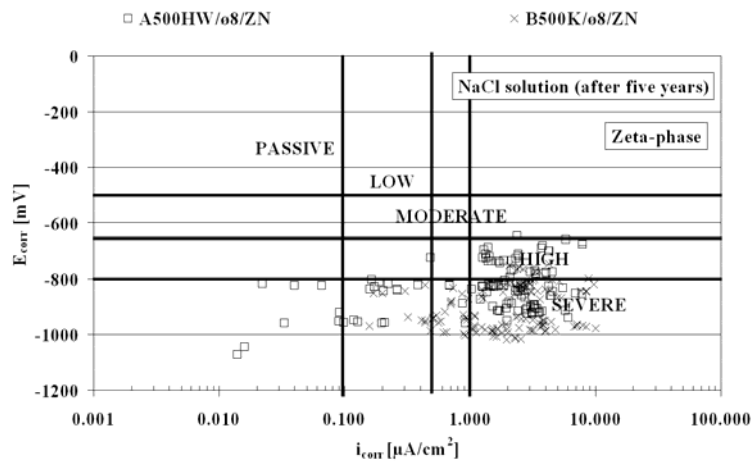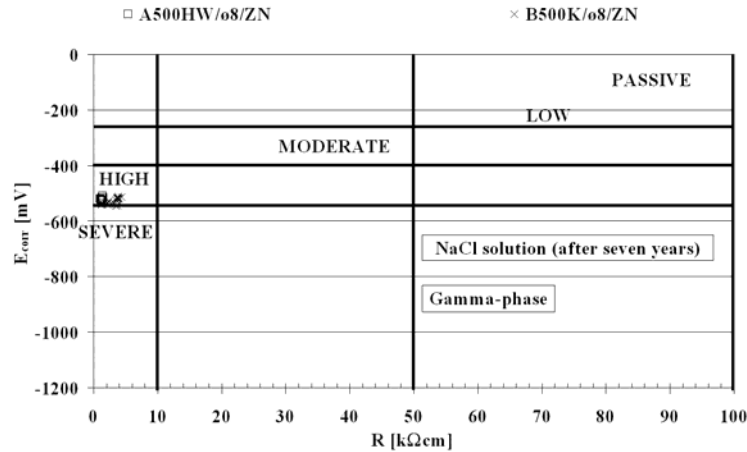
Fig. 88. E_{corr} – R graphs of hot-dip galvanised reinforcement bars for the cylinder specimens exposed to sodium chloride solution after seven years of exposure.

From Fig. 65 - Fig. 88 it can be seen that the relationships between the corrosion current i_{corr}, corrosion potential E_{corr} and the resistivity of the concrete R are generally suggestive. E_{corr} – log i_{corr} graphs are probably better comparable with microscopic examination of corrosion conditions (Chapter 4.3.8 and Chapter 4.3.9) on the reinforcement bars than log i_{corr} – R or E_{corr} – R graphs. This conclusion is based on the visual and subjective estimation of the state of corrosion. It should be pointed out that the number of analysed specimens among other factors affects the reliability of the estimation.

There are a number of sources of errors related to the electrochemical measurements. One of the major problems is non-uniform corrosion along the reinforcement bar, while the results obtained represent an average rate of corrosion. Consequently, local severe corrosion is not detected. Furthermore, the values obtained are not absolute and can be used for comparison between the specimens. Another issue is the effect of the cracks on the measured values. It is commonly accepted[1] that with a larger crack width the corrosion current and rate of corrosion should increase, while the corrosion potential and resistivity of the concrete should decrease. This tendency was not found in the present studies. In the author's opinion it could be related to varying crack widths and the occasional clogging of the cracks with leaching products, for instance; see Fig. 89. The reinforcement bars were already loaded to their yield limit before the corrosion tests and the testing arrangements differ from the stresses found in the service limit state, which have a secondary effect on the usability of the results of the electrochemical and crack width measurements. Furthermore, it should be noted that the structure may also crack as a result of imposed deformations[2].

Chlorides, cracks, and the drying of the specimens are the sources of the errors in the results. Cracks cause the signal to deviate from the required electrolytic path, giving misleading readings. The presence of chlorides may lead to an overestimated rate of corrosion values as corrosion is homogeneous when compared to visual and microscopic examination[3]. It should be pointed out that the general accepted concept of chloride induced pitting corrosion with a pitting factor α is from five to ten. This pitting

---

[1] Andrade, C. et al. (2004). Recommendations of RILEM TC-154-EMC.
[2] Nagy, A. (1997). Cracking in Reinforced Concrete Structures Due to Imposed Deformations.
[3] Andrade, C. et al. (2004). Recommendations of RILEM TC-154-EMC.

130

factor means that the measured corrosion rate underestimates the actual corrosion. However, that factor was not used in this study (see Chapter 4.3.5) because it was in conflict with visual and microscopic examination.

Other factors influencing the results of the electrochemical measurements are the corrosion products which form on the surfaces of the reinforcement bar or environmental conditions, such as moisture content and temperature[1]. On the basis of the measurement results shown in Table 35 it can be concluded that there was a local anodic area in the reinforcement bar at the crack which was surrounded by a large cathodic area extending away from the crack into the sound concrete; see Fig. 52. This means that even in a high-quality concrete cracking has significance for the durability of the reinforcement bar materials by reducing macro-level corrosion. This is understandable because with a high water-to-binder ratio anodic areas may spread near the crack into the uncracked area. In that case micro-level corrosion currents also increased in widespread anodic areas. The water-to-binder ratio has a significant influence on the formation of macro-level corrosion, and the values of macro- and micro-level corrosion[2,3]. This is comparable with the corrosion behaviour of the cylinder specimens. Furthermore, localised corrosion with a low water-to-binder ratio may lead to the passivation of the steel as a result of the settlement of the crack by corrosion products and alkalis.

a) Beam specimens in tap water after six months of exposure

	w = 0.00 mm	w = 0.01 0.10 mm	w = 0.11 0.20 mm	w = 0.21 0.30 mm	w = 0.31 0.40 mm	w = 0.41 0.50 mm	w > 0.50 mm	Total
0	7	0	0	0	0	0	0	7
1	0	6	4	1	1	0	0	12
2	0	2	4	0	0	0	0	6
3	4	23	11	8	4	2	4	56
Sum	11	31	19	9	5	2	4	81

b) Beam specimens in NaCl solution after six months of exposure

	w = 0.00 mm	w = 0.01 0.10 mm	w = 0.11 0.20 mm	w = 0.21 0.30 mm	w = 0.31 0.40 mm	w = 0.41 0.50 mm	w > 0.50 mm	Total
0	10	0	0	0	0	0	0	10
1	0	11	1	0	1	0	0	13
2	0	5	1	0	0	0	0	6
3	1	18	15	7	10	7	4	62
Sum	11	34	17	7	11	7	4	91

c) Beam specimens in tap water after five years of exposure

	w = 0.00 mm	w = 0.01 0.10 mm	w = 0.11 0.20 mm	w = 0.21 0.30 mm	w = 0.31 0.40 mm	w = 0.41 0.50 mm	w > 0.50 mm	Total
0	5	0	0	0	0	0	0	5
1	1	13	3	3	7	0	1	28
2	2	0	0	0	0	0	0	2
3	0	28	9	2	4	3	0	46
Sum	8	41	12	5	11	3	1	81

d) Beam specimens in NaCl solution after five years of exposure

	w = 0.00 mm	w = 0.01 0.10 mm	w = 0.11 0.20 mm	w = 0.21 0.30 mm	w = 0.31 0.40 mm	w = 0.41 0.50 mm	w > 0.50 mm	Total
0	11	0	0	0	0	0	0	11
1	1	18	6	4	7	1	0	37
2	1	0	0	0	0	0	0	1
3	0	19	11	3	14	4	5	56
Sum	13	37	17	7	21	5	5	105

Class:
0 = no visible crack;
1 = crack partly settled;
2 = crack settled;
3 = crack not settled

Fig. 89.   Clogging of the cracks for beam specimens exposed to (a) tap water after six months of exposure, (b) sodium chloride solution after six months of exposure, (c) tap water after five years of exposure, and (d) sodium chloride solution after five years of exposure. The same phenomenon also applies to the cylinder specimens.

[1] Andrade, C. et al. (2000). Recommendations of RILEM TC-154-EMC.
[2] Mohammed, T. et al. (2003). Corrosion of Steel Bars in Cracked Concrete.
[3] Otsuki, N. et al. (2000). Influences of Bending Crack and Water-Cement Ratio on Chloride-Induced Corrosion of Main Reinforcing Bars and Stirrups.

The results shown in Fig. 38 and Table 35 revealed no signs of corrosion in the case of austenitic stainless steel, either exposed to tap water or to the sodium chloride solution, in comparison with the other types of steel bars studied. The remaining types showed higher rates of corrosion and larger corroded surface areas. Surprisingly, the galvanised steel showed a slightly higher amount of corrosion with the beam specimens when exposed to tap water in comparison with the sodium chloride solution. As shown in Table 35, the total corroded area reached 13% of the surface exposed to tap water and 10% of that exposed to the sodium chloride solution. A similar trend was revealed in the case of the weathering steel, although the actual corroded areas were significantly larger.

4.4.2 The microscopic examination of the zinc layer of the reinforcement bars of the specimens

As shown in Fig. 57, Fig. 58, Fig. 59, and Fig. 60, different degrees of corrosion were observed in the specimens exposed either to tap water or the sodium chloride solution. The analysis of the BSE images confirmed the existence of three possible deterioration mechanisms for the reinforcement embedded into cementitious matrix and exposed to pure water or water with a high concentration of chlorides[1]. The first mechanism consists of a local dissolution of the eta (η) and zeta (ζ) phases of the zinc layer. In the second mechanism, as a result of a non-uniform zinc coating, the local dissolution of the eta (η) and zeta (ζ) phases, together with longitudinal and perpendicular cracking in the zinc layer, may lead to the local separation of the zinc layer. In the third mechanism, as a result of a non-uniform zinc coating, the full dissolution of the eta (η) and partial dissolution of the zeta (ζ) phase, together with longitudinal and perpendicular cracking in ferrite, may lead to the local separation of the zinc layer and ferrite.

The first mechanism involves the local dissolution of the eta (η) phase, which is more prone to dissolution in concrete with a high pH. This mechanism is also described by Yeomans[2] and Andrade et al.[3]. The measured pH values for the tap water and sodium chloride solution varied between 7.4 and 9.3 (see Table 31). In the results there was no significant difference between these two types of solutions, presumably as a result of the leaching of alkalis from the concrete specimens, which seems independent of the solution used. Furthermore, the carbonation of leached alkali in the solutions may hide the difference in leaching rate. According to the SEM-BSE images, in particular those of the thickness of the dissoluted zinc layer, it can be concluded that the zeta (ζ) phase was dissolved as well. The dissolved zinc layer is visible as a darker area (see Fig. 57). This darker area could be caused by a lower average atomic number of the phases, which filled porous zones, or also by the presence of the resin which was used to impregnate the specimens. The average atomic number of the resin is also lower in comparison with that of zinc. The EDS results presented in Table 37 seem to comply with this conclusion, as the amount of Ca and Si ions was significantly higher in comparison with the non-dissolved zone. The non-dissolved zone is visible as a brighter area thanks to the higher average atomic number caused by the higher amount of heavy elements.

---

[1] Sistonen, E. et al. (2008). Corrosion Mechanism of Hot-dip Galvanised Reinforcement Bar in Cracked Concrete.
[2] Yeomans, S.R. (2004). Galvanized Steel in Reinforced Concrete.
[3] Andrade, et al. (2004). Electrochemical Aspects of Galvanized Reinforcement Corrosion.

The second mechanism, which was also proposed by Yeomans[1] and Andrade et al.[2], and which assumes a general dissolution of the eta (η) phase, could occur at the same time as the local dissolution described above. However, as result of the discrepancies already described, it appeared initially as local dissolution. The eta (η) phase is anode and the zeta (ζ) phase is cathode (local galvanic corrosion). Local dissolution of the zinc layer can be caused by its non-uniform thickness, which varied significantly depending on its location on the reinforcement bar; see Fig. 55. As a result, the dissolution rate could vary along the reinforcement bar. Furthermore, the access of the aggressive medium certainly differs locally as a result of, for instance, non-homogeneous microstructure and increased porosity caused by the local microbleeding of the binder matrix ITZ.

It should be pointed out that in the literature the nature of the attack affected the galvanised coating during its passivation period or shorter exposure period than in this study. Thus, the first and the second mechanism were also found at propagation stage. Furthermore, non-uniformness of zinc coating and significant long exposure time affected determined corrosion mechanisms in this study.

According to the BSE images of severely corroded core specimens, a third mechanism could be distinguished, which includes the corrosion of the steel reinforcement bar beneath a virtually un-corroded or slightly corroded zinc layer. Certainly, this mechanism will occur in combination with the two already described. Cathodic protection is not yet active for the steel, as the long exposure time affected the effect of the cathodic protection. A layer of only partly dissolved zinc which is still connected to a layer of un-corroded steel is shown in Fig. 60. In all three corrosion mechanisms pulverised or spalling corrosion products are possible[3], and were observed during the visual examination of the deteriorated specimens. A schematic presentation of the proposed corrosion mechanisms, including their mutual interaction, is presented in Fig. 90. The order of the different phases is presented in Fig. 1.

The results described confirm earlier observations that the thicknesses of the zinc phases influence the extent of the corrosion. The rate of corrosion determined by the electrochemical measurements complies with the SEM studies and proposed corrosion mechanism. It is known that, for instance, the eta (η) phase contains the highest amount of zinc and is the main layer providing the passivity of the reinforcement bar. Its local or general deterioration can open up access to the subsequent layers, which corrode at higher rates. The dissolution of the eta (η) phase may occur at low and high pH values. Furthermore, the presence of chlorides as described by Andrade causes a general dissolution of the eta (η) phase, followed by a localised corrosion of the alloyed layers. Andrade and Alonso[4] indicated that in the presence of chlorides the dissolved zinc creates a cathodic protection system which prevents further attacks on the exposed steel. In the present study the extensive corrosion of the galvanised bars was caused by the long exposure time, which extended beyond the time when the cathodic protection system created by the zinc was functional. This means that the damaged area of zinc coating in the later stage is too wide and the cathodic protection cannot exist any more. Furthermore, propagation stage for ordinary reinforcement bar is possible due to the

---

[1] Yeomans, S.R. (2004). Galvanized Steel in Reinforced Concrete.
[2] Andrade, et al. (2004). Electrochemical Aspects of Galvanized Reinforcement Corrosion.
[3] Belaïd, F. et al. (2000). Corrosion Products of Galvanized Rebars Embedded in Chloride-Contaminated Concrete.
[4] Yeomans, S.R. (2004). Galvanized Steel in Reinforced Concrete.

wide damaged area of zinc coating first local and later uniformly spread. It was found that especially in chloride-contaminated concrete the cathodic protection was disturbed.

Additional data concerning the corrosion products were provided by the EDS analysis. The high content of Ca^{2+} ions could originate from Portlandite, which often forms in the ITZ[1], and might occur as visible separate crystals or in the form of microcrystals intermixed with Calcium Silicate Hydrate (CSH). Furthermore, Ca^{2+} ions could originate from Calcium Hydroxozincate (CaHZn), which forms during the early stages of hydration as a partial dissolution of the eta (η) phase of zinc and proves to be beneficial from the point of view of the risk of corrosion, as a passivity layer. The source of Ca^{2+} ions in the corrosion process is presented, for instance, in Fig. 5 and Equation (5). Unfortunately, the environment the SEM-EDS system that was used in this research and was operated at a relatively high accelerating voltage and a low vacuum, induced the so-called electron beam skirting effect[2]. The skirting effect causes excitement of the elements in a relatively large area. According to the previous research, the electron beam could have a diameter as great as 40 μm. Therefore, it is impossible to conclude in which compound the Ca ions were present. In the author's opinion, all forms were present.

[1] Yeomans, S.R. (2004). Galvanized Steel in Reinforced Concrete.
[2] Cwirzen, A. (2004). Effects of the Transition Zone and Aging on the Frost Damage of the High Strength Concretes.
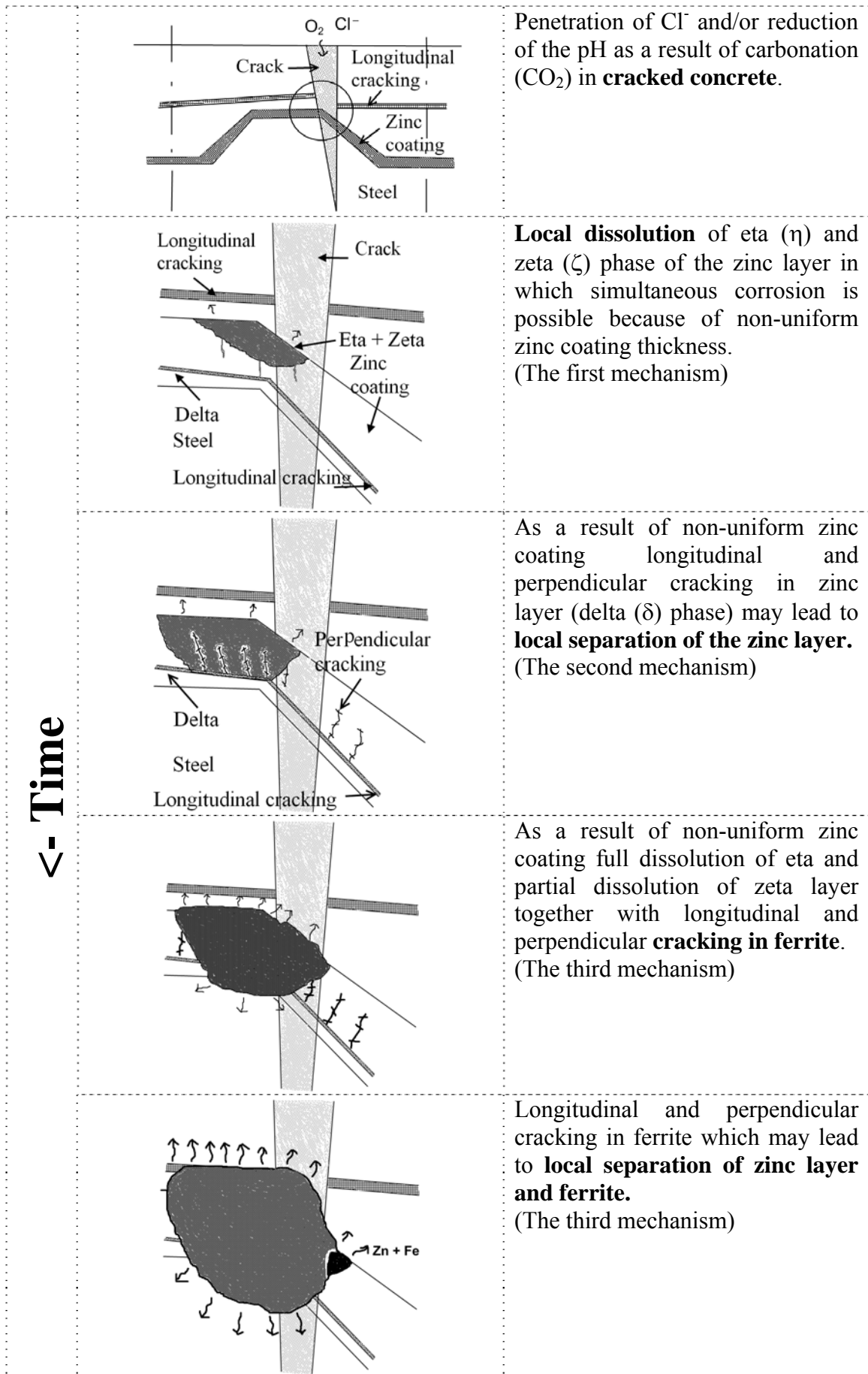
<- Time	(diagram)	Description
	O_2 Cl^- — Crack — Longitudinal cracking — Zinc coating — Steel	Penetration of Cl^- and/or reduction of the pH as a result of carbonation (CO_2) in **cracked concrete**.
	Longitudinal cracking — Crack — Eta + Zeta Zinc coating — Delta Steel — Longitudinal cracking	**Local dissolution** of eta (η) and zeta (ζ) phase of the zinc layer in which simultaneous corrosion is possible because of non-uniform zinc coating thickness. (The first mechanism)
	PerPendicular cracking — Delta Steel — Longitudinal cracking	As a result of non-uniform zinc coating longitudinal and perpendicular cracking in zinc layer (delta (δ) phase) may lead to **local separation of the zinc layer.** (The second mechanism)
	(diagram)	As a result of non-uniform zinc coating full dissolution of eta and partial dissolution of zeta layer together with longitudinal and perpendicular **cracking in ferrite**. (The third mechanism)
	Zn + Fe	Longitudinal and perpendicular cracking in ferrite which may lead to **local separation of zinc layer and ferrite.** (The third mechanism)

Fig. 90.   Corrosion mechanisms of hot-dip galvanised reinforcement bar in cracked concrete. Figures are not full-scale.

4.4.3   Statistical analysis

The data processing and analysis included data and statistical most suitable distribution models from electrochemical, crack width, and zinc coating thickness measurements. Regression curves for the parameters determined in the measurements were studied for the reliability analysis of service life planning. In the theoretical probability-based service life prediction of concrete structures, measured values are analysed with low fractals. The reason for this is that in conservative emphasised models the accepted probability of damage is low and extreme values are needed for use as input values. Thus, extreme values were analysed compared with all values. In the analysis p-values greater than 0.5, KS-values less than 0.03, and AD-values less than 1.5 represent the goodness of the most suitable regression curve, i.e. a close fit. With different electrochemical measurements, the parameters that illustrate the same corrosion phenomenon may have different types of distribution curves (Table 43 and Table 44). The most suitable distribution type for the thickness of the zinc coating before exposure for the beam and cylinder specimens was Gamma distribution.

Table 43.   *Most suitable distribution types (beam specimen: hot-dip galvanised steel reinforcement bar).*

Duration of exposure [years]	Condition	Crack width w [mm]	Corrosion current I_{corr} [μA/cm^2]	Corrosion potential E_{corr} [mV]	Rate of corrosion v_{corr} [μm/a]	Resistivity of concrete R [kΩcm]
0.5	Tap water	Triangular	Normal	Logistic	Normal	Lognormal
0.5	NaCl solution	Exponential	Exponential	Gamma	Exponential	Lognormal
5	Tap water	Triangular	Gamma	Gamma	Gamma	Gamma
5	NaCl solution	Exponential	Weibull	Normal	Gamma	Lognormal
A close fit						

Table 44.   *Most suitable distribution types (cylinder specimen: hot-dip galvanised steel reinforcement bar).*

Duration of exposure [years]	Condition	Crack width w [mm]	Corrosion current I_{corr} [μA/cm^2]	Corrosion potential E_{corr} [mV]	Rate of corrosion v_{corr} [μm/a]	Resistivity of concrete R [kΩcm]
0.3	Tap water	-	Logistic	Normal	Logistic	Pareto
0.3	NaCl solution	-	Gamma	Logistic	Gamma	Weibull
7	Tap water	Triangular	Lognormal	Triangular	Lognormal	Gamma
7	NaCl solution	Lognormal	Normal	Uniform	Normal	Lognormal
A close fit						

The electrochemical, crack width, and zinc coating thickness measurements for the beam and cylinder specimens exposed to tap water and the sodium chloride solution are shown in Appendix C. The coefficient of variation for the beam specimens exposed to tap water and the sodium chloride solution for all values and extreme values is shown in Fig. 91, Fig. 92, Fig. 93, and Fig. 94. The coefficient of variation for the cylinder specimens exposed to tap water and the sodium chloride solution for all values and extreme values is shown in Fig. 95, Fig. 96, Fig. 97, and Fig. 98. All the values represent the number of measurements that are shown in Appendix C. The extreme values represent the minimum or maximum values of the sample space of the measurement values, depending on the parameter studied. Examples of the distribution curves of the hot-dip galvanised reinforcement beam and cylinder specimens exposed to

tap water and the sodium chloride solution for all and extreme values are shown in Appendix D. Comparison examples between all and extreme values with 90-100% low fractals of the hot-dip galvanised reinforcement beam and cylinder specimens exposed to tap water and the sodium chloride solution are shown in Appendix E.

In some cases with low fractals the extreme values were contradictory when compared to all values. Inadequate measurement data affect this. It was noticed that the use of extreme values significantly reduces the benefit of hot-dip galvanised reinforcement bars. For instance, the thickness of the zinc coating is low and the rate of corrosion is high with low fractals. The same effect takes place with the other reinforcement bar materials studied. However, the longer the target service life, the lower the accepted yearly-based probability of damage should be. Thus, the use of extreme values is needed. This also relates to repaired concrete structures, where the level of confidence in the old structure decreases.

The coefficients of variations for hot-dip galvanised reinforcement bars are at the same level during exposure but higher than those presented in Chapter 3.1. In general, the sources of error in the measurements affect these higher values. Furthermore, the values presented in Fig. 91 - Fig. 98 are momentary. This differs from the values presented in Table 9, Table 10, Table 11, and Table 12, which are yearly. It should be noted that different electrochemical measurement parameters that illustrate the same corrosion phenomenon have considerable differences in their values of coefficients of variation. Generally, the coefficients of variations for hot-dip galvanised reinforcement bars are on the same level compared to the other reinforcement bar types studied. The coefficients of variation for the beam and cylinder specimens for all values and extreme values are slightly higher in the case of those exposed to tap water than those exposed to the sodium chloride solution. High values of variations partly indicate corrosion phenomena. That can be observed in the proposed corrosion mechanisms.
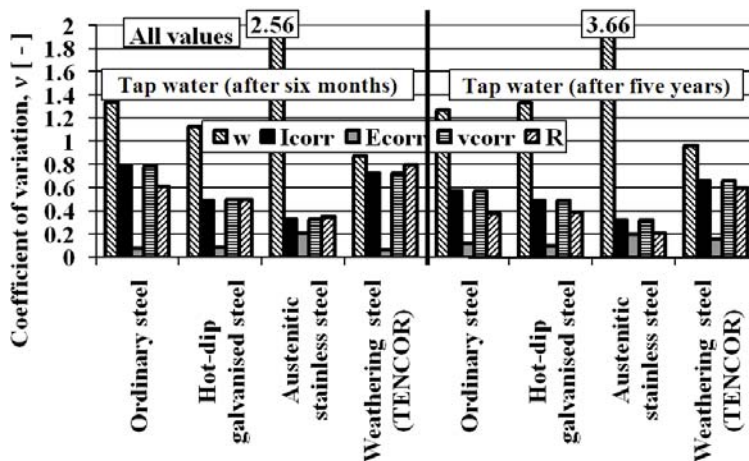
Fig. 91.   *Coefficient of variation for the beam specimens exposed to tap water for all values. Explanation of notations: w is crack width; I_{corr} is corrosion current; E_{corr} is corrosion potential; v_{corr} is rate of corrosion; R is resistivity of concrete.*
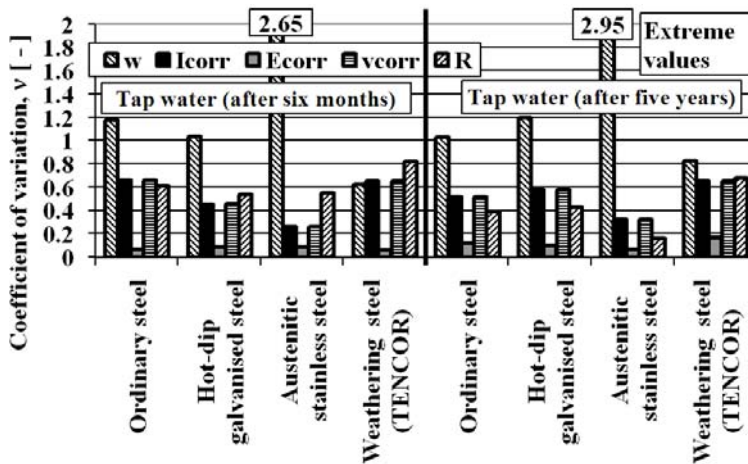
Fig. 92.   *Coefficient of variation for the beam specimens exposed to tap water for extreme values. Explanation of notations: w is crack width; I_{corr} is corrosion current; E_{corr} is corrosion potential; v_{corr} is rate of corrosion; R is resistivity of concrete.*
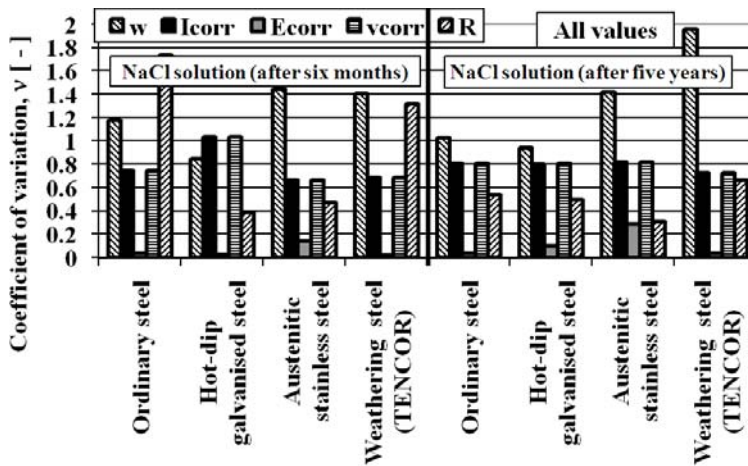
Fig. 93.   *Coefficient of variation for the beam specimens exposed to sodium chloride solution for all values. Explanation of notations: w is crack width; I_{corr} is corrosion current; E_{corr} is corrosion potential; v_{corr} is rate of corrosion; R is resistivity of concrete.*
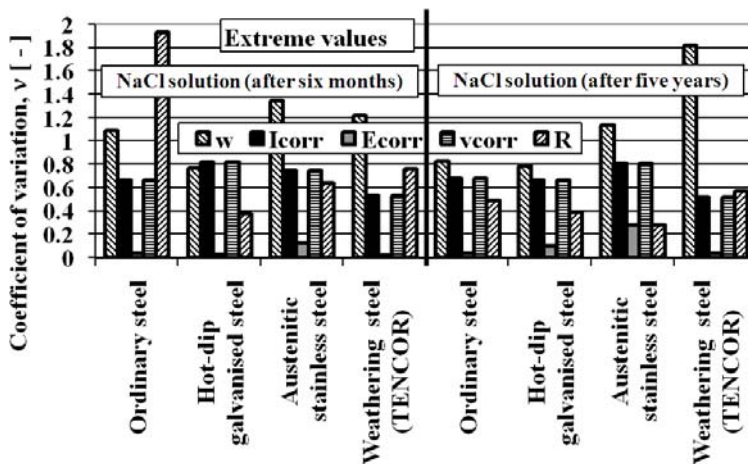
Fig. 94.   *Coefficient of variation for the beam specimens exposed to sodium chloride solution for extreme values. Explanation of notations: w is crack width; I_{corr} is corrosion current; E_{corr} is corrosion potential; v_{corr} is rate of corrosion; R is resistivity of concrete.*
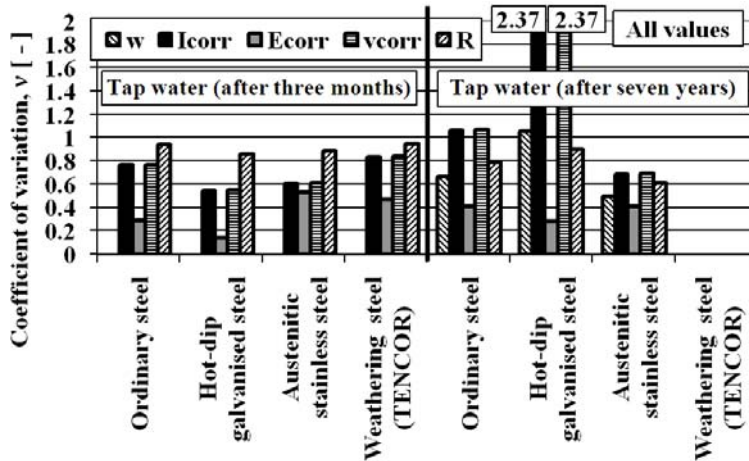
Fig. 95.   Coefficient of variation for the cylinder specimens exposed to tap water for all values. Explanation of notations: w is crack width; I_{corr} is corrosion current; E_{corr} is corrosion potential; v_{corr} is rate of corrosion; R is resistivity of concrete.
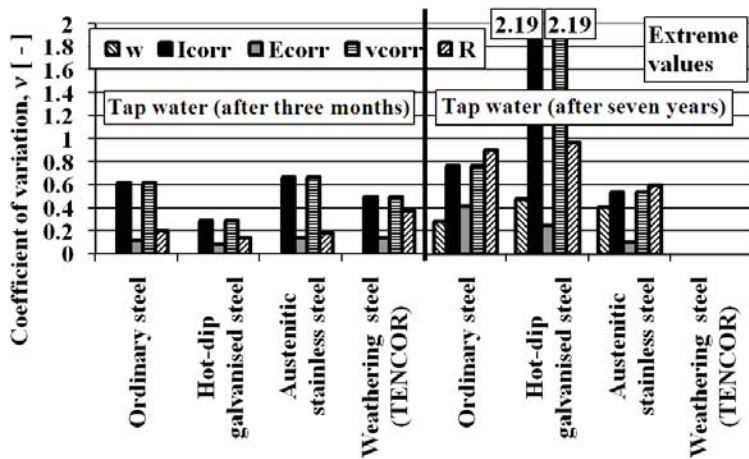
Fig. 96.   Coefficient of variation for the cylinder specimens exposed to tap water for extreme values. Explanation of notations: w is crack width; I_{corr} is corrosion current; E_{corr} is corrosion potential; v_{corr} is rate of corrosion; R is resistivity of concrete.
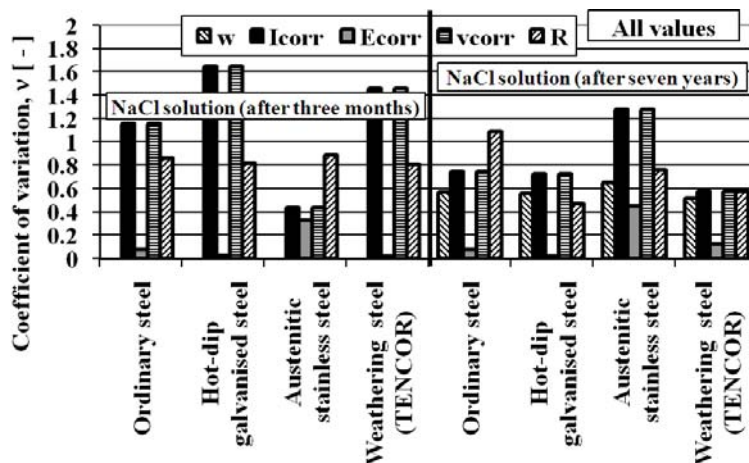
Fig. 97.   Coefficient of variation for the cylinder specimens exposed to sodium chloride solution for all values. Explanation of notations: w is crack width; I_{corr} is corrosion current; E_{corr} is corrosion potential; v_{corr} is rate of corrosion; R is resistivity of concrete.
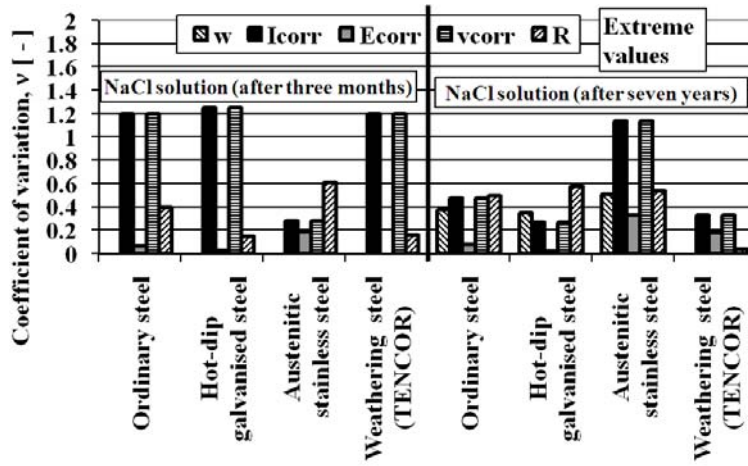
Fig. 98.   *Coefficient of variation for the cylinder specimens exposed to sodium chloride solution for extreme values. Explanation of notations: w is crack width; I_{corr} is corrosion current; E_{corr} is corrosion potential; v_{corr} is rate of corrosion; R is resistivity of concrete.*

5   DISCUSSION

5.1   Service life calculation of hot-dip galvanised reinforcement bars based on the results of durability tests

The service life of hot-dip galvanised reinforcement bars is discussed below on the basis of the measured mean values presented in Chapters 2, 3, and 4, and Appendix C. Service life calculation formulae are presented in Table 6. Concrete properties are presented in Table 19 and Table 21. The reinforcement bar diameter is assumed to be 8 mm for all the reinforcement bar types studied. In carbonated uncracked concrete exposed to rain, the initiation time is calculated on the basis of Equation (27), and the coefficient of carbonation with Equation (28). The thickness of the concrete cover and the carbonation depth are set to 5 mm for the beam specimens and to 18 mm for the cylinder specimens. The calculated values for the coefficient of carbonation are 1.2 mm/a$^{1/2}$ for the beam specimens and 2.0 mm/a$^{1/2}$ for the cylinder specimens. The measured values for the coefficient of carbonation under outdoor conditions were much lower (see Chapter 4.3.1) as a result of the full saturation of the concrete surface. However, a conservative assumption of the calculated value of the coefficient of carbonation is used here. The initiation time in carbonated uncracked concrete for the beam specimens is calculated to be 19 years and for the cylinder specimens 84 years.

The critical chloride content in carbonated and chloride-contaminated concrete for different reinforcement bar types is assumed to be the lower limit values presented in Table 7. The surface chloride content is assumed to be 5 wt%$_{CEM}$, which corresponds to a concrete structure in sea water in the Atlantic Ocean. The chloride diffusion coefficient of the concrete is calculated from Equation (31) with the concrete strength values presented in Table 21. The calculated value of the chloride diffusion coefficient of the concrete is 51 mm^2/a for the beam specimens and 186 mm^2/a for the cylinder specimens. The calculated initiation time in chloride-contaminated uncracked concrete with ordinary, hot-dip galvanised, and weathering steel reinforcement bars for the beam and cylinder specimens is less than one year. The calculated initiation time in chloride-contaminated uncracked concrete with austenitic stainless steel reinforcement bars is four years for the beam specimens and for cylinder specimens 13 years.

The service life of reinforced concrete structures with hot-dip galvanised reinforcement bars, assuming uncracked concrete and a uniform rate of corrosion for beam and cylinder specimens, is shown in Table 45. A comparison of the calculated service life values between hot-dip galvanised, ordinary, weathering, and stainless steel reinforcement bars is also presented. Hot-dip galvanised steel is not compared with austenitic stainless steel in carbonated concrete, where the initiation time for austenitic stainless steel is, in practice, infinity.

When a decreasing rate of corrosion is assumed, the calculated values for the coefficient of the rate of corrosion are presented in Table 39. The service life of hot-dip galvanised reinforcement bars and a comparison with ordinary, weathering, and stainless steel reinforcement bars for beam and cylinder specimens exposed to tap water and a sodium chloride solution, assuming uncracked concrete and a decreasing rate of corrosion, is shown in Table 46. The basis for the calculation values in uncracked concrete presented in Table 45 and Table 46 is in the research results, which showed no correlation

between crack width and electrochemical measurement values (see Fig. 63) and clogging of the cracks (see Fig. 89).

Table 45. *Service life of hot-dip galvanised reinforcement bars **according to the results of** **durability tests** and comparison with ordinary, weathering, and stainless steel reinforcement bars for beam and cylinder specimens exposed to tap water and sodium chloride solution assuming **uncracked concrete** and **uniform rate of corrosion**.*

Reinforcement bar type	Hot-dip galvanised steel t_L [a]	Compared to ordinary steel $t_L/(t_0+t_2)$ [-]	Compared to weathering (TENCOR) steel $t_L/(t_0+t_2)$ [-]	Compared to austenitic stainless steel $t_L/(t_0+t_2)$ [-]
Beam specimen in tap water	61[a] 106[b]	2.4[a] 2.8[b]	2.2[a] 2.9[b]	-[a] -[b]
Beam specimen in NaCl solution	4[a] 6[b]	8.3[a] 9.5[b]	4.3[a] 5.3[b]	0.10[a] 0.15[b]
Cylinder specimen in tap water	155[c] 452[d]	1.5[c] 1.6[d]	1.1[c] Not measured[d]	-[c] -[d]
Cylinder specimen in NaCl solution	2[c] 4[d]	2.0[c] 2.3[d]	2.9[c] 2.0[d]	0.004[c] 0.04[d]

[a] after six months of exposure
[b] after five years of exposure
[c] after three months of exposure
[d] after seven years of exposure

Table 46. *Service life of hot-dip galvanised reinforcement bars **according to the results of** **durability tests** and comparison with ordinary, weathering, and stainless steel reinforcement bars for beam and cylinder specimens exposed to tap water and sodium chloride solution assuming **uncracked concrete** and **decreasing rate of corrosion**.*

Reinforcement bar type	Hot-dip galvanised steel t_L [a]	Compared to ordinary steel $t_L/(t_0+t_2)$ [-]	Compared to weathering (TENCOR) steel $t_L/(t_0+t_2)$ [-]	Compared to austenitic stainless steel $t_L/(t_0+t_2)$ [-]
Beam specimen in tap water	533[a] 254[b]	14[a] 7.0[b]	10[a] 7.6[b]	-[a] -[b]
Beam specimen in NaCl solution	5[a] 1[b]	37[a] 16[b]	14[a] 11[b]	0.01[a] 0.03[b]
Cylinder specimen in tap water	2990[c] 2627[d]	6.0[c] 1.6[d]	0.81[c] Not measured[d]	-[c] -[d]
Cylinder specimen in NaCl solution	1[c] 1[d]	2.1[c] 2.2[d]	3.1[c] 2.0[d]	0.00001[c] 0.003[d]

[a] after six months of exposure
[b] after five years of exposure
[c] after three months of exposure
[d] after seven years of exposure

With the same electrochemical measurement values the service life of concrete structures with different reinforcement bar types can also be calculated for cracked concrete. The assumed values are 1.0 for the coefficient of the relative rib area, 0.2 mm for the crack width, and 500 μm for the maximum permitted corrosion depth of the reinforcement. The calculated initiation time in carbonated cracked concrete and chloride-contaminated cracked concrete with ordinary, hot-dip galvanised, and weathering steel reinforcement bars for beam and cylinder specimens is less than one year. Thus, the service life of a concrete structure with the calculation assumptions used is determined by the propagation time.

The service life of reinforced concrete structures with hot-dip galvanised reinforcement bars, assuming cracked concrete and a uniform rate of corrosion for beam and cylinder specimens, is shown in Table 47. A comparison of the calculated service life values between hot-dip galvanised, ordinary, weathering, and stainless steel reinforcement bars is also presented, expect for stainless steel in carbonated concrete.

The service life of hot-dip galvanised reinforcement bars and a comparison with ordinary, weathering, and stainless steel reinforcement bars for beam and cylinder specimens exposed to tap water and a sodium chloride solution, assuming cracked concrete and a decreasing rate of corrosion is shown in Table 48. The calculated values for the coefficient of the rate of corrosion are presented in Table 39.

Table 47. *Service life of hot-dip galvanised reinforcement bars **according to the results of durability tests** and comparison with ordinary, weathering, and stainless steel reinforcement bars for beam and cylinder specimens exposed to tap water and sodium chloride solution assuming **cracked concrete** and **uniform rate of corrosion**.*

Reinforcement bar type	Hot-dip galvanised steel t_L [a]	Compared to ordinary steel $t_L /(t_0+t_2)$ [-]	Compared to weathering (TENCOR) steel $t_L /(t_0+t_2)$ [-]	Compared to austenitic stainless steel $t_L /(t_0+t_2)$ [-]
Beam specimen in tap water	105[a] 254[b]	1.5[a] 1.4[b]	1.1[a] 1.5[b]	-[a] -[b]
Beam specimen in NaCl solution	7[a] 10[b]	1.9[a] 2.0[b]	0.87[a] 1.0[b]	0.02[a] 0.03[b]
Cylinder specimen in tap water	110[c] 724[d]	1.8[c] 1.3[d]	0.66[c] Not measured[d]	-[c] -[d]
Cylinder specimen in NaCl solution	2[c] 6[d]	1.3[c] 1.4[d]	2.0[c] 1.2[d]	0.002[c] 0.03[d]

[a] after six months of exposure
[b] after five years of exposure
[c] after three months of exposure
[d] after seven years of exposure

Table 48. *Service life of hot-dip galvanised reinforcement bars **according to the results of durability tests** and comparison with ordinary, weathering, and stainless steel reinforcement bar for beam and cylinder specimens exposed to tap water and sodium chloride solution assuming **cracked concrete** and **decreasing rate of corrosion**.*

Reinforcement bar type	Hot-dip galvanised steel t_L [a]	Compared to ordinary steel $t_L /(t_0+t_2)$ [-]	Compared to weathering (TENCOR) steel $t_L /(t_0+t_2)$ [-]	Compared to austenitic stainless steel $t_L /(t_0+t_2)$ [-]
Beam specimen in tap water	2418[a] 1925[b]	1.3[a] 1.1[b]	0.75[a] 1.3[b]	-[a] -[b]
Beam specimen in NaCl solution	10[a] 2[b]	1.8[a] 2.0[b]	0.40[a] 0.53[b]	0.0003[a] 0.0005[b]
Cylinder specimen in tap water	5716[c] 12828[d]	1.8[c] 1.1[d]	0.21[c] Not measured[d]	-[c] -[d]
Cylinder specimen in NaCl solution	2[c] 1[d]	1.1[c] 1.2[d]	2.6[c] 0.98[d]	0.000002[c] 0.001[d]

[a] after six months of exposure
[b] after five years of exposure
[c] after three months of exposure
[d] after seven years of exposure

The calculated values for service life in carbonated uncracked and cracked concrete are very high as a result of the long calculated propagation time. These values mean that the

deterioration of the concrete structure being studied may not concentrate on reinforcement corrosion. Service life values of more than 200 years are unrealistic. The reason for this is that other deterioration types (for instance frost deterioration) may be predominant and the effect of interacting deterioration parameters on the service life of concrete structures may be significant.

As shown in Table 45, Table 46, Table 47, and Table 48, austenitic stainless steel outperformed the other reinforcement bar types. Furthermore, the service life increases substantially both in uncracked and cracked carbonated concrete when a decreasing rate of corrosion is assumed. Thus, there is significant potential for improving the service life of reinforced concrete structures. However, it should be proved that an increased rust layer reduces oxygen diffusion. In the durability tests of the study it was noticed that the rate of corrosion decreased.

The calculated service life values for cylinder specimens in chloride-contaminated uncracked and cracked concrete are comparable with the research results obtained from durability tests (Chapter 4.3.9). On the other hand, the estimated values for beam specimens in chloride-contaminated uncracked and cracked concrete are too conservative. Furthermore, the calculated service life values for beam and cylinder specimens in carbonated concrete are too high, especially with a decreasing rate of corrosion.

When the calculated values between uncracked and cracked concrete exposed to tap water are compared, it can be noticed that the service life increases in cracked concrete. The reason for this lies in the value 500 μm used for the maximum permitted corrosion depth of the reinforcements in cracked concrete. According to Equation (22) the calculated corrosion depth during the propagation time in uncracked concrete, where the corrosion products spall the concrete cover is 50 μm for the beam specimens and 180 μm for the cylinder specimens. In the cracked concrete the corrosion products may migrate from the structure and thus allow the use of higher value for the corrosion depth compared to uncracked concrete. Cracking may affect only the aesthetic symptoms on the concrete structure. Furthermore, with the assumed reinforcement bar diameter the reduced cross-sectional area of steel bar in cracked concrete is approximately six per cent. That may not be too high for adequate load-bearing capacity of the reinforced concrete structures.

The estimated service life based on the proposed propagation of corrosion mechanisms (Fig. 90) is almost identical to the calculated service life values for cylinder specimens in chloride-contaminated uncracked and cracked concrete. The calculated service life values for beam specimens in chloride-contaminated uncracked and cracked concrete are too pessimistic compared to the estimated service life based on the proposed propagation of corrosion mechanisms. For the other cases studied, the calculated service life values are too optimistic compared to the estimated service life based on the proposed propagation of corrosion mechanisms (see Chapter 4). For instance, local dissolution of the zinc coating can be seen in Fig. 57 and Fig. B.5 (see Appendix B) for cylinder and beam specimens exposed to tap water. The results are incompatible with the values presented in Table 45, Table 46, Table 47, and Table 48.

5.2 Service life calculation of hot-dip galvanised reinforcement bars based on validation of theoretical analysis

The validation of the service life calculation was performed by comparing the results achieved with the service life calculation of the laboratory experiments with the results given by the service life evaluation presented in Chapter 3. The corrosion parameters in the propagation stage by which the service life of hot-dip galvanised reinforcement bars may be influenced compared to ordinary steel reinforcement bars are presented in Fig. 99. The same applies with cracked concrete. These corrosion parameters are here used in the validation of the service life calculation. By means of the comparison an analysis was performed of how well the service life calculations describe the accuracy of the calculation.

Explanation of notations:

t_1 is propagation time for zinc coating;

t_2 is propagation time for ordinary steel reinforcement bar;

Zn is zinc coating;

Fe is ordinary steel reinforcement bar;

r_1 is rate of corrosion for hot-dip galvanised reinforcement bar;

d is thickness of zinc coating;

r_s is rate of corrosion for ordinary steel reinforcement bar;

k_1 is coefficient of the rate of corrosion for hot-dip galvanised reinforcement bar;

k_s is coefficient of the rate of corrosion for ordinary steel reinforcement bar

Fig. 99.   Corrosion parameters in the propagation stage used in validation (uncracked concrete).

The thickness of the zinc coating is stated as a typical value shown in Table 8. The rate of corrosion and coefficient of the rate of corrosion for different reinforcement bar types are stated as typical values shown in Table 9, Table 10, Table 11, and Table 12. Other corrosion parameters are the same as those presented in Chapter 5.1. The results of the service life calculation according to the theoretical analysis are shown in Table 49, Table 50, Table 51, and Table 52. In validation a comparison is made between Table 45 and Table 49, Table 46 and Table 50, Table 47 and Table 51, and Table 48 and Table 52. The validation of the service life calculation of hot-dip galvanised reinforcement bars is presented in Fig. 100, Fig. 101, Fig. 102, Fig. 103, Fig. 104, Fig. 105, and Fig. 106.

Table 49.   *Service life of hot-dip galvanised reinforcement bars **according to theoretical analysis** and comparison with ordinary, weathering, and stainless steel reinforcement bars for beam and cylinder specimens exposed to tap water and sodium chloride solution assuming **uncracked concrete** and **uniform rate of corrosion**.*

Reinforcement bar type	Hot-dip galvanised steel t_L [a]	Compared to ordinary steel $t_L /(t_0+t_2)$ [-]	Compared to weathering (TENCOR) steel $t_L /(t_0+t_2)$ [-]	Compared to austenitic stainless steel $t_L /(t_0+t_2)$ [-]
Beam specimen in tap water	92	3.6	3.2	-
Beam specimen in NaCl solution	11	10	6.4	0.81
Cylinder specimen in tap water	173	1.6	1.4	-
Cylinder specimen in NaCl solution	14	3.7	2.3	0.29

Table 50.   *Service life of hot-dip galvanised reinforcement bars **according to theoretical analysis** and comparison with ordinary, weathering, and stainless steel reinforcement bars for beam and cylinder specimens exposed to tap water and sodium chloride solution assuming **uncracked concrete** and **decreasing rate of corrosion**.*

Reinforcement bar type	Hot-dip galvanised steel t_L [a]	Compared to ordinary steel $t_L /(t_0+t_2)$ [-]	Compared to weathering (TENCOR) steel $t_L /(t_0+t_2)$ [-]	Compared to austenitic stainless steel $t_L /(t_0+t_2)$ [-]
Beam specimen in tap water	232	8.4	7.7	-
Beam specimen in NaCl solution	17	32	22	0.58
Cylinder specimen in tap water	400	2.0	1.8	-
Cylinder specimen in NaCl solution	22	3.7	2.4	0.07

Table 51.   *Service life of hot-dip galvanised reinforcement bars **according to theoretical analysis** and comparison with ordinary, weathering, and stainless steel reinforcement bars for beam and cylinder specimens exposed to tap water and sodium chloride solution assuming **cracked concrete** and **uniform rate of corrosion**.*

Reinforcement bar type	Hot-dip galvanised steel t_L [a]	Compared to ordinary steel $t_L /(t_0+t_2)$ [-]	Compared to weathering (TENCOR) steel $t_L /(t_0+t_2)$ [-]	Compared to austenitic stainless steel $t_L /(t_0+t_2)$ [-]
Beam specimen in tap water	90	1.8	1.4	-
Beam specimen in NaCl solution	15	1.8	1.2	0.30
Cylinder specimen in tap water	90	1.8	1.4	-
Cylinder specimen in NaCl solution	15	1.8	1.2	0.31

Table 52.   *Service life of hot-dip galvanised reinforcement bars **according to theoretical analysis** and comparison with ordinary, weathering, and stainless steel reinforcement bars for beam and cylinder specimens exposed to tap water and sodium chloride solution assuming **cracked concrete** and **decreasing rate of corrosion**.*

Reinforcement bar type	Hot-dip galvanised steel t_L [a]	Compared to ordinary steel $t_L /(t_0+t_2)$ [-]	Compared to weathering (TENCOR) steel $t_L /(t_0+t_2)$ [-]	Compared to austenitic stainless steel $t_L /(t_0+t_2)$ [-]
Beam specimen in tap water	201	1.3	0.98	-
Beam specimen in NaCl solution	38	1.2	0.97	0.06
Cylinder specimen in tap water	201	1.3	0.98	-
Cylinder specimen in NaCl solution	38	1.2	0.97	0.06
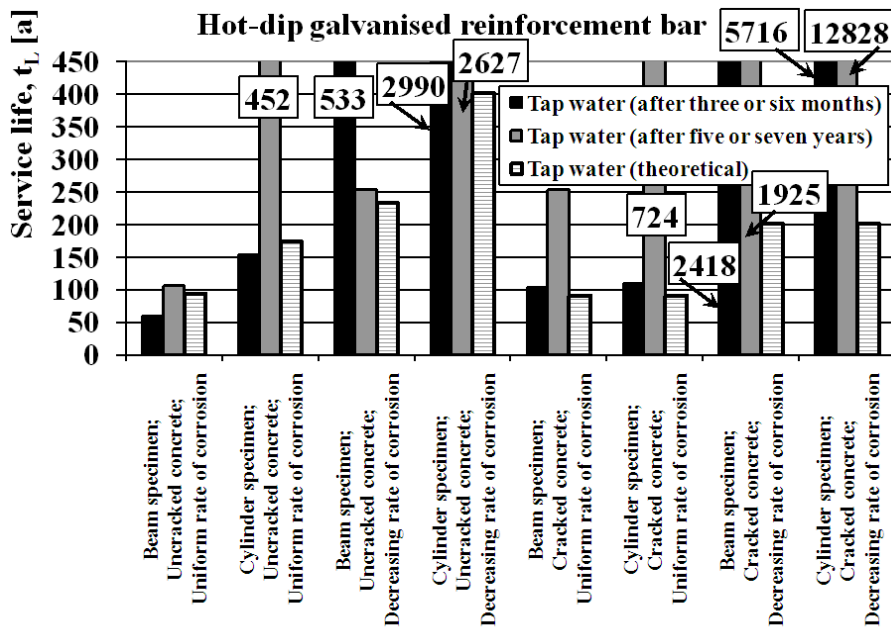
Fig. 100.   *Comparison of the results achieved with the service life calculation of laboratory experiments with the results given by the service life evaluation in tap water.*
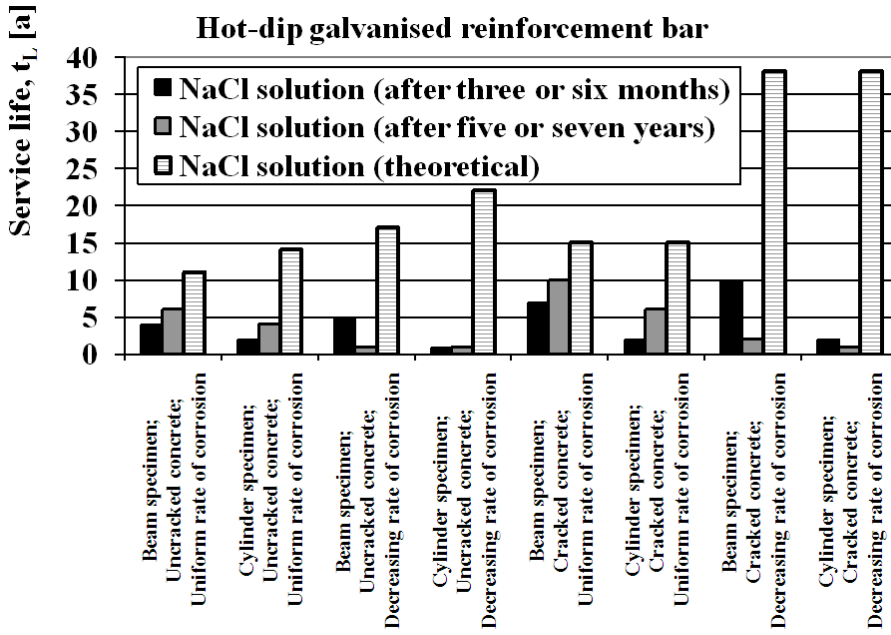
Fig. 101. Comparison of the results achieved with the service life calculation of laboratory experiments with the results given by the service life evaluation in sodium chloride solution.
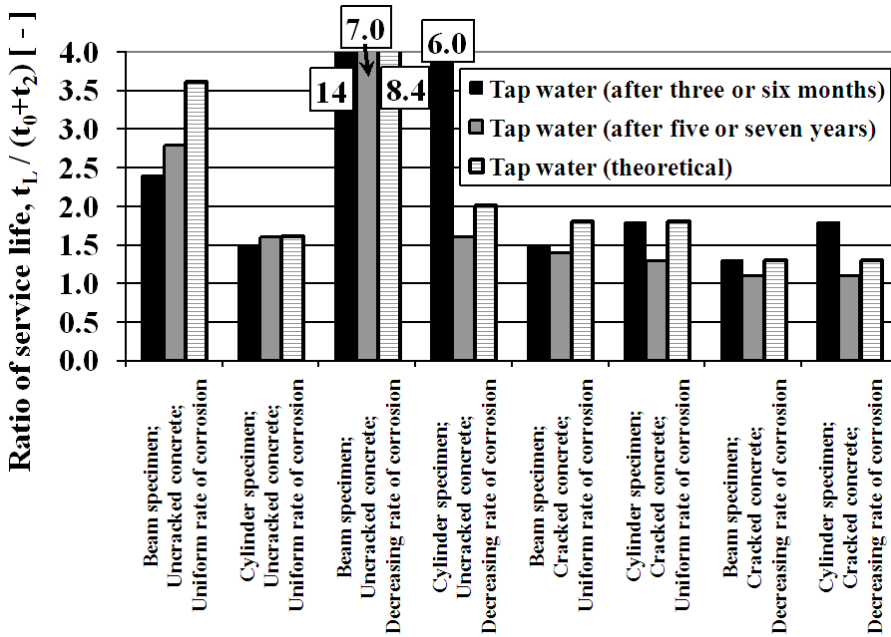
Fig. 102. Ratio of service life (service life of hot-dip galvanised reinforcement bars **compared to ordinary** steel reinforcement bars) given by the laboratory experiments and the theoretical analysis in tap water.
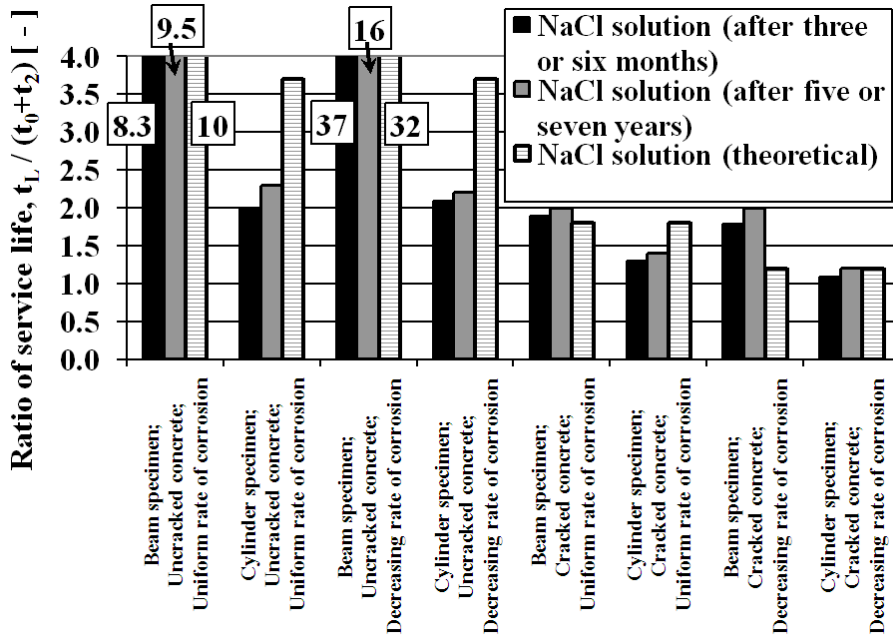
Fig. 103.   *Ratio of service life (service life of hot-dip galvanised reinforcement bars **compared to ordinary** steel reinforcement bars) given by the laboratory experiments and the theoretical analysis in sodium chloride solution.*
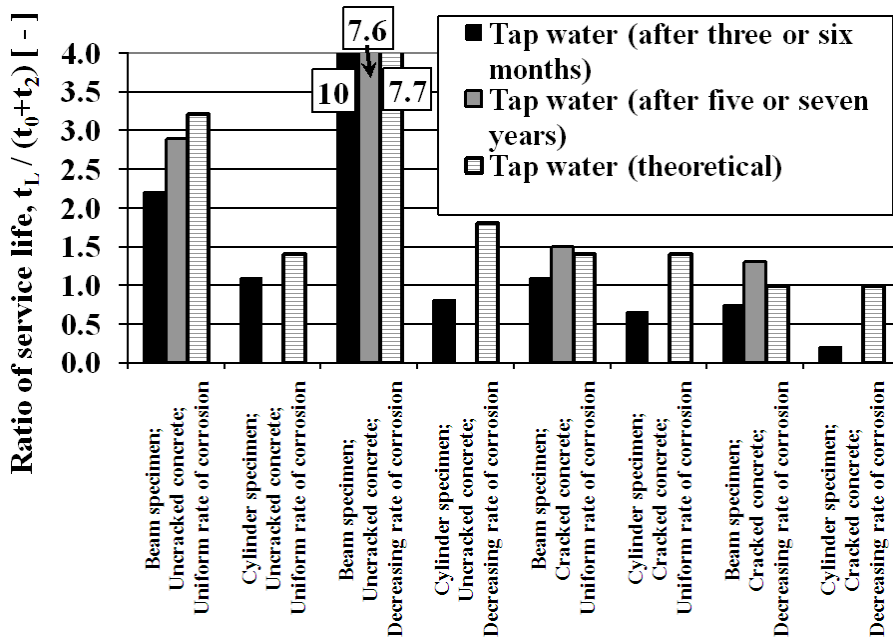
Fig. 104.   *Ratio of service life (service life of hot-dip galvanised reinforcement bars **compared to weathering** steel reinforcement bars) given by the laboratory experiments and the theoretical analysis in tap water.*
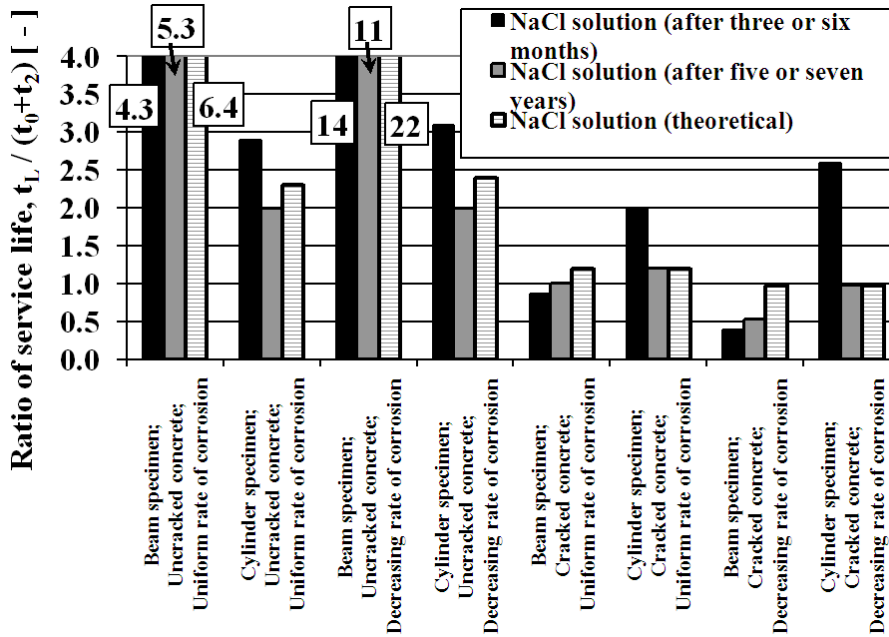
Fig. 105.   *Ratio of service life (service life of hot-dip galvanised reinforcement bars **compared to weathering** steel reinforcement bars) given by the laboratory experiments and the theoretical analysis in sodium chloride solution.*
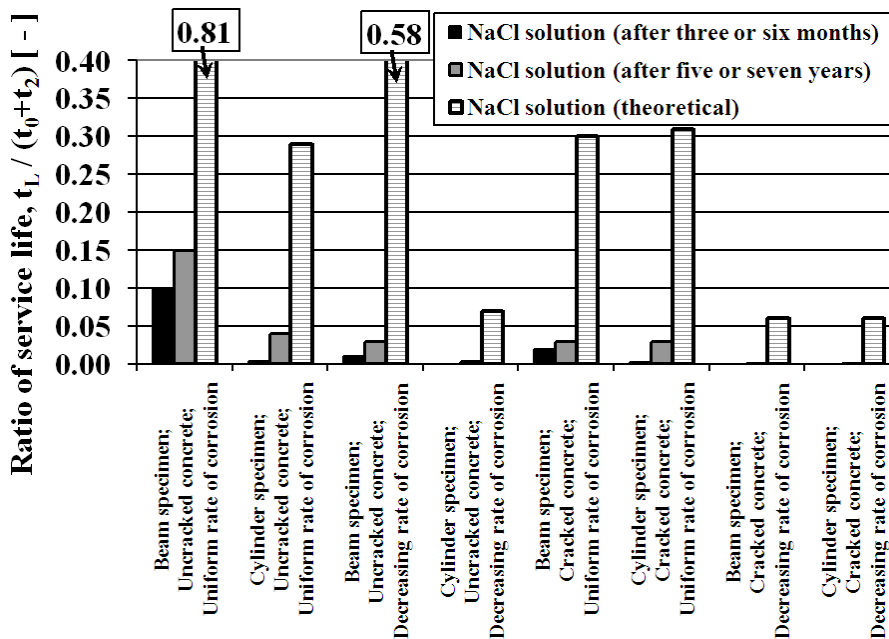
Fig. 106.   *Ratio of service life (service life of hot-dip galvanised reinforcement bars **compared to austenitic** stainless steel reinforcement bars) given by the laboratory experiments and the theoretical analysis in sodium chloride solution.*

As can be seen in Fig. 100, the calculated values of service life in tap water according to the laboratory experiments differ greatly in many cases from the estimated values of service life according to the theoretical analysis. The reason for this is that the measured values of the rate of corrosion (see Chapter 4.3) were lower than the estimated values (see Chapter 3.1). On the other hand, in the sodium chloride solution the noticed difference was due to the high measured values of the rate of corrosion (see Fig. 101).

The service life of hot-dip galvanised reinforcement bars, compared to ordinary or weathering steel reinforcement bars, is on the same level in almost every case (see Fig. 102, Fig. 103, Fig. 104, and Fig. 105). The recognised differences have an influence on the measured low values of rate of corrosion (see Chapter 4.3). As can be seen in Fig. 106, the calculated values of service life in the sodium chloride solution according to the laboratory experiments differ greatly in many cases from the estimated values of service life according to the theoretical analysis. The reason for this is that the measured values of the rate of corrosion (see Chapter 4.3) were lower than the estimated values (see Chapter 3.1). The thickness of the zinc coating has a minor effect on the comparable values because the measured and estimated values are at the same level. On the basis of the validation of the theoretical analysis, the results given by the service life evaluation are realistic in most of the cases. Furthermore, it can be concluded that the values of the rate of corrosion measured approximately less than one year after the durability tests had begun reduced the reliability of calculated service life estimations. The reason for this is that the values of the rate of corrosion show a decreasing trend with a long period of exposure. Thus, the rate of corrosion ought to be measured over a long period of time.

5.3 Improvement of the service life by using hot-dip galvanised reinforcement bars

On the basis of the literature used (Chapter 2), the service life calculations (Chapters 3 and 5.1), the validation (Chapter 5.2), and the sensitivity analysis, an approximation of the improvement in the service life of reinforced outdoor concrete structures by restricting cracks and protecting reinforcements is presented in Table 53. The use of hot-dip galvanised reinforcement bars will extend the service life of concrete structures that normally suffer from carbonation-induced reinforcement corrosion. In carbonated intact and cracked concrete the use of hot-dip galvanised reinforcement bars could double the service life compared with the use of ordinary steel reinforcement bars. In chloride-contaminated intact concrete an improvement in durability by using hot-dip galvanised reinforcement bars (a service life 3-5 times longer than that of an ordinary steel reinforcement bar) is based mainly on the high critical water-soluble chloride content, 1.0-1.5 wt%$_{CEM}$. In chloride-induced reinforcement corrosion, the extendibility of the service life is almost entirely dependent on whether the critical threshold value of hot-dip galvanised reinforcement bars is exceeded. It has been observed that when the chloride threshold value of hot-dip galvanised reinforcement bars (C_{cr} equal to 1.0-1.5 wt%$_{CEM}$) is reached, the rate of corrosion is high.[1,2,3,4]

[1] Yeomans, S.R. (1998). Corrosion of the Zinc Alloy Coating in Galvanized Reinforced Concrete.
[2] Yeomans, S.R. (2004). Galvanized Steel Reinforcement in Concrete.
[3] Proverbio, E. et al. (1998). Long Term Exposure Tests on Galvanized Steel in Different Concrete Types.
[4] Sistonen, E. et al. (2005). Improvement in the Durability of Reinforced outdoor Concrete Structures by Restricting Cracks and Protecting Reinforcement.

Table 53. Relative improvement in the service life of reinforced outdoor concrete structures by restricting cracks and protecting reinforcements.

Reference reinforcement bar (A500HW, weldable hot-rolled ribbed steel reinforcement bar; B500K, cold-worked ribbed steel reinforcement bar)	Relative improvement in the service life of cracked concrete structures	
Researched reinforcement bar (A500HW/ZN, B500K/ZN, hot-dip galvanised reinforcement bar)	Carbonated concrete	Chloride-contaminated concrete
d = 100 μm; c = 30 mm; w = 0.2 mm	1.2…1.6	1.1…1.3
d = 200 μm; c = 30 mm; w = 0.2 mm	1.4…2.0	1.2…1.5
Reference reinforcement bar (A500HW, weldable hot-rolled ribbed steel reinforcement bar; B500K, cold-worked ribbed steel reinforcement bar)	Relative improvement in the service life of uncracked concrete structures	
Researched reinforcement bar (A500HW/ZN, B500K/ZN, hot-dip galvanised reinforcement bar)	Carbonated concrete	Chloride-contaminated concrete
d = 100 μm; c = 20 mm	1.3…2.0	2…4
d = 200 μm; c = 20 mm	1.4…2.1	2…5
d = 100 μm; c = 30 mm	1.2…1.8	3…5
d = 200 μm; c = 30 mm	1.3…1.9	4…5

c is the concrete cover [mm], w is the crack width [mm], and d is the zinc coating thickness [μm].

The mean values, range, and coefficient of variation used with the corrosion parameters (Chapter 3) differ from the values measured in the laboratory work (Chapter 4). The calculated values for the rate of corrosion, the coefficient of the rate of corrosion, and the coefficient of the critical chloride content were higher than those presented in Table 8, Table 9, Table 10, Table 11, and Table 12. The same applies with the measured values for the coefficient of variation in chloride-contaminated concrete and the thickness of the zinc coating. Furthermore, the values used for cracked concrete and for corrosion depth (Fig. 17) contradict the results found in the laboratory work (Fig. 38). It should be noticed that the measured values in the laboratory work represent momentary values. Thus, the values shown in Table 8, Table 9, Table 10, Table 11, and Table 12 are assumed to be long-term mean values including seasonal variation. However, the comparison ratios in Table 45, Table 46, Table 47, and Table 48 are on the same level as those presented in Table 53.

5.4   Summary

The deterioration and service life of hot-dip galvanised reinforcement bars, together with their material cost, are an important factor in their selection. The hypothesis for this should be that there is, for instance, a 20-30% increase in their service life compared with that of an ordinary steel reinforcement bar in carbonated concrete. As long a service life as possible should be ensured with certain requirements.

Providing the necessary research and development can be guaranteed, a hot-dip galvanised reinforcement bar could be a feasible product, which contractors, constructors, and manufacturers can utilise in the future. Although it is more expensive (compared with an ordinary steel reinforcement bar), it can be cost-effective. However, for a hot-dip galvanised reinforcement bar to be used for building purposes, certain changes need to be made to the prescriptive design rules.[1,2,1]

---

[1] Sistonen, E. et al. (2005). Improvement in the Durability of Reinforced Outdoor Concrete Structures by Restricting Cracks and Protecting Reinforcement.

[2] Sistonen, E. et al. (2005). The Influence of Rebar Material on the Durability of Outdoor Reinforced Concrete Structures.

The service life of hot-dip galvanised reinforcement bars can be added to the relevant material properties. Concrete properties such as a lower water-to-binder ratio, a lower pore solution pH value (app. 12.5-13.2), and rapid-hardening concrete are required to ensure a durable reinforced concrete structure with hot-dip galvanised reinforcement bars. Steel properties such as the silicon (target value 0.15%) and phosphorus content (target value 0.020%) of ordinary steel reinforcement bars, and the thickness of the zinc coating and its uniform quality are also demanded. Furthermore, the properties of the galvanising method, the formation and structure of the zinc coating, the properties and reactions of hot-dip galvanised reinforcements in concrete, and mechanical properties have an influence on increasing the probability of a lower and decreasing rate of corrosion. It should be noted that the use of hot-dip galvanised reinforcement bars demands strict limits for the concrete mix and the chemical composition and geometrical properties of the steel.

The service life of hot-dip galvanised reinforcement bars is strongly linked with the quality requirements for hot-dip galvanised reinforcement bars. Thus, there is a need for further research: 1) to investigate the interfacial transition zone (ITZ) between the cement paste and the hot-dip galvanised steel reinforcement bar; 2) to confirm that it is possible to meet the durability requirements of the new National Building Code of Finland (Part B4 Concrete Structures) by using hot-dip galvanised reinforcement bars; 3) to specify requirements for quality, and 4) to develop software concerning the service life calculation method for hot-dip galvanised reinforcements to make it possible to incorporate the results into product models and ITC applications in the building industry.

---

[1] Sistonen, E. et al. (2006). Stochastic Method and Monte Carlo Simulation for Predicting Service Life of Hot-Dip Galvanised Reinforcement.

6　CONCLUSIONS

The study presented the influence of hot-dip galvanised reinforcement bars on the durability of outdoor concrete structures. The paper presented a literature review of the research topic studied. The study of the service life calculation focused on a stochastic method based on the probability of damage, Monte Carlo simulation, and reliability analysis. A long-term laboratory test with two concrete and four reinforcement bar types was presented. The effects of hot-dip galvanised reinforcing steels on the service life of outdoor concrete structures were estimated through calculations.

The literature study revealed that several factors have an influence on the thickness and formation of the zinc coating and the formation of the passive layer of the hot-dip galvanised reinforcement bar, which are linked to the durability and service life of hot-dip galvanised reinforcement bars.

In the stochastic evaluation, the most suitable deterministic formulae might be the ones that are of a power of three at the most. Because of possible sources of error in service life calculation, it is recommendable that priority is given to determining which of the parameters are the most significant in view of the target service life instead of placing reliance on the estimates as such. The main problems in service life evaluation are as follows: the reliability of the distribution of parameters in a deterministic formula (a lack of sufficient statistical data); the accuracy of the distribution function chosen to describe a deterministic model (a deterministic formula may take account of only one deterioration mechanism), and the choice of a probability of damage that ensures that the deterioration probability of the formula is sufficiently low.

The durability tests confirmed that the rate of corrosion was decreasing. This phenomenon may have a positive effect on improvement of the service life of reinforced concrete structures. The research result was not dependent on the water-to-cement ratio of concrete. The comparison of the measured crack width of concrete with the rate of corrosion values showed no correlation independent of the exposure duration or type of aggressive liquid. Other measured values, such as the corrosion potential, the resistivity of the concrete and mechanical properties of steel, did not reveal any correlation with crack width either.

There was a local anodic area on the reinforcement bar at a crack which was surrounded by a large cathodic area extending away from the crack into the sound concrete. This means that in high-quality concrete cracking has significance for the durability of the reinforcement bar materials. Approximated half-cell potential limits for different reinforcement bar materials measured with a copper/copper sulphate half-cell, CSE, were proposed on the basis of the performed corrosion tests, theoretical analyses, and literature.

Three different corrosion mechanisms were proposed for hot-dip galvanised reinforcement bars in cracked concrete (the first and the second one were also found by other researchers). The first mechanism consists of a local dissolution of the eta (η) and zeta (ζ) phase of the zinc layer, the simultaneous corrosion of which is possible as a result of the non-uniform thickness of the zinc coating. The second mechanism consists additionally of longitudinal and perpendicular cracking in the zinc layer (delta (δ) phase), which may lead to the local separation of the zinc layer. The last mechanism includes all the factors mentioned in the previous two mechanisms, supported

additionally by longitudinal and perpendicular cracking in the ferrite, which may lead to the local separation of the zinc layer and ferrite.

The results obtained and mechanisms described confirmed earlier observations that the thicknesses of the zinc phases influence the extent of the corrosion. The rate of corrosion determined by the electrochemical measurements agreed with the SEM studies and proposed corrosion mechanisms. Data processing and analysis showed that with different electrochemical measurements the parameters that illustrate the same corrosion phenomenon may have different types of distribution curves.

The limit values that considerably extend the service life were presented, including cracking. The estimated service life calculations agreed with the literature review and the proposed corrosion mechanisms that hot-dip galvanised steel used as a method for protecting reinforcements against corrosion could improve the durability of even cracked, carbonated, and chloride-contaminated concrete. In carbonated intact and cracked concrete the use of hot-dip galvanised reinforcement bars could double the service life compared with the use of ordinary steel reinforcement bars.

In chloride-contaminated intact concrete the improvement in the service life by using hot-dip galvanised reinforcement bars is 3-5 times longer compared with ordinary steel reinforcement bars. This conclusion is based on the results received with the critical water-soluble chloride content of 1.0-1.5 wt%$_{CEM}$, which is substantially higher than the critical water-soluble chloride content of 0.3-0.4 wt%$_{CEM}$ for ordinary steel reinforcement bars. In chloride-induced reinforcement corrosion, the extendibility of the service life is almost entirely dependent on whether the critical threshold value of hot-dip galvanised reinforcement bars is exceeded.

The lack of knowledge in the field of the manufacturing, transportation, installation, and service life of hot-dip galvanised bars as reinforcement is evident. To encourage the construction industry to increase its use of hot-dip galvanised reinforcement bars on a large scale in Finland it is necessary to improve the quality of hot-dip galvanised reinforcement bars remarkably, to speed up the manufacturing process of hot-dip galvanised reinforcement bars, and to prove the durability properties of hot-dip galvanised reinforcement bars with quality requirements from the point of view of their service life. The use of hot-dip galvanised reinforcement bars demands strict limits for the concrete mix and the chemical composition and geometrical properties of the steel.

Further research is needed to define proposed corrosion mechanisms with different moisture contents and concrete types. Furthermore, a numerical model for the estimation of the degradation of concrete with hot-dip galvanised reinforcement bars is needed. Analysis with the finite element method (FEM) should concentrate on the corrosion parameters studied in this dissertation, i.e. cracking, the rate of corrosion of hot-dip galvanised reinforcement bars compared to ordinary steel reinforcement bars, and the thickness of the zinc coating.

7   REFERENCES

Alonso, C., Sánchez, J., Fullea, J., Andrade, C., Tierra, P., Bernal, M. (2000). The Addition of Ni to Improve the Corrosion Resistance of Galvanized Reinforcement. 19th Intern. Galvanizing Conference and Exhibition. Intergalva, Berlin, Germany.

Andersson, K., Allard, B., Bengtsson, M., Magnusson, B. (1989). Chemical Composition of Cement Pore Solutions. *Cement and Concrete Research*, Vol. **19**, No. 3, pp. 327-332. 0008-8846/89.

Andrade, C., Alonso, C. (2001). On-Site Measurements of Corrosion Rate of Reinforcements. *Construction and Building Materials*, Vol. **15**, No. 2-3, pp. 141-145.

Andrade, C., Alonso, C. (2004). Electrochemical Aspects of Galvanized Reinforcement Corrosion. In: Yeomans, S.R. (Editor). Galvanized Steel in Reinforced Concrete, Elsevier B.V., Amsterdam, The Netherlands, 2004, 297 p. ISBN 0-08-044511-X.

Andrade, C., Alonso, C., Gulikers J., Polder, R., Cigna, R., Vennesland, Ø., Salta, M., Raharinaivo, A., Elsener, B. (2004). Recommendations of RILEM TC-154-EMC: "Electrochemical Techniques for measuring Metallic Corrosion" Test Methods for On-site Corrosion Rate Measurement of Steel Reinforcement in Concrete by means of the Polarization Resistance Method. *Materials and Structures*, Vol. **37**, No. 273, pp. 623-643.

Andrade, C., Arteaga, A., López-Hombrados, C., Vázquez, A. (2001). Tests on Bond of Galvanized Rebar and Concrete Cured in Seawater. *Journal of Materials in Civil Engineering*, Vol. **13**, No. 5, pp. 319-324. September/October, 2001.

Andrade, C., Gulikers J., Polder, R., Vennesland, Ø., Elsener, B., Weider, R., Raupach, M. (2000). Recommendations of RILEM TC-154-EMC: "Electrochemical Techniques for measuring Metallic Corrosion" Test Methods for On-site Measurement of Resistivity of Concrete. *Materials and Structures*, Vol. **33**, No. 234, pp. 603-611.

Andrade, C., Holst, J.D., Nürnberger U., Whiteley, J.D., Woodman, N. (1992). Protection Systems for Reinforcement. Lausanne, Switzerland: CEB, 1992. 82 p. (Bulletin D'Information No 211). ISBN 2-88394-016-9.

Andrade, C., Holst, J.D., Nürnberger, U., Whiteley, J.D., Woodman, N. (1995). Coating Protection for Reinforcement, State of the art report. London, UK: Thomas Telford Publications. 51 p. (CEB Bulletin d'Information 211. 1992) ISBN: 0 7277 2021 X.

Andrade, C., Macias, A., Molina, A., Gonzalez, J.A. (1985). Advances in the Study of the Corrosion of Galvanized Reinforcement Embedded in Concrete. Tehnical symposia – Corrosion 85, paper 270. Publ. by NACE, Houston, TX, USA, 9 p.

Andrade, C., Molina, A., Huete, F., Gonzalez, J.A. (1983). Relation between the Alkali Content of Cements and the Corrosion Rates of the Galvanized Reinforcements. In: Crane, A.P. (Editor). Corrosion of Reinforcement in Concrete Construction. London, 13-15 June, 1983. Chichester, UK: Ellis Horwood Limited, 1983, pp. 343-355. ISBN 0-85312-600-3.

Angst, U., Vennesland, Ø. (2007). Critical chloride content - State of the Art. SINTEF Building and Infrastructure, SINTEF Report SBF BK A07037, Trondheim, Norway, 54 p. ISBN 978-82-536-0997-3.

Arliguie, G. (2001). Performance of Galvanized Rebar. COST 521 Workshop, Tampere 17-20 June, 2001. pp. 47-54. Mattila, J. (editor) COST 521. Corrosion of Steel in Reinforced Concrete Structures. Proceedings of the 2001 Workshop, Department of Civil Engineering, Tampere, Finland. 293 p. ISBN 952-15-0634-2.

ASTM A143/A143M-03 (2003). Standard Practice for Safeguarding Against Embrittlement of Hot-Dip Galvanized Structural Steel Products and Procedure for Detecting Embrittlement, American Society for Testing and Materials, 3 p.

ASTM A153/A153M-03 (2003). Standard Specification for Zinc Coating (Hot-Dip) on Iron and Steel Hardware, American Society for Testing and Materials, 4 p.

ASTM A385-03 (2003). Standard Practice for Providing High Quality Zinc Coatings, American Society for Testing and Materials, 9 p.

ASTM A767/A 767M-00b (2000). Standard Specification for Zinc-Coated (Galvanized) Steel Bars for Concrete Reinforcement, American Society for Testing and Materials, 4 p.

156

ASTM C457-98 (1998). Standard Test Method for Microscopical Determination of Parameters of the Air-Void System in Hardened Concrete, American Society for Testing and Materials, 14 p.

ASTM C856-04 (2004). Standard Practice for Petrographic Examination of Hardened Concrete, American Society for Testing and Materials, 17 p.

ASTM C876-91 (1999). Standard Test Method for Half-Cell Potentials of Uncoated Reinforcing Steel in Concrete, American Society for Testing and Materials, 6 p.

ASTM C1218/C1218M-99 (1999). Standard Test Method for Water-Soluble Chloride in Mortar and Concrete, American Society for Testing and Materials, 3 p.

Aubriet, F., Maunit, B., Muller, J-F. (2000). Studies on Alkali and Alkaline Earth Chromate by Time-of-flight Laser Microprobe Mass Spectrometry and Fourier Transform Ion Cyclotron Resonance Mass Spectrometry. Part I: Differentiation of Chromate Compounds. *International Journal of Mass Spectrometry*, Vol. **198**, No. 3, 2000, pp. 189–211.

Baboian, R. (1976). Electrochemical Techniques for Predicting Galvanic Corrosion. In: Baboian, R., France, W.D., Jr., Rowe, L.C., Rynewicz, J.F. (editors). Galvanic and Pitting Corrosion – Field and Laboratory Studies. Two symposia on Galvanic and Pitting Corrosion. Detroit, MI. 22-23 Oct. 1976. pp. 5-19, ASTM stp 576.

Bautista, A., Gonzalez, J.A. (1996). Analysis of the Protective Efficiency of Galvanizing Against Corrosion of Reinforcements Embedded in Chloride Contaminated Concrete. *Cement and Concrete Research*, Vol. **26**, No. 2, 1996, pp. 215-224. ISNN 0008-8846.

Belaïd, F., Arliguie, G., François, R. (2000). Corrosion Products of Galvanized Rebars Embedded in Chloride-Contaminated Concrete, *Corrosion Engineering Section*, Vol. **56**, No. 9, pp. 960-965.

Belaïd, F., Arliguie, G., François, R. (2001). Porous structure of the ITZ around galvanized and ordinary steel reinforcements. *Cement and Concrete Research*, Vol. **31**, pp. 1561-1566.

Bellezze, T., Malavolta, M., Quaranta, A., Ruffini, N., Roventi, G., (2006). Corrosion behaviour in concrete of three differently galvanized steel bars, *Cement and Concrete Composites*, Vol. **28**, pp. 246-255.

Bentur, A., Diamond, S., Berke, N.S. (1997). Steel Corrosion in Concrete: Fundamentals and Civil Engineering Practice. London, United Kingdom: Spon, 1997. 201 p. ISBN 0-419-22530-7.

Bertolini, L., Elsener, B., Pedeferri, P., Polder, R. (2004). Corrosion of Steel in Concrete – Prevention, Diagnosis, Repair. WILEY-VCH, Weinheim, Germany. 392 p. ISBN 3-527-30800-8.

Boyd, W.K., Tripler, A.B. (1968). Corrosion of Reinforced Steel Bars in Concrete, *Materials Protection*, Vol. **7**, No. 10, pp. 40-47.

Broomfield, J.P. (1997). Corrosion of Steel in Concrete. London, United Kingdom: E & FN Spon, 238 p. ISBN 0-419-19630-7.

By 32 (1992). Durability Guideline and Service Life Dimensioning of Concrete Structures, Concrete Association of Finland, 1992. (in Finnish).

By 50 (2004). Concrete Code 2004, Concrete Association of Finland, 2004. (in Finnish).

Camitz, G., Pettersson, K. (1989). Corrosion protection of steel in concrete - Stage 1, Cathodic corrosion protection of steel reinforcement in concrete - the literature review. Stockholm, Sweden: Gotab. 70 p. CBI offprint 3:90. Swedish Corrosion Institute, R 63 185: 1989. ISSN 1101-1297 (in Swedish).

Clifton, J.R., Pommersheim, J.M., (1992). Methods for Predicting the remaining service life of concrete in structures. NISTIR 4954. Gaithersburg, MD: NIST, 1992.

Collepardi, M. (2000). Ordinary and Long-Term Durability of Reinforced Concrete Structures. pp. 1-17. In: Malhotra, V.M. (editor), Fifth CANMET/ACI International Conference on Durability of Concrete, Vol. I, Barcelona, Spain. 644 p.

Compton, K.G., Turley, J.A. (1976). Electrochemical Examination of Fused Joints Between Metals. In: Baboian, R., France, W.D., Jr., Rowe, L.C., Rynewicz, J.F. (editors). Galvanic and Pitting Corrosion – Field and Laboratory Studies. Two symposia on Galvanic and Pitting Corrosion. Detroit, MI. 22-23 Oct. 1976. pp. 56-68, ASTM stp 576.

Concrete Institute of Australia (1984). The Use of Galvanized Reinforcement in Concrete. 3 p. Current Practice Note 17. ISBN 0 909375 21 6.

Corderoy, D.J.H., Herzog, H. (1980). Passivation of Galvanized Reinforcement by Inhibitor Anions. In: Tonini, D.E., Gaidis, J.M. (editors). Corrosion of Reinforcing Steel in Concrete. A Symposium on Corrosion of Metals, Bal Harbour, Fla., 4-5 Dec.1978. Philadelphia, Pa, USA: ASTM, American Society for Testing and Materials, pp. 142-159. ASTM stp 713.

Cwirzen, A. (2004). Effects of the Transition Zone and Aging on the Frost Damage of the High Strength Concretes. Helsinki University of Technology, Building Materials Technology, Report 17 (Dissertation). Espoo, Finland. 190 p. + app. 65 p.

EN ISO 1461 (1999). Hot Dip Galvanized Coatings on Fabricated Iron and Steel Articles – Specifications and Test Methods (ISO 1461:1999). European Standard, February 1999, 18 p.

Fagerlund, G. (1990). Durability of Concrete Structures, Summary Review. 2. Edition. AW Grafiska: Uppsala 1990. 101 p. ISBN 91-87334-00-3 (in Swedish).

Finnish Association of Civil Engineers (1995). RIL 183-4.9-1995. Service Life of Construction Materials and Structures. Methods of Appraisal. 4.9: Service Life Design of Concrete Structures. Vantaa, Finland: Finnish Association of Civil Engineers, RIL, ISBN 951-758-344-3, 120 p. (in Finnish).

Foct, J., Reumont, G., Perrot, P. (1993). How does Silicon lead the Kinetics of the Galvanizing Reaction to lose its solid-solid Character. *Journal De Physique IV*, Colloque C7, Supplément au Journal de Physique III, Vol. **3**, Novembre 1993, pp. 961-966.

Fratesi, R., Moriconi, G., Coppola, I. (1996). The Influence of Steel Galvanization on Rebars Behaviour in Concrete. In: Page, C.L., Bamforth, P.B. & Figg, J.W. (editors), Corrosion of Reinforcement in Concrete Construction, pp. 630-641. Royal Society of Chemistry.

Galvanizers' Association of Australia (1999). After-Fabrication Hot Dip Galvanizing. A practical Reference for Designers, Specifiers, Engineers, Consultants, Manufacturers and Users – to introduce AS/NZS 4680. Melbourne, Australia, 72 p.

Ghosh, R., Singh, D.D.N. (2007). Kinetics, Mechanism and Characterisation of passive Film formed on Hot Dip Galvanized Coating exposed in simulated Concrete Pore Solution. *Surface and Coatings Technology*, Vol. **201**, No. 16-17, pp. 7346-7359.

Gowripalan, N., Mohamed, H.M. (1998). Chloride-Ion Induced Corrosion of Galvanized and Ordinary Steel Reinforcement in High-Performance Concrete. *Cement and Concrete Research*, Vol. **28**, No. 8, pp. 1119-1131.

Hausmann, D.A. (1967). Steel Corrosion in Concrete: How Does It Occur? *Materials Protection*, No. 6, pp. 19-23.

Hime, W.G., Machin, M. (1993). Performance Variances of Galvanized Steel in Mortar and Concrete. *Corrosion Science*, Vol. **49**, No. 10, pp. 858-860.

Hisamatsu, Y. (1989). Science and technology of zinc and zinc alloy coated sheet steel. GALVATECH '89. Tokyo: The Iron and Steel Institute of Japan. p. 3.

Ho-Jong, Lee (2001). Effect of Ni Addition in Zinc Bath on Formation of Inhibition Layer during Galvannealing of Hot-dip Galvanized Sheet Steels, *Journal of Materials Science Letters* Vol. **20**, pp. 955-957.

Hoke, J.H., Pickering, H.W., Rosengarth, K. (1981). Cracking of Reinforced Concrete. ILZRO Project ZE-271. International Lead Zinc Research Organisation, Research Triangle Park, NC, USA.

http://www.hdgasa.org.za/ (12.04.2009).

Høyland, A., Rausand, M. (1993). System Reliability Theory. Models and Statistical Methods. Wiley Series in Probability and Mathematical Statistics, New York, 523 p.

Jokela, J. (1986). Dimensioning of Strain or Deformation-controlled Reinforced Concrete Beams. Espoo, Finland: VTT, 1986. 53 p. Publications 33, Technical Research Centre of Finland.

Lachowski, E., Mohan, K., Taylor, H.F.W. (1980). Analytical Electron Microscopy of Cement Pastes: II, Pastes of Portland Cements and Clinkers. *Journal of the American Ceramics Society*, Vol. **63**, No. 7-8, pp. 447-452.

Locke, C.E. (1984). Corrosion of Steel in Portland Cement Concrete: Fundamental Studies. In: Chaker, V. (editor). Corrosion Effect of Stray Currents and the Techniques for Evaluating Corrosion of Rebars in

Concrete, A symposium on Corrosion of Metals, Williamsburg, VA, 28 Nov. 1984. Baltimore, USA: ASTM. pp. 5-14, ASTM stp 906. ISBN 0-8031-0468-5.

Luping, T. (2002). Calibration of the Electrochemical Methods for the Corrosion Rate Measurement of Steel in Concrete, NORDTEST Project No. 1531-01, SP Swedish National Testing and Research Institute, Building Technology, SP Report 2002:25, Borås, Sweden.

Maahn, E. and Sorensen, B. (1996). Influence of Microstructure on the Corrosion Properties of Hot-dip Galvanized Reinforcement in Concrete. *Corrosion* (Houston), Vol. **42**, No. 4, pp. 187-196. ISSN 0010-9312.

Maldonado, L., Pech-Canul, M.A., Alhassan, S. (2006). Corrosion of Zinc-coated Reinforcing Bars in Tropical Humid Marine Environments. *Anti-Corrosion Methods and Materials*, Vol. **53**, No. 6, pp. 357-361.

Mansfeld, F., Kenkel, J.V. (1976). Laboratory Studies of Galvanic Corrosion of Aluminum Alloys. In: Baboian, R., France, W.D., Jr., Rowe, L.C., Rynewicz, J.F. (editors). Galvanic and Pitting Corrosion – Field and Laboratory Studies. Two symposia on Galvanic and Pitting Corrosion. Detroit, MI. 22-23 Oct. 1976. pp. 20-47, ASTM stp 576.

Marder, A.R. (2000). The Metallurgy of Zinc-Coated Steel. *Progress in Materials Science*, Vol. **45**, No. 3, pp. 191-271.

Matala, S. (1991). Calculation Methods of Service Life. In: Finnish Association of Civil Engineers. RIL K145-1991. Durability, Damage and Repair of Concrete Structures. Vantaa, Finland. 165 p. ISBN 951-758-271-4 (in Finnish). Unpublished.

Mohammed, T., Otsuki, N., Hamada, H. (2003). Corrosion of Steel Bars in Cracked Concrete, Journal *of Materials in Civil Engineering*, Vol. **15**, No. 5, pp. 460-469.

Nagy, A. (1997). Cracking in Reinforced Concrete Structures Due to Imposed Deformations, (Doctoral thesis) Lund Institute of Technology, Rapport TVBK-1012. Lund, Sweden, 90 p. ISSN 0349-4969.

Nishimoto, A., Inagaki, J., Nakaoka, K. (1986). Effects of surface microstructure and chemical composition of steels on formation of Fe-Zn compounds during continuous galvanizing. The Iron and Steel Institute of Japan. Trans ISIJ 1986; 26: 807.

Notowidjojo, B.D., Wingrove, A.L., Kennon, N.F. (1989). Possible Source of Dross Formation in Zinc-0.l% Nickel Galvanizing Process. *Materials Forum*, Vol. **13**, pp.73-75.

Nürnberger, U. (2000). Supplementary Corrosion Protection of Reinforcing Steel. *Otto-Graf-Journal*, Vol. **11**, pp. 77-108.

Okamura, H., Hisamatsu, Y. (1976). Effect of Use of Galvanized Steel on the Durability of Reinforced Concrete. *Materials Performance*, Vol. **15**, No. 7, pp. 43-47.

Otsuki, N., Miyazato, S., Diola, N., Suzuki, H. (2000). Influences of Bending Crack and Water-Cement Ratio on Chloride-Induced Corrosion of Main Reinforcing Bars and Stirrups, *ACI Materials Journal*, Vol. **97**, No. 4, pp. 454-464.

Pentti, M. (1999). The Accuracy of the Extent-of-Corrosion Estimate Based on the Sampling of Carbonation and Cover Depths of Reinforced Concrete Facade Panels, (Doctoral thesis) Tampere University of Technology, Publication 274. Tampere, Finland, 164 p.

Pfeifer, D.W., Landgren, J.R., Zoob, A.B. (1987). Protective Systems for New Prestressed and Substructure Concrete, FHWA Report No. FHWA/RD 86/193. Springfield, Virginia, USA: National Technical Information Service.

Porter, F. (1991). Zinc Handbook, Properties, Processing, and Use in Design. New York, USA: Marcel Dekker, Inc. 629 p. ISBN 0-8247-8340-9.

Pourbaix, M. (1963). Atlas of Electrochemical Equilibria in Aqueous Solutions. Pergamon Press, Brussels, Belgium, 644 p. (in French).

PrEN 13295 (2003). Products and Systems for the Protection and Repair of Concrete Structures. Test Methods. Determination of Resistance to Carbonation. European Standard, November 2003, 14 p.

Proverbio, E., Meloni, M., Fratesi, R., Luminari, M. (1998). Long Term Exposure Tests on Galvanized Steel in Different Concrete Types. In: Gjørv, O.E., Sakai, K., Banthia, N. (editors). Concrete under Severe Conditions 2, Environment and Loading. Proceedings of the 2nd International Conference on

Concrete under severe Conditions CONSEC '98. Tromsø, Norway, June 21-24, 1998. Vol. 1. London, U.K.: E&FN Spon, pp. 509-518. ISBN 0 419 23860 3.

Ramirez, E., Gonzalez, J.A., Bautista, A. (1996). The Protective Efficiency of Galvanizing Against Corrosion of Steel in Mortar and in $Ca(OH)_2$ Saturated Solutions Containing Clorides. *Cement and Concrete Research*, Vol. **26**, No. 10, pp. 1525-1536. ISNN 0008-8846.

Reumont, G., Perrot, P., Foct, J. (1998). Thermodynamic Study of the Galvanizing Process in a Zn–0.1%Ni bath. *Journal of Materials Science*, Vol. **33** No. 19, pp. 4759-4768.

RILEM TC (1994). RILEM Recommendations for the Testing and Use of Constructions Materials, RC 6 Bond Test for Reinforcement Steel. 2. Pull-out Test, 1983, E & FN SPON, pp. 218 - 220. ISBN 2351580117 (pdf).

Rostam, S. (2002). Service Life Design of Concrete Structures - A Challenge to Designers as well as to Owners. *Asian Journal of Civil Engineering (Building and Housing)*, Vol. **6**, No. 5, pp. 423-445.

Sandoval-Jabalera, R., Nevárez-Moorillón, G., Chacón-Nava, J., Malo-Tamayo, J., Martínez-Villafañe, A. (2006). Electrochemical Behaviour of 1018, 304 and 800 Alloys in Synthetic Wastewater. J. *Journal of the Mexican Chemical Society*, Vol. **50**, No. 1, Sociedad Química de México, pp. 14-18.

Sarja, A. (2006). European Symposium on Service Life and Serviceability of Concrete Structures, ESCS-2006, Proceedings, Helsinki, Finland, June 12-14, 2006, 406 p.

Sarja, A. (2000). Integrated Life-Cycle Design of Materials and Structures, ILCDES 2000. Proceedings PRO 14, Proceedings of the RILEM/CIB/ISO International Symposium, Helsinki, Finland, May 22-24, 2000, 549 p. ISSN 0356-9403. ISBN 951-758-408-3.

Sarja, A., Jokela, M., Metso J. (1984). Zinc-coated Concrete Reinforcement. Espoo, Finland. VTT, 92 p. Research Reports 306, Technical Research Centre of Finland. ISBN 957-38-2134-X.

Sarja, A., Vesikari, E. (1996). Durability Design of Concrete Structures. RILEM Report 14, Report of TC 130-CSL, E & FN SPON, 165 p.

Schießl, P. (1976). Regarding the Question of maximum Crack Width and the required Concrete Cover in Reinforced Concrete Structures paying particular Attention to the Carbonation of the Concrete. Berlin, Germany, deutscher Ausschuß für Stahlbeton, Heft 255. 175 p. (in German).

Scrivener, K.L. (2004). Backscattered Electron Imaging of Cementitious Microstructures: Understanding and Quantification, *Cement and Concrete Composites*, Vol. **26**, No. 8, pp. 935-945.

SFS 1215 (1996). Reinforcing steels. Weldable Hot Rolled Ribbed Steel Bars A500HW. Finnish Standards Association SFS, 6 p. (in Finnish).

SFS 1257 (1996). Reinforcing steels. Cold Worked Ribbed Steel Bars B500K. Finnish Standards Association SFS, 6 p. (in Finnish).

SFS 4475 (1988). Concrete. Frost resistance. Protective pore ratio. Finnish Standards Association SFS, 2 p. (in Finnish).

SFS-EN 206-1 (2001). Concrete. Part 1: Specification, Performance, Production and Conformity. Finnish Standards Association SFS, 73 p. (in Finnish).

Schneider, J. (1997). Introduction to Safety and Reliability of Structures, Structural Engineering Documents 5. International Association for Bridge and Structural Engineering, IABSE. Zürich, Switzerland, 139 p.

Shimada, H., Nishi, S. (1983). Sea Water Corrosion Attack on Concrete Blocks Embedding Zinc Galvanized Steel Rebars. In: Crane, A.P. (editor). Corrosion of Reinforcement in Concrete Construction. Chichester, West Sussex, England: Ellis Horwood Limited, pp. 407-418. ISBN 0-85312-600-3.

Short, N.R., Zhou, Z., Dennis, J.K. (1994). Corrosion Behaviour of Zinc Alloy Coated Steel in Hardened Cement Pastes. In: Swamy, R.N. (editors). Corrosion and Corrosion Protection of Steel in Concrete. Sheffield, United Kingdom: Sheffield Academic Press Ltd, pp. 1287-1298. ISBN 1-85075-723-2.

Siemens, A., Vrouwenvelder, A., van den Beukel, A. (1985). Durability of Buildings: A Reliability Analysis. Heron **30**, 3. pp. 3-48.

Sistonen, E. (2001). The Main Corrosion Parameters and their Influence on the Durability of Outdoor Concrete Structures, Licentiate Thesis, Espoo, Finland, TKK, 84 p. + app. 20 p. (in Finnish).

Sistonen, E., Cwirzen, A., Puttonen J. (2008). Corrosion Mechanism of Hot-dip Galvanised Reinforcement Bar in Cracked Concrete, *Corrosion Science*, Vol. **50**, No. 12. pp. 3416-3428.

Sistonen, E., Huovinen, S. (2005). Improvement in the Durability of Reinforced Outdoor Concrete Structures by restricting Cracks and protecting Reinforcement, Nordic Concrete Research - Research Projects 2005, Proceedings Nordic Concrete Research Meeting, XIX Symposium on Nordic Concrete Research & Development - A meeting place for research and practice; Sandefjord, Norway, 12.-15.6.2005, Publication no. 33, pp. 259-261.

Sistonen, E., Huovinen, S. (2005). The Main Corrosion Parameters and their Influence on the Durability of Outdoor Concrete Structures, Nordic Concrete Research - Research Projects 2005, Proceedings Nordic Concrete Research Meeting, XIX Symposium on Nordic Concrete Research & Development - A meeting place for research and practice; Sandefjord, Norway, 12.-15.6.2005, Publication No. 33, pp. 271-273.

Sistonen, E., Huovinen, S. (2005). Possibilities of controlling Cracks and improving the Durability of Outdoor Reinforced Concrete Structures, Nordic Concrete Research - Research Projects 2005, Proceedings Nordic Concrete Research Meeting, XIX Symposium on Nordic Concrete Research & Development - A meeting place for research and practice; Sandefjord, Norway, 12.-15.6.2005, Publication No. 33, pp. 262-264.

Sistonen, E., Huovinen, S. (2005). Problems in Service life Modelling of Corroded Outdoor Concrete Structures, Nordic Concrete Research - Research Projects 2005, Proceedings Nordic Concrete Research Meeting, XIX Symposium on Nordic Concrete Research & Development - A meeting place for research and practice; Sandefjord, Norway, 12.-15.6.2005, Publication No. 33, pp. 265-267.

Sistonen, E., Kari, O-P., Tukiainen, P., Huovinen, S. (2006). Stochastic Method and Monte Carlo Simulation for Predicting Service Life of Hot-Dip Galvanised Reinforcement, 2nd International RILEM Symposium on Advances in Concrete through Science and Engineering, Quebec City, Canada, September 11-13, 2006, RILEM proceedings PRO 51 (editors: Marchand, J. et al.) (Abstract at p. 289 and the paper number 45 is 23 pages on symposium CD-ROM proceedings).

Sistonen, E., Kari, O-P., Tukiainen, P., Huovinen, S. (2007). The Influence of the Crack Width on the Durability of different Reinforcement Bar Materials, CONSEC'07, Concrete under severe conditions: Environment and loading, Tours, France, (editors: Toutlemonde, F. et al.) June 4-6, 2007. pp. 419-428.

Sistonen, E., Peltola, S. (2005). Quality Specifications for Hot-Dip Galvanised Reinforcement to Ensure the Target Service Life, Nordic Concrete Research - Research Projects 2005, Proceedings Nordic Concrete Research Meeting, XIX Symposium on Nordic Concrete Research & Development - A meeting place for research and practice; Sandefjord, Norway, 12.-15.6.2005, Publication No. 33, pp. 133-134.

Sistonen, E., Tukiainen, P. (2005). The Influence of Rebar Material on the Durability of Outdoor Reinforced Concrete Structures, Nordic Concrete Research - Research Projects 2005, Proceedings Nordic Concrete Research Meeting, XIX Symposium on Nordic Concrete Research & Development - A meeting place for research and practice; Sandefjord, Norway, 12.-15.6.2005, Publication No. 33, pp. 268-270.

Sistonen, E., Tukiainen, P., Huovinen, S. (2005). Bonding of Hot Dip Galvanised Reinforcement in Concrete, *Nordic Concrete Research*; Publication No. **34**, 2/2005, The Nordic Concrete Federation, Oslo, Norway, 2005, pp 1-14.

Sistonen, E., Tukiainen, P., Laitala, M., Huovinen, S. (2000). Restricting Corrosion Risk in Reinforced Concrete Structures under Outdoor Conditions, Espoo, Finland, TKK-TRT-111, 141 p+ app. 47 p. (in Finnish).

Sistonen, E., Tukiainen, P., Peltola, S., Skriko, S., Huovinen, S. (2002). Restricting Corrosion Risk in Reinforced Concrete Structures under Outdoor Conditions – Part II, Espoo, Finland, TKK-TRT-121, 212 p+ app. 101 p. (in Finnish).

Sistonen, E., Tukiainen, P., Peltola, S., Kari, O-P., Huovinen, S. (2006). Service Life and Quality Specifications for Hot-Dip Galvanised Reinforcement, European Symposium on Service Life and Serviceability of Concrete Structures, ESCS-2006, Proceedings, Helsinki, Finland, June 12-14, 2006, pp. 395-400.

Swamy, R.N. (1990). Resistance to Chlorides of Galvanized Rebars. In: Corrosion of Reinforcement in Concrete, Page, C., Treadaway, K.W.J, and Bamforth, P.B. (editors), Elsevier Appl. Sci., London-New York, pp. 586-600.

Sykes, J.M. (1995). Electrochemical Studies on Steel in Concrete, Materials Science Forum Vols. 192-194, pp. 833-842. In: Electrochemical Methods in Corrosion Research V.

Taylor, H.F.W., Newbury, D.E. (1984). An Electron Microprobe Study of a Mature Cement Paste. *Cement and Concrete Research*, Vol. **14**, No. 4, pp. 1561-1566.

Treadaway, K.W.J., Brown, B.L., Cox, R.N. (1980). Durability of Galvanized Steel in Concrete. In: Tonini, D.E., Gaidis, J.M. (editors). Corrosion of Reinforcing Steel in Concrete. ASTM, pp. 102-131.

Treadaway, K.W.J. (1989). Durability of Corrosion Resisting Steels in Concrete. In: Proceedings of the Institution of Civil Engineers. pp. 305-331.

Vesikari, E. (2009). Carbonation and Chloride Penetration in Concrete - with Special Objective of Service Life Modelling by the Factor Approach. Espoo, Finland, 38 p. Research Report VTT-R-04771-09, Technical Research Centre of Finland.

Vesikari, E. (1981). Corrosion of Reinforcing Steels at Cracks in Concrete. VTT, Espoo, Finland, 39 p. + app. 4 p. Research Reports 11/1981, Technical Research Centre of Finland.

Vesikari, E. (1988). Service Life of Concrete Structures with regard to Corrosion of Reinforcement. VTT, Espoo, Finland, 53 p. Research Reports 553, Technical Research Centre of Finland.

Vinka, T.-G., Becker, M. (1998). Corrosion of Galvanised Steel in Concrete. 1998-08-21. 40 p. Swedish Corrosion Institute, Project Report 63 282:1 (in Swedish).

WSP TutkimusKORTES Oy (Ltd.) (2006). Research report 6462/06. 6 p. (in Finnish).

WSP TutkimusKORTES Oy (Ltd.) (2007). Research report 7300/07. 5 p. (in Finnish).

Yeomans, S.R. (1994). A Conceptual Model for the Corrosion of Galvanized Reinforcement in Concrete. In: Swamy, R.N. (editor). Corrosion and Corrosion Protection of Steel in Concrete. Sheffield, United Kingdom: Sheffield Academic Press Ltd, pp. 1299-1309. ISBN 1-85075-723-2.

Yeomans, S.R. (1993). Coated Steel Reinforcement in Concrete Part 1. *Corrosion Management*, Vol. **2**, No. 4, pp. 18-29.

Yeomans, S.R. (1994). Coated Steel Reinforcement in Concrete Part 2. *Corrosion Management*, Vol. **3**, No. 1, pp. 18-25.

Yeomans, S.R. (1998). Corrosion of the Zinc Alloy Coating in Galvanized Reinforced Concrete. Presentation at NACE Corrosion '98, San Diego, USA, March 22-27, Paper No. 98-653.

Yeomans, S.R. (2004). Galvanized Steel in Reinforced Concrete, Elsevier B.V., Amsterdam, The Netherlands, 297 p. ISBN 0-08-044511-X.

Yeomans, S.R. (1987). Galvanized Steel Reinforcement in Concrete. First National Structural Engineering Conference 1987. Melbourne, Australia, 26-28 August 1987. pp. 662-667.

Yeomans, S.R. (2004). Galvanizing of Steel Reinforcement for Use in Building and Construction, A presentation to a seminar on Galvanized Rebars in Construction and Infrastructure, Mumbai, India, 27 October, 2004.

Yeomans S.R. (1994). Performance of black, galvanized, and epoxy-coated reinforcing steel in chloride-contaminated concrete, *Corrosion*, Vol. **50**, No. 1, pp. 72-81.

APPENDIX A STANDARD DEVIATION AND DISTRIBUTION FUNCTIONS

The standard deviation of the service life can be estimated with the formula:

$$\sigma^2(t_L) = \sum_{i=1}^{n}\left[\frac{\partial\mu(t_L)}{\partial x_i}\cdot\sigma(x_i)\right]^2 = \sum_{i=1}^{n}\left[\frac{\partial\mu(t_L)}{\partial x_i}\cdot v_i\cdot\mu(x_i)\right]^2, \qquad (A.1)$$

where $\sigma(t_L)$ is the standard deviation of the service life [a],
$\sigma(x_i)$ is the standard deviation of variable x_i [-],
$\partial\mu(t_L)/\partial x_i$ is the partial derivate of the service life for variable x_i [-],
$\mu(x_i)$ is the mean value of the service life for variable x_i [-],
v_i is the coefficient of variation for factor i [-], and
n   is the number of variables [-].

The relative significance of parameters in the deterministic service life formula (influence on maximum error) can be determined with:

$$RI(x_i) = \frac{\left|\frac{\partial\mu(t_L)}{\partial x_i}\cdot\sigma(x_i)\right|}{\left|\sum_{i=1}^{n}\left(\frac{\partial\mu(t_L)}{\partial x_i}\cdot\sigma(x_i)\right)\right|}\cdot 100\% = \frac{\left|\frac{\partial\mu(t_L)}{\partial x_i}\cdot v_i\cdot\mu(x_i)\right|}{\left|\sum_{i=1}^{n}\left(\frac{\partial\mu(t_L)}{\partial x_i}\cdot v_i\cdot\mu(x_i)\right)\right|}\cdot 100\%, \quad (A.2)$$

where $RI(x_i)$ is the relative significance of factor i [-], and
$\mu(t_L)$ is the mean value of service life [-].

The number of variable combinations in sensitive analysis can be calculated as follows:

$$S_K = \sum_{k=1}^{n-1}(n-k), \qquad\qquad (A.3)$$

where S_K is the number of variable combinations [-],
n   is the number of variables [-], and
k   is a summing term [-].

Lognormal distribution function

The standard deviation and mean value of the lognormal distribution function can be calculated with:

$$\sigma^2(Y) = \ln\left(1+\left(\frac{\sigma(t_L)}{\mu(t_L)}\right)^2\right), \qquad\qquad (A.4)$$

$$\mu(Y) = \ln\mu(t_L) - \frac{1}{2}\cdot\sigma^2(Y), \qquad\qquad (A.5)$$

where $\sigma(Y)$ is the standard deviation of the lognormal distribution function [-],
$\sigma(t_L)$ is the standard deviation of the service life [a],
$\mu(t_L)$ is the mean value of the service life [a], and
$\mu(Y)$ is the mean value of the lognormal distribution function [-].

The lognormal density and cumulative distribution function as time is expressed with:

$$f(t) = \frac{1}{t \cdot \sqrt{2 \cdot \pi} \cdot \sigma(Y)} \cdot e^{\left[-\frac{1}{2 \cdot \sigma^2(Y)} \cdot (\ln t - \mu(Y))^2 \right]} ,$$ (A.6)

$$F(t) = \Phi \left[\frac{\ln t - \mu(t_L)}{\sigma(t_L)} \right] ,$$ (A.7)

where   t   is the time [a], and
       $\Phi[.]$ is the (0,1)-normal cumulative distribution function.

The target service life expressed with the probability of damage is as follows:

$$t_{Ltarg} = \frac{e^{\mu(Y)}}{e^{[\beta \cdot \sigma(Y)]}} ,$$ (A.8)

$$\beta = \frac{\mu(Y) - \ln(t)}{\sigma(Y)} ,$$ (A.9)

where t_{Ltarg} is the target service life [a],
       $\mu(Y)$ is the mean value of the lognormal distribution function [a],
       $\sigma(Y)$ is the standard deviation of the lognormal distribution function [a], and
       β is the test parameter for the (0,1)-normal cumulative distribution function ø [-].

Weibull distribution function

The standard deviation and mean value of the Weibull distribution function can be calculated with:

$$f_W(t) = \alpha \cdot \lambda \cdot (\lambda \cdot t)^{\alpha - 1} \cdot e^{-(\lambda \cdot t)^\alpha} ,$$ (A.10)

$$F(t) = 1 - e^{-(\lambda \cdot t)^\alpha} ,$$ (A.11)

where α is the shape parameter in Weibull distribution [-],
       λ is the scale parameter in Weibull distribution [-], and
       t   is the time [a].

The standard deviation and mean value of the Weibull distribution function can be calculated with:

$$\mu(t_L) = \left(\frac{1}{\lambda} \right) \cdot \Gamma \left(1 + \frac{1}{\alpha} \right) ,$$ (A.12)

$$\sigma(t_L) = \sqrt{\frac{1}{\lambda^2} \left[\Gamma \left(1 + \frac{2}{\alpha} \right) - \left(\Gamma \left(\frac{1}{\alpha} + 1 \right) \right)^2 \right]} ,$$ (A.13)

where $\mu(t_L)$ is the mean value of the service life [a],
       $\sigma(t_L)$ is the standard deviation of the service life [a], and
       Γ is the Gamma function.

APPENDIX B   ESEM IMAGING AND EDS SPOT ANALYSIS

Fig. B.1.   *SEM (Hot-dip galvanised reinforcement cylinder specimen, A500HW/Ø8/ZN, sodium chloride solution, after seven years of exposure).*

Table B.1.   *EDS spot analysis in Fig. B.1 (Hot-dip galvanised reinforcement cylinder specimen, A500HW/Ø8/ZN, sodium chloride solution, after seven years of exposure).*

Spot	Na [%]	Mg [%]	Al [%]	Si [%]	Cl [%]	K [%]	Ca [%]	Mn [%]	Fe [%]	Zn [%]	Ca /Si [-]	(Al+Fe) /Ca [-]	Zn /Fe [-]
1.	3.46	0.93	1.1	2.11	0.5	1.07	25.54	1.97	12.9	50.4	12.1	0.5	3.9
2.	0	2.18	3.98	16.14	2.13	2.58	1.44	1.78	64.93	4.86	0.1	47.9	0.1
3.	0	1.91	2.41	4.46	1.9	1.28	1.41	2.13	80.13	4.37	0.3	58.5	0.1
4.	0	1.47	1.5	3.16	1.69	1.53	1.56	1.88	83.75	3.46	0.5	54.6	0.0
5.	0	1.47	1.5	3.16	1.69	1.53	1.56	1.88	83.75	3.46	0.5	54.6	0.0
6.	0	2.13	3.61	10.61	2.02	2.1	2.64	2.31	67.93	6.64	0.2	27.1	0.1
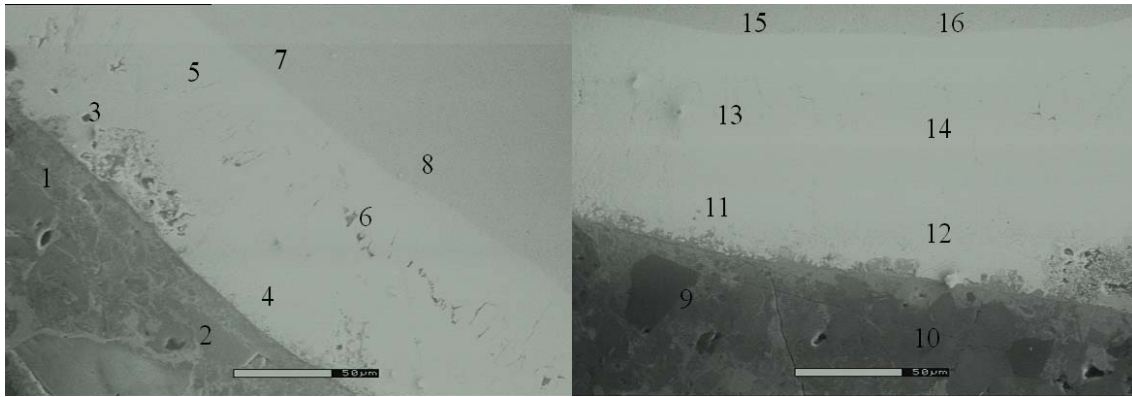
Fig. B.2. SEM (Hot-dip galvanised reinforcement cylinder specimen, B500K/Ø8/ZN, tap water, after seven years of exposure). Grid line is 50 μm.

Table B.2. EDS spot analysis in Fig. B.2 (Hot-dip galvanised reinforcement cylinder specimen, B500K/Ø8/ZN, tap water, after seven years of exposure).

Spot	Na [%]	Mg [%]	Al [%]	Si [%]	Cl [%]	K [%]	Ca [%]	Mn [%]	Fe [%]	Zn [%]	Ca/Si [-]	(Al+Fe)/Ca [-]	Zn/Fe [-]
1.	6.37	0	0.55	5.73	0	0.22	6.4	0.19	7.18	73.37	1.1	1.2	10.2
2.	0	0	2.26	12.79	0	0.32	8.71	0.17	8.82	66.92	0.7	1.3	7.6
3.	0	2.02	4.1	9.25	1.65	2.59	28.68	2.01	9.02	40.68	3.1	0.5	4.5
4.	0	1.24	1.53	2.01	1.1	1.3	2.28	1.81	9.43	79.29	1.1	4.8	8.4
5.	0	1.05	1.28	1.54	1.06	1.11	1.39	1.65	14.62	76.31	0.9	11.4	5.2
6.	0	0.99	1.32	1.61	1.19	1.22	1.28	1.64	15.84	74.93	0.8	13.4	4.7
7.	0	0	0	0.06	0	0.19	0.36	1.32	90.25	7.83	6.0	250.7	0.1
8.	0	0.94	0.97	1.16	0.91	1.3	1.32	2.4	80.58	10.41	1.1	61.8	0.1
9.	0	1.4	2.3	5.57	0.99	1.31	5.39	1.9	16.38	64.76	1.0	3.5	4.0
10.	0	1.42	2.32	5.64	0.95	1.31	5.51	1.55	16.53	64.77	1.0	3.4	3.9
11.	0	1.75	3.48	8.06	1.49	1.82	12.77	2.13	9.98	58.52	1.6	1.1	5.9
12.	0.00	0.94	1.57	2.10	1.06	1.17	1.89	1.84	6.64	82.79	0.9	4.3	12.5
13.	0.00	0.92	1.33	1.58	1.64	1.24	1.18	1.62	14.55	75.94	0.7	13.5	5.2
14.	0.00	0.98	1.20	1.42	0.82	1.17	1.36	1.62	14.57	76.85	1.0	11.6	5.3
15.	0.00	1.11	0.90	1.20	1.08	1.34	1.01	2.33	79.62	11.41	0.8	79.7	0.1
16.	0.00	0.00	0.00	0.00	0.00	0.00	0.24	1.22	88.98	9.56		370.8	0.1
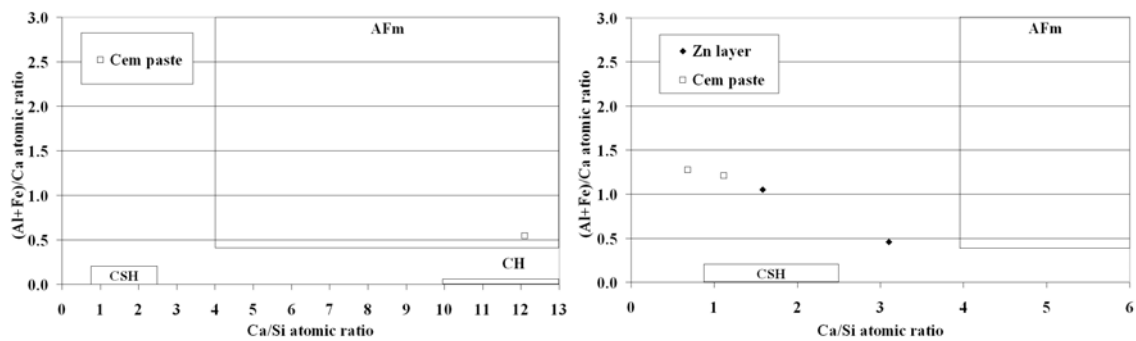
Fig. B.3. Proportions of (Al+Fe)/Ca to Ca/Si atomic ratios for hot-dip galvanised reinforcement cylinder specimen after seven years of exposure in sodium chloride solution (A500HW/Ø8/ZN) (left) and tap water (B500K/Ø8/ZN) (right).

Fig. B.4.   *SEM (Hot-dip galvanised reinforcement cylinder specimen, B500K/Ø8/ZN, sodium chloride solution, after seven years of exposure). Grid line is 50 μm.*

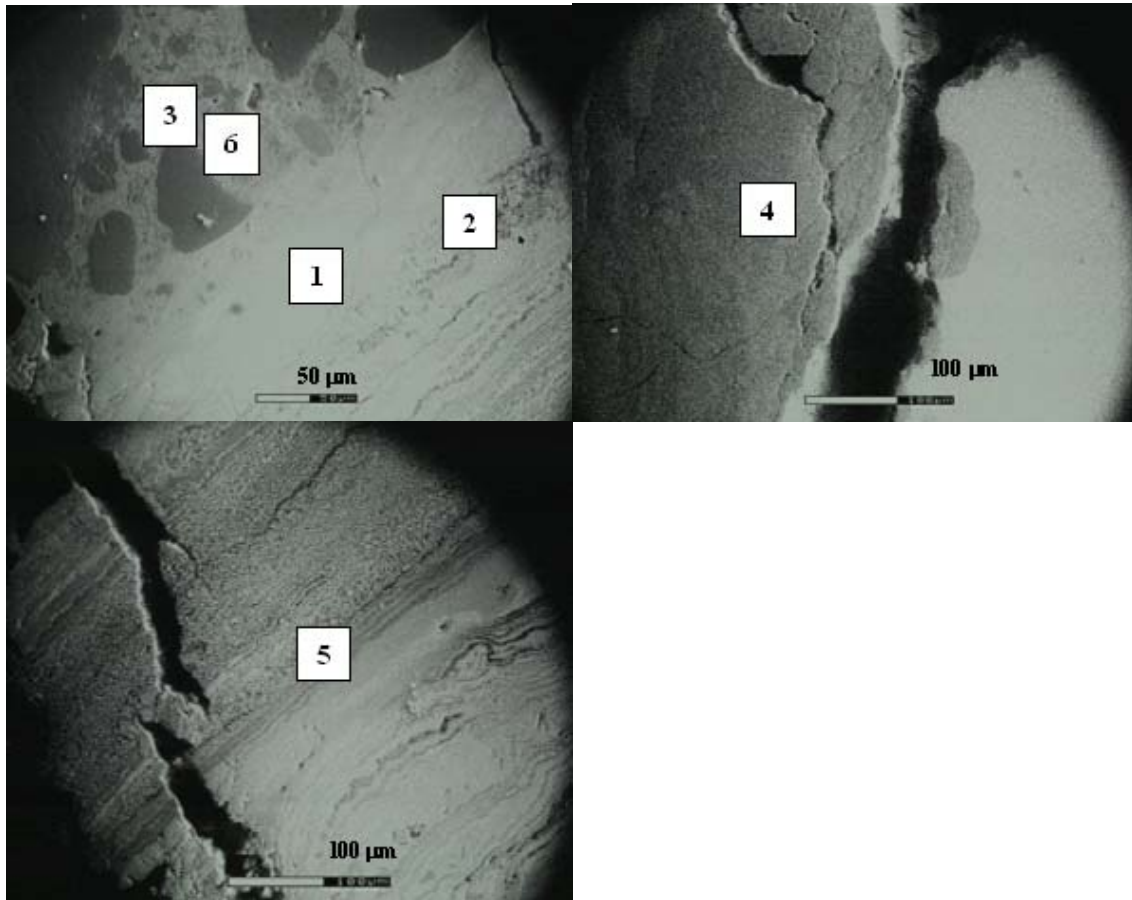*Table B.3.*   *EDS spot analysis in Fig. B.4 (Hot-dip galvanised reinforcement cylinder specimen, B500K/Ø8/ZN, sodium chloride solution, after seven years of exposure).*

| Spot	Na [%]	Mg [%]	Al [%]	Si [%]	Cl [%]	K [%]	Ca [%]	Mn [%]	Fe [%]	Zn [%]	Ca /Si [-]	(Al+Fe) /Ca [-]	Zn /Fe [-]
1.	0	0	0	1.22	0.99	0	0.67	0.43	92.29	4.41	0.5	137.7	0.0
2.	0	0	0	0	1.15	0	0.63	0.43	93.96	3.83		149.1	0.0
3.	0	0	0	1.58	3.63	0	0.13	0.32	92.02	2.32	0.1	707.8	0.0
4.	0	0	0	2.29	2.13	0	0.56	0.18	91.42	3.42	0.2	163.3	0.0
5.	0	0	0	1.87	1.36	0	0.61	0.31	93.71	2.15	0.3	153.6	0.0
6.	0	0.18	0	1.79	1.29	0.08	0.52	0.23	93.96	1.95	0.3	180.7	0.0
7.	0	0	0.36	7.41	3.29	0	1.35	0.5	85.28	1.81	0.2	63.4	0.0
8.	0	0	0.56	6.55	2.97	0	1.01	0.4	84.75	3.76	0.2	84.5	0.0
9.	1.49	0	18.29	47.7	0.75	1.13	9.7	0.3	19.28	1.36	0.2	3.9	0.1
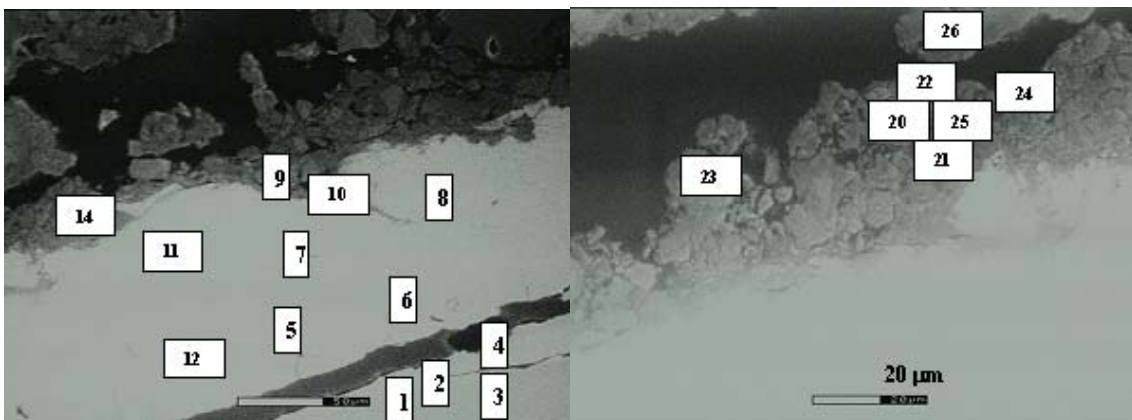
Fig. B.5.   *SEM (Hot-dip galvanised reinforcement beam specimen, A500HW/Ø8/ZN, tap water, after five years of exposure). Grid line is 50 μm (left) and 20 μm (right).*

Table B.4.   *EDS spot analysis in Fig. B.5 (Hot-dip galvanised reinforcement beam specimen, A500HW/Ø8/ZN, tap water, after five years of exposure).*

| Spot	Na [%]	Mg [%]	Al [%]	Si [%]	Cl [%]	K [%]	Ca [%]	Mn [%]	Fe [%]	Zn [%]	Ca /Si [-]	(Al+Fe) /Ca [-]	Zn /Fe [-]
1.	2.13	0.68	0.61	0.97	0.86	1.13	1.19	2.28	73.26	16.9	1.2	62.1	0.2
2.	0	0	0	0.21	0	0.24	0.7	1.2	76.32	21.34	3.3	109.0	0.3
3.	0	0	0	0	0	0.1	0.61	1.37	87.58	10.35		143.6	0.1
4.	4.83	0	0	0	0	0.14	0.73	0.76	20.64	72.89		28.3	3.5
5.	7.29	0	0	0	0	0.15	0.85	0.38	12.65	78.68		14.9	6.2
6.	10.46	0	0	0.3	0	0.11	0.89	0.46	12.6	75.19	3.0	14.2	6.0
8.	11.54	0	0	0.97	0	0.12	2.3	0.56	6.62	77.9	2.4	2.9	11.8
9.	4.25	0	0	5.6	0	0.69	24.32	0.21	9.54	55.38	4.3	0.4	5.8
10.	0	0	0	3.99	0	0.44	20.3	0.4	10.45	64.43	5.1	0.5	6.2
11.	8.46	0	0	0.81	0	0.14	1.64	0.44	5.6	82.91	2.0	3.4	14.8
12.	14.71	0	0	0.24	0	0.12	0.86	0.61	12.11	71.34	3.6	14.1	5.9
13.*													
14.	0	0	0.42	10.28	0	0.83	43.06	0.36	9.4	35.64	4.2	0.2	3.8
15.*													
16.*													
17.*													
18.*													
19.*													
20.	0	0	3.01	10.81	2.24	1.93	12.78	0	25.85	43.37	1.2	2.3	1.7
21.*													
22.	0	0	0.86	7.86	0	1.8	41.68	0	13.3	34.51	5.3	0.3	2.6
23.	0	4.5	1.11	11.9	0	1.37	50.58	0.4	11.24	18.91	4.3	0.2	1.7
24.	0	0	1.24	7.69	0	1.92	38.12	0.32	12.11	38.59	5.0	0.4	3.2
25.	0	0	1.21	10.51	0	1.82	42.91	0.45	12.97	30.12	4.1	0.3	2.3
26.*													

* Not done (equipment error)

Fig. B.6.   *Proportions of (Al+Fe)/Ca to Ca/Si atomic ratios for hot-dip galvanised reinforcement cylinder specimen after seven years of exposure 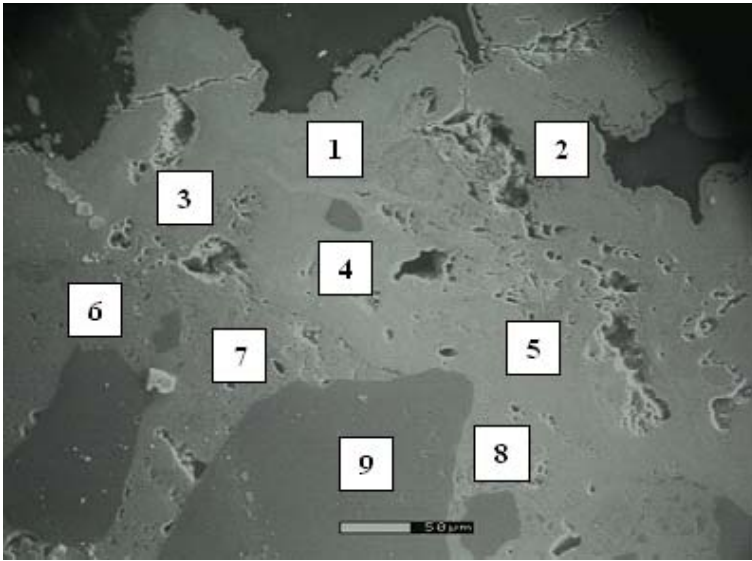in sodium chloride solution (B500K/Ø8/ZN) (left) and for hot-dip galvanised reinforcement beam specimen after five years of exposure in tap water (A500HW/Ø8/ZN) (right).*
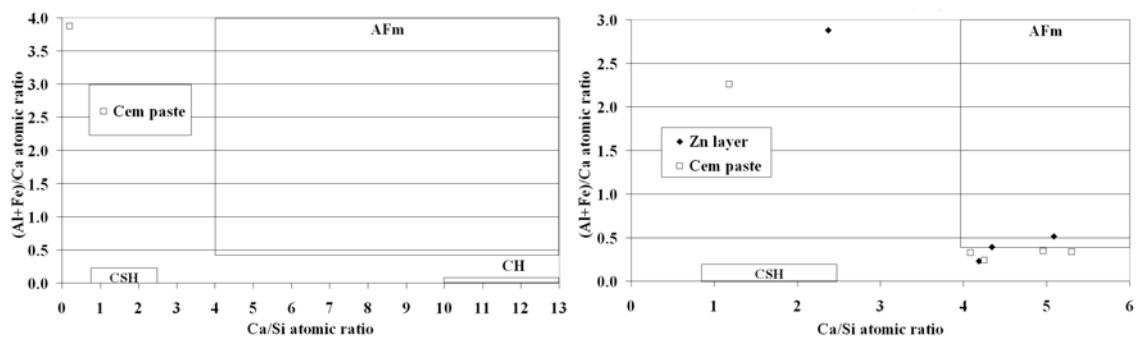
APPENDIX C ELECTROCHEMICAL, CRACK WIDTH, AND ZINC COATING THICKNESS MEASUREMENTS FOR BEAM AND CYLINDER SPECIMENS EXPOSED TO TAP WATER AND SODIUM CHLORIDE SOLUTION

Table C.1.   Electrochemical and crack width measurements for beam specimens exposed to tap water and sodium chloride solution after six months of exposure.

Tap water (after six months of exposure)

Type of beam	Crack width, w					Resistivity of concrete, R				
	Mean value $\bar{x}$ [mm]	Standard deviation s [mm]	Coefficient of variation V [-]	Number of measurements n [-]	Number of measured beams n [-]	Mean value $\bar{x}$ [kΩcm]	Standard deviation s [kΩcm]	Coefficient of variation V [-]	Number of measurements n [-]	Number of measured beams n [-]
A500HW/ø8	0.07	0.16	2.27	46	14	53.8	34.3	0.64	17	4
A500HW/ø8/ZN	0.11	0.10	0.91	42	14	64.2	37.5	0.58	23	6
B500K/ø8	0.12	0.21	1.65	42	14	42.5	19.7	0.46	25	6
B500K/ø8/ZN	0.06	0.08	1.43	42	14	54.0	16.9	0.31	20	5
B500K/ø7	0.24	0.16	0.66	45	15	37.0	20.2	0.55	22	5
B600KX/ø7	0.02	0.04	2.56	40	13	55.1	19.0	0.35	20	5
A500HW/ø12	0.12	0.18	1.53	37	12	37.0	25.9	0.70	25	6
TENCOR/ø12	0.17	0.15	0.87	32	10	32.3	25.8	0.80	24	6
Ordinary steel	0.14	0.18	1.27	170	55	42.8	24.1	0.56	89	21
Hot-dip galvanised steel	0.08	0.09	1.10	84	28	59.9	28.8	0.48	43	11

Type of beam	Corrosion current, i_{corr}				Rate of corrosion, v_{corr}			Corrosion potential, E_{corr}			Number of measurements n [-]	Sum Number of measured beams n [-]
	Mean value $\bar{x}$ [μA/cm^2]	Standard deviation s [μA/cm^2]	Coefficient of variation V [-]	Number of measurements n [-]	Mean value $\bar{x}$ [μm/a]	Standard deviation s [μm/a]	Coefficient of variation V [-]	Mean value $\bar{x}$ [mV]	Standard deviation s [mV]	Coefficient of variation V [-]		
A500HW/ø8	0.5	0.3	0.60	79	5.7	3.5	0.60	-668	47	0.07	79	14
A500HW/ø8/ZN	0.3	0.2	0.63	68	4.7	3.0	0.63	-920	67	0.07	68	14
B500K/ø8	0.6	0.3	0.60	68	6.6	4.0	0.60	-743	51	0.07	68	14
B500K/ø8/ZN	0.4	0.1	0.34	64	5.5	1.9	0.34	-911	97	0.11	64	14
B500K/ø7	1.0	0.6	0.63	75	11.6	7.3	0.63	-734	38	0.05	75	15
B600KX/ø7	0.1	0.0	0.33	56	0.7	0.2	0.33	-334	72	0.21	56	13
A500HW/ø12	0.3	0.3	0.76	67	4.0	3.0	0.76	-682	45	0.07	67	12
TENCOR/ø12	0.5	0.4	0.73	46	5.4	4.0	0.73	-697	48	0.07	46	10
Ordinary steel	0.6	0.4	0.70	289	7.2	5.0	0.70	-709	54	0.08	289	55
Hot-dip galvanised steel	0.3	0.1	0.42	132	5.2	2.2	0.42	-916	84	0.09	132	28

NaCl solution (after six months of exposure)

Type of beam	Crack width, w					Resistivity of concrete, R				
	Mean value $\bar{x}$ [mm]	Standard deviation s [mm]	Coefficient of variation V [-]	Number of measurements n [-]	Number of measured beams n [-]	Mean value $\bar{x}$ [kΩcm]	Standard deviation s [kΩcm]	Coefficient of variation V [-]	Number of measurements n [-]	Number of measured beams n [-]
A500HW/ø8	0.16	0.23	1.42	45	15	4.7	1.8	0.39	24	6
A500HW/ø8/ZN	0.17	0.13	0.78	48	16	5.2	2.4	0.47	28	7
B500K/ø8	0.17	0.24	1.41	39	13	3.4	2.0	0.60	27	6
B500K/ø8/ZN	0.11	0.10	0.89	39	13	5.7	1.8	0.32	30	6
B500K/ø7	0.31	0.18	0.58	30	10	4.1	1.9	0.45	18	4
B600KX/ø7	0.16	0.21	1.32	21	7	7.5	3.7	0.49	23	5
A500HW/ø12	0.14	0.16	1.20	33	11	27.2	27.4	1.01	21	5
TENCOR/ø12	0.06	0.09	1.41	36	12	13.6	18.0	1.32	33	8
Ordinary steel	0.20	0.20	1.02	147	49	9.9	14.3	1.45	90	21
Hot-dip galvanised steel	0.14	0.12	0.83	87	29	5.4	1.4	0.25	58	13

Type of beam	Corrosion current, i_{corr}				Rate of corrosion, v_{corr}			Corrosion potential, E_{corr}			Number of measurements n [-]	Sum Number of measured beams n [-]
	Mean value $\bar{x}$ [μA/cm^2]	Standard deviation s [μA/cm^2]	Coefficient of variation V [-]	Number of measurements n [-]	Mean value $\bar{x}$ [μm/a]	Standard deviation s [μm/a]	Coefficient of variation V [-]	Mean value $\bar{x}$ [mV]	Standard deviation s [mV]	Coefficient of variation V [-]		
A500HW/ø8	6.0	3.6	0.59	88	69.5	41.3	0.59	-729	29	0.04	88	15
A500HW/ø8/ZN	3.6	3.7	1.03	91	53.4	55.3	1.03	-1073	39	0.04	91	16
B500K/ø8	12.2	6.4	0.53	72	141.0	74.6	0.53	-760	29	0.04	72	13
B500K/ø8/ZN	3.5	3.7	1.05	71	52.7	55.1	1.05	-1083	24	0.02	71	13
B500K/ø7	18.0	11.4	0.63	43	209.1	131.8	0.63	-750	20	0.03	43	10
B600KX/ø7	0.1	0.1	0.65	28	1.5	1.0	0.65	-368	58	0.16	28	7
A500HW/ø12	8.2	5.1	0.62	55	95.3	59.0	0.62	-743	32	0.04	55	11
TENCOR/ø12	5.4	3.7	0.69	57	60.6	42.0	0.69	-749	16	0.02	57	12
Ordinary steel	11.1	7.7	0.69	258	128.7	89.7	0.70	-746	29	0.04	258	49
Hot-dip galvanised steel	3.7	3.7	0.99	162	55.6	55.3	0.99	-1077	34	0.03	162	29

169

Table C.2. *Electrochemical and crack width measurements for beam specimens exposed to tap water and sodium chloride solution after five years of exposure.*

Tap water (after five years of exposure)

Type of beam	Crack width, w					Resistivity of concrete, R				
	Mean value $\bar{x}$ [mm]	Standard deviation s [mm]	Coefficient of variation V [-]	Number of measurements n [-]	Number of measured beams n [-]	Mean value $\bar{x}$ [kΩcm]	Standard deviation s [kΩcm]	Coefficient of variation V [-]	Number of measurements n [-]	Number of measured beams n [-]
A500HW/ø8	0.09	0.17	1.86	46	14	29.5	9.1	0.31	112	14
A500HW/ø8/ZN	0.10	0.10	0.94	50	13	34.1	12.0	0.35	104	13
B500K/ø8	0.10	0.12	1.19	56	15	29.2	10.8	0.37	120	15
B500K/ø8/ZN	0.03	0.07	2.12	48	14	31.3	13.1	0.42	112	14
B500K/ø7	0.19	0.15	0.80	58	16	34.9	15.0	0.43	128	16
B600KX/ø7	0.02	0.07	3.66	51	13	32.7	7.0	0.21	104	13
A500HW/ø12	0.07	0.13	1.74	44	11	37.9	11.2	0.29	88	11
TENCOR/ø12	0.21	0.20	0.96	43	11	29.4	17.6	0.60	88	11
Ordinary steel	0.12	0.14	1.11	204	56	32.6	10.9	0.34	448	56
Hot-dip galvanised steel	0.07	0.09	1.17	98	27	32.6	11.4	0.35	216	27

Type of beam	Corrosion current, i_{corr}				Rate of corrosion, v_{corr}			Corrosion potential, E_{corr}				Sum
	Mean value $\bar{x}$ [μA/cm²]	Standard deviation s [μA/cm²]	Coefficient of variation V [-]	Number of measurements n [-]	Mean value $\bar{x}$ [μm/a]	Standard deviation s [μm/a]	Coefficient of variation V [-]	Mean value $\bar{x}$ [mV]	Standard deviation s [mV]	Coefficient of variation V [-]	Number of measurements n [-]	Number of measured beams n [-]
A500HW/ø8	0.2	0.1	0.46	112	2.4	1.1	0.46	-531	40	0.08	107	14
A500HW/ø8/ZN	0.2	0.1	0.41	104	2.3	1.0	0.41	-645	44	0.07	103	13
B500K/ø8	0.3	0.2	0.61	120	3.2	1.9	0.61	-581	53	0.09	119	15
B500K/ø8/ZN	0.2	0.1	0.48	112	3.1	1.5	0.48	-592	61	0.10	112	14
B500K/ø7	0.3	0.1	0.47	128	3.3	1.5	0.47	-536	52	0.10	127	16
B600KX/ø7	0.1	0.0	0.32	104	0.8	0.2	0.32	-349	69	0.20	103	13
A500HW/ø12	0.1	0.1	0.45	88	1.7	0.8	0.45	-463	38	0.08	88	11
TENCOR/ø12	0.3	0.2	0.66	88	2.9	1.9	0.66	-482	79	0.16	87	11
Ordinary steel	0.2	0.1	0.41	448	2.7	1.1	0.41	-532	61	0.12	441	56
Hot-dip galvanised steel	0.2	0.1	0.36	216	2.7	1.0	0.36	-618	60	0.10	215	27

NaCl solution (after five years of exposure)

Type of beam	Crack width, w					Resistivity of concrete, R				
	Mean value $\bar{x}$ [mm]	Standard deviation s [mm]	Coefficient of variation V [-]	Number of measurements n [-]	Number of measured beams n [-]	Mean value $\bar{x}$ [kΩcm]	Standard deviation s [kΩcm]	Coefficient of variation V [-]	Number of measurements n [-]	Number of measured beams n [-]
A500HW/ø8	0.14	0.18	1.31	64	16	1.8	0.8	0.44	128	16
A500HW/ø8/ZN	0.15	0.14	0.93	60	15	1.9	0.8	0.41	120	15
B500K/ø8	0.18	0.20	1.12	56	14	1.1	0.6	0.54	112	14
B500K/ø8/ZN	0.13	0.12	0.96	60	16	2.8	1.3	0.47	128	16
B500K/ø7	0.28	0.16	0.58	49	13	1.3	0.7	0.51	104	13
B600KX/ø7	0.33	0.47	1.42	55	14	3.7	1.1	0.31	112	14
A500HW/ø12	0.16	0.19	1.17	47	12	1.1	0.5	0.48	96	12
TENCOR/ø12	0.05	0.10	1.96	43	11	1.4	0.9	0.67	88	11
Ordinary steel	0.19	0.17	0.89	216	55	1.3	0.7	0.53	440	55
Hot-dip galvanised steel	0.13	0.11	0.86	120	31	2.3	1.1	0.46	248	31

Type of beam	Corrosion current, i_{corr}				Rate of corrosion, v_{corr}			Corrosion potential, E_{corr}				Sum
	Mean value $\bar{x}$ [μA/cm²]	Standard deviation s [μA/cm²]	Coefficient of variation V [-]	Number of measurements n [-]	Mean value $\bar{x}$ [μm/a]	Standard deviation s [μm/a]	Coefficient of variation V [-]	Mean value $\bar{x}$ [mV]	Standard deviation s [mV]	Coefficient of variation V [-]	Number of measurements n [-]	Number of measured beams n [-]
A500HW/ø8	4.1	2.8	0.67	128	47.9	31.9	0.67	-667	27	0.04	126	16
A500HW/ø8/ZN	2.3	1.7	0.76	120	34.0	26.0	0.76	-832	84	0.10	120	15
B500K/ø8	9.5	5.9	0.61	112	110.7	68.1	0.61	-706	19	0.03	111	14
B500K/ø8/ZN	2.6	2.1	0.81	128	39.3	32.0	0.81	-908	76	0.08	128	16
B500K/ø7	11.3	6.5	0.57	104	130.7	74.8	0.57	-685	24	0.04	104	13
B600KX/ø7	0.1	0.1	0.82	112	1.5	1.3	0.82	-349	100	0.29	112	14
A500HW/ø12	8.7	8.5	0.97	96	100.9	98.3	0.97	-651	17	0.03	96	12
TENCOR/ø12	4.5	3.2	0.73	88	50.4	36.6	0.73	-642	28	0.04	88	11
Ordinary steel	8.2	5.9	0.72	440	95.0	68.1	0.72	-677	29	0.04	437	55
Hot-dip galvanised steel	2.4	1.4	0.59	248	36.7	21.6	0.59	-871	88	0.10	248	31

Table C.3.   Electrochemical and crack width measurements for cylinder specimens exposed to tap water and sodium chloride solution after three months of exposure.

Tap water (after three months of exposure)

Type of cylinder	Crack width, w					Resistivity of concrete, R				
	Mean value $\bar{x}$ [mm]	Standard deviation s [mm]	Coefficient of variation V [-]	Number of measurements n [-]	Number of measured cylinders n [-]	Mean value $\bar{x}$ [kΩcm]	Standard deviation s [kΩcm]	Coefficient of variation V [-]	Number of measurements n [-]	Number of measured cylinders n [-]
A500HW/ø8	-	-	-	0	0	4.1	2.1	0.51	12	2
A500HW/ø8/ZN	-	-	-	0	0	7.2	6.8	0.94	9	2
B500K/ø8	-	-	-	0	0	6.1	6.9	1.12	21	2
B500K/ø8/ZN	-	-	-	0	0	5.7	4.2	0.75	11	2
B500K/ø7	-	-	-	0	0	8.1	6.3	0.77	10	2
B600KX/ø7	-	-	-	0	0	15.4	13.7	0.89	7	2
A500HW/ø12	-	-	-	0	0	5.4	4.2	0.79	11	2
TENCOR/ø12	-	-	-	0	0	10.6	10.1	0.95	12	2
Ordinary steel	-	-	-	0	0	5.9	5.5	0.94	54	8
Hot-dip galvanised steel	-	-	-	0	0	6.4	5.4	0.86	20	4

Type of cylinder	Corrosion current, i_{corr}				Rate of corrosion, v_{corr}			Corrosion potential, E_{corr}				Sum
	Mean value $\bar{x}$ [μA/cm²]	Standard deviation s [μA/cm²]	Coefficient of variation V [-]	Number of measurements n [-]	Mean value $\bar{x}$ [μm/a]	Standard deviation s [μm/a]	Coefficient of variation V [-]	Mean value $\bar{x}$ [mV]	Standard deviation s [mV]	Coefficient of variation V [-]	Number of measurements n [-]	Number of measured cylinders n [-]
A500HW/ø8	1.0	0.7	0.70	12	11.9	8.3	0.70	-457	141	0.31	12	2
A500HW/ø8/ZN	0.2	0.1	0.54	10	3.3	1.8	0.54	-839	116	0.14	9	2
B500K/ø8	0.6	0.5	0.83	21	6.6	5.5	0.83	-446	111	0.25	21	2
B500K/ø8/ZN	0.3	0.2	0.57	13	4.0	2.3	0.57	-888	129	0.15	11	2
B500K/ø7	0.7	0.5	0.79	10	7.7	6.1	0.79	-373	107	0.29	10	2
B600KX/ø7	0.0	0.0	0.61	7	0.3	0.2	0.61	-233	124	0.53	7	2
A500HW/ø12	0.8	0.5	0.63	11	8.9	5.6	0.63	-451	142	0.31	11	2
TENCOR/ø12	0.3	0.2	0.84	12	3.0	2.5	0.84	-368	173	0.47	12	2
Ordinary steel	0.7	0.6	0.77	54	8.4	6.5	0.77	-436	124	0.29	54	8
Hot-dip galvanised steel	0.2	0.1	0.55	23	3.7	2.1	0.55	-866	123	0.14	20	4

NaCl solution (after three months of exposure)

Type of cylinder	Crack width, w					Resistivity of concrete, R				
	Mean value $\bar{x}$ [mm]	Standard deviation s [mm]	Coefficient of variation V [-]	Number of measurements n [-]	Number of measured cylinders n [-]	Mean value $\bar{x}$ [kΩcm]	Standard deviation s [kΩcm]	Coefficient of variation V [-]	Number of measurements n [-]	Number of measured cylinders n [-]
A500HW/ø8	-	-	-	0	0	0.1	0.1	0.90	17	2
A500HW/ø8/ZN	-	-	-	0	0	0.3	0.3	0.87	12	2
B500K/ø8	-	-	-	0	0	0.1	0.1	0.98	11	2
B500K/ø8/ZN	-	-	-	0	0	0.3	0.2	0.79	13	2
B500K/ø7	-	-	-	0	0	0.1	0.1	0.74	9	2
B600KX/ø7	-	-	-	0	0	0.3	0.2	0.89	8	2
A500HW/ø12	-	-	-	0	0	0.1	0.1	0.83	13	2
TENCOR/ø12	-	-	-	0	0	0.1	0.1	0.81	15	2
Ordinary steel	-	-	-	0	0	0.1	0.1	0.86	50	8
Hot-dip galvanised steel	-	-	-	0	0	0.3	0.2	0.82	25	4

Type of cylinder	Corrosion current, i_{corr}				Rate of corrosion, v_{corr}			Corrosion potential, E_{corr}				Sum
	Mean value $\bar{x}$ [μA/cm²]	Standard deviation s [μA/cm²]	Coefficient of variation V [-]	Number of measurements n [-]	Mean value $\bar{x}$ [μm/a]	Standard deviation s [μm/a]	Coefficient of variation V [-]	Mean value $\bar{x}$ [mV]	Standard deviation s [mV]	Coefficient of variation V [-]	Number of measurements n [-]	Number of measured cylinders n [-]
A500HW/ø8	26.2	13.9	0.53	17	304.1	161.2	0.53	-666	59	0.09	17	2
A500HW/ø8/ZN	10.8	9.9	0.92	13	161.6	148.9	0.92	-988	24	0.02	13	2
B500K/ø8	66.3	66.4	1.00	11	769.2	770.5	1.00	-675	56	0.08	11	2
B500K/ø8/ZN	34.1	49.8	1.46	13	511.7	746.8	1.46	-964	27	0.03	13	2
B500K/ø7	16.8	10.7	0.64	10	195.1	124.0	0.64	-642	46	0.07	10	2
B600KX/ø7	0.0	0.0	0.44	9	0.5	0.2	0.44	-213	71	0.33	9	2
A500HW/ø12	21.1	12.8	0.61	13	244.7	148.5	0.61	-652	53	0.08	13	2
TENCOR/ø12	59.3	86.7	1.46	15	687.6	1006.0	1.46	-640	11	0.02	15	2
Ordinary steel	31.7	36.8	1.16	51	367.9	426.4	1.16	-660	54	0.08	51	8
Hot-dip galvanised steel	22.4	37.1	1.65	26	336.7	557.0	1.65	-976	28	0.03	26	4

Table C.4. *Electrochemical and crack width measurements for cylinder specimens exposed to tap water and sodium chloride solution after seven years of exposure.*

Tap water (after seven years of exposure)

Type of cylinder	Crack width, w					Resistivity of concrete, R				
	Mean value $\bar{x}$ [mm]	Standard deviation s [mm]	Coefficient of variation V [-]	Number of measurements n [-]	Number of measured cylinders n [-]	Mean value $\bar{x}$ [kΩcm]	Standard deviation s [kΩcm]	Coefficient of variation V [-]	Number of measurements n [-]	Number of measured cylinders n [-]
A500HW/ø8	0.29	0.13	0.45	32	4	201.9	136.7	0.68	32	4
A500HW/ø8/ZN	0.17	0.19	1.12	176	23	531.4	398.2	0.75	184	23
B500K/ø8	0.24	0.23	0.95	40	5	632.5	402.1	0.64	40	5
B500K/ø8/ZN	0.16	0.16	0.98	156	22	279.5	276.4	0.99	176	22
B500K/ø7	0.26	0.13	0.51	36	5	713.7	451.6	0.63	40	5
B600KX/ø7	0.37	0.18	0.50	108	14	487.9	297.3	0.61	112	14
A500HW/ø12	-	-	-	0	0	-	-	-	0	0
TENCOR/ø12	-	-	-	0	0	-	-	-	0	0
Ordinary steel	0.26	0.17	0.67	108	14	538.5	425.0	0.79	112	14
Hot-dip galvanised steel	0.17	0.18	1.06	332	45	408.2	366.0	0.90	360	45

Type of cylinder	Corrosion current, i_{corr}				Rate of corrosion, v_{corr}			Corrosion potential, E_{corr}				Sum	
	Mean value $\bar{x}$ [μA/cm²]	Standard deviation s [μA/cm²]	Coefficient of variation V [-]	Number of measurements n [-]	Mean value $\bar{x}$ [μm/a]	Standard deviation s [μm/a]	Coefficient of variation V [-]	Mean value $\bar{x}$ [mV]	Standard deviation s [mV]	Coefficient of variation V [-]	Number of measurements n [-]	Number of measurements n [-]	Number of measured cylinders n [-]
A500HW/ø8	0.1	0.1	1.24	32	0.8	1.0	1.24	-237	50	0.21		32	4
A500HW/ø8/ZN	0.1	0.2	2.47	184	1.4	3.6	2.47	-503	141	0.28		184	23
B500K/ø8	0.1	0.1	0.77	40	1.2	0.9	0.77	-217	60	0.28		40	5
B500K/ø8/ZN	0.0	0.0	0.90	176	0.7	0.7	0.90	-473	127	0.27		176	22
B500K/ø7	0.1	0.1	1.36	40	0.6	0.8	1.36	-128	74	0.58		40	5
B600KX/ø7	0.0	0.0	0.69	112	0.2	0.2	0.69	-255	104	0.41		112	14
A500HW/ø12	-	-	-	0	-	-	-	-	-	-		0	0
TENCOR/ø12	-	-	-	0	-	-	-	-	-	-		0	0
Ordinary steel	0.1	0.1	1.07	112	0.9	0.9	1.07	-191	79	0.41		112	14
Hot-dip galvanised steel	0.1	0.2	2.37	360	1.1	2.6	2.37	-489	135	0.28		360	45

NaCl solution (after seven years of exposure)

Type of cylinder	Crack width, w					Resistivity of concrete, R				
	Mean value $\bar{x}$ [mm]	Standard deviation s [mm]	Coefficient of variation V [-]	Number of measurements n [-]	Number of measured cylinders n [-]	Mean value $\bar{x}$ [kΩcm]	Standard deviation s [kΩcm]	Coefficient of variation V [-]	Number of measurements n [-]	Number of measured cylinders n [-]
A500HW/ø8	0.44	0.23	0.52	164	21	3.6	1.5	0.43	168	21
A500HW/ø8/ZN	0.46	0.25	0.55	4	1	1.3	0.2	0.12	8	1
B500K/ø8	0.29	0.19	0.66	168	22	5.2	5.2	1.00	176	22
B500K/ø8/ZN	0.27	0.14	0.50	20	3	2.8	1.1	0.38	24	3
B500K/ø7	0.39	0.18	0.45	100	13	4.6	7.1	1.53	104	13
B600KX/ø7	0.52	0.34	0.65	96	13	1.3	1.0	0.76	104	13
A500HW/ø12	-	-	-	0	0	-	-	-	0	0
TENCOR/ø12	0.57	0.30	0.52	8	2	4.7	2.8	0.58	16	2
Ordinary steel	0.37	0.21	0.57	432	56	4.4	4.8	1.09	448	56
Hot-dip galvanised steel	0.30	0.17	0.56	24	4	2.4	1.1	0.47	32	4

Type of cylinder	Corrosion current, i_{corr}				Rate of corrosion, v_{corr}			Corrosion potential, E_{corr}				Sum	
	Mean value $\bar{x}$ [μA/cm²]	Standard deviation s [μA/cm²]	Coefficient of variation V [-]	Number of measurements n [-]	Mean value $\bar{x}$ [μm/a]	Standard deviation s [μm/a]	Coefficient of variation V [-]	Mean value $\bar{x}$ [mV]	Standard deviation s [mV]	Coefficient of variation V [-]	Number of measurements n [-]	Number of measurements n [-]	Number of measured cylinders n [-]
A500HW/ø8	12.5	7.5	0.52	168	145.1	87.5	0.60	-546	44	0.08		168	21
A500HW/ø8/ZN	4.3	2.8	0.66	8	64.0	42.2	0.66	-518	6	0.01		8	1
B500K/ø8	10.2	9.5	0.93	176	118.6	110.7	0.93	-573	38	0.07		176	22
B500K/ø8/ZN	7.6	5.3	0.69	24	114.1	78.9	0.69	-531	10	0.02		24	3
B500K/ø7	11.3	8.0	0.71	104	131.2	93.0	0.71	-562	38	0.07		104	13
B600KX/ø7	0.2	0.3	1.28	104	2.3	2.9	1.28	-303	136	0.45		104	13
A500HW/ø12	-	-	-	0	-	-	-	-	-	-		0	0
TENCOR/ø12	10.0	5.8	0.58	16	113.3	65.9	0.58	-543	72	0.13		16	2
Ordinary steel	11.3	8.5	0.75	448	131.5	98.9	0.75	-560	42	0.08		448	56
Hot-dip galvanised steel	6.8	4.9	0.73	32	101.6	74.2	0.73	-528	11	0.02		32	4

Table C.5. *Statistics of zinc coating thickness before exposure for beam and cylinder specimens for all values (reinforcement bar diameter, Ø = 7mm, 8 mm, and 12 mm).*

Beam and cylinder specimen, Hot-dip galvanised steel	Zinc coating thickness
Tap water and NaCl solution	d
Before exposure	[μm]
Mean value, μ	184.54
Standard deviation, σ	102.76
Coefficient of variation, ν	0.56
Minimum value	62.47
Maximum value	495.60
Number of measurements, n	139
p-value (>0.5)	0.4437
KS-value (<0.03)	0.0644
AD-value (<1.5)	0.4727
Distribution type	Gamma
Distribution parameter 1	L = 62.20
Distribution parameter 2	α = 101.19
Distribution parameter 3	β = 1.21
A close fit	

Table C.6. *Statistics of zinc coating thickness before exposure for beam and cylinder specimens for extreme values (reinforcement bar diameter, Ø = 7mm, 8 mm, and 12 mm).*

Beam and cylinder specimen, Hot-dip galvanised steel	Zinc coating thickness
Tap water and NaCl solution	d
Before exposure	[μm]
Mean value, μ	147.59
Standard deviation, σ	69.94
Coefficient of variation, ν	0.47
Minimum value	62.47
Maximum value	417.60
Number of measurements, n	33
p-value (>0.5)	0.8131
KS-value (<0.03)	0.0887
AD-value (<1.5)	0.3174
Distribution type	Extreme
Distribution parameter 1	m = 118.28
Distribution parameter 2	α = 48.59
Distribution parameter 3	-
A close fit	

APPENDIX D   EXAMPLES OF THE DISTRIBUTION CURVES OF THE HOT-DIP GALVANISED REINFORCEMENT BEAM AND CYLINDER SPECIMENS FOR ALL AND EXTREME VALUES EXPOSED TO TAP WATER AND SODIUM CHLORIDE SOLUTION
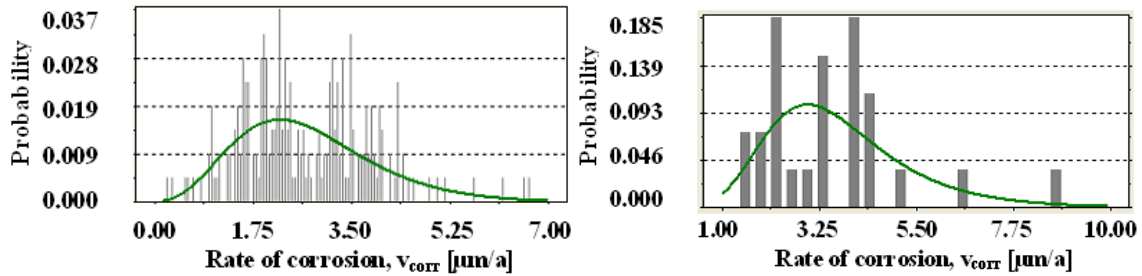
Fig. D.1.   Rate of corrosion of the hot-dip galvanised reinforcement beam specimens after five years of exposure in tap water for all values (left) (n = 216 pc/Gamma distribution) and extreme values (right) (n = 27 pc/Extreme value distribution (Type 1)).
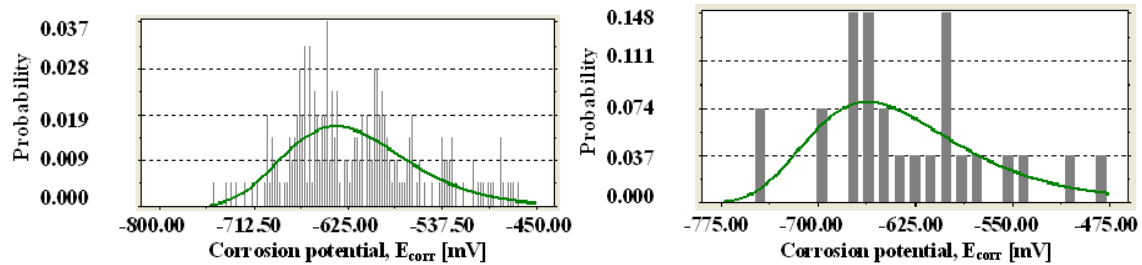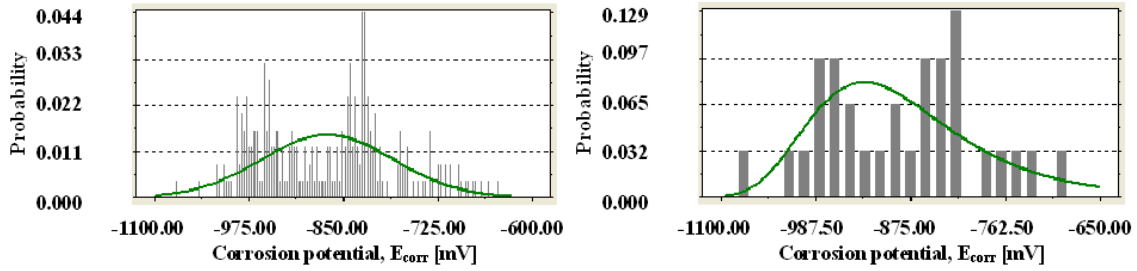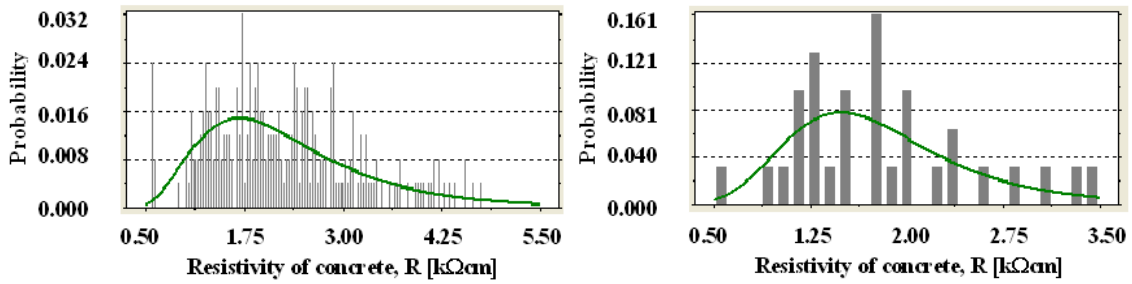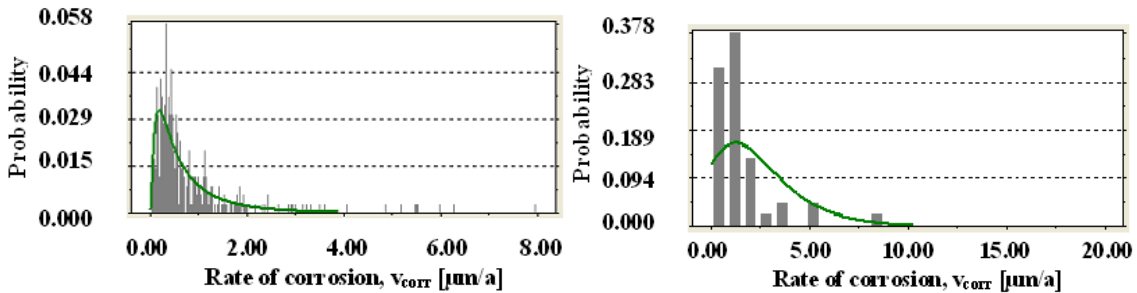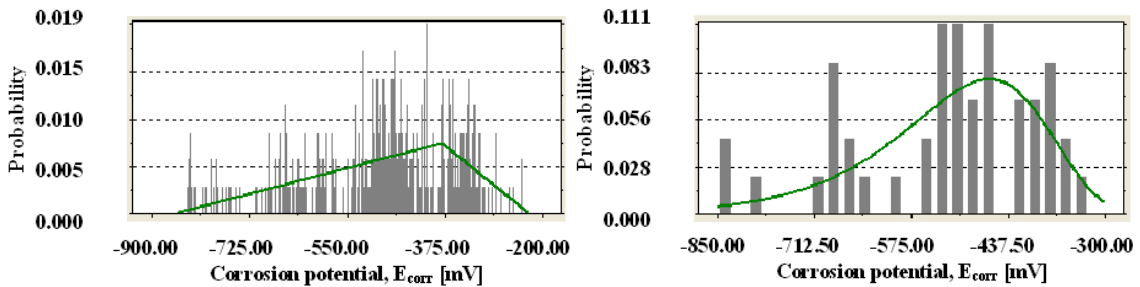

Fig. D.2.   Corrosion potential of the hot-dip galvanised reinforcement beam specimens after five years of exposure in tap water for all values (left) (n = 215 pc/Gamma distribution) and extreme values (right) (n = 27 pc/Extreme value distribution (Type 1)).
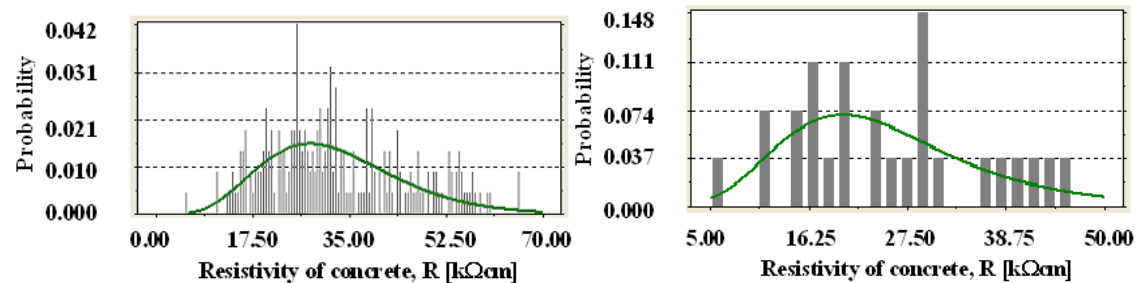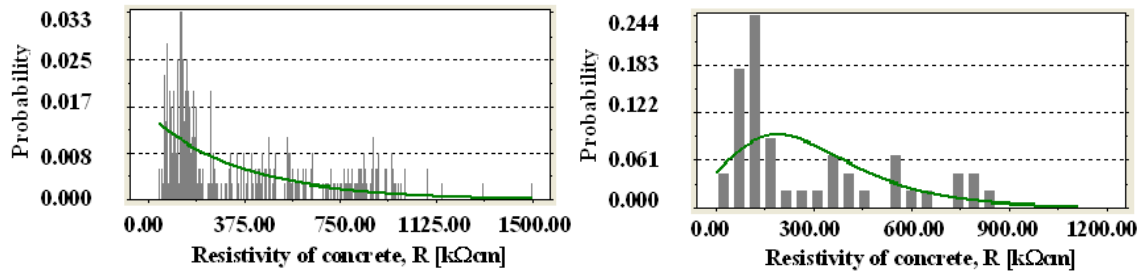

Fig. D.3.   The resistivity of concrete of the hot-dip galvanised reinforcement beam specimens after five years of exposure in tap water for all values (left) (n = 216 pc/Gamma distribution) and extreme values (right) (n = 27 pc/Extreme value distribution (Type 1)).
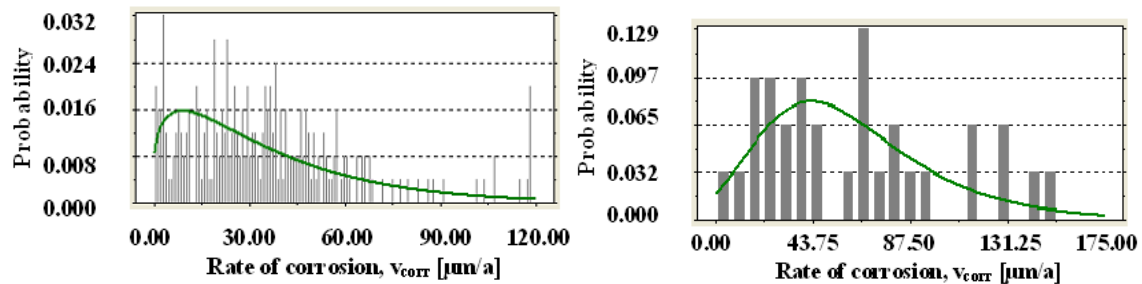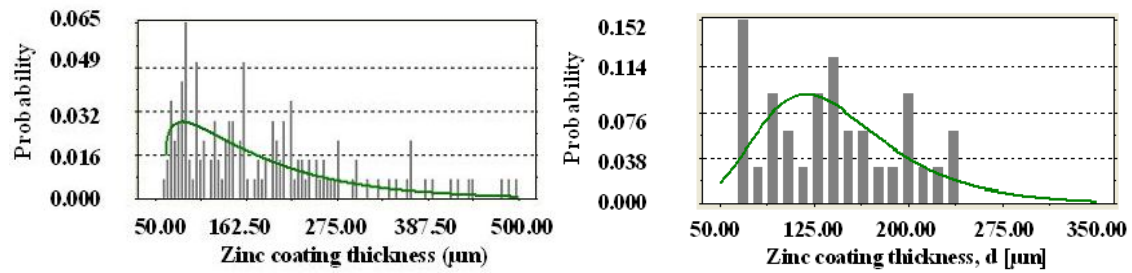

Fig. D.4.   Rate of corrosion of the hot-dip galvanised reinforcement beam specimens after five years of exposure in sodium chloride solution for all values (left) (n = 248 pc/Gamma distribution) and extreme values (right) (n = 31 pc/Extreme value distribution (Type 1)).

Fig. D.5.   Corrosion potential of the hot-dip galvanised reinforcement beam specimens after five years of exposure in sodium chloride solution for all values (left) (n = 248 pc/Normal distribution) and extreme values (right) (n = 31 pc/Extreme value distribution (Type 1)).

Fig. D.6.   The resistivity of concrete of the hot-dip galvanised reinforcement beam specimens after five years of exposure in sodium chloride solution for all values (left) (n = 248 pc/Lognormal distribution) and extreme values (right) (n = 31 pc/Extreme value distribution (Type 1)).

Fig. D.7.   Rate of corrosion of the hot-dip galvanised reinforcement cylinder specimens after seven years of exposure in tap water for all values (left) (n = 360 pc/Lognormal distribution) and extreme values (right) (n = 45 pc/Extreme value distribution (Type 1)).

Fig. D.8.   Corrosion potential of the hot-dip galvanised reinforcement cylinder specimens after seven years of exposure in tap water for all values (left) (n = 360 pc/Triangular distribution) and extreme values (right) (n = 45 pc/Extreme value distribution (Type 1)).

Fig. D.9.   *The resistivity of concrete of the hot-dip galvanised reinforcement cylinder specimens after seven years of exposure in tap water for all values (left) (n = 360 pc/Gamma distribution) and extreme values (right) (n = 45 pc/Extreme value distribution (Type 1)).*

Fig. D.10.   *Zinc coating thickness before exposure for beam and cylinder specimens for all values (left) (n = 139 pc/Gamma distribution) and extreme values (right) (n = 33 pc/Extreme value distribution (Type 1)).*

APPENDIX E   COMPARISON EXAMPLES BETWEEN ALL AND EXTREME VALUES WITH **90 - 100 %** FRACTAL OF THE HOT-DIP GALVANISED REINFORCEMENT BEAM AND CYLINDER SPECIMENS EXPOSED TO TAP WATER AND SODIUM CHLORIDE SOLUTION
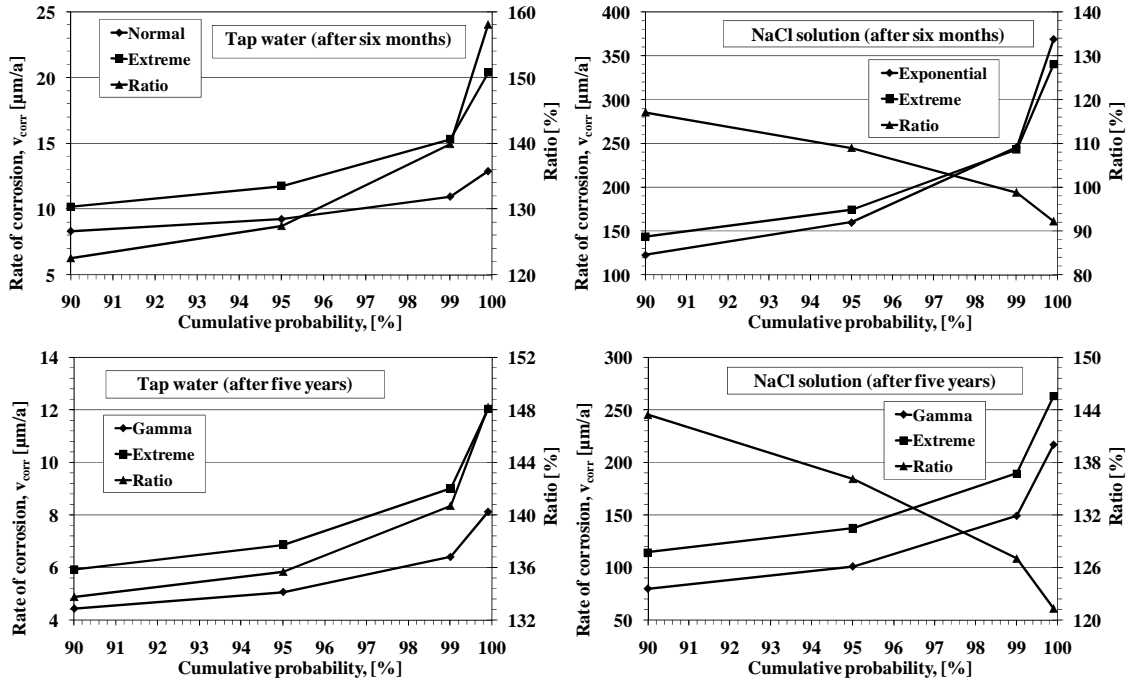
Fig. E.1.   *Rate of corrosion as a function of cumulative probability of hot-dip galvanised reinforcement bars for the beam specimens exposed to tap water (left) and sodium chloride solution (right). (Ratio = Extreme/chosen distribution curve).*
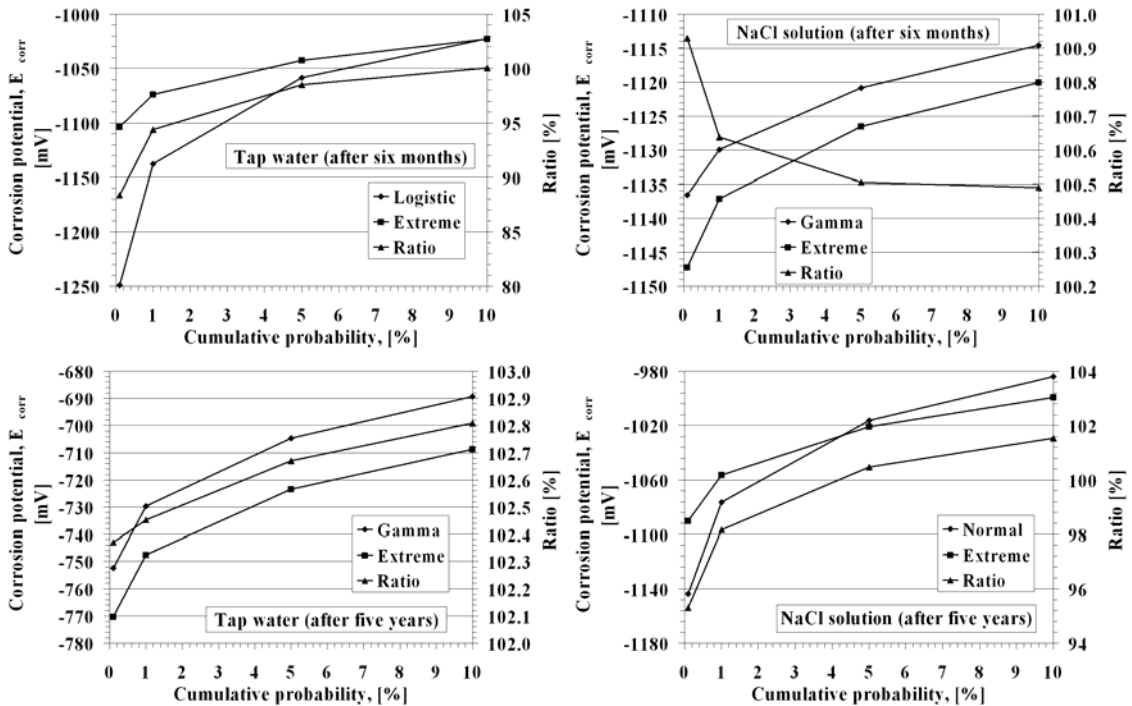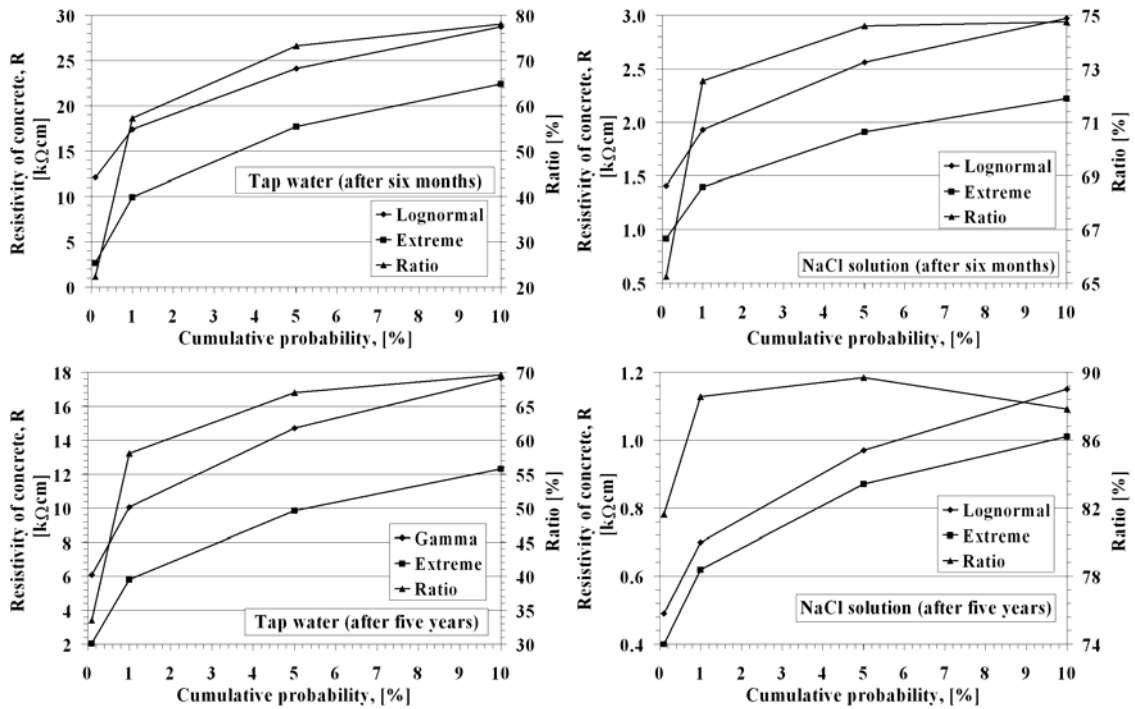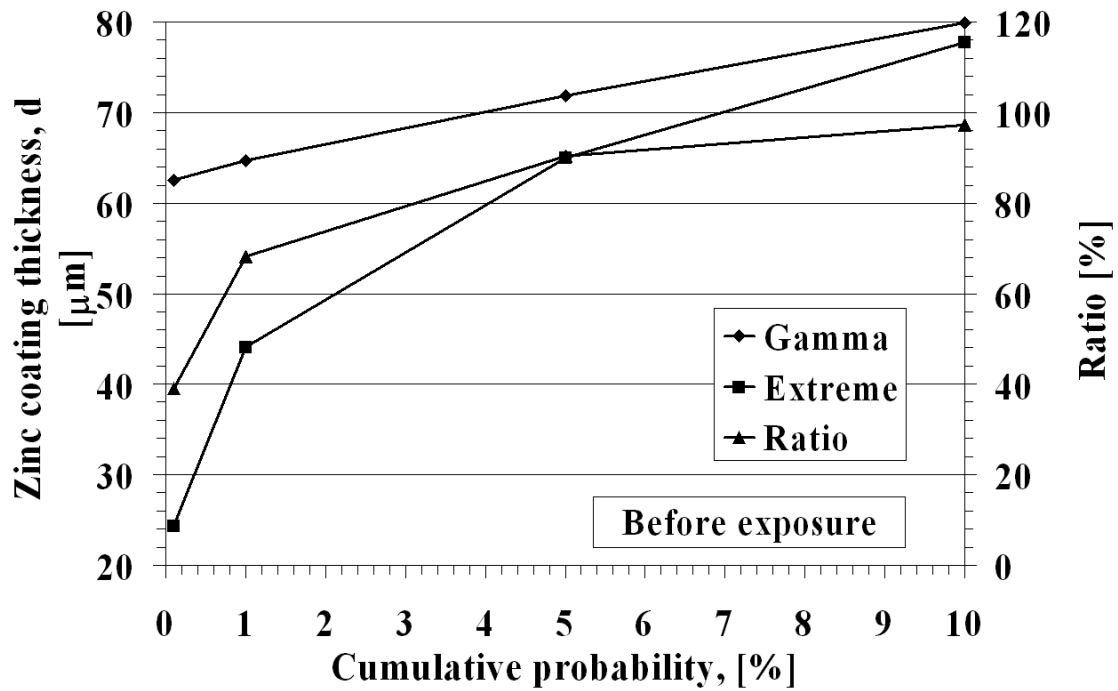

Fig. E.2.   *Corrosion potential as a function of cumulative probability of hot-dip galvanised reinforcement bars for the beam specimens exposed to tap water (left) and sodium chloride solution (right). (Ratio = Extreme/chosen distribution curve).*

Fig. E.3.   *Resistivity of concrete as a function of cumulative probability of hot-dip galvanised reinforcement bars for the beam specimens exposed to tap water (left) and sodium chloride solution (right). (Ratio = Extreme/chosen distribution curve).*

Fig. E.4.   *Zinc coating thickness as a function of cumulative probability of hot-dip galvanised reinforcement bars for the beam and cylinder specimens exposed to tap water and sodium chloride solution. (Ratio = Extreme/chosen distribution curve).*